BNL-52497-97/01-~~REV~~ Rev.
UC - 406

FLOW REVERSAL POWER LIMIT

FOR THE HFBR

Lap Y. Cheng
and
Paul R. Tichler

January, 1997

Formal Report

Reactor Division

Brookhaven National Laboratory
Brookhaven Science Associates

Under Contract No. DE-AC02-98CH10886 with the
UNITED STATES DEPARTMENT OF ENERGY

DISCLAIMER

Portions of this document may be illegible electronic image products. Images are produced from the best available original document.

BNL-52497-97/01-~~REV~~ Rev.
UC-406

FLOW REVERSAL POWER LIMIT

FOR THE HFBR

January 1997

Lap Y. Cheng and Paul R. Tichler
Brookhaven National Laboratory

DISCLAIMER

ABSTRACT

The High Flux Beam Reactor (HFBR) is a pressurized heavy water moderated and cooled research reactor that began operation at 40 MW. The reactor was subsequently upgraded to 60 MW and operated at that level for several years. The reactor undergoes a buoyancy-driven reversal of flow in the reactor core following certain postulated accidents. Questions which were raised about the afterheat removal capability during the flow reversal transition led to a reactor shutdown and subsequent resumption of operation at a reduced power of 30 MW. An experimental and analytical program to address these questions is described in this report. The experiments were single channel flow reversal tests under a range of conditions. The analytical phase involved simulations of the tests to benchmark the physical models and development of a criterion for dryout. The criterion is then used in simulations of reactor accidents to determine a safe operating power level. It is concluded that the limit on the HFBR operating power with respect to the issue of flow reversal is in excess of 60 MW. Direct use of the experimental results and an understanding of the governing phenomenology supports this conclusion.

ACKNOWLEDGEMENTS

The authors would like to express their thanks to Dr. H.K. Fauske and Professor R.T. Lahey, Jr. for their suggestions during the planning of the flow reversal tests, and Professor P. Griffith for his review and comments on the original version of this report. The authors also have benefitted from helpful discussions with Dr. G.L. Yoder, Jr. who reviewed the report for the Reactor Safety Committee at Brookhaven National Laboratory. The current version of the report (Rev. 01/97) reflects the comments and recommendations made by D. Pedersen, M. Ishii and C.C. Chu who reviewed the report for the Department of Energy.

The flow reversal tests were conducted at the Heat Transfer Research Facility of Columbia University and the authors gratefully acknowledge the effort of the staff there.

The authors thank Ms. Judith Spara for preparing this report and her patience in accommodating many revisions.

TABLE OF CONTENTS

LIST OF FIGURES

LIST OF TABLES

I. EXECUTIVE SUMMARY

A. Introduction

This report describes the results of an experimental and analytical program to address the flow reversal issue in the High Flux Beam Reactor. The original version of this report was reviewed by a team from Argonne National Laboratory for the Department of Energy, Office of Nuclear Energy, Science and Technology. This review resulted in revisions to the original report and reissuing it as the current version (Rev. 01/97). The revisions are intended to clarify and focus the report and to provide a more complete assessment of the importance of assumptions and approximations made in the experimental and analytical phases of the program.

B. Background

The HFBR at Brookhaven National Laboratory (BNL) is a research reactor which is fueled by 93% enriched uranium and is cooled, moderated, and reflected by heavy water. The core is composed of 28 fuel elements with each element made up of 18 fuel plates in a parallel plate array. The aluminum clad fuel plates are 0.05 inch thick and are spaced to provide coolant channels about 0.1 inch thick and 2.5 inch in width. During normal operation the coolant flow direction, as indicated in Figure 1, is downward through the core. For emergency shutdown heat removal, the HFBR employs a scheme that provides a return path around the core so that natural circulation cooling can be established. The return path is provided by the opening of four spring-loaded flow reversal valves. These valves are held closed during normal operation by the head developed across any one of the two primary and shutdown coolant pumps. If all pumping power is cut off, either by loss of electrical pumping power or because of automatic safety action, flow coastdown will begin. The flow reversal valves open automatically when the head developed by the pumps can no longer maintain the valve springs in tension. When the downward core flow reaches a value at which the thermal buoyancy head is comparable to the friction losses in the core, flow reversal occurs.

At the time that the reactor was being designed (1960) there were data [1] that indicated that while the decay heat removal capacity with natural circulation was more than adequate, there were little data on the flow reversal transient itself. Accordingly a series of tests [2] were undertaken at that time to establish the limiting shutdown heating rate. These tests were simple, go, no-go tests in which the success criterion was the absence of rapid temperature excursions in the test section. In 1982 after a number of plant modifications were made the reactor power was increased from 40 to 60 MW. During the period 1989-1991 reviews by the Department of Energy (DOE) raised the issue of the prototypicality and the applicability of these earlier tests to 60

MW operation of the HFBR. At that time, critical heat flux data and correlations were available for steady-state upflow and downflow in channel geometries and conditions similar to the HFBR [3,4]. However, because of the transient nature of the flow reversal process it was not apparent how these steady-state correlations should be used. Therefore, a more conservative heat removal limit was formulated for the HFBR based on the flooding limit and the nominal operating power level was reduced to 30 MW.

In an effort to provide a more realistic and defensible estimate of the flow reversal heat removal limit and thereby increase the HFBR power level, a series of flow reversal tests were conducted for BNL at the Heat Transfer Research Facility (HTRF) of Columbia University. In conjunction with these tests, models of the test loop and the HFBR were developed using the thermal hydraulics code, RELAP5. The purpose of this modeling effort was to benchmark the code against the test results and then use the HFBR model to analyze loss of flow accidents.

C. Test Program

The tests were designed to reproduce as closely as possible the dominant features of the flow reversal transient in the reactor. The tests were performed with an electrically heated single channel section representing the core, an orifice or throttle valve representing the flow reversal valves, a variable speed pump to simulate the flow coastdown, and auxiliary piping and equipment to simulate other pertinent structures in the reactor vessel. The test loop was set up to preserve the vertical height of the natural circulation flow path in the HFBR vessel. The heated section was a full-size mockup of a typical channel in a HFBR fuel element. The flow areas of the test loop were scaled to correspond to a typical coolant channel in the HFBR. The top of the upper plenum region was open to the atmosphere. Demineralized water was the working fluid of the test loop.

The fuel plates were simulated in the test by 6061 aluminum plates of similar thickness and powered by DC heating. Two separate heater arrangements were used in the experiments. The single-sided arrangement had one heater plate and a transparent plate separated by the coolant gap. The double-sided heater had a heater plate on each side of the coolant gap.

The test loop was instrumented to continuously record water temperatures, heated plate temperatures, flow rates and power (voltage and current) to the heated plate. The plates were protected from overheating during the experiments by two types of power trips - on plate temperature rise and on increase in voltage across the plate. A voltage increase would occur when the plate temperature increased because of the increased plate resistance with temperature. The trip settings on temperature and voltage rise were conservatively set so that the heated plate was not

damaged and could be reused in subsequent tests.

In each test, steady forced flow conditions were established at a fixed power and a flow rate corresponding to a time in the reactor loss of flow accident where the primary flow rate has fallen to about 7% of its operating value. The test was then initiated by linearly reducing the pump flow to simulate the final coastdown of the reactor pumps to zero flow. The test was considered to be a successful flow reversal, if natural circulation cooling was sustained without a trip of the power for 30 seconds. For a given set of test conditions, the flow reversal experiment was repeated at increasing power levels until the thermal limit was bracketed within about 0.5 kW.

Appropriate scaling laws were followed in the design of the test loop. However, there were a number of areas where it was not practical to achieve exact similitude between the test and reactor. By expanding the range of variables examined in the tests and with the aid of RELAP5 simulations of the tests and reactor, it has been demonstrated that the differences either do not have a significant effect on the applicability of the results or the test results are conservative. The areas where similitude was not achieved are as follows:

(a) Single channel in test vs. multiple channels in reactor with varying heating rates.

(b) External loop containing centrifugal pumps and check valves in reactor vs. a loop containing a positive displacement pump in test.

(c) Fuel plate in reactor cooled on two sides vs. heated plate(s) cooled on one side in test.

(d) Each fuel element in reactor has inlet tube section which is common to nineteen coolant channels. Test channel has one inlet tube section.

D. Flow Reversal and Dryout Mechanism

Steady state conditions were established at the beginning of each test. The downflow rate was then decreased according to the specified coastdown time. When the downflow rate through the channel had decreased sufficiently, boiling initiated at the bottom of the channel. Evidence of reversal was the appearance of large voids rising in the channel. Other evidence of upflow was the vertical temperature gradient in the heated surface which showed increasing temperatures toward the top of the channel.

The experimental evidence indicates that there are several stages in the flow reversal process. These are: a) initiation of boiling at the bottom of the channel, b) slug formation, and c)

periodic slug expulsion and liquid re-entry. If the liquid fails to re-enter the heated channel periodically then dryout occurs. When a temperature excursion did not occur the lower section of the channel was all liquid and the upper section appeared to be in the churn-turbulent flow regime. When a temperature excursion did occur it generally occurred within a few seconds after the coolant had gone through the transition from downflow to upflow. A temperature excursion typically occurred near the top of the channel and the flow regime appeared to be annular in a large fraction of the channel. This suggested that film dryout is the cause of the temperature excursion and is consistent with the work of Mishima and Ishii [5] who observed that for comparable conditions of mass flow and pressure, the transition from churn to annular flow was the cause of CHF.

E. RELAP5 and Dryout Criterion

In evaluating the RELAP5 simulations of the tests it was found that the calculated plate temperature was not a reliable indicator of dryout. The calculated temperatures tended to be higher than the measured values and there was no consistent trend from test to test. The heat transfer correlations in RELAP5 are based primarily on data developed for rod bundle geometry and high pressure conditions applicable to power reactors. The applicability of these correlations to narrow channel geometry and low pressure conditions existing in the HFBR and test has not been established. Instead an alternative dryout criterion involving the channel void fraction was developed.

The use of void fraction as a dryout criterion was prompted by the visual observations of flow reversal noted above. In order to provide support for the use of RELAP5 for reliable void prediction, comparisons of RELAP5 predictions were made with the prediction of a drift-flux model [6]. The comparisons were made using several steady-state CHF correlations for upflow under conditions of pressure and geometry that were similar to our test conditions. The void fraction calculated by the drift flux model was in good agreement with RELAP5 results. In addition the void fraction near the exit (top) of the channel was calculated to be above 90% by both models. This is consistent with the conclusion that CHF in the tests upon which the correlations were based is due to dryout.

Because of the transient nature of flow reversal, it is not possible to use a steady-state correlation of the type referred to above. In addition, the high void fractions associated with annular flow and dryout under steady-state conditions would not necessarily lead to dryout under cyclic conditions where the heated surface is periodically rewet. The approach taken to characterize the need to maintain a high void condition for a sustained period was to time smooth the void fraction transient predicted by RELAP5 to obtain a running average void fraction. With a suitable smoothing time selected, the maximum value of the time smoothed

void fraction following reversal would be a measure of the potential for dryout.

Sensitivity studies were done to determine the best smoothing time and whether the spatial averaging should cover the full channel or only the upper quadrant where the highest void fractions and temperatures occurred. Although there were not large differences, a two second smoothing time and a full channel spatial average was judged the best. The maximum time smoothed void fraction was calculated from the RELAP5 simulations of the tests. For each test condition two simulations were done. One represented the test power at which no dryout was observed and the other represented a test at a slightly higher power (≈0.5 kW) at which dryout (temperature or voltage trip) occurred. There were 17 sets of tests representing a range of initial water temperature, coastdown times, return path flow impedances, liquid level and include both one sided and two sided heating tests.

For purposes of establishing a conservative criterion, only the no dryout data were used. The sample mean and standard deviation of the maximum time smoothed void fraction for the 17 data points were obtained. The mean was 0.725 and the standard deviation was 11.9%. A 95%/95% one sided tolerance limit of 0.51 was calculated. This limit was established as a conservative dryout threshold in the evaluation of potential reactor accidents using RELAP5.

F. Simulations of Reactor Accidents

A detailed model of the HFBR primary system was constructed. The channel to channel variation and time dependence of heating in the core was accounted for. The primary loop, including the heat exchanger, pumps and valves were explicitly modeled. However where equivalent structures were in parallel such as the 2 parallel loops and 4 flow reversal valves, they were lumped into one equivalent structure. Plant data were used to benchmark the primary pump model and the depressurization of the reactor via the depressurization valve.

There are a number of accident scenarios that lead to a loss of forced flow cooling and flow reversal. The accident selected as limiting is the one that leads to the maximum decay heat at the time the primary flow has coasted down to a point where flow reversal can occur.

A nominal reactor power of 60 MW was assumed in the analysis. The actual power used in the analysis was higher (64.05 MW) to account for uncertainties in the measurement of reactor power (5%) and operational variations in power (± 1 MW). The nominal decay heating was also increased by 22.8% to account for uncertainties in the calculation of decay heating and the helium void effect. Helium voids were not explicitly modeled in the accident analysis.

The helium void correction applied to the decay heating is based on data obtained from the experimental program.

Sensitivity studies were performed to evaluate the effect of changes in the input parameter or of modeling assumptions. These included the following:

a. Non-uniform axial power distribution in core.

b. One flow reversal valve failing to open.

c. Variation in pump coastdown.

d. Channel dimension variations due to manufacturing tolerances.

e. Channel to channel heat transfer via common fuel plate.

f. Common inlet region above fuel channels in each fuel element.

g. Backward flow loss coefficient for the flow reversal valves.

h. Modeling of individual hot channels.

i. Doubling of reactor power (120 MW).

A maximum time smoothed channel void fraction was calculated for the various cases analyzed and compared with the dryout limit of 0.51. For all the 60 MW analyses this parameter was in the range of 0.3 ± 5% which is well below the limit. The 120 MW sensitivity calculation resulted in a void fraction value of 0.5 which is slightly below the limit. Except for the case in which the power was doubled, the sensitivity cases resulted in relatively small changes in the void fraction. The safety of steady-state operation at 120 MW has not been nor needs to be examined. This high power level was assumed only to determine the safety factor for safe flow reversal at 60 MW. For reasons not related to flow reversal (e.g., heat exchanger capacity, reactivity induced power transients), the HFBR cannot be operated at power levels significantly above the nominal value of 60 MW.

G. Conclusion

In applying the void fraction criterion to the RELAP5 analysis of loss of flow accidents in the HFBR, it is concluded that flow reversal can occur without fuel damage at afterheat rates corresponding to reactor power levels in excess of a nominal 60 MW with a margin of at least a factor of two. Similar conclusions can be drawn by examining the test data directly, independent of the RELAP5 analyses. Successful flow reversal occurred in the Columbia tests at power levels that are greater than the decay power in the hottest HFBR channel at the time of flow reversal following 60 MW operation. The test which most closely matches the conditions in

a multichannel core had a thermal limit which is 2.4 times the decay power in the hot channel in the core at the time of flow reversal. If it is unrealistically assumed that the heating rates in all the channels are the same and equal to the hot channel heating rate and all channels reversed simultaneously, the margin is 1.12. These margins conservatively account for analytical and other uncertainties, i.e., the margins would be about 30% larger if these uncertainties were ignored.

THIS PAGE IS BLANK

II. TEST PROGRAM

A. Objective

This section discusses the important aspects of the tests including the objectives, test description and results. More detailed information is given in Appendix A.

The program was designed to capture, as closely as possible, the essential features of the flow reversal transient in the reactor.

1. Scaling to achieve similar thermal-hydraulic responses.

2. Spatial variation of heat generation.

3. Rate of flow coastdown on loss of pumping power.

4. Effect of flow impedance of flow reversal valves.

5. Effect of liquid level.

6. Effect of pressure.

7. Effect of initial water temperature.

8. Effect of helium evolution on depressurization.

Another objective of the test program, separate from the issue of prototypicality, was to provide a means of visualizing the flow reversal process. This was accomplished by designing the test channel with one side heated and one side transparent. Recordings were taken with a video camera. A small number of tests were conducted with both sides of the channel heated.

B. Description

The tests were performed with an electrically heated single channel section representing the core, an orifice representing the flow reversal valves, a variable speed pump to simulate the flow coastdown, and auxiliary piping and equipment to simulate other pertinent structures in the reactor vessel. The test loop was set up to preserve the vertical height of the natural circulation flow path in the HFBR vessel. The heated section was a full-size mockup of a typical channel in a HFBR fuel element. The flow areas of the test loop were scaled to correspond to a typical coolant channel in the HFBR. The top of the upper plenum region was open to the atmosphere. Demineralized water was the working fluid of the test loop.

Figure 2 is a drawing of the test loop used for the first series of tests showing nominal component dimensions. The loop was

modified to extend the range of variables investigated. However, the overall dimension of the loop was unchanged. Figures 3 through 5 are schematics of the various test loop configurations used.

The fuel plates were simulated in the test by 6061 aluminum plates of similar thickness and powered by DC heating. Two separate heater arrangements were used in the experiments. The single-sided arrangement had one heater plate and a transparent LEXAN plate separated by the coolant gap. The double-sided heater had a heater plate on each side of the coolant gap. The cross-sectional view of the single-sided heater is shown in Figure 6. The channel gap was maintained by two spacer rails installed along the side edges of the channel, overlapping the heater plate(s) by ~0.05 inch. The dimensions of the two heated sections are shown in Table 1.

The heated section was powered by a set of direct current generators rated at 250 volts. The low electrical resistance of aluminum resulted in a voltage drop of only ~2 volts across the length of the heater plates. At low voltages the generator output was prone to drift. A ballast was installed in series with the heater plates(s) to raise the total resistance seen by the generator and stabilize the output voltage.

The initial flow through the heated section and the bypass orifice was provided by an eccentric screw pump which has the characteristics of a positive displacement pump. The effect of flow coastdown was created by using a programmable speed controller to vary the rotational speed of the pump motor.

The test loop was instrumented to continuously record water temperatures, heated plate temperatures, flow rates and power (voltage and current) to the heated plate. The instrumentation layout for the various test configurations are shown in Figures 3 to 5.

The plates were protected from overheating during the experiments by two types of power trips - on plate temperature rise and on increase in voltage across the plate. A voltage increase would occur when the plate temperature increased because of the increased plate resistance with temperature. The trip settings on temperature and voltage rise were conservatively set so that the heated plate was not damaged and could be reused in subsequent tests.

A number of parameters were varied in the tests to examine their effects on the thermal limit. In the first series of tests these parameters were rate of flow coastdown, inlet subcooling, water level in the upper plenum, single-sided vs. two-sided heating and bypass ratio (ratio of initial flow through the heated section to initial flow through the bypass path). This ratio is a measure of the flow impedance in flow path which simulates the flow

reversal valves in the reactor. A schematic of the test loop for the first test series is shown in Figure 3.

In the second series of tests the loop was modified to permit simulation of the evolution of helium. In the reactor, helium gas is evolved from solution when the reactor which is normally pressurized with helium to 200 psig, is depressurized. Depressurization occurs in accidents involving loss of coolant. The maximum anticipated void fraction is 15%. Since the test loop was not designed for 200 psig, the helium void effect was achieved in the tests by saturating a volume of water with helium in a separate pressurized tank and injecting the depressurized solution into the test loop. A range of bypass ratios were also examined in this test series. The schematic of the test loop for this test series is shown in Figure 4.

In the last series of tests the test loop was modified to expand the range of one of the parameters investigated, the bypass ratio (see Figure 5). This was done to test the RELAP5 model against a broader data base and to provide a way to simulate the effects of multiple parallel channels in a single channel test. Since all the channels in the core are not heated equally and therefore do not reverse simultaneously, the cooler channels which are in downflow provide a secondary return path in parallel with the flow reversal valve path. The parallel channel simulation is achieved by reducing the flow impedance of this path relative to the test channel which in turn reduced the bypass ratio from a nominal 2:1 to 1:3.4. Another effect related to the presence of multiple parallel channels in the core was examined in this test. While the core is in downflow, the water temperature in the plenum region below the core will represent the average temperature of all the channels rather than the hottest channels. When reversal occurs in a channel the water entering this channel will be at this average temperature. In a single channel test this effect is simulated by injecting unheated water into the region below the test section so that it mixed with the hot water exiting the test section.

As seen in Figure 5, the schematic for the last series of tests, a turbine flowmeter that was in series with the test section in the earlier tests was eliminated and replaced with a magnetic flow meter. It turned out that the pressure loss in the turbine flow meter (0.3 psi at 2 gpm) was substantial in comparison with the test channel pressure drop (≈0.15 psi). This was overlooked and was not recognized until after the first 2 test series were completed and the last test series began. The pressure loss in the magnetic flow meter is relatively low (≈ 0.03 psi) and is comparable to the pressure loss in the reflector region of the reactor.

In each test, steady forced flow conditions were established at a fixed power and a flow rate corresponding to a time in the

reactor loss of flow accident where the primary flow rate has fallen to about 7% of its operating value. The test was then initiated by linearly reducing the pump flow to simulate the final coastdown of the reactor pumps to zero flow. The test was considered to be a successful flow reversal, if natural circulation cooling was sustained without a trip of the power for 30 seconds. For a given set of test conditions, the flow reversal experiment was repeated at increasing power levels until the thermal limit was bracketed within about 0.5 kW.

C. Corrections to Test Section Power

Two heat loss corrections were made to the electrical power delivered to the test section. One is the steady state loss. This was based on a comparison of the measured electrical power to the power obtained from a heat balance using the measured flow rate through the heated channel and the temperature rise across the channel. These measurements were made during the steady state period established at the start of the test. The steady state heat loss was 4% for the one-sided heater and 5% for the two-sided heater.

A transient heat loss occurs during the flow coastdown and reversal period when temperatures are rapidly changing. There are two components to the transient loss. One is the heat loss from the heated aluminum plate to the insulation backing and the other is the loss from the water in the channel to the transparent window. Since temperatures are varying with time during the test, the rate of loss also varies with time. The average rate of loss during the short interval in which flow reversal occurs was considered the appropriate value to use.

The transient heat loss calculations used as input measured temperatures in the test. Based on these calculations [7] an expression that was used to estimate the transient heat loss as a function of power to the test section was developed.

$$THL = 11.55 - 0.45\ P,\% \quad \text{(Single-sided heater)}$$
$$THL = 12.26 - 0.54\ P,\% \quad \text{(Double-sided heater)}$$

The transient heat loss (THL) is given as a % of the power, P (kW).

In estimating the total heat loss from the test section, the transient loss is not added to the steady state loss. The higher of the two values is used.

D. Test Results

Based on observation of the flow reversal tests, the reversal process can conceptually be divided into four stages. The progression of a flow reversal transient is depicted in Figure 7.

The four stages of a flow reversal transient are:

1. Coastdown Stage

   As the flow is coasting down in the heated channel, the coolant temperature gradually increases to the point when steam voids begin to appear in the channel.

2. Vapor Generation Stage

   The steam voids continue to grow and start to move in an upward direction.

3. Oscillatory Flow Stage

   This is a transitional stage before a more stable natural circulation flow is established. This stage is characterized by a cyclic behavior in which steam voids are first generated followed by reflood from the bottom. The expulsion of coolant due to steam generation and the refilling of the coolant channel by bottom reflood are visible through the oscillation of the boiling boundary in the heated section. The upper portion of the channel is in the churn-turbulent flow regime. The sequence of expulsion and reflood generally lasts for a few cycles.

4. Natural Circulation Flow Stage

   Natural circulation flow is established in the heated section and there is no overheating of the channel walls.

In the tests, all safe flow reversal cases eventually went through the four stages described above. For those cases which ended in a power trip the rapid generation of steam in the heated section impeded the return of the liquid during the oscillatory flow stage. In successive reflood cycles less and less liquid entered the heated section. A power trip occurred as a substantial portion of the channel stayed in a voided state for more than a couple of seconds. The large voids suggests that the presence of annular flow was the cause of the temperature excursion and trip. In a couple of cases that were conducted at higher powers, a power trip occurred before the flow reversal.

Detailed results of all the tests conducted are presented in the reports by Columbia University [8]. These reports include a tabulation of lower power tests in addition to the threshold power for a given set of test conditions. The Columbia tabulation has been consolidated for presentation here by eliminating the lower power tests and only including two test results for each set of conditions. One is the highest power level at which successful flow reversal occurred and the other is the power level at which a trip of the power occurred.

The results for the first series of tests are shown in Tables 2.1 and 2.2. The helium evolution tests results are shown in Table 2.3 and the final test series results are shown in Table 2.4. Note that while the first test series used both single sided and two sided heating arrangements, the remaining tests were all performed with a single sided heater. Also note that the last test series most closely matched reactor conditions because of the loop modification which eliminated the high flow impedance of the turbine flow water.

Several observations can be made from the test results.

1. Depending on the test conditions, the threshold power (highest power for successful flow reversal varied from 7 to 19 kW.

2. The power limit increases with decreasing coolant inlet temperature.

3. The power limit increases with shorter coastdown time. The increase in the power limit from the base case coastdown time of 40 seconds to the pump trip case (≈1.5 seconds) was about 50%.

4. The power limit increases with an decrease in flow impedance of bypass paths. The power limit increased about 50% when the bypass ratio was changed from the base case value of 2:1 to 1:3.4.

5. The highest threshold power (19 kW) occurred in the pump trip case with low impedance in the return path. This power is about three times the power in the hottest core channel during potential accidents. The true threshold power was not reached for these test conditions. When the power was raised to 21 kW the power trip occurred while the power was being increased and before the pump was shutoff.

6. Two-sided heating results in a slightly higher power limit than one-sided heating.

7. The height of water in the upper plenum has a negligible effect on the power limit.

8. The reduction in the power limit due to helium voids will not exceed 10%.

9. The results are reproducible.

There are qualitative explanations for these results. Flow reversal is generally initiated prior to the end of the coastdown of the pump. With the flow still present in the bypass path, the pressure drop across the bypass resistance acts in opposition to the thermal buoyancy which is driving the reversal. If this

opposing force is large enough and lasts long enough dryout will occur. Thus a shorter coastdown time and a smaller impedance in the bypass path will increase the dryout power. The highest dryout power measured in the tests was for the case of a pump trip with low impedance in the bypass path. For the pump trip tests the coastdown time is short (≈ 1.5 seconds) so that the flow impedance which is already small disappears quickly.

A lower water temperature at the inlet to the channel will delay the onset of flow reversal so that reversal occurs later in the coastdown period. The pump flow and bypass flow rates are lower at this time and therefore the flow resistance in the bypass path is lower.

The two-sided heating vs. one-sided heating results indicate that the thermodynamic condition of the fluid as determined by the power input is much more important than local heat flux in determining dryout.

The difference in liquid level would be expected to affect the dryout power because of the difference in saturation temperature and vapor density. The static pressure in the channel at the two liquid levels are 18.7 and 23.2 psia. Evidently the differences in saturation properties are not large enough to be distinguished by the tests which can only bracket the dryout power within 5-10%.

The presence of helium voids would be expected to affect the flow reversal process through its effect on hydraulics (flow is two phase before boiling begins) and because it adds to the voids produced by steam. However the void fraction due to helium is only 15% and the relatively high rate of steam generated will rapidly displace the helium in the heated channel.

THIS PAGE IS BLANK

III. RELAP5 ANALYSIS OF TESTS AND DEVELOPMENT OF DRYOUT CRITERION

More detailed information about the code and the test comparisons is given in Appendix B.

A. Comparison of Tests and RELAP5 Simulations

RELAP5 is a system thermal-hydraulics code developed at the Idaho National Engineering Laboratory (INEL) for the analysis of power reactors. Recent updates to RELAP5 has made the code more applicable to DOE research reactors. The version of RELAP5 used in the simulation of the flow reversal tests is mod 3.1.1.1 released to BNL by INEL in July 1994. During the development of the RELAP5 model for the flow reversal tests, it was observed that high steam condensation rates were calculated at the steam-water interface resulting in unrealistic simulation of the tests. The interfacial heat transfer coefficient on the liquid side was modified to reflect the conditions observed during the actual tests. In effect, the coefficients are reduced for the bubbly subcooled liquid and the slug subcooled liquid flow regimes.

RELAP5 simulations of selected tests were generated for detailed comparison with the test data. In summary, the RELAP5 simulations of the flow reversal tests are found to reproduce the general aspects of the observed behavior of the tests. These include the timing of the onset of flow reversal, the period of flow and void oscillations, and the extensive voiding that was observed visually prior to dryout. In addition, comparisons have been made between RELAP5 predictions and the initial steady-state data from the flow reversal tests. Two parameters from the test data are available for comparison with the initial conditions predicted by RELAP5. They are the channel pressure drop and the water temperature rise across the heated section. Agreement was found to be very good for both of these parameters (see Appendix B, Section D for the validation of RELAP5).

One parameter where RELAP5 did not reliably reproduce the test data was the heated plate temperature. The calculated temperatures tended to be higher than the measured values and there was no consistent trend from test to test. The heat transfer correlations in RELAP5 are based primarily on data developed for rod bundle and tube geometries and high pressure conditions applicable to power reactors. The accuracy of applying the existing heat transfer correlations to narrow channel geometry and low pressure conditions has not been established. An alternative dryout criterion is developed in Section C which is based on the use of channel void fraction.

B. Comparison of RELAP5 with Drift-Flux Model

Further validation of RELAP5 was obtained by performing comparisons with a drift-flux based numerical model. First a

comparison was made for the prediction of steady state void fraction. These calculations were done for a range of coolant flow rates and channel powers which corresponded to critical heat fluxes (CHF) given by three existing correlations developed specifically for narrow channel geometry. The results show good agreement between RELAP5 and the drift-flux model [6]. Comparisons were made of the predictions by RELAP5 and the drift-flux model of natural circulation flow after flow reversal [9]. Excellent agreement was obtained. The drift-flux model was not in good agreement with RELAP5 in the prediction of the flow transient phase from downflow to upflow. The drift-flux model had been simplified by assuming that the flow in the heated channel is axially uniform and therefore could not be expected to predict this transient phase accurately.

C. Channel Void Fraction as Dryout Criterion

There are several reasons for selecting void fraction as a basis for a dryout criterion. First it was observed in the tests that when a temperature excursion was seen, it occurred after the flow had reversed. Evidence of reversal was the appearance of large void regions rising in the channel. Other evidence of upflow was that a thermocouple at the top of the channel would initiate the trip of the channel power by exhibiting a rapid rise in temperature. In upflow in a uniformly heated channel, the highest temperatures would occur at the top of the channel.

The flow behavior after reversal was cyclic with a period of steam generation (voiding) followed by refilling of the coolant channel by bottom reflood. When a temperature excursion did <u>not</u> occur the lower section of the channel was all liquid and the upper section appeared to be in the churn-turbulent flow regime. When a temperature excursion did occur it typically occurred, as noted above, near the top of the channel and the flow regime appeared to be annular in a large fraction of the channel. This suggested that film dryout is the cause of the temperature excursion and is consistent with the work of Mishima and Ishii [5] who observed that for comparable conditions of mass flow and pressure, the transition from churn to annular flow was the cause of CHF. For the pressure and flow conditions of interest this transition occurs at a high void fraction - about 0.8 [5, 10].

Further evidence that the condition of the coolant rather than the heat flux determines when a temperature excursion occurs is provided by a comparison of the one-sided heating tests with the two-sided heating tests. The channel powers at which the temperature excursion occurred in the two-sided tests were only slightly higher than in the one-sided tests while the heat flux in the one-sided tests were about twice as high.

As noted earlier, the use of RELAP5 for reliable void prediction is supported by comparisons of RELAP5 and drift-flux

model predictions of channel void fractions using several steady-state CHF correlations for upflow under conditions of pressure and geometry similar to our test conditions. The void fraction near the exit (top) of the channel was calculated to be above 90% in both models. This is consistent with the conclusion that the CHF in the tests upon which the correlations were based is due to dryout.

Because of the transient nature of flow reversal, it is not possible to use a steady-state correlation of the type referred to above. In addition, the high void fractions associated with annular flow and dryout under steady-state conditions would not necessarily lead to dryout under cyclic conditions where the heated surface is periodically rewet. The approach taken to characterize the need to maintain a high void condition for a sustained period was to time smooth the void fraction transient predicted by RELAP5 to obtain a running average void fraction. With a suitable smoothing time selected, the maximum value of the time smoothed void fraction following reversal would be a measure of the potential for dryout.

A value of the maximum time smoothed void fraction was calculated for each test which bracketed the dryout threshold. The appropriate smoothing time and the region of the channel that should be used in the averaging calculation was obtained semi-empirically. With respect to the choice of smoothing times, several times were considered ranging from 1 to 4 seconds. This range of values was considered for a number of reasons. First it was visually observed that the time between voiding and reflood cycles following reversal was about 2 seconds. Typically if dryout occurred it took place within one to two voiding and reflood cycles. Furthermore, a fast Fourier transform analysis (FFT) of the test data showed a dominant period of 1-2 seconds [11]. Finally the RELAP5 simulations of the test exhibited an approximately two second period.

With respect to the issue of what fraction of the channel should be considered in this averaging process two options were selected. In one only the top quarter of the channel was used and in the other a full channel average was obtained. For all the RELAP5 simulations, maximum time smoothed void fractions were obtained for the following cases:

Spatial Average	Smoothing Time
Full Channel	1, 2, 3, 4 seconds
Upper Quarter	1, 2, 3, 4 seconds

For each averaging scheme (spatial and time) a mean ($\bar{v}$) and standard deviation (s.d.) of the maximum time smoothed void fraction were obtained for all the test simulations.

A quantitative criterion was used to determine if there was a "best" averaging scheme. The scheme with the smallest standard deviation in void fraction is not necessarily the best. The best scheme is one that will result in the smallest uncertainty in the prediction of the channel power at dryout. The sensitivity of the void fraction to channel power will vary with the averaging scheme used. This sensitivity can be quantified by using the results of the RELAP5 simulations for the dryout and no dryout tests at the same test conditions. Since the tests in which dryout occurred were conducted at a higher power than the no dryout tests, the ratio of the percent change in maximum time smoothed void fraction to percent change in power can be calculated. An average value of this ratio for all the tests in which the dryout and no dryout powers were measured is calculated. This ratio is defined as $\Delta V/\Delta P$. A measure of the uncertainty in the predictions of channel power is obtained by dividing the standard deviation (s.d.) calculated for the scheme by the value of $\Delta V/\Delta P$ for that scheme. The smaller the value of this parameter the smaller is the uncertainty.

A comparison of the parameter values for the eight averaging schemes indicated that the full channel spatial averages were generally better than the quarter channel schemes. Among the full channel schemes, the 1 second smoothing time was inferior to the 2, 3 and 4 second schemes which were close in value. Since the criterion could not distinguish between the remaining smoothing times (2, 3 and 4 seconds) we selected 2 seconds because it corresponded to the voiding and reflood cycle time experimentally observed and predicted by RELAP5.

The maximum 2 second time averaged void fraction for each of the test simulations is shown in Table 3. As expected, the value for no dryout is lower than the dryout value for each test condition. For purposes of establishing a conservative criterion for the dryout threshold only the no dryout data are used. The sample mean and standard deviation for the 17 points are calculated as $x = 0.725$ and $s = 11.9\%$. A 95%/95% one sided tolerance limit of 0.51 is calculated.

IV. SIMULATIONS OF REACTOR ACCIDENTS

More detailed information on reactor accident simulations is given in Appendix C.

A. RELAP5 Model of Reactor

In the core region, the 532 channels are divided into two channel types, hot and average. The model has 3 hot channel groups representing the different channel dimensions (Numbers 2, 3 and 4 in the fuel element). There is more than one potentially hot channel because of the possibility that a narrower channel with a slightly lower heating rate will be more limiting than a wider channel with a higher heating rate. The average channel type contains geometrically identical average channels. This type is divided into 7 groups, each with a different heating rate. Within these 7 groups, group No. 7 has the highest heating per channel and group No. 1 has the lowest. Each of the 3 hot channel groups contain 14 channels and each of the 7 average channel groups contain 70 channels.

Fission and decay heat are modeled as a volumetric source uniformly distributed in the fuel cermet. Cladding is included in the model. In the base case calculation there is no axial or spanwise variation. The effect of axial variations are examined in a separate calculation. The time dependence of power density following shutdown is modeled. The time dependent shutdown power for the highest powered channel is shown in Figure 10 [12]. The shape of the power vs. time curve is similar for other channel groups.

The base case power at a nominal 60 MW is increased in the RELAP5 calculation to 64.05 MW to account for operational variations in reactor power (± 1 MW) and power measurement uncertainty (5%). An additional factor of 1.23 is applied to the decay power to account for the uncertainty in the calculation of decay power and the helium evolution effect (10%) which could not be explicitly included in the model. The 10% helium evolution effect is based on the tests which showed that the effect will reduce the power by no more than 10%.

The other important structures in the primary system were explicitly modeled. However where equivalent structures were in parallel such as the 2 parallel loops and the 4 flow reversal valves, they were lumped into one equivalent structure. In the case of the flow reversal valves an additional calculation was done with one of the 4 valves in a failed state. The shutdown pumps and pony motors were assumed not to operate.

Plant data were used to benchmark the primary pump model and the depressurization of the reactor via the valve HCe-102. Sensitivity studies were done to examine the effect of different

pump coastdowns. Trip setting used were obtained from the 60 MW accident analysis.

B. Analysis of Reactor Accidents

There are two types of potential accident scenarios which could lead to loss of forced flow cooling and flow reversal. One is a loss of cover gas pressure with the shutdown and pony motors not available. The other type is a LOCA event which results in the liquid level dropping below the 197 inch level at which pump trip occurs. In these accidents a reactor trip occurs first and is followed by a trip of the primary pumps. The time interval between these 2 events determines the decay power at the time flow reversal occurs. The shorter is this interval, the higher is the decay power. The accident scenario which has the shortest interval between reactor trip and pump trip is a cover gas depressurization in which the depressurization is caused by a breach in the cover gas system. The breach size is a circular opening 1.39 in^2 in area and is based on the design basis break in the 60 MW FSAR. In this accident, both reactor and pump trips occur within 2 seconds of accident initiation and the reactor is completely depressurized in 14 seconds.

Several variations of the cover gas depressurization accident were performed using RELAP5 to determine the effect of changes in some of the input parameters. The base case will be discussed in some detail first and the results of the other cases will then be summarized. More detailed results are given in Appendix C.

The initial power for the base case was 64.05 MW and that corresponded to a nominal reactor power of 60 MW. Both the reactor trip and the primary pump trip were activated by the low pressure trip setpoints for the cover gas. Figure 11 shows the rapid depressurization of the cover gas following the break initiation at time zero.

The primary pump coastdown began in less than one second after the reactor trip. Figure 12 shows the primary flow rate of the primary pump as a function of time.

The junction mass flow rates at the top and bottom of the heated section of the three hot channel groups are shown in Figures 13 and 14 respectively. In these figures the positive flow direction was downward. It is seen that flow reversal occurs in each channel periodically for the duration of the calculation (≈100 sec.). The first flow reversal in the three hot channel groups occurred at about the same time (≈47 sec. after reactor trip). Among the three hot channel groups, the first to go through flow reversal was group number 3 which had the lowest power of the hot channels but the narrowest channel gap (0.095 inches).

The periodic flow behavior also occurs in the seven average channel groups except that the magnitude of the flow fluctuations is smaller than for the hot channel groups and the first flow reversal occurs later.

The state of the coolant in the channel is characterized by the channel void fraction which is shown for several channel groups in Figure 15. The periodic behavior of the channel void fraction can be characterized by two stages, a boiling stage and a heat up stage. When the coolant reached the boiling condition, the generation of steam voids in a channel resulted in a rapid increase in the channel void fraction. Flow began to enter the channel because of the density difference between the coolant channel and the reflector region. The coolant quickly condensed or displaced the steam in the channel and cooled down the heated wall. When the channel was occupied by single-phase liquid, the mass flow was reduced and the coolant in the channel began to heat up to boiling again. The flow in the heated channel was seen to alternate between two-phase and single-phase conditions.

The 2 second time averaged channel void fraction as a function of time is shown in Figures 16 and 17 for a hot and average channel group. The channel groups selected contain the highest value of the 2 second void fraction. The maximum value is 0.28 for the hot channel group and 0.31 for the average channel group. These figures are typical of all the groups except for the lowest powered of the average groups, group Nos. 1 and 2. In these the time averaged void fractions are less than 0.02.

In the case of the HFBR with variable heating rates in the channels, flow reversal does not occur simultaneously in all channels. With some of the channels in upflow while others in downflow, the coolant from the downflow channels becomes an extra source for feeding the upflow channels. This extra source supplements the core bypass flow and the flow through the flow reversal valves. The existence of downflow channels is similar in effect to an increase in the bypass orifice used in the single-channel flow reversal test. The apparent increase in the bypass flow area in the HFBR is the principal cause of a lower channel void fraction calculated for the reactor as compared to the single-channel test.

Another aspect of the flow reversal in the reactor is the effect flow reversal has on the rate at which the flow rate in the primary system decays. The thermal buoyancy generated in the core as the coolant temperature rises and as channels begin to reverse acts as an increased flow resistance and will cause the flow generated by the centrifugal pump, as it coastdown, to fall more rapidly than it otherwise would. Thus a single channel test with a rapid flow coastdown is more representative of reactor conditions.

It is of interest to compare the relatively low channel void fraction calculated for the multichannel reactor (0.31) with the single channel test simulations with the object of determining what single channel test conditions most closely approximated the multichannel reactor core. Previous discussions suggest that a single channel test with a rapid coastdown and a large bypass can be considered a good representation of flow reversal in a multichannel core. The test that most closely approximates these conditions is Test No. B081795C in Table 3. It has a bypass ratio of 1:3.4:0.6, a short coastdown time (≈2 sec) and a power of 19 kW. The two second void fraction calculated by RELAP5 is shown in Figure 18. Also shown in this figure is the RELAP5 calculation of the two second void fraction under the assumption that the test conditions were the same but the channel power was 7.8 kW instead of 19 kW. Note that a test at this low power was not actually conducted under these conditions. The lowest power in this test series was 14 kW. In any event it is seen from Figure 18 that the maximum two second void fraction for the 7.8 kW case is 0.32 which is almost identical to the two second void fraction computed for the identically powered hot channel in the reactor. This comparison supports the applicability of the previously discussed single channel test conditions to the reactor.

In order to provide added confidence in the ability of the RELAP5 code to predict flow reversal in a multi-channel configuration another simpler numerical model based on the drift-flux formula was developed [15]. Both codes were used to simulate flow reversal in a simplified model of the reactor core which had the same ten channel groups and channel geometry as the full reactor model. The codes predicted similar flow behavior and fairly good agreement in the timing of flow reversal was obtained.

C. Sensitivity Study

A number of RELAP5 analyses have been performed to evaluate the effect of changes in the input parameter or of modeling assumptions. These include the following:

1. Non-uniform axial power distribution in the core.
2. Doubling of reactor power (120 MW nominal).
3. Closure of one flow reversal valve.
4. Variation in the duration of pump coastdown.
5. Modeling of individual hot channels in a fuel element.
6. Common inlet region above fuel channels in each fuel element.
7. Two-sided heat transfer from a fuel plate.

8. Channel dimension variations due to manufacturing tolerances.

9. Different pressure loss coefficients for the flow reversal valves in the forward and backward flow direction.

A maximum time averaged channel void fraction was calculated for the various sensitivity cases and compared with the base case value. The comparison shows that except for the doubling of reactor power, the base case value is either comparable or conservative with respect to the sensitivity cases. Details of the sensitivity study are given in Appendix C.

THIS PAGE IS BLANK

V. DISCUSSION OF SIMILARITY BETWEEN FLOW REVERSAL TEST AND THE HFBR

A. Introduction

The application of the flow reversal test data to the HFBR requires an understanding of the similarities and differences between the test and the reactor. The purpose of this section is to discuss the similitude of the test loop with respect to the reactor. For areas that do not have similitude, it is demonstrated that either the consequence is negligible or the test results are conservative.

B. The Three Time Phases of Flow Reversal

Flow reversal in the HFBR can be divided into three time phases, namely the coastdown phase, the reversal phase, and the natural circulation phase. The flow transient starts in the coastdown phase which represents the decay of the primary flow as a result of the slowing down of the primary pumps. The reversal phase begins when the coolant reverses flow direction in the core. Flow reversal is a form of flow excursion and it occurs in a coolant channel with initial downflow when the buoyancy force exceeds the frictional force exerted on the coolant. The mechanism of flow excursion depends only on steady-state laws. Hence the inertia of the coolant flow and the type of pump used to drive flow through the reactor do not matter up to the point of flow reversal. During the reversal phase there is a redistribution of coolant flow from the reversed channel(s) to the bypass flow paths and the other coolant channels which are still in downflow. The transient will reach the natural circulation phase more quickly if there is less resistance to the redistribution of the coolant flow. The driving force behind the redistribution of flow is the buoyancy force generated in the core region. The amount of voiding in the core depends on the buoyancy force required to overcome the resistance to the redistribution of flow. The two factors that influence the magnitude of the resistance are the amount of forced downflow and the size of the bypass flow paths to accommodate the redistributed flow. A faster coastdown and/or a bigger bypass would then imply a lesser resistance to the flow reversal. Once the flow transient has passed through the reversal phase without experiencing a channel dryout event, it reaches the natural circulation phase. By this time the forced downflow has subsided and natural circulation cooling removes the decay heat from the reactor core.

The dominant thermal-hydraulic processes in different time phases of the flow reversal transient are:

Coastdown phase - forced flow cooling

Reversal phase - flow excursion, buoyancy driven flow, and flow distribution.

Natural circulation phase - natural circulation cooling

For a given power level and channel geometry, the two principal parameters that affect the thermal-hydraulic processes in a flow reversal transient are the rate of flow coastdown and the flow resistance of the bypass flow path. Maintenance of similitude with the reactor for these two parameters was an important consideration in the design of the test loop. The following paragraphs describe how the test loop approximates the reactor system and the consequences of the approximations.

C. Flow Loops in the Reactor System

There are two flow loops in the reactor system, an external loop and an internal loop. Under normal operation, the external loop constitutes the flow path of the primary coolant which cools the reactor core. The internal loop forms a closed circuit through the reactor core and the reflector region via the bypass flow path. The bypass flow path has two branches. One of the branches is always open and it represents the fraction of primary flow that cools the control rods or leaks around the fuel elements. The other branch represents the flow path through the flow reversal valves. Normally the pressure drop developed across the core maintains the flow reversal valves in the closed position. They start to open when the core pressure drop falls below 3 psi. The core pressure drop is a function of the primary flow rate. After a pump trip the primary flow first decays rapidly at an exponential rate and then slows down to a roughly linear decay rate. Based on the decay heat of a 60 MW reactor and the coastdown characteristics of the primary flow, flow reversal would not occur until the primary flow rate is sufficiently low that the flow reversal valves are essentially fully open. At this reduced flow rate the rate of flow decay is roughly linear and the inertia of the external loop has little influence on the distribution of the primary flow between the core flow and the bypass flow (via two branches). Since the early stage of the primary flow decay has little bearing on the flow reversal transient, it is then possible to skip directly to the later stage and track the flow transient from a time when the flow reversal valves are fully open. It is then also appropriate to use a linear flow coastdown to represent the primary flow decay.

There is a check valve in the external loop of the reactor system and so once the primary flow has subsided, the external loop will have little interaction with the internal loop. During the reversal phase of the transient the pump head produced by the centrifugal pumps in the external loop may impede the flow reversal by forcing flow into the reactor core. However at reduced flow rate this pump head is easily overcome by the buoyancy force

generated in the reactor core. Hence the external loop will not present a significant impediment to flow reversal. During the reversal phase the buoyancy force generated in the reactor core acts to oppose the flow in the external loop and at the same time promotes closed loop natural circulation in the internal loop. Because of the opposition by the buoyancy force the primary flow in the external loop will decay more rapidly than it would if buoyancy was not present. This leads to the conclusion that if the feedback effect of the buoyancy force on the pump flow was not present, flow reversal will become more difficult. In the flow reversal test, a screw pump which had the characteristics of a positive displacement pump provided the flow in the external loop. The linear flow decay was simulated by varying the speed of the pump motor. The use of a flow boundary condition (i.e., imposing flow driven by a positive displacement pump) to represent the external loop is conservative because there is no feedback mechanism for the buoyancy force to affect the forced flow. The beneficial effect of the buoyancy feedback has been verified by comparing the results of two RELAP5 simulations [13]. The first was a RELAP5 simulation of the flow reversal test with a screw pump (positive displacement pump) driving the forced flow. The second simulation replaced the screw pump with a centrifugal pump that had the same performance characteristics as the primary pump in the reactor. The rate of linear flow coastdown in the first case was adjusted such that flow reversal occurred at the same time in the two RELAP5 simulations which had identical initial conditions. The calculated maximum two second time averaged void fraction was 0.811 for the screw pump case and 0.764 for the centrifugal pump case. A higher void fraction in the case of the screw pump indicates that a bigger buoyancy force is required to achieve flow reversal. This confirms the argument that the flow boundary condition that existed in the actual flow reversal test imposed a more restrictive environment on the reversing flow than the pressure boundary condition that corresponded to a centrifugal pump. It is then conservative to apply the flow reversal test data to the reactor because the test condition is more restrictive to flow reversal than the condition that exists in the reactor.

D. Test Loop Representation of the HFBR

The flow reversal test loop was a full height representation of the internal loop of the reactor. The test used a single heated rectangular channel to represent the core of the reactor. The geometry of the heated channel was similar to an average coolant channel in the reactor. In sizing the rest of the test loop a uniform reactor core was assumed, i.e., all the coolant channels were identical in size and power [14]. As a result of this scaling assumption, the flow reversal test represents a conservative limiting condition for flow reversal in which all coolant channels reverse simultaneously in the reactor. In the real situation because of varying channel gap and heating rate when the first flow reversal occurs in the reactor most of the cooler channels will

still be in downflow. The cooler channels in effect provide additional bypass flow paths to accommodate the coolant diverted from the reversing channels and thus reducing the resistance to the establishment of natural circulation flow. One bypass flow path with fixed flow area was used in the test loop to represent the two branches of the bypass flow path in the reactor. The scaling of the test loop preserved the similitude in loop inertia and loop resistance. The relative flow resistance between the reactor core and the bypass flow path was preserved in the test loop by adjusting the resistance in the bypass flow path. The adjustment was to achieve in both the test and the reactor the same initial flow split between the heated section (core region) and the unheated section (bypass flow path). Since the heated sections in the reactor and the test loop have similar flow resistance, satisfying the initial flow split also implies the preservation of similitude in loop resistance. Assuming the four flow reversal valves are fully open the initial flow split ratio was determined to be 2:1 (core to bypass) which became the flow split ratio for the base case test condition [14]. The 2:1 ratio represents the most limiting condition for flow reversal in the reactor because it assumes flow reversal occurring simultaneously in all channels. An effective flow split ratio for the reactor can be estimated by including the coolant channels still in downflow as part of the bypass flow path. Based on a RELAP5 analysis of the reactor using multiple channel groups of varying power levels to model the core region, a conservative effective flow split ratio of 1:3.4 was obtained (see Appendix C). In the last series of tests, the test loop was modified to provide a flow split of 1:3.4 and a flow reversal power limit was determined for this more realistic flow ratio.

In applying the test results to determine a power limit for the reactor, the power to the test section is conservatively assumed to correspond to the highest powered coolant channel in the reactor. The correspondence of test section power to hot channel power contributes to yet another conservatism in the test data, namely a higher temperature in the lower plenum of the test loop prior to flow reversal than in the reactor. It has been shown by both test and RELAP5 analysis that a lower temperature in the lower plenum led to a higher power limit for flow reversal. Since the coolant temperature in the lower plenum of the reactor corresponds to the average power and not the hot channel power as in the case of the test, the power limit for the hottest channel in the reactor is expected to be higher than the measured value in the test.

In the natural circulation phase of the test, the coolant in the heated section was predominately in the churn-turbulent flow regime. The observed oscillation period for the natural circulation flow was about one to two seconds. A fast Fourier transform (FFT) of the test data showed oscillation periods in the one to two second range [11]. Most of the RELAP5 simulations of the tests predicted an oscillation period of about two seconds.

The oscillation period predicted by RELAP5 for a similar transient in the reactor was four to five seconds [12]. The only difference between the RELAP5 model of the test and the reactor was that in the case of the reactor, there were ten coolant channel groups representing the core (only one heated channel in the test). Additional analyses were done to study the cause of the difference in the oscillation period [15]. In one case, a RELAP5 model was created to represent the whole reactor core by uniform coolant channels, similar to the condition assumed in the scaling analysis of the test loop. The case of a uniform core gave an oscillation period of approximately two seconds which agreed with the period predicted for the test loop. This confirms that the application of the scaling laws was correct in the design of the test loop. A second analysis involved the simulation of flow reversal in a multi-channel core (same ten channel groups as in the RELAP5 model) using a drift-flux model. The drift-flux model of the reactor core predicted an oscillation period of about four seconds which agreed well with the RELAP5 prediction. It is then concluded that the flow oscillation and the corresponding period predicted by RELAP5 in a multi-channel core are due to the dynamics of multiple coolant channels and not because of numerical instability.

The HFBR core consists of twenty eight fuel elements. Each element has an unheated inlet tube section shared by nineteen coolant channels. There are eighteen plates in a fuel element. Each fuel plate is cooled on both sides by coolant flowing in adjacent coolant channels. The representation of the reactor core by a single heated channel in the test differed somewhat from the configuration of a fuel element. Using only one heated channel in the test, it was unable to simulate the condition of a shared inlet tube section. Also it was not possible to simulate the transfer of heat from one fuel plate to two adjacent coolant channels. However it has been shown by way of RELAP5 analyses [16] that the test configuration yielded results that were conservative in comparison with those obtained from a model which matched the configuration of a fuel element.

Most of the flow reversal tests were conducted with heating on one side of the heated section only. For the few tests conducted with two-sided heating the power limit was about 10% higher than the corresponding value for the single-sided heating. The test result indicates that the thermal limit for flow reversal is not primarily a function of local parameters, like the wall heat flux, but a function of the channel power. This supports the use of a global variable, in this case, the channel averaged void fraction as a success criterion for safe flow reversal.

In addition to satisfying the similitudes in loop inertia and loop resistance, the prototypicality of the flow reversal test is assured by,

(a) Use of similar coolant - demineralized domestic water in the

test and heavy water in the reactor.

(b) Similar thermal state in the test and the reactor prior to flow reversal.

(c) Same material for the heated wall, Al-6061.

(d) Same wall thickness.

(e) Similar channel geometry in height, width and gap.

(f) Similar power to volume ratio.

It follows from the discussions above that the ratio π_{Gr} of the buoyancy over frictional forces [17] is similar for the test and the reactor where,

$$\pi_{Gr} = \frac{g\,\rho_o^2\,\beta_T\,H\,\dot{Q}_o}{C_p\,W_o^3 \sum_{loop} \frac{K + f\,L/d}{A^2}}$$

The ratio π_{Gr} characterizes the natural circulation flow in the internal loop of the reactor. Furthermore, the dynamic response time, t_d (characterizing the time for flow reversal), the fluid residence time, t_r (characterizing the time for fluid heatup), and the thermal response time, t_{th} are similar for the test and the reactor, where

$$t_d = \frac{\rho_o \sum_{loop} L/A}{W_o \sum_{loop} \frac{K + f\,L/A}{A^2}}$$

$$t_r = \frac{\rho_o\,V}{W_o}$$

and,

$$t_{th} = \frac{(M\,C_p)_{fuel}}{A_{fuel}\,h_c}$$

In summary, the heated channel of the test and the coolant channels in the reactor are expected to have similar heat transfer and fluid flow characteristics. Therefore the flow reversal test results are directly applicable to the HFBR.

THIS PAGE IS BLANK

VI. CONCLUSION

A. Summary

It is concluded that if flow reversal were to occur due to a loss of coolant accident while operating at 60 MW (nominal), the transient would occur without fuel damage. The margin to the onset of fuel damage is substantial and can be calculated in a number of ways. Numerical values for these margins presented as "safety factors" are listed below. These factors should be interpreted as a number by which the 60 MW decay heat needs to be multiplied to reach the fuel damage threshold. It should be recognized that, for reasons unrelated to the flow reversal issue, the HFBR is not designed to operate above 60 MW. The safety factor conservatively accounts for analytical uncertainties; i.e. the factor would be larger if the uncertainties were ignored.

1. Based on application of 2 second time averaged void fraction: >2.0.

2. Based on test results only: 1.12-2.4 (see discussion below).

B. Discussion

The following uncertainties are included in the safety factor estimate.

1. Operational variations in reactor power: (± 1 MW) 1.67%
2. Reactor power measurement: 5%
3. Decay power calculation: 11.6%
4. Helium void fraction effect: 10%

The uncertainty in the measurement of the power to the test section is insignificant (0.5%). Other uncertainties in the test have been conservatively accounted for in the RELAP5 modeling. The four uncertainties listed above are combined multiplicatively rather than statistically. The combined factor due to uncertainties is therefore 1.31.

The safety factor of >2.0 based on the analysis for the reactor accident and applying the two second channel void fraction criterion was calculated as follows.

A RELAP5 simulation of a reactor accident with an initial power of 157.26 MW (Section IV.C.2) resulted in a maximum two second channel void fraction of 0.5. A slightly higher reactor power would be required to reach the 0.51 critical void fraction value. The safety factor is therefore greater than 157.26/(60 x 1.31) = 2.0.

The safety factor developed from the test data independent of the void fraction criterion depends on a judgement as to the appropriate test result to compare with reactor conditions. A conservative factor is obtained by using the test results for base case conditions (130°F inlet temperature, 2:1 bypass ratio, 40 second coastdown time). The power limit for this case is 8.7 kW (Table 3, Reference test no. B081395E). This is compared with the decay power input to the hottest channel in the core at the time of reversal (47 seconds). The decay power, 7.8 kW, includes all the uncertainties listed above. The safety factor for this case is calculated as 8.7/7.8 = 1.12. Note that this represents an unrealistically low value since it would apply to a reactor in which all the channels in the core had a heating rate equal to the hottest channel and all the channels reversed simultaneously.

A safety factor which is considered to be more realistic can be obtained by using a test result which is based on conditions more representative of the multi-channel core. Since the heating rates in the core channels vary, flow reversal will not occur in all channels at the same time. As explained in Section IVB, the hottest channels, which reverse first, are supplied with coolant not only from the flow reversal valves but also from channels still in downflow. A second effect that needs to be considered is that the primary pump flow rate will fall very rapidly at the time of flow reversal (Figure 12). The rapid flow reduction is caused by the increased buoyancy head that the centrifugal pump "sees" as the water in the core heats up. The test with a 40 second coastdown and a positive displacement pump will not represent this condition. Thus the test condition that most closely approximates reactor conditions is the test with a small bypass ratio and a rapid flow coastdown (Table 3, Reference test no. B081795C). The thermal limit for this case is 19 kW and the safety factor is 2.43 (19/7.8).

References:

[1] Gambill, W.R. and Bundy, R.D., 1960, "Burnout Heat Fluxes for Low-Pressure Water in Natural Circulation," ORNL-3026.

[2] Tichler, P.R., and Hill, F.B., 1963, "Experimental Evaluation of the HFBR Emergency Cooling System," BNL-12476 (issued in May 1968).

[3] Mishima, K. and Nishihara, H., 1982, "The Effect of Flow Direction and Magnitude on CHF for Low Pressure Water in Thin Rectangular Channels," Nuclear Engineering and Design, 86, pp 165-181.

[4] Sudo, Y., et.al., 1985, "Experimental Study of Differences in DNB Heat Flux between Upflow and Downflow in Vertical Rectangular Channels," J. Nuclear Science and Technology, 22, pp 604-618.

[5] Mishima, K. and Ishii, M., 1982, "Critical Heat Flux Experiments Under Low Flow Conditions in a Vertical Annulus," NUREG/CR-2647 (ANL-82-6).

[6] Cheng, L.Y., 1996, "Comparison of Steady-State Void Fraction Calculated by RELAP5 and a Drift-Flux Model," (Revised September 24, 1996), BNL Memorandum to Files.

[7] Tichler, P., 1996, "Transient Heat Losses from Test Section During Flow Reversal Tests," BNL Reactor Division Calculation SEG-65-0.

[8A] Yang, B.W., et.al., 1993, "Brookhaven National Laboratory Single Channel Test Program for the HFBR," Columbia University Heat Transfer Research Facility, CU-HTRF-93-05 (Final Report, Vols. I and II).

[8B] Yang, B.W., et.al., 1994, "Brookhaven National Laboratory Single Channel Test Program for the HFBR - Helium Evolution and Bypass Flow Restriction Effects," Columbia University Heat Transfer Research Facility, CU-HTRF-94-02 (Final Report Vols. I and II).

[8C] Yang, B.W., et.al., 1995, "Brookhaven National Laboratory Single Channel Test Program for the HFBR - Flow Reversal With Reduced Bypass Flow Restriction," Columbia University Heat Transfer Research Facility, CU-HTRF-95-03 (Final Report Vols. I and II).

[9] Cheng, L.Y., 1995, "Comparison of RELAP5 and a Drift Flux Model in the Calculation of Multi-Channel Flow Reversal," BNL Memorandum to Files.

[10] Jones, O.C., Jr. and Zuber, N., 1979, "Slug-Annular Transition with Particular Reference to Narrow-Rectangular Ducts," in Two-Phase Momentum, Heat and Mass Transfer in Chemical, Process and Energy Engineering Systems, Vol. 1, Durst, F., Tsiklauri, G.V., and Afgan, N.H. (eds.), Hemisphere Publishing Co., p 345-355.

[11] Cheng, Lap Y., 1996, "Fast Fourier Transform of Flow Reversal Test Data," BNL Memorandum to Files.

[12] Cheng, L.Y., 1995, "Flow Reversal Limited Operating Power for the HFBR," BNL Reactor Division Calculation, SEG-57-0.

[13] Cheng, Lap Y., 1996, "A RELAP5 Simulation of the Flow Reversal Test with a Pressure Boundary Condition," BNL Memorandum to Files.

[14] Cheng, Lap Y., 1992, "Scaling Criteria for the Single-Channel Test," BNL Memorandum to Files.

[15] Cheng, Lap Y., 1996, "Comparison of Calculation by RELAP5 and a Drift-Flux Model of Multi-Channel Flow Reversal in the HFBR," BNL Memorandum to Files.

[16] Cheng, Lap Y., 1996, "A RELAP5 Analysis of the Reactor with One Hot Fuel Element and an Average Core Group," BNL Memorandum to Files.

[17] Wulff, Wolfgang, 1996, "Scaling of Thermohydraulic Systems," Nuclear Engineering and Design 163, pp 359-395.

TABLE 1 HEATED SECTION DIMENSIONS	
Single Sided Heater	
width of channel	2.160 inches
channel gap	0.10 - 0.113 inches
channel length	24.00 inches
heater width	2.25 inches
heater length	22.750 inches
heater thickness	0.050 inches
Double Sided Heater	
width of channel	2.160 inches
channel gap	0.098 - 0.116 inches
channel length	24.00 inches
heater width	2.25 inches
heater length	22.750 inches
thickness of heaters	0.025 inches

TABLE 2.1

SUMMARY OF FIRST TEST SERIES' SINGLE-SIDED HEATING

TEST NUMBER	ORIFICE DIAMETER (inches)	BYPASS" RATIO	WATER LEVEL (ft.)	INLET TEMP. (°F)	COASTDOWN TIME (sec.)	NOMINAL POWER (kW)	FR POWER (kW)	TRIP POWER (kW)	TEST'" OUTCOME
B021393F	0.199	2:1	14.43	130	40	7.0	7.30	-	FR
B021393H	0.199	2:1	14	130	40	7.5	-	7.95	T/C #1
B021393I	0.199	2:1	14	130	30	7.5	7.90	-	FR
B021393K	0.199	2:1	14	130	30	8.0	-	8.70	T/C #1,4
B021393N	0.199	2:1	14	130	Pump trip	9.0	9.35	-	FR
B021393P	0.199	2:1	14	130	Pump trip	10.0	10.4	10.65	FR then T/C #1
B021393O	0.199	2:1	14	130	Pump trip	10.5	10.85	11.05	FR then T/C #1
B021393Q	0.199	2:1	14	110	40	8.0	8.65	9.20	FR then trip after 4 min.
B021393R	0.199	2:1	14	110	40	9.0	-	9.50	Voltage
B030493B	0.199	2:1	14	130	40	7.0	7.10	-	FR
B030493A	0.199	2:1	14	130	40	7.5	-	8.4	T/C #2 and Voltage
B030493D	0.199	2:1	3.67	130	40	7.0	7.15	-	FR
B030493E	0.199	2:1	3.67	130	40	7.5	-	8.10	T/C #1
B080394B	0.199	2:1	14	130	40	7.0	7.40	-	FR
B080394A	0.199	2:1	14	130	40	7.5	-	8.00	Voltage

TABLE 2.1

SUMMARY OF FIRST TEST SERIES' SINGLE-SIDED HEATING

TEST NUMBER	ORIFICE DIAMETER (inches)	BYPASS** RATIO	WATER LEVEL (ft.)	INLET TEMP. (°F)	COASTDOWN TIME (sec.)	NOMINAL POWER (kW)	FR POWER (kW)	TRIP POWER (kW)	TEST*** OUTCOME
B080394E	0.129	5:1	14	130	40	6.2	6.70	-	FR
B080394D	0.129	5:1	14	130	40	6.5	-	7.10	Voltage
B080394G	0.28	1.5:1	14	130	40	7.5	8.2	-	FR
B080394H	0.28	1.5:1	14	130	40	7.8	-	8.55	T/C #1, 2 and Voltage

Notes:

* Test loop configuration shown in Figure 3 was used. Powers listed are uncorrected for heat loss.

** The ratio of flow in test section to flow in bypass under initial conditions. Combined initial flow rate was 3 gpm for all tests.

*** FR signifies absence of trip for 30 seconds after flow reversal. T/C or voltage indicates that a plate temperature excursion or plate voltage excursion caused trip. Number of T/C indicates thermocouple location on plate by a number 1 to 9 starting at top of plate.

TABLE 2.2

SUMMARY OF FIRST TEST SERIES* - TWO-SIDED HEATING

TEST NUMBER	ORIFICE DIAMETER (inch)	BYPASS** RATIO	WATER LEVEL (ft.)	INLET TEMP. (°F)	COASTDOWN TIME (sec.)	NOMINAL POWER (kW)	FR POWER (kW)	TRIP POWER (kW)	TEST*** OUTCOME
B061293E	0.199	2:1	14	130	40	8.0	8.7	-	FR
B061293G	0.199	2:1	14	130	40	8.5	-	9.4	Voltage
B061293H	0.199	2:1	14	130	Pump Trip	10.5	11.4	12.0	FR then Voltage
B061293J	0.199	2:1	14	150	40	6.5	6.7	-	FR
B061293I	0.199	2:1	14	150	40	7.0	-	7.7	T/C
B061293L	0.199	2:1	14	130	60	6.5	7.3	-	FR
B061293K	0.199	2:1	14	130	60	7.0	-	7.85	Voltage

Notes:

* Test loop configuration shown in Figure 3 was used. Powers listed are uncorrected for heat loss.

** The ratio of flow in test section to flow in bypass under initial conditions. Combined initial flow rate was 3 gpm for all tests.

*** FR signifies absence of trip for 30 seconds after flow reversal. T/C or voltage indicates that a plate temperature excursion or plate voltage excursion caused trip. Number of T/C indicates thermocouple location on plate by a number 1 to 9 starting at top of plate.

TABLE 2.3

SUMMARY OF HELIUM EFFECTS TESTS#

TEST NUMBER	HELIUM	UPPER* PLENUM VOID FRACTION	ORIFICE DIAMETER (inches)	BYPASS** RATIO	COASTDOWN TIME (sec)	NOMINAL POWER (kW)	FR POWER (kW)	TRIP POWER (kW)	TEST*** OUTCOME
B101694B	NO	0.0	0.199	1.42:1	40	7.5	7.85	-	FR
B101694E	YES	0.11	0.199	1.42:1	40	7.0	7.60	-	FR
B101694C	NO	0.0	0.199	1.42:1	40	8.0	-	8.90	Voltage
B101694D	YES	0.13	0.199	1.42:1	40	7.5	-	8.10	Voltage & T/C #1
B101694G	NO	0.0	0.199	1.42:1	60	6.5	7.00	-	FR
B101694H	YES	0.065	0.199	1.42:1	60	6.5	6.70	-	FR
B101694F	NO	0.0	0.199	1.42:1	60	7.0	-	7.75	Voltage
B101694I	YES	0.045	0.199	1.42:1	60	7.0	-	7.50	Voltage
B101694L	NO	0.0	0.129	2.78:1	40	6.4	6.95	-	FR
B101694M	YES	≈0.0	0.129	2.78:1	40	6.5	7.00	-	FR
B101694K	NO	0.0	0.129	2.78:1	40	6.6	-	7.20	Voltage
B101694N	YES	0.038	0.129	2.78:1	40	7.0	-	7.75	Voltage

Notes:

\# All tests were done with water level at 14' above the inlet section, an inlet water temperature of 130°F, and single-sided heating. Test loop configuration shown in Figure 4. Powers listed are uncorrected for heat loss.

* Approximate void fraction at the time of flow reversal; calculated from a pressure difference measurement in the upper plenum.

** The ratio of flow in test section to flow in bypass under initial conditions. Combined initial flow rate was 3.4 gpm for all tests.

*** FR signifies absence of trip for 30 seconds after flow reversal. T/C or voltage indicates that a plate temperature excursion or plate voltage excursion caused trip. Number of T/C indicates thermocouple location on plate by a number 1 to 9 starting at top of plate.

TABLE 2.4

SUMMARY OF EXTENDED BYPASS RATIO TESTS+

TEST NUMBER	TOTAL INITIAL FLOW (gpm)	BYPASS* RATIO	WATER** LEVEL (ft.)	INLET TEMP. (°F)	COASTDOWN TIME (sec.)	NOMINAL POWER (kW)	FR POWER (kW)	TRIP POWER (kW)	TEST*** OUTCOME
B081395E	3.0	2:1:0	14	130	40	9.0	9.45	-	FR
B081395F	3.0	2:1:0	14	130	40	9.5	-	10.25	T/C #1
B081395K	8.8	1:3.4:0	14	130	40	14.0	14.35	-	FR
B081395L	8.8	1:3.4:0	14	130	40	14.5	-	15.00	T/C #9
B081395M	10.0	1:3.4:0.6	14	130	40	14.5	-	14.9	T/C #9
B081395N	10.0	1:3.4:0.6	14	130	40	14.0	14.2	-	FR
B081395O	10.0	1:3.4:0.6	14	130	30	14.5	-	15.02	T/C #9
B081395U	4.2	2:1:1.2	14	130	40	11.5	12.0	-	FR
B081395V	4.2	2:1:1.2	14	130	40	12.5	-	13.75	Voltage
B081795C	10.0	1:3.4:0.6	14	130	Pump Trip	19.0	19.8	-	FR
B081795D	10.0	1:3.4:0.6	14	130	##	21.0	-	21.65	Voltage

Notes:

\+ Test loop configuration shown in Figure 5. Powers listed are uncorrected for heat loss.

* The ratio of flow in test section to flow in primary bypass to flow in secondary bypass under initial conditions.

** Height of column of water above top of the inlet section.

*** FR signifies absence of trip for 30 seconds after flow reversal. T/C or voltage indicates that a plate temperature excursion or plate voltage excursion caused trip. Number after T/C indicates thermocouple location on plate by a number 1 to 9 starting at top of plate.

A voltage trip occurred while power was being raised and before pump was shut off.

TABLE 3

LIST OF RELAP5 SIMULATIONS OF FLOW REVERSAL TESTS

RELAP5 RUN NO.	REFERENCE' TEST NO.	TEST" OUTCOME	CHANNEL+ POWER (kW)	ORIFICE'' DIAMETER (in.)	BYPASS'' RATIO	NUMBER SIDES HEATED	INLET TEMP. (°F)	COASTDOWN TIME (sec.)	MAXIMUM++ VOID FRACTION
101	B021393F[1]	FR	7.0/6.7	0.199	2:1	1	130	40	0.696/.663
102	B021393H[1]	Trip	7.6/7.3	0.199	2:1	1	130	40	0.761/.728
103	B021393I[1]	FR	7.6/7.3	0.199	2:1	1	130	30	0.716/.688
104	B021393K[1]	Trip	8.4/8.1	0.199	2:1	1	130	30	0.789/.761
107	B021393Q[1]	FR	8.3/8.0	0.199	2:1	1	110	40	0.704/.678
108	B021393R[1]	Trip	9.1/8.8	0.199	2:1	1	110	40	0.771/.745
109	B030493D[1]	FR	6.9/6.6	0.199	2:1	1	130	40	0.762/.739
110	B030493E[1]	Trip	7.8/7.5	0.199	2:1	1	130	40	0.829/.807
112	B080394D[1]	Trip	6.8/6.5	0.129	5:1	1	130	40	0.884/.866
113	B080394E[1]	FR	6.4/6.1	0.129	5:1	1	130	40	0.860/.841
114	B080394G[1]	FR	7.9/7.6	0.28	1.5:1	1	130	40	0.739/.711
115	B080394H[1]	Trip	8.2/7.9	0.28	1.5:1	1	130	40	0.766/.739
302	B101694B[2]	FR	7.5/7.2	0.199	1.42:1	1	130	40	0.819/.793
303	B101694C[2]	Trip	8.5/8.2	0.199	1.42:1	1	130	40	0.904/.878
304	B101694F[2]	Trip	7.4/7.1	0.199	1.42:1	1	130	60	0.851/.819
305	B101694G[2]	FR	6.7/6.4	0.199	1.42:1	1	130	60	0.777/.744
306	B101694K[2]	Trip	6.9/6.6	0.129	2.78:1	1	130	40	0.895/.893
307	B101694L[2]	FR	6.7/6.4	0.129	2.78:1	1	130	40	0.894/.892

TABLE 3 (CONTINUED)

LIST OF RELAP5 SIMULATIONS OF FLOW REVERSAL TESTS

RELAP5 RUN NO.	REFERENCE* TEST NO.	TEST# OUTCOME	CHANNEL+ POWER (kW)	ORIFICE** DIAMETER (in.)	BYPASS## RATIO	NUMBER SIDES HEATED	INLET TEMP. (°F)	COASTDOWN TIME (sec.)	MAXIMUM++ VOID FRACTION
201	B061293E(1)	FR	8.3/8.0	0.199	2:1	2	130	40	0.784/.766
202	B061293G(1)	Trip	8.9/8.6	0.199	2:1	2	130	40	0.819/.801
204	B061293I(1)	Trip	7.3/7.0	0.199	2:1	2	150	40	0.824/.797
205	B061293J(1)	FR	6.4/6.1	0.199	2:1	2	150	40	0.743/.715
206	B061293K(1)	Trip	7.5/7.2	0.199	2:1	2	130	60	0.775/.737
207	B061293L(1)	FR	6.9/6.6	0.199	2:1	2	130	60	0.701/.664
1	B081395E(3)	FR	9.0/8.7	-	2:1:0	1	130	40	0.713/.690
2	B081395F(3)	Trip	9.8/9.5	-	2:1:0	1	130	40	0.774/.751
10	B081395K(3)	FR	13.8/13.6	-	1:3.4:0	1	130	40	0.860/.850
21	B081395N(3)	FR	13.8/13.6	-	1:3.4:0.6	1	130	40	0.668/.656
6	B081395U(3)	FR	11.5/11.2	-	2:1:1.2	1	125	40	0.55/.53
5	B081395V(3)	Trip	13.2/13.0	-	2:1:1.2	1	130	40	0.667/.653
11	B081795C(3)	FR	19.0/19.0	-	1:3.4:0.6	1	130	1.5	0.718/.718

Notes:

* The number in parenthesis after the test number is the test loop configuration: (1) refers to Figure 3; (2) refers to Figure 4; (3) refers to Figure 5.

\# FR means a successful flow reversal without a power trip for 30 seconds after initiation of flow reversal.

\+ Channel power corresponds to either the flow reversal power or the trip power given in Tables 2. The first number is the channel power after a reduction of 4% and 5% to account for steady-state heat loss from the single-sided and two-sided heaters respectively. The second number is the effective channel power after accounting for the higher of steady-state and transient heat losses.

** A numerical value indicates orifice diameter in bypass path in test configurations (1) and (2). A (-) indicates use of throttling valve in bypass path.

\## Refers to ratio of flow rates under initial conditions. First number applies to section flow, second number applies to primary bypass flow and third number, if present, applies to secondary bypass flow in test configuration 3.

++ Maximum time-averaged void fraction during the 10 second interval following reversal in RELAP5 calculation. The time averaging period is two seconds. The first number is based on a channel power accounting only for steady-state heat loss. The second number is based on the effective channel power which accounts for the higher of steady-state and transient heat losses.

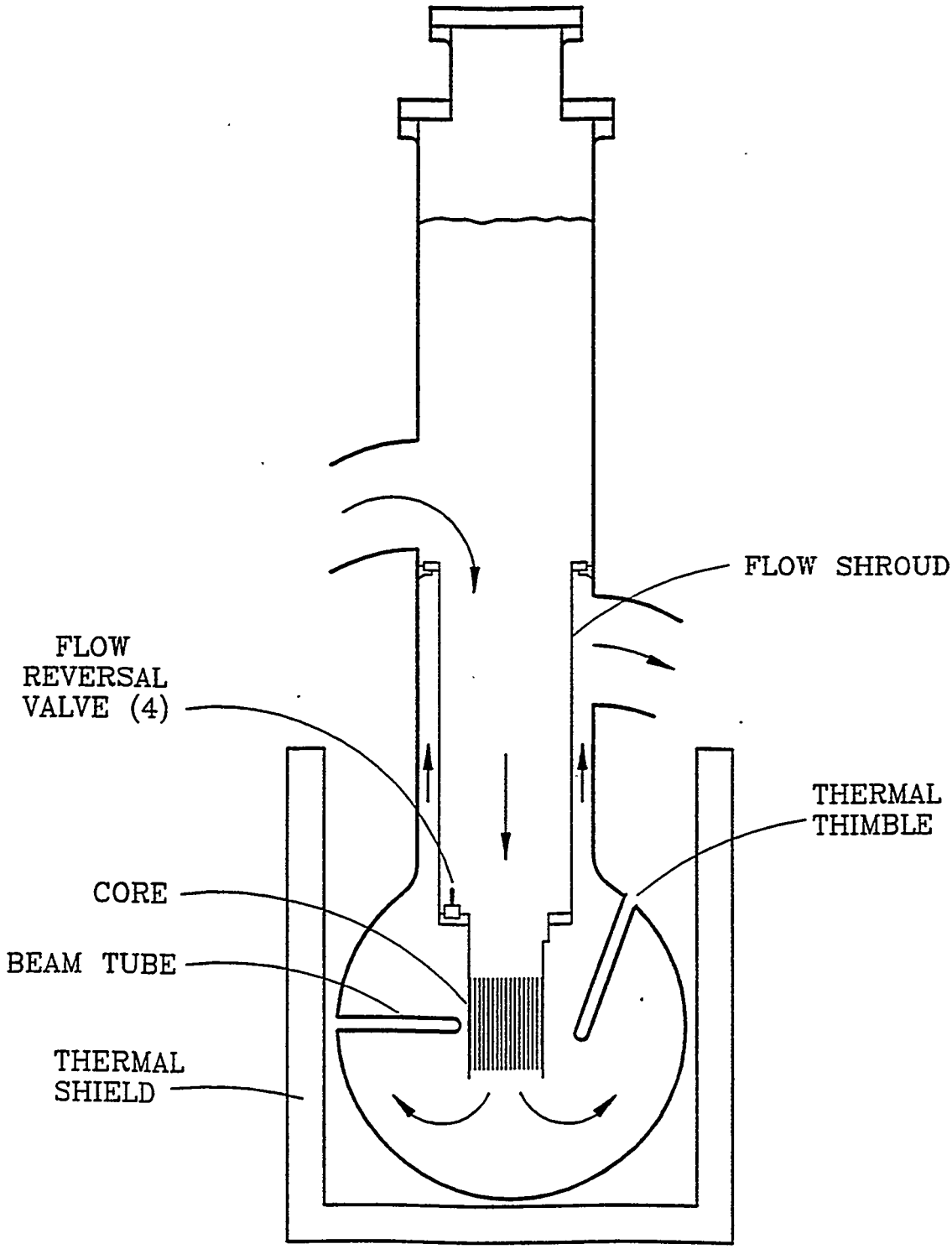

Figure 1 HFBR Vessel Showing Normal Flow Direction

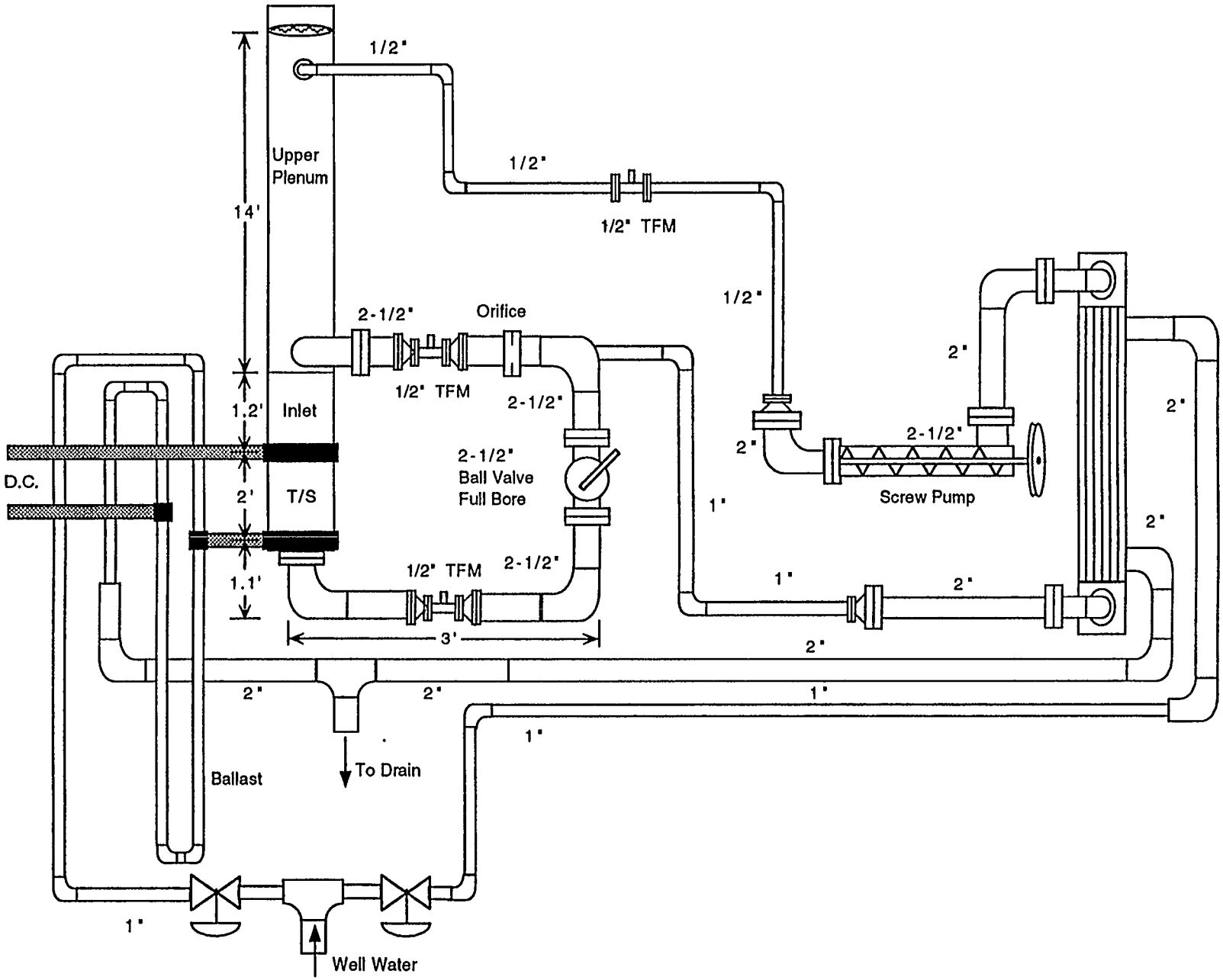

Figure 2 Schematic of the Flow Reversal Test Loop

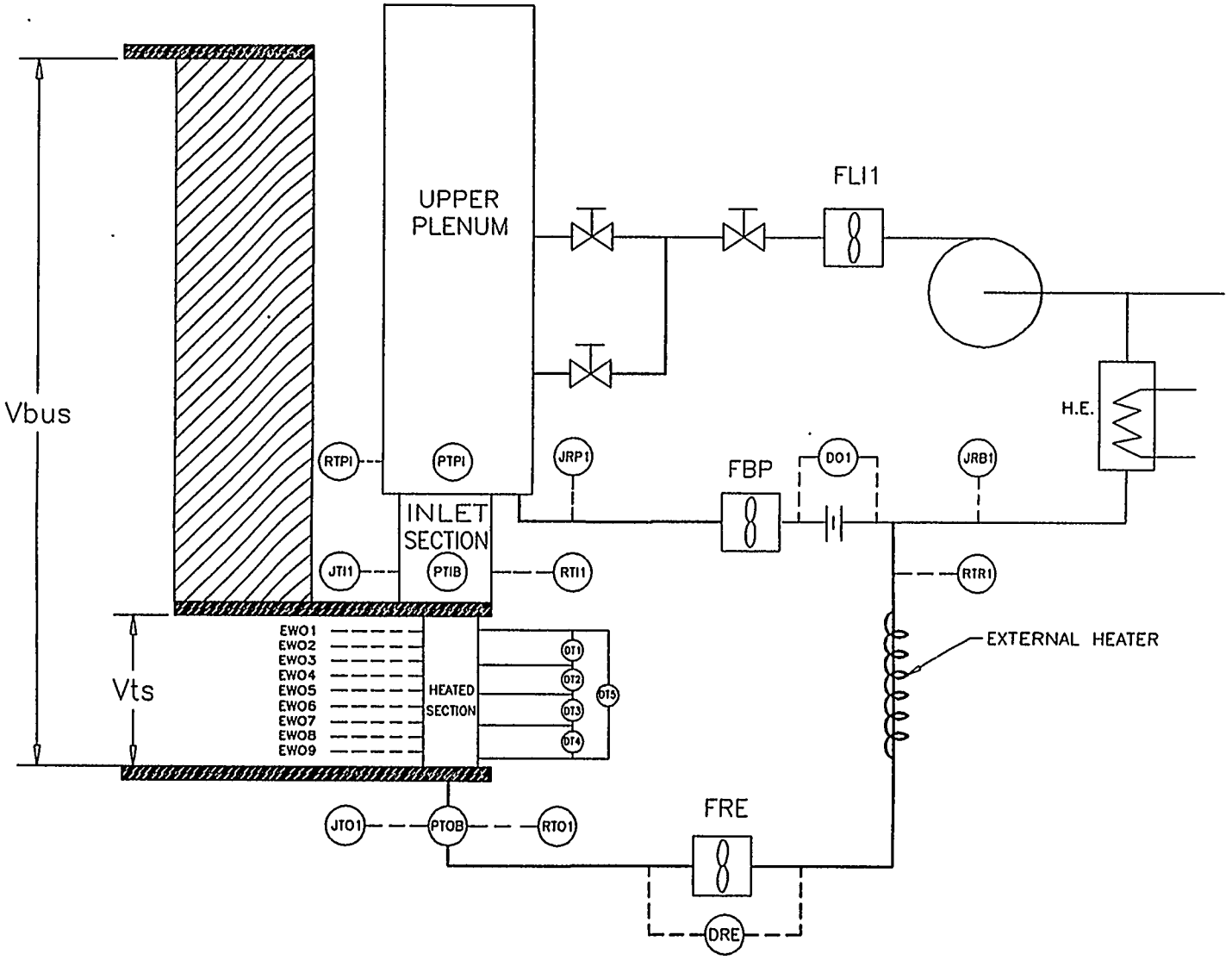

Figure 3 Schematic of Test Loop for First Test Series

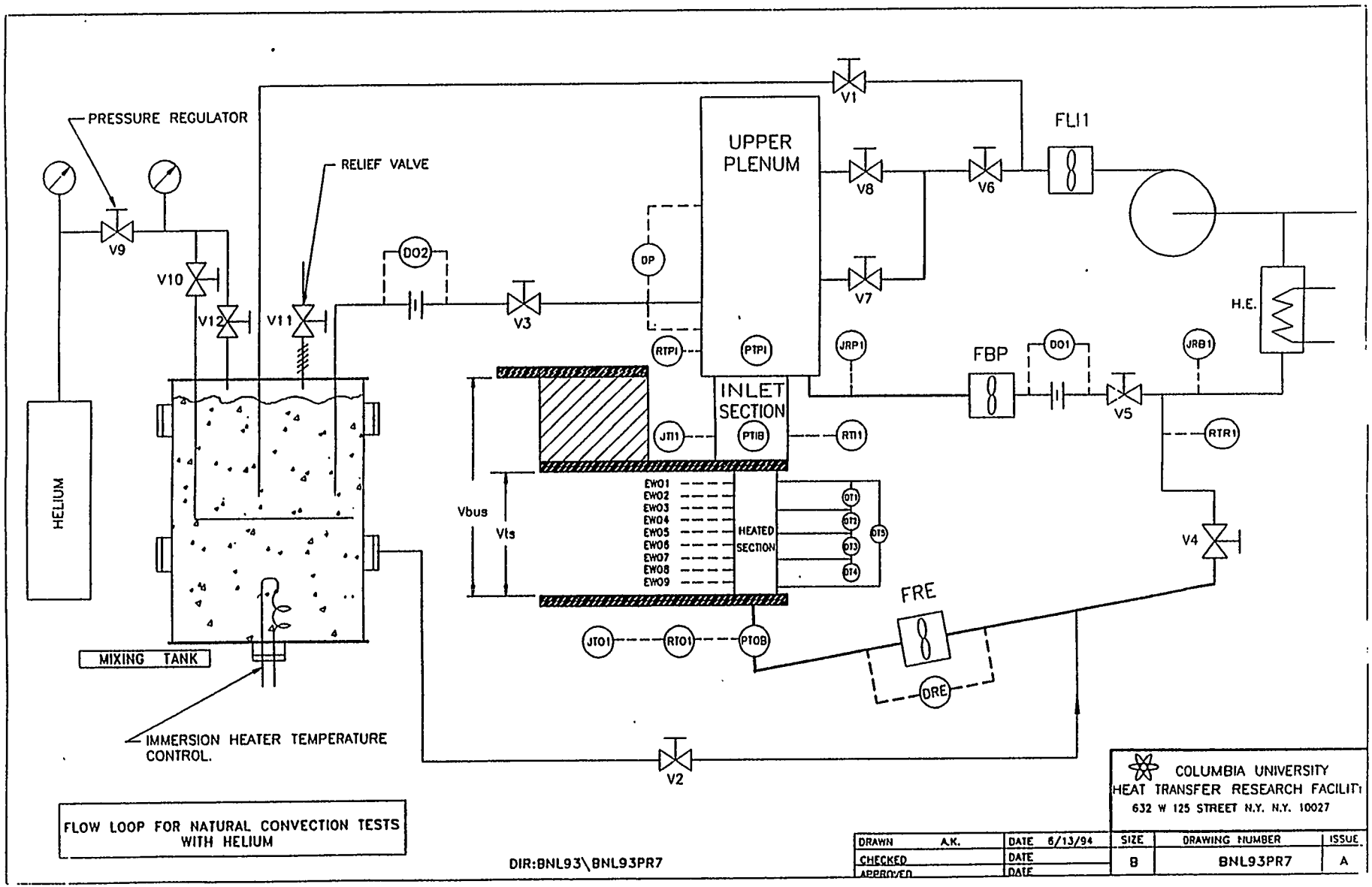

Figure 4 Schematic of Test Loop for Helium Tests

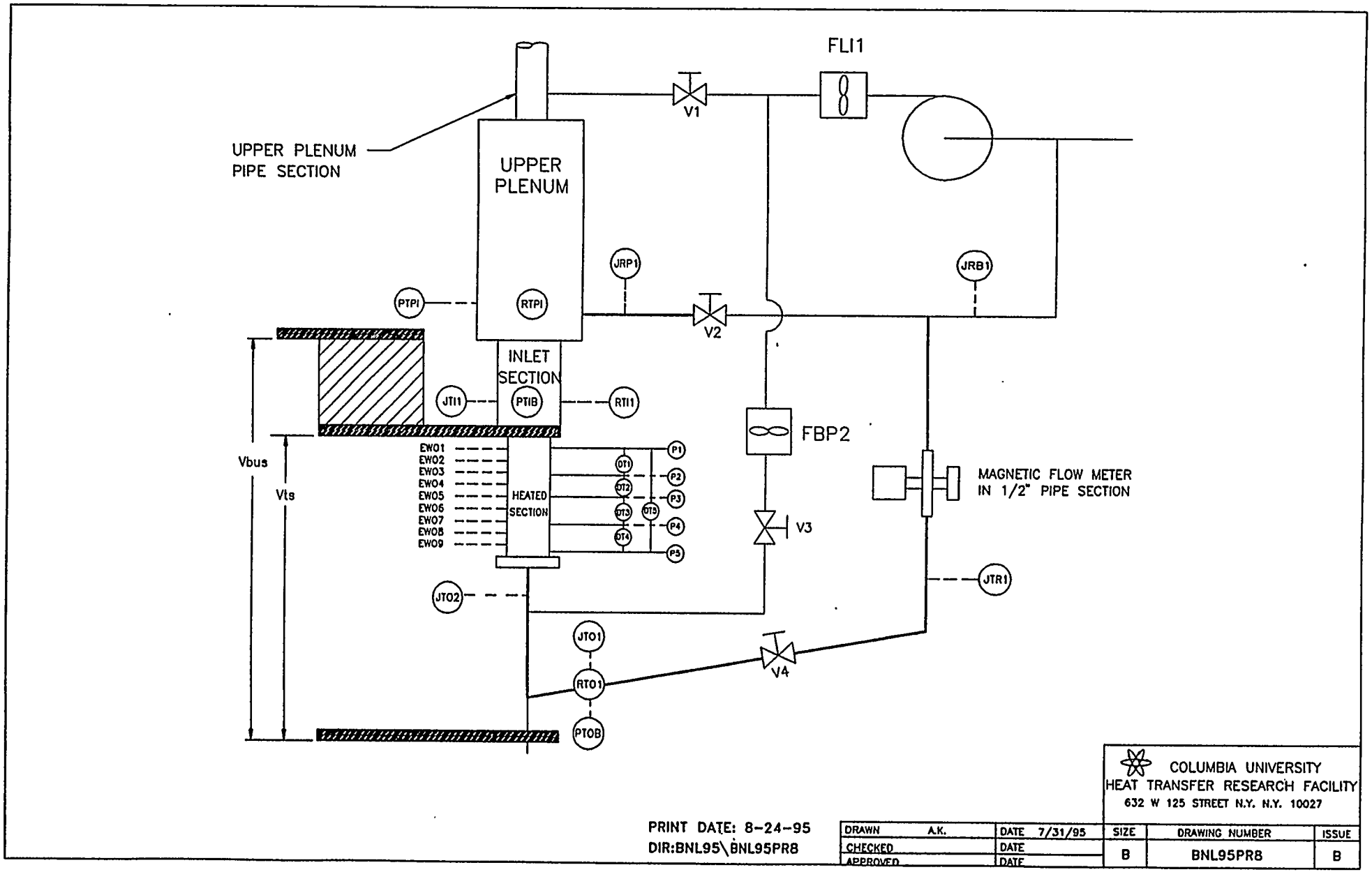

Figure 5 Schematic of Test Loop for Extended Bypass Ratio Tests

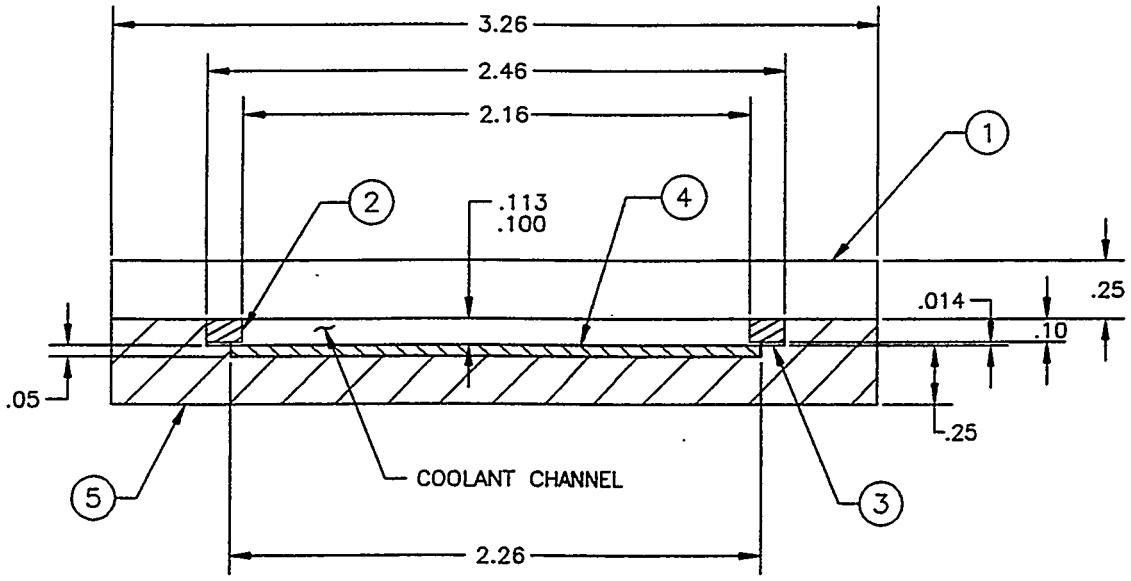

ITEM NO.	QTY.	DESCRIPTION
1	–	LEXAN
2	–	SIDE RAIL (ASBESTOS PHENOLIC)
3	–	KAPTON TAPE (4 LAYERS)
4	–	ALUMINUM HEATER STRIP (WIDTH = 2.25)
5	–	INSULATOR (PEEK)

NOTE:

1. ALL DIMENSIONS ARE NOMINAL VALUES AND IN INCHES.

Figure 6 Cross-Section of the Single-Heater Test Section

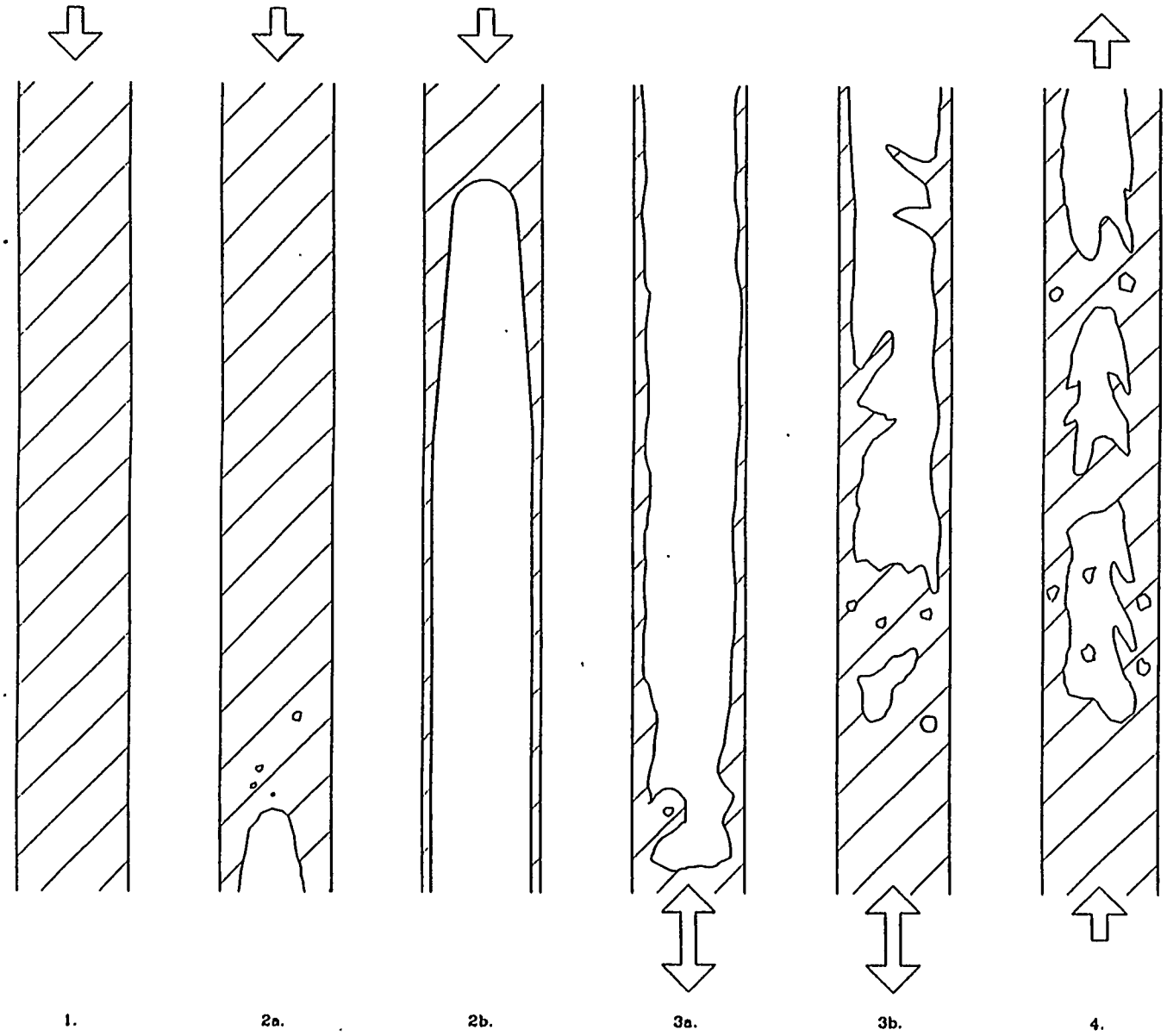

Figure 7 Stages of the Flow Reversal Process

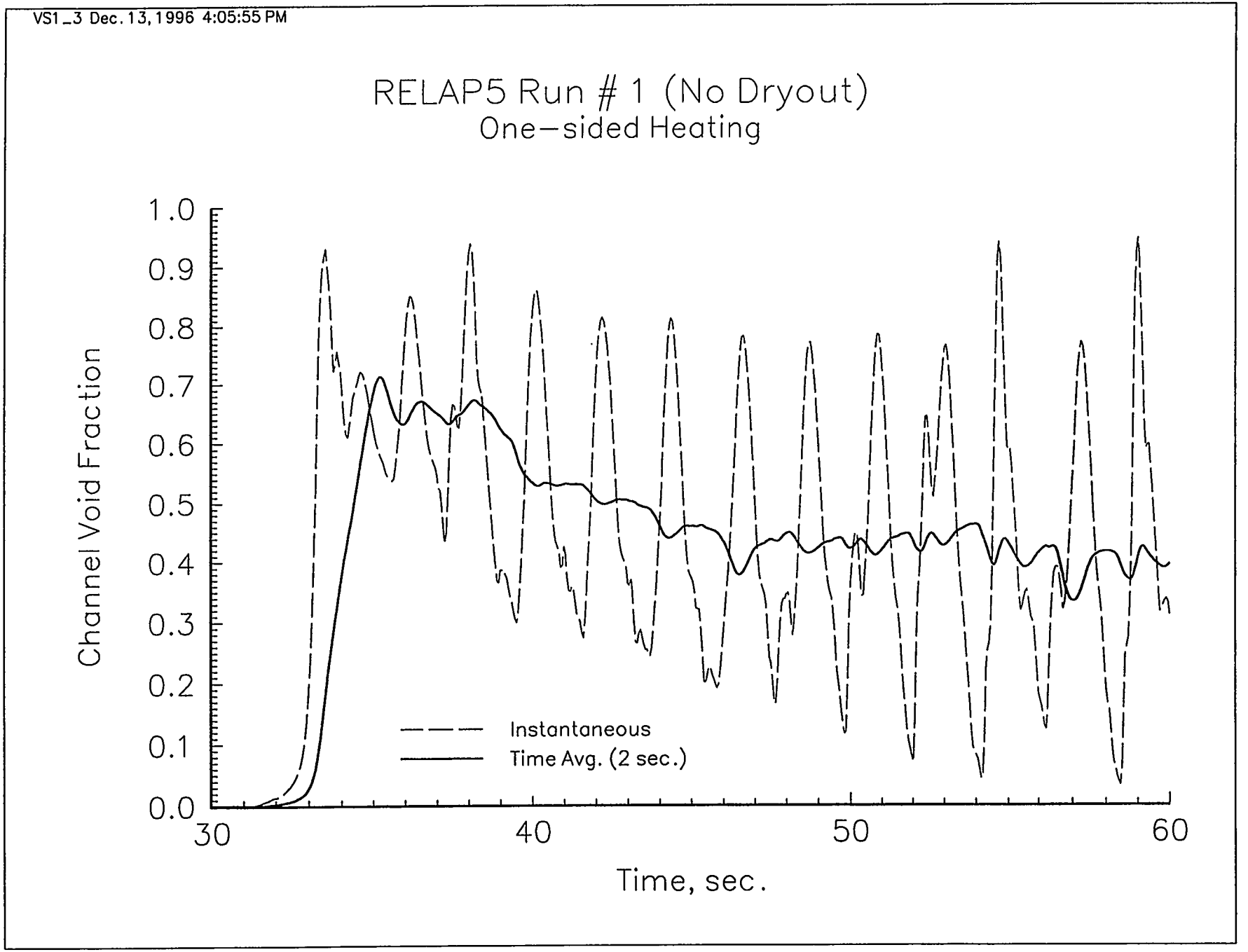

Figure 8 Typical Trace of Time Averaged Channel Void Fraction

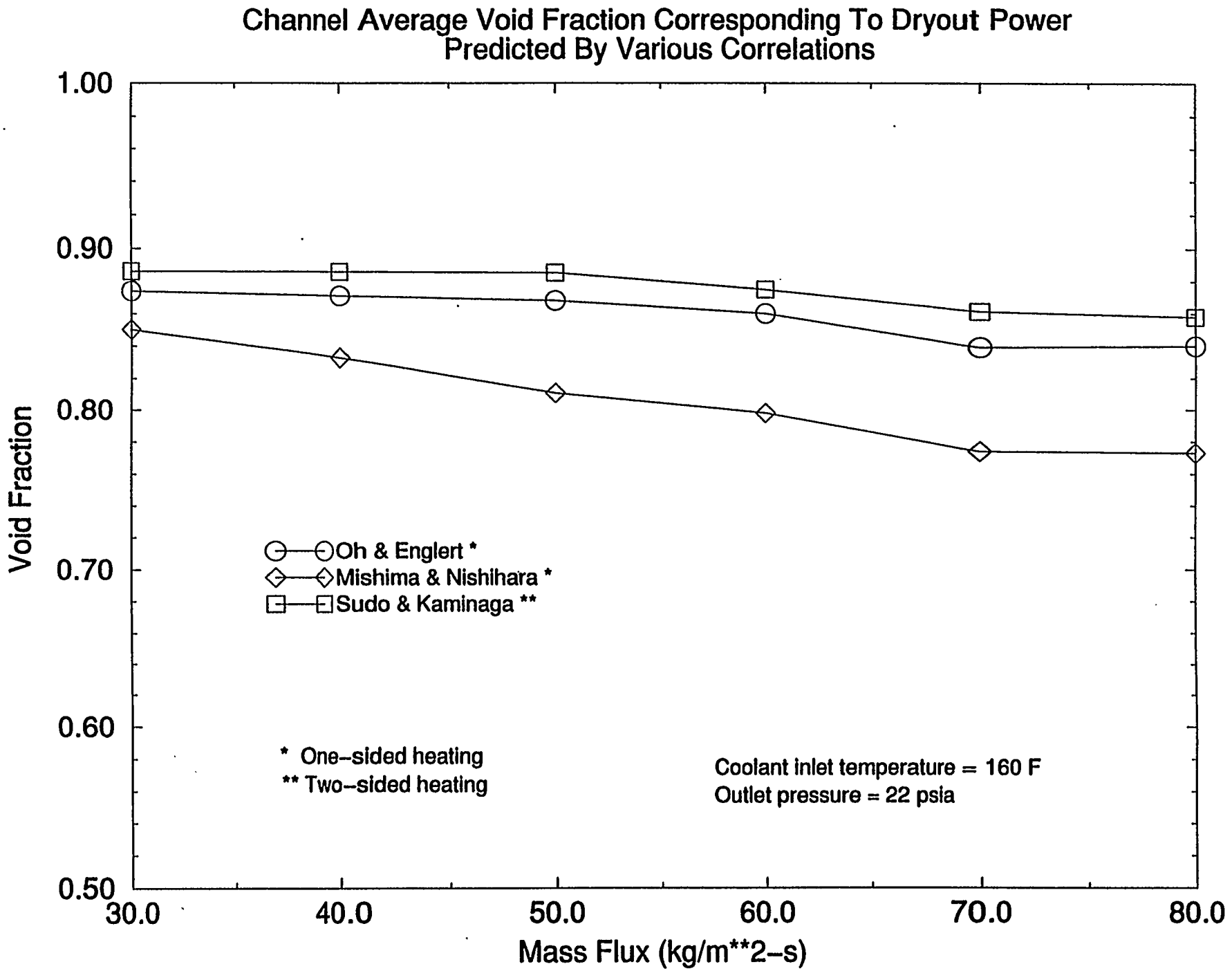
Channel Average Void Fraction Corresponding To Dryout Power
Predicted By Various Correlations
1.00
0.90
0.80
0.70
0.60
0.50
Void Fraction
Oh & Englert *
Mishima & Nishihara *
Sudo & Kaminaga **
* One-sided heating
** Two-sided heating
Coolant inlet temperature = 160 F
Outlet pressure = 22 psia
30.0
40.0
50.0
60.0
70.0
80.0
Mass Flux (kg/m**2-s)

Figure 9

DECAY2 Apr. 18, 1995 10:53:09 AM

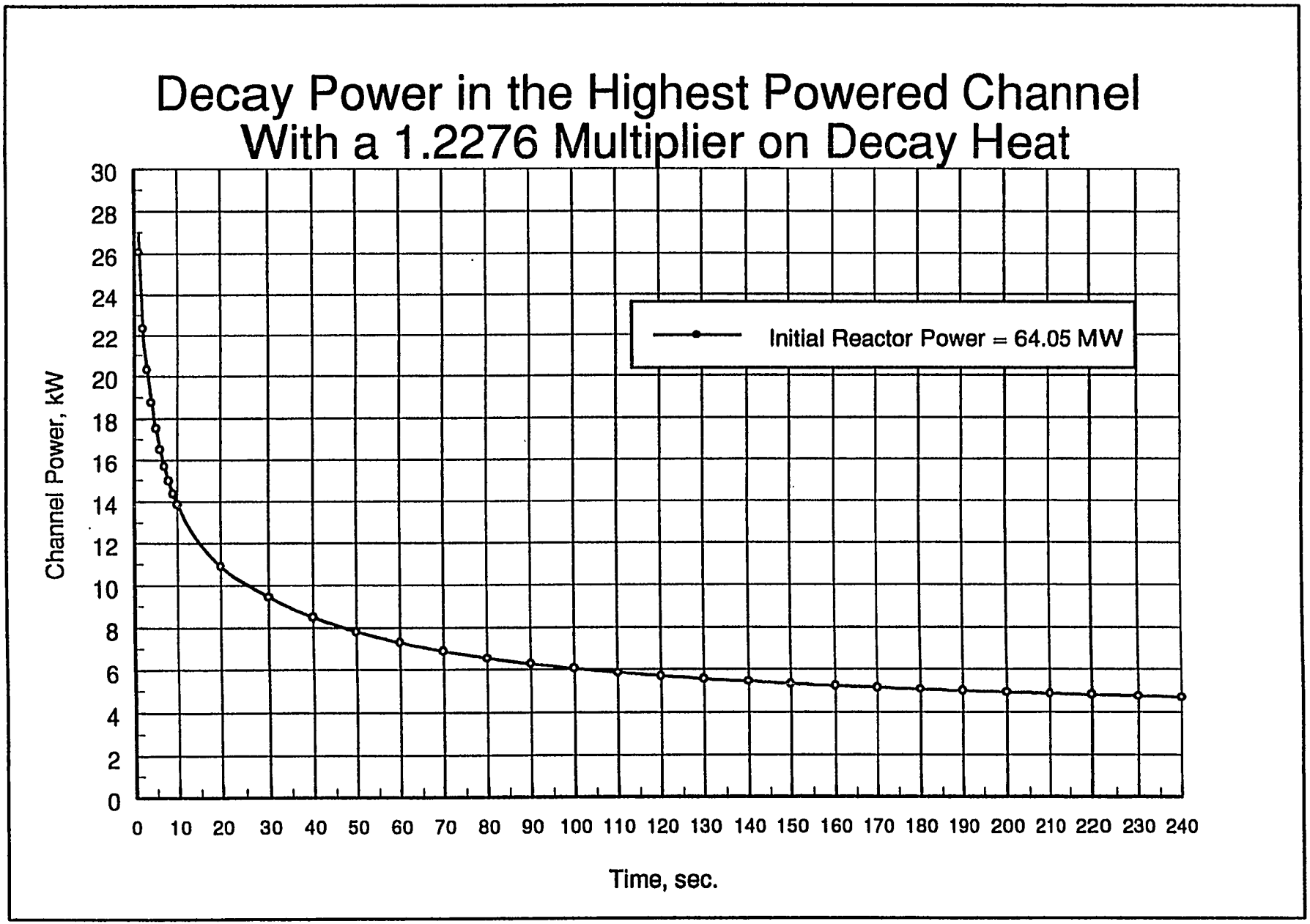

Figure 10 Decay Power vs. Time After Shutdown

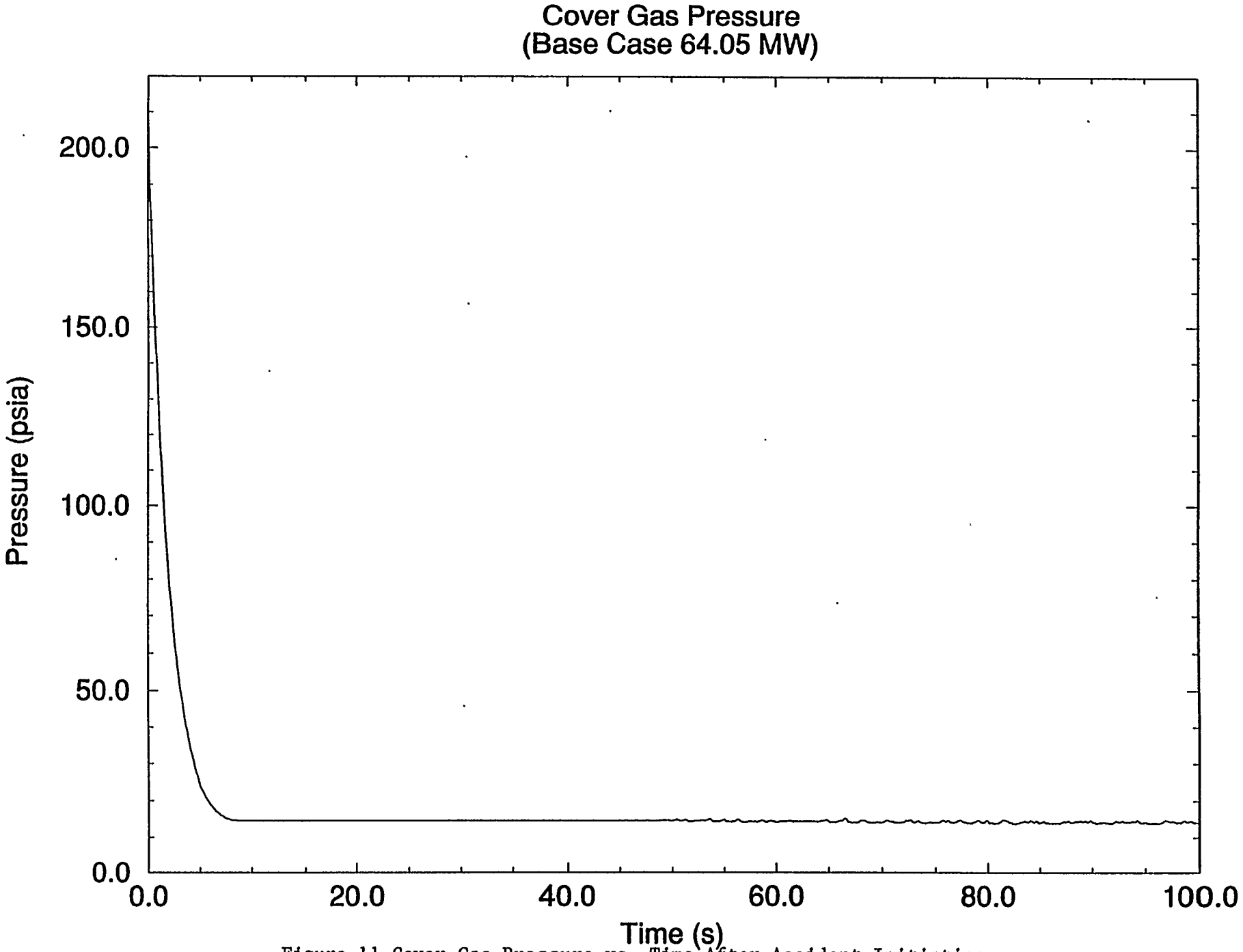

Figure 11 Cover Gas Pressure vs. Time After Accident Initiation

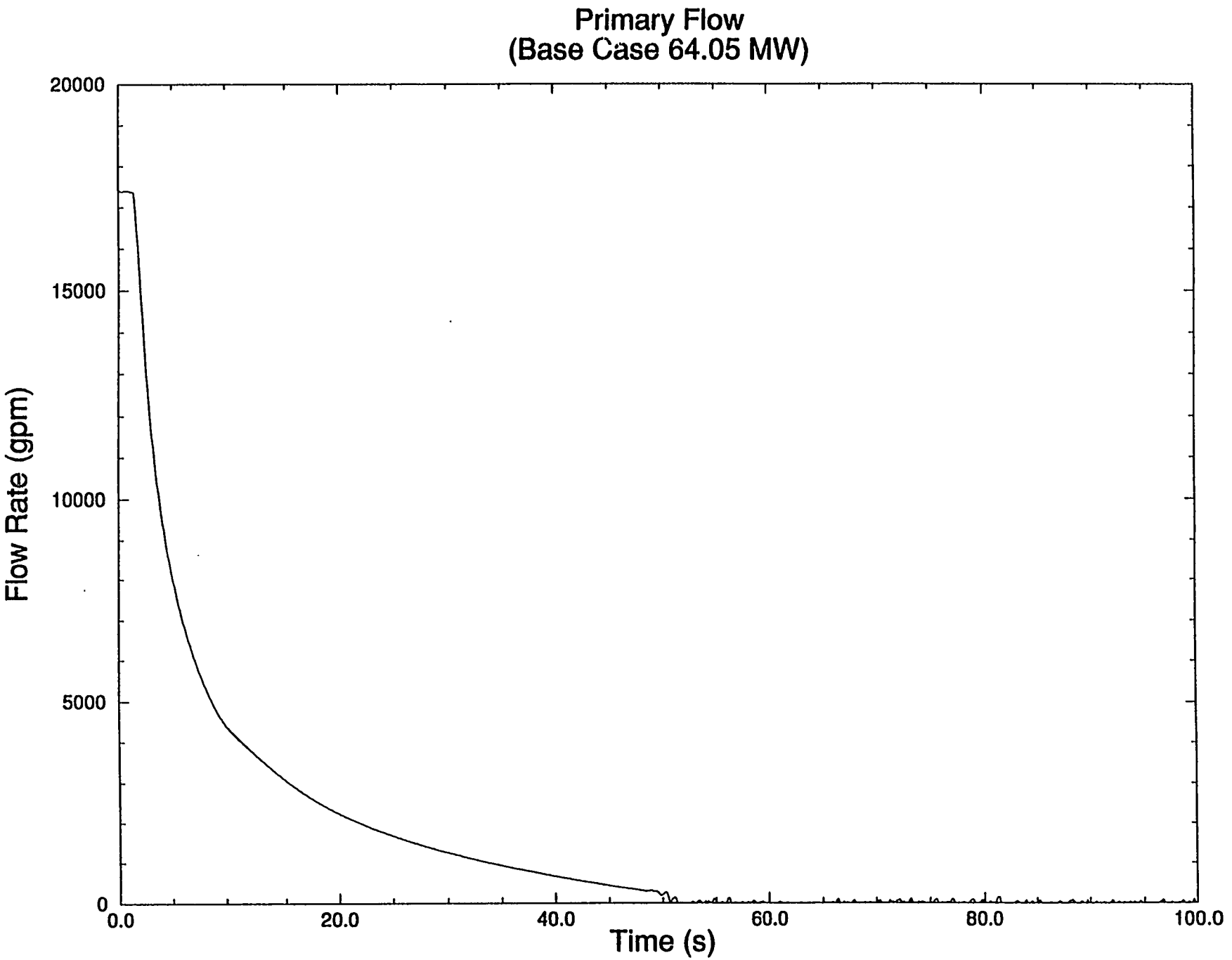

Figure 12 Primary Flow Rate vs. Time After Accident Initiation

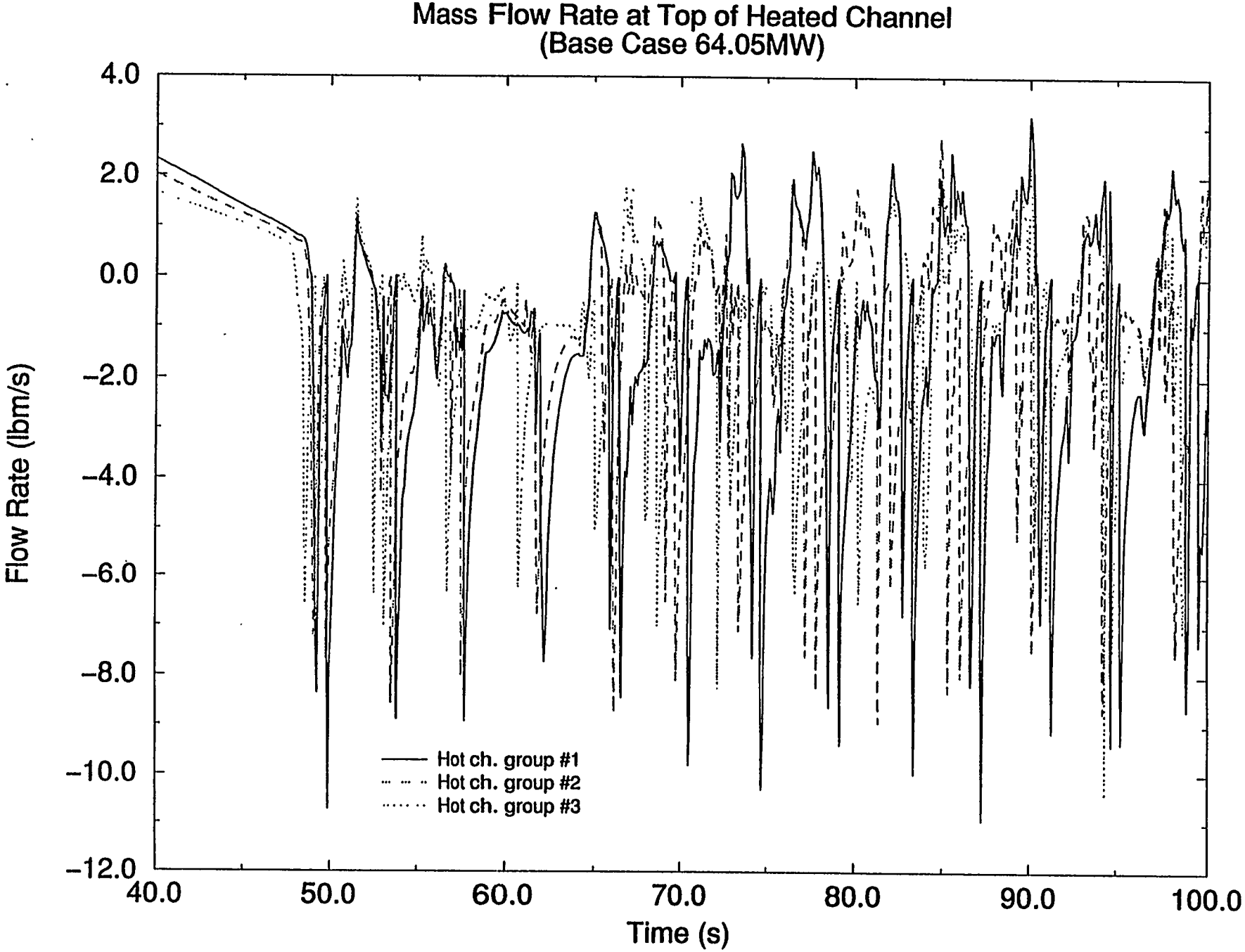

Figure 13 Mass Flow Rate At Top of Heated Channels vs. Time

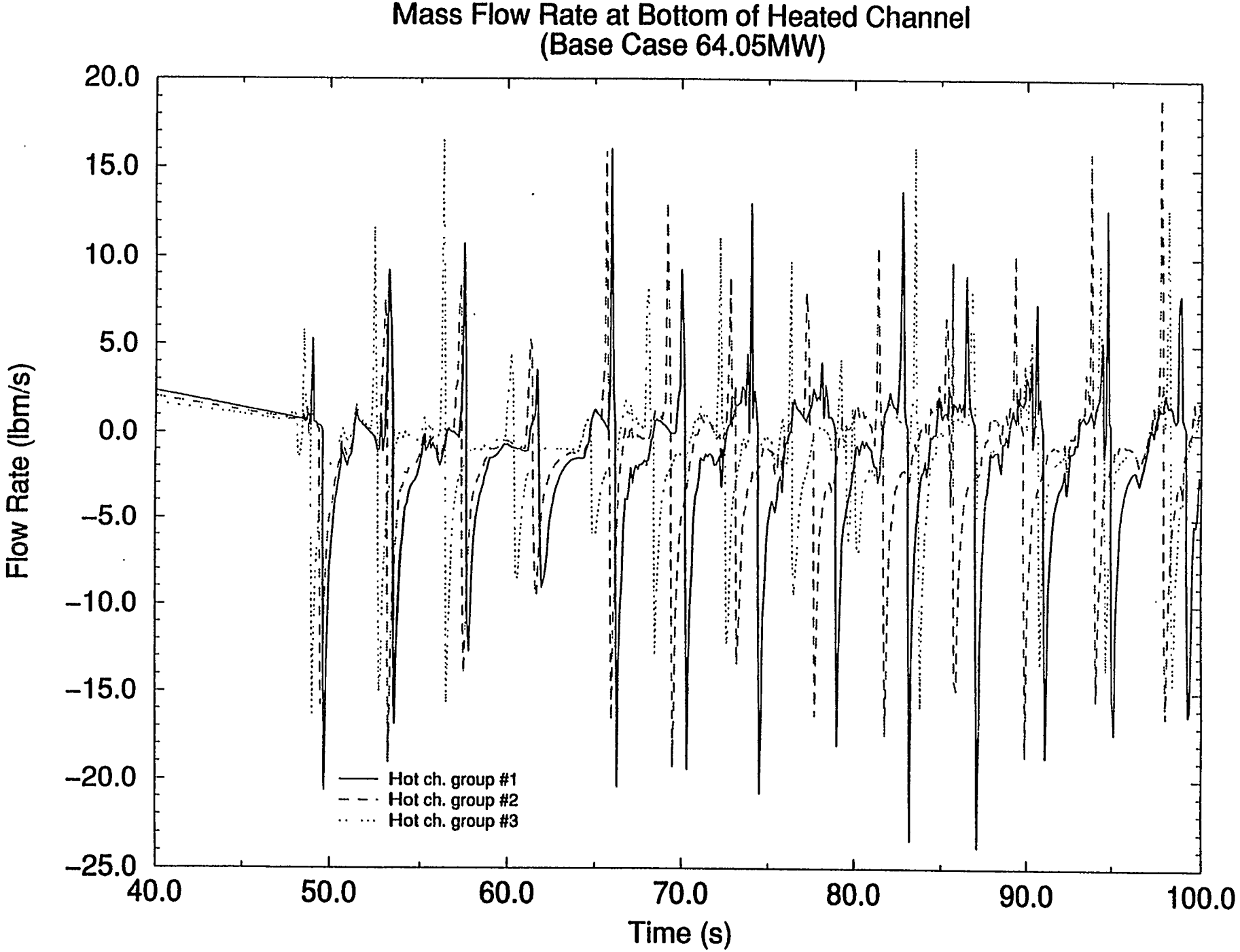

Figure 14 Mass Flow Rate at Bottom of Heated Channels vs. Time

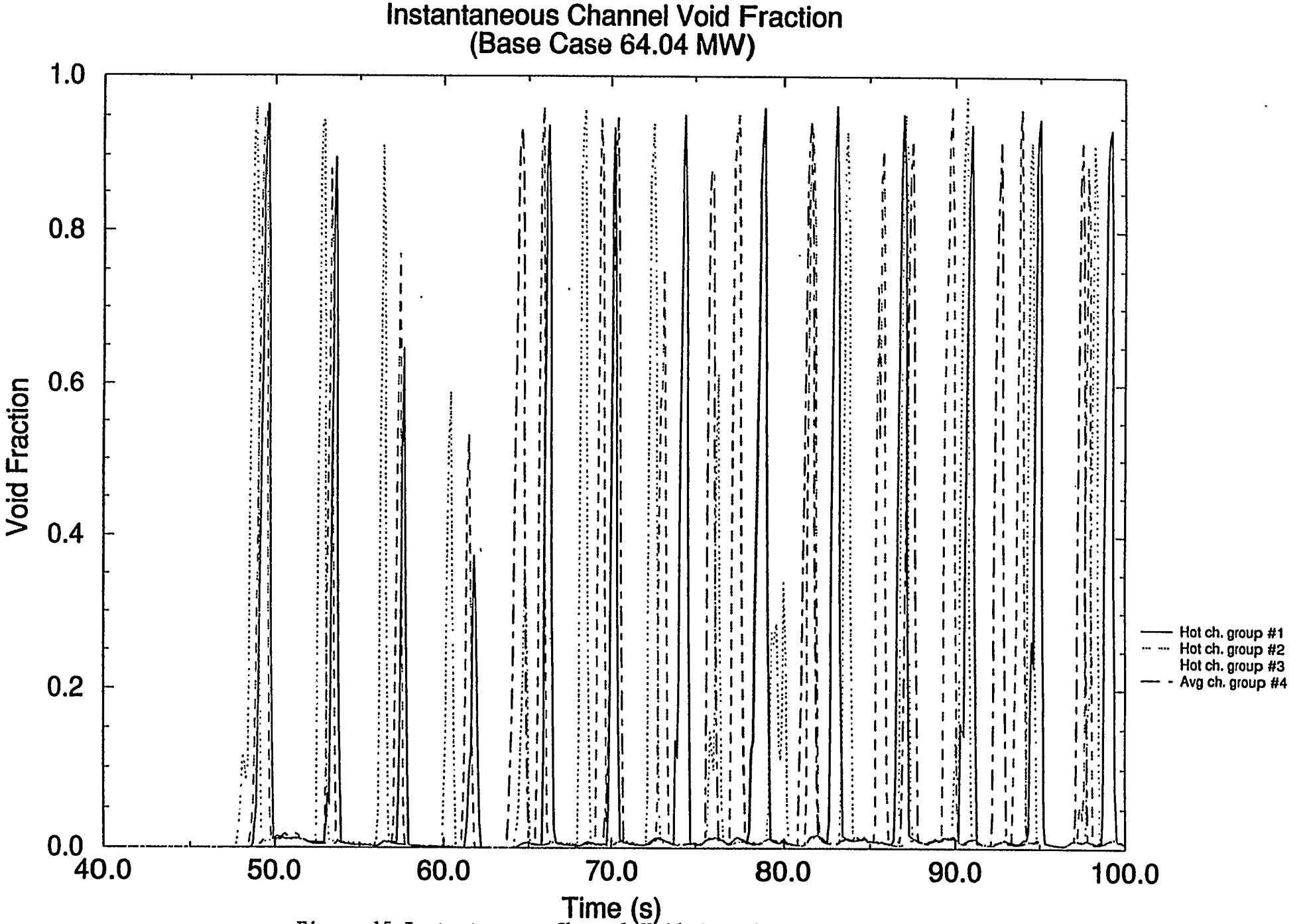

Figure 15 Instantaneous Channel Void Fraction vs. Time

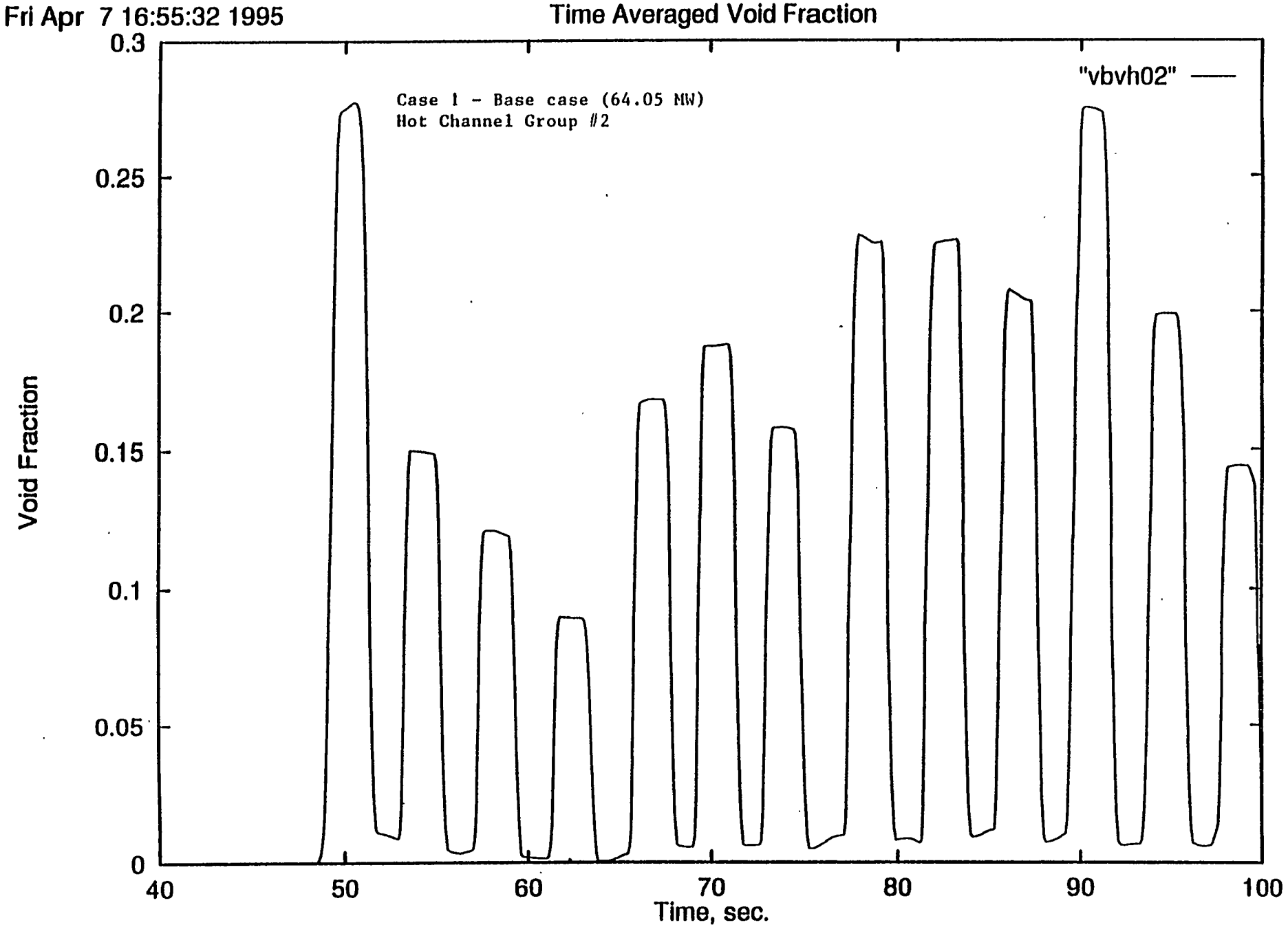

Figure 16 Time Averaged Channel Void Fraction vs. Time (Average Channel Group 2)

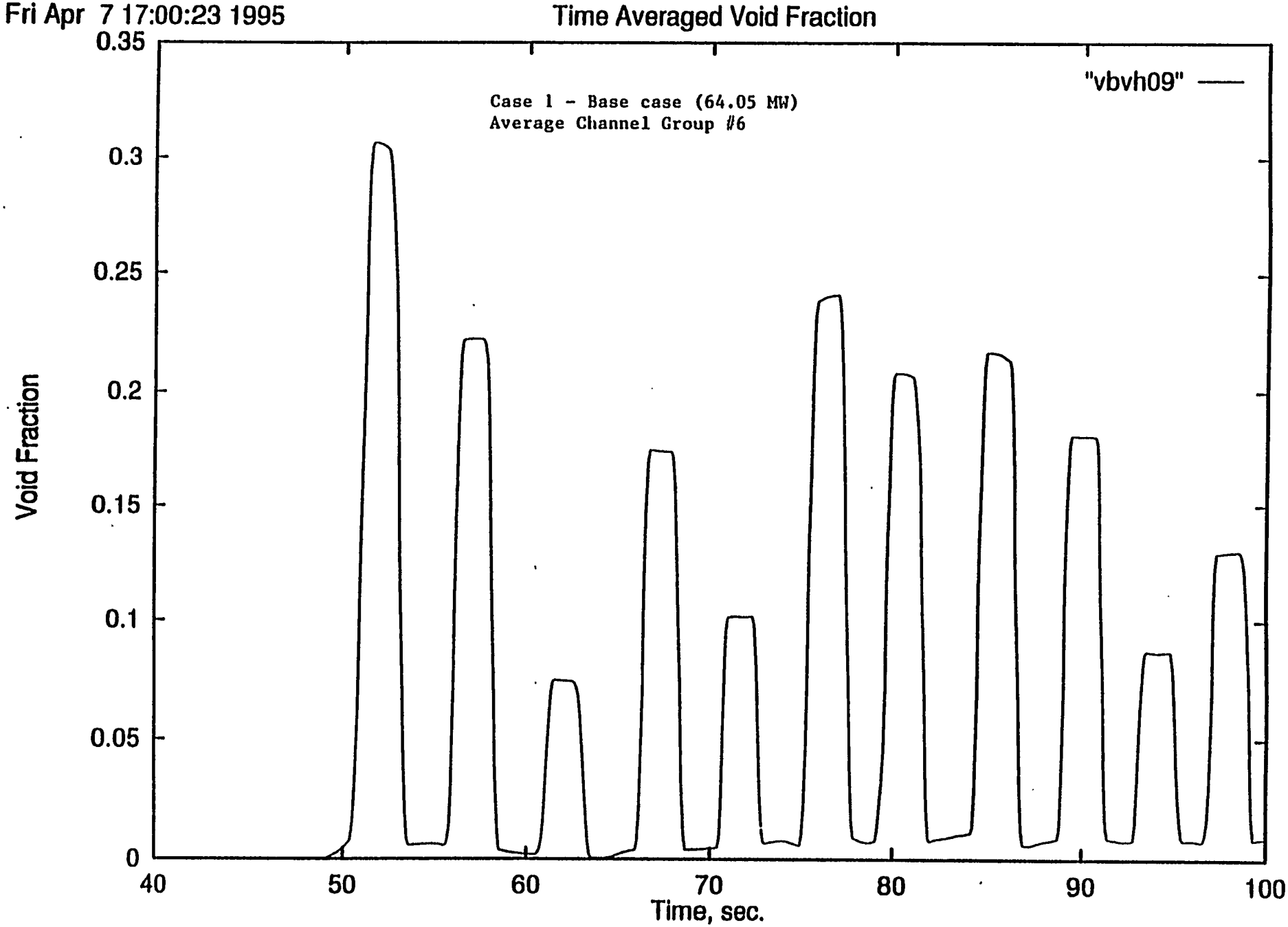

Figure 17 Time Averaged Channel Void Fraction vs. Time (Average Channel Group 6)

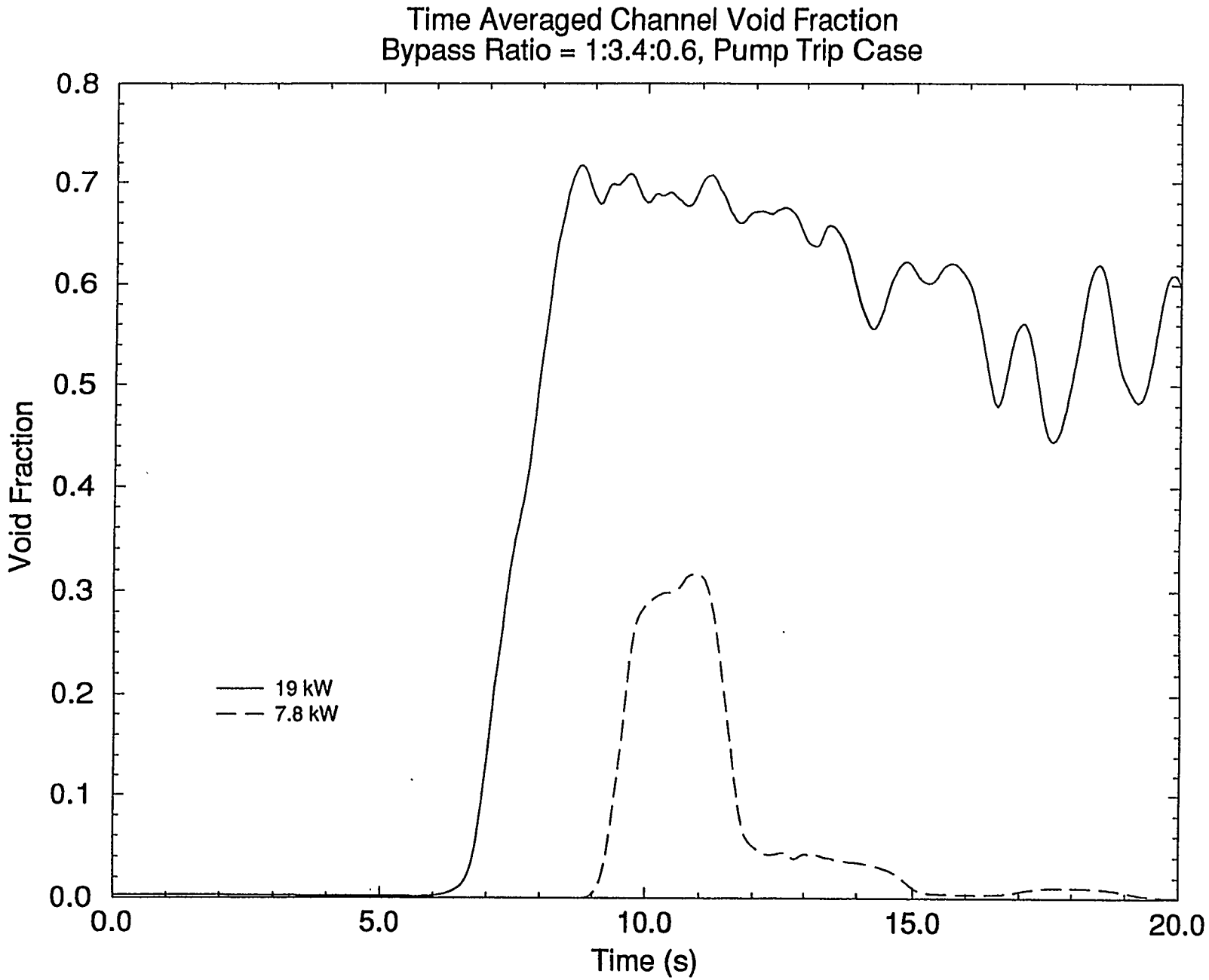

Figure 18 Time Averaged Channel Void Fraction at 2 Power Levels (Pump Trip Test Simulations)

APPENDIX A

TEST PROGRAM

A. GENERAL OBJECTIVES

The test program was developed with the assistance of consultants Richard Lahey and Hans Fauske, experts in the thermal-hydraulics area. The program was designed to capture, as closely as possible, the essential features of the flow reversal transient in the reactor.

1. Scaling to achieve similar thermal-hydraulic responses.

2. Spatial variation of heat generation.

3. Rate of flow coastdown on loss of pumping power.

4. Effect of flow impedance of flow reversal valves.

5. Effect of liquid level.

6. Effect of pressure.

7. Effect of initial water temperature.

8. Effect of helium evolution on depressurization.

Another objective of the test program, separate from the issue of prototypicality, was to provide a means of visualizing the flow reversal process. This was accomplished in one series of tests by designing the test channel with one side heated and one side transparent. Recordings were taken with a video camera.

The test program, as originally outlined, involved multichannel testing following completion of the single channel tests. However, after the single channel tests and modeling effort were completed, it was concluded that the delay associated with the fabrication of a multichannel loop could not be justified. Simulation of multi-channel effects is discussed in Section C.5 of this appendix.

B. DESCRIPTION OF TESTS

Three series of flow reversal tests were conducted under somewhat different test loop configurations. These changes were made to extend the range of test conditions to include the investigation of the helium void effect and the effect of very low impedance in the bypass path. The information given in B.1, B.2 and B.3 below applies to the first series of tests. The modifications for the helium void effect are described in Section

B.4. Section B.5 describes the modifications to lower the bypass path impedance.

1. Test Loop

The tests were performed with an electrically heated section representing the core, an orifice representing the flow reversal valves, a variable speed pump to simulate the flow coastdown, and auxiliary piping and equipment to simulate other pertinent structures in the reactor vessel [A1]. Figure A1 shows the various components of the test loop and their general arrangement. The test loop was set up to preserve the vertical height of the natural circulation flow path in the HFBR vessel. The heated section was a full-size mockup of a typical channel in a HFBR fuel element. The flow areas of the test loop were scaled to correspond to a typical coolant channel in the HFBR. The top of the upper plenum region was open to the atmosphere. Demineralized water was the working fluid of the test loop.

The fuel plates were simulated in the test by 6061 aluminum plates of similar thickness and powered by direct DC heating. The heated section was 2 feet in height. Two separate heater arrangements were used in the experiments. The single-sided arrangement had one heater plate and a transparent LEXAN plate separated by the coolant gap. The double-sided heater had a heater plate on each side of the coolant gap. The cross-sectional view of the single-sided heater is shown in Figure A2. The channel gap was maintained by two spacer rails installed along the side edges of the channel, overlapping the heater plate(s) by ~0.05 inch. The dimensions of the two heated sections are shown in Table A1.

The heated section was powered by a set of direct current generators. The low electrical resistance of aluminum resulted in a voltage drop of only 2 volts across the length of the heater plates. At low voltages the generator output was prone to drift. A ballast, made up of a twenty-foot length of water cooled stainless steel pipe, was installed in series with the heater plates(s) to raise the total resistance seen by the generator and stabilize the output voltage.

An orifice was used to simulate the flow impedance of the four flow reversal valves in the reactor and other core bypass paths. The nominal flow condition of the four open valves and other paths was simulated by a 0.199 inch diameter orifice. The nominal flow split between the heated section and the bypass was 2:1. Additional tests were done with other orifice sizes to determine the effect of bypass flow impedance.

The initial flow through the heated section and the bypass orifice was provided by an eccentric screw pump which has the

characteristics of a positive displacement pump. The pump capacity is 10 gpm. The effect of flow coastdown was created by using a programmable speed controller to vary the rotational speed of the pump motor.

The as-built dimensions of the test loop for the three test series are summarized in Tables A2-1, A2-2 and A2-3.

2. Instrumentation

The instrumentation layout is shown in Figure A3 and Table A3 provides functional information. The test loop was instrumented to monitor the temperature, pressure, and flow rate of the coolant. Each heater plate was monitored for current, voltage, and wall temperatures at nine locations. All data were collected digitally by a computer controlled data acquisition system. In addition, video recordings were made for all the single-sided heater tests.

The total loop flow rate was measured by a 0.5-inch turbine flowmeter (FLI1) located downstream of the circulation pump discharge. Two bi-directional turbine flowmeters were installed in the bypass line and the reflector section to measure the bypass flow (FBP) and the test section flow (FRE). The turbine flowmeters were calibrated in place for single-phase water flow in the range of 0.2 - 3.0 gpm. In case of two-phase flow or high frequency flow oscillation both the flow rate and the directional signals from the flowmeters became difficult to interpret. A differential pressure transducer (DO1) was installed across the bypass orifice plate as a backup for the bypass flow measurement. A similar transducer (DRE) was installed across the reflector turbine flowmeter (FRE).

Three pressure transducers were used to measure the absolute pressure at the inlet section (PTIB), the lower plenum (PTOB), and the upper plenum (PTP1). Five differential pressure transducers were used to measure the pressure drop along the heated section. One transducer measured the pressure drop in each quarter of the heated section (DT1, DT2, DT3, DT4), and one was for the overall heated section pressure drop measurement (DT5). The five pressure taps were located on the narrow side of the heated channel at 5 inch intervals. The differential pressure indications did not include the hydrostatic head because the zero reading was taken when the test loop and the pressure lines were filled with water. Hence, the differential pressure transducers only measured the frictional and acceleration pressure drop.

The water temperature was monitored by two types of sensors, namely, iron-constantan thermocouples and resistance temperature detectors (RTD). Test section inlet and exit

temperatures were measured by RTD's located in the inlet section (RTI1) and the lower plenum (RTO1). In addition, two thermocouples (JTI1 and JTO1) were installed at the same locations as backup measurements. Two other RTD's were located in the upper plenum (RTP1) and the reflector region (RTR1) to monitor the trend of temperature variation during the course of flow reversal and natural circulation. For the same purpose, three additional thermocouples were used in the lower plenum (JRB1), the bypass line (JRP1) and at the junction, upstream of the pump suction, where the fluid streams from the reflector and the bypass sections recombined (JRB1).

The wall temperatures of the heater plates were measured by 0.064-inch thermocouples. Each thermocouple was installed through an eyelet pinned directly to the heater plate. Nine thermocouples were evenly distributed along the middle of the heater plate at 2.5 inch intervals. They were identified from top to bottom by numbers EW01 to EW09 for the single-sided heater, and EW101 to EW109 for the first plate and EW201 to EW209 for the second plate of the double-sided heater.

The heater plates were protected from overheating during the flow reversal experiments by two types of power trips, a temperature trip and a voltage trip. Depending on the power level, all wall temperature trips were set at a temperature of about 30 - 40 degrees F above the test section exit saturation temperature. Typical temperature trip setpoint was between 260 to 280 °F. There was an increase in the electrical resistance of the aluminum plates as their temperatures rose during the course of the flow reversal transient. The upward drift in voltage was about 5 - 7 % for a coolant temperature rise from 130°F to saturation. The voltage trip was set at 10 % above the initial operating voltage. This setting was found to be high enough to avoid spurious trips while protecting the heater plates from overheating.

Power to the test section was calculated from the measured current and voltage applied to the heater plates. The current was measured separately by two calibrated shunts. The test section voltage was measured by two separate calibrated voltage divider setups. For the double-sided heater the two heater plates were installed in series. An excursion in the wall temperature or an over-shoot in the voltage across a heater plate would result in an automatic power cut off to the heated section. This was used as an indication that the thermal limit had been exceeded.

3. Test Procedure

In each test, flow reversal in the heated section was initiated by a reduction in the forced flow provided by the

circulation pump. The pump flow was ramped down linearly in time to simulate the coastdown of the HFBR primary pumps from the shutdown flow rate. A number of parameters were varied in the tests to examine their effects on the thermal limit. Among the parameters varied were the rate of flow coastdown, inlet subcooling, water level in the upper plenum, bypass ratio (ratio of initial flow through the heated section to initial flow through the bypass orifice), and single versus double-sided heating. The baseline test conditions were:

Mode of heating: single-sided
Water level: 14 feet above the top of the inlet section
Inlet temperature: 130 °F, entering the heated section
Coastdown time: 40 seconds
Bypass ratio: 2:1

For a given set of test conditions the flow reversal experiment was repeated at increasing power levels to the heated section until the thermal limit was bracketed within a 0.5 kW interval. The power was maintained at the specified level throughout each test run. However there was a small upward drift in power due to the changing electrical resistance of the heated section as the temperature increased. A successful flow reversal was defined as a test where natural circulation cooling was sustained without a power trip for more than 30 seconds after flow reversal.

4. Modifications for Helium Evolution Tests

Since the HFBR vessel is pressurized by helium to 200 psig during normal operation the coolant is saturated with dissolved helium. The vessel is automatically depressurized on loss of coolant and the dissolved helium will evolve from the coolant in the form of small bubbles. The maximum anticipated void fraction is ≈15% [A2]. The helium bubbles may influence the heat transfer and coolant flow in the heated channels during flow reversal.

Since the flow reversal test loop was not designed to operate at 200 psig, the helium dissolution effect was simulated by preparing a saturated solution of helium in water at 200 psig in a separate tank and feeding the helium saturated water at a controlled rate to the test loop through a supply valve which dropped the pressure in the water to close to atmospheric [A3]. The flow reversal test was initiated as soon as the test loop was filled with the helium-water mixture to minimize the coalescence and separation of the evolved helium that would normally occur after a period of time. The void fraction was determined from the static pressure difference between two elevations in the upper plenum of the test loop.

During the first tests with helium, large gas bubbles were observed to rise from the bottom of the heated section when the forced flow had coasted down to almost zero. The gas bubbles were from the helium gas accumulated in the vertically oriented open space in the bottom plenum adapter section. In the HFBR vessel, there is no confined vertical space below the core region and hence any significant accumulation of helium in the lower plenum region is unlikely.

Three modifications were made to the test loop to limit helium accumulation in the bottom plenum section. The vertical section of the bottom plenum was shortened. A filler piece was inserted in the vertical section to eliminate extra open space. The horizontal portion of the bottom plenum was tilted upward at a 10 degree angle to prevent helium accumulation. The modified test loop is shown in Figure A4.

The preliminary helium test not only indicated a need to limit the helium accumulation but also a need to conduct further tests to study the effects of bypass flow restriction. An earlier test result (1993) [A1] indicated a slightly higher thermal limit for a smaller bypass orifice. This result was contrary to the expectation that an increase in flow restriction would lower the thermal limit. When flow reversal tests conducted as part of the preliminary helium tests indicated a slightly lower thermal limit with increased flow restriction, it was decided that further tests be done with a variety of bypass flow restrictions to clarify the issue before modifying the loop for the helium tests. In these tests care was exercised not to disturb the channel gap clearance which could be affected (within specified tolerances) by adjustments made to the test section. In the earlier 1993, test series, such adjustments may have affected gap clearance sufficiently to cause the higher thermal limit. The results of the tests in which the bypass orifice size was varied, confirmed the expectation that a smaller (more restrictive) bypass orifice reduces the thermal limit.

5. Modification to Lower the Bypass Path Impedance

After reviewing the results of previous tests and analyses it was concluded that the data base should be expanded to develop more confidence in the RELAP5 simulations of the tests and the ability to predict dryout in the multi-channel HFBR core. As discussed in detail in Section C.5, the multichannel core with channel to channel variations in heating rates is equivalent in some respects to a single channel with a low impedance in the bypass path. One measure of the bypass impedance is the bypass ratio which as noted earlier is the ratio of flow in the channel to flow in the bypass path under initial flow conditions. The baseline condition for the bypass ratio is 2:1 which is the ratio of flow in the core to the flow in

bypass paths when all channels are in downflow. However, the cooler channels can be considered as part of the bypass path since they are still in downflow when the hot channels reverse. The effective bypass ratio in this situation is much smaller. If only the hottest channels are considered it is estimated that the effective bypass ratio is about 1:14. Achieving this bypass ratio would require a substantial increase in the size of the pump and major changes to the loop and was considered impractical. Instead a compromise value of 1:3.4 was selected. This was judged to be sufficiently different from the earlier tests to achieve the desired effect.

Several modifications to the loop were made as can be seen from the Figure A5 which is a schematic of the modified loop [A4]. The corresponding isometric drawing of the modified loop is shown in Figure A6.

1. The positive displacement pump was replaced with a larger capacity pump. The diameter of the supply and return line to the pump was increased and the flowmeter in the pump discharge line was replaced with one of increased capacity. Neither of these changes affected the bypass path flow impedance.

2. The bypass line (the line containing valve V2 in Figure A5) originally had a 1/2" turbine flow meter and an orifice to simulate the flow reversal valves. The flow meter and orifice plate were eliminated and replaced with a valve (V2) for flow adjustment.

3. The 1/2" turbine flow meter in the reflector section was replaced with a section of 2 1/2" diameter pipe.

4. A magnetic flowmeter which consisted of a foot long section of 1/2" diameter pipe was installed in the vertical section of the reflector.

5. A line was added from the pump discharge (near flowmeter FLI 1) to the line below the heated section. This was a 1" line which contained a 3/4" turbine flowmeter and a gate valve. This line was intended to simulate another aspect of the multiple channels in the core. While in downflow the water temperature change from inlet to outlet is determined by the average core power rather than the hot channel power. Thus the water temperature entering the bottom of the channels when reversal occurs would be lower than would be the case with a single channel test with a hot channel. This secondary line injects unheated water into the region below the heated section at a rate that when mixed with the water from the heated section, will result in an average temperature that will be approximately equal to the water temperature

below the core. An earlier version of this bypass line was located such that the line ran from above the inlet section to below the heated section. This path would exactly simulate an unheated parallel channel. However it was not possible to achieve the necessary flow with this arrangement so that location of the high pressure end of the line was changed. The ratio of the channel flow to this bypass flow was 1:0.6.

C. COMPARISON OF TEST AND REACTOR CONDITIONS

In Part A the general objectives of the test program were outlined. How these objectives were met are discussed below.

1. Initial Conditions for the Test

In principle, the initial conditions for the tests should match the conditions in the HFBR at the beginning of flow coastdown. However the relatively high heat transfer coefficients with the core, the low thermal inertia of the fuel element and slow flow transients result in essentially steady state conditions existing from the start of coastdown where coolant velocities in the core are 35-40 ft/sec to shutdown cooling flow levels where velocities are 2-3 ft/sec. This fact simplified the experimental requirements by making it possible to initiate the tests at relatively low flow rates (≈3 gpm). This flow rate was analogous to a total reactor flow rate of 1300 gpm which is the flow rate when a single pony motor driven pump provides the shutdown cooling flow.

During the flow coastdown period, the water temperature at the inlet to the core will remain constant at the full power steady state value of 130°F (nominal) until the water at the heat exchanger outlet has been transported to the core inlet. The water that enters the core after this time will be at or below 130°F depending on the timing of the reactor trip with respect to the initiation of pump coastdown. Conducting the base case test at a constant inlet temperature of 130°F will therefore be conservative. However, to assess the magnitude of the temperature effect and to determine the effect of variations in full power core inlet temperature, flow reversal tests were also performed at 110 and 150°F.

2. Scaling of Test Loop

The scaling criteria for the test loop were based on the similarity rules derived by Ishii and Kataoka [A5]. The following assumptions were used in establishing the scaling criteria.

a. Identical coolant channel dimensions.

b. Dynamic similarity (inertia and pressure loss) preserved for the natural circulation loop. It should be noted that in the first and second series of tests (Figure A3, A4) the pressure loss due to a turbine flow meter in series with the test section was overlooked. For these tests the pressure loss in the loop was relatively higher than in the reactor. In the last test series (Figure A5) the turbine flowmeter was replaced with a low impedance magnetic flowmeter. In this latter test configuration the pressure losses were similar to the reactor losses.

c. Similar thermal inertia, particularly in the large volume regions which are the upper and lower plenum and reflector.

With respect to the channel dimensions there are 4 different channel sizes in the HFBR fuel element. They all have the same height (24") and width (2.46") but have nominal gaps of 0.100", 0.118", 0.108" and 0.096". A nominal value of 0.100" was selected for the test channel gap. Because it was necessary to allow for thermal expansion of the heated plates, the plate could not be rigidly fixed and as a result there was some uncertainty in the channel gap. The design specification resulted in a gap that could vary between 0.10" and 0.113" for the single sided heater and between 0.098" and 0.116" for the two-sided heater. In analyzing the test data, the maximum gap value was conservatively assumed. A channel with a larger flow area will have a larger heat removal capacity, all other things being equal.

In Table 1 it is seen that the heated width of the reactor channel (2.25") is matched in the test channel. However the reactor channel width (2.46") is larger than the heated width while the test channel width (2.16") is slightly smaller than the heated width. The original design of the test section called for making the channel and heated widths the same, 2.25". This was a design simplification which was considered to be conservative. However when buckling of the heated plate was experienced during preliminary testing, the design was modified again by using spacer rails along the side edges of the plate to maintain the gap. These rails overlapped the heater plate(s) by about 0.05" and thereby reduced the channel width. This modification was also considered conservative since it reduced the heat transfer area exposed to the coolant and thereby increased the heat flux.

The dimensions of the heated channel could also be affected by deflection of the transparent LEXAN plate due to internal water pressure and thermal expansion. An analysis of these effects indicates that the plate deflection is not large enough to require a correction to the experimental results [A6].

Details of the scaling analysis are given in Reference [A7].

3. Spatial Variation of Heat Generation in Fuel

In the reactor the heat generation rate varies from fuel plate to fuel plate and within a single plate. This applies to full power operation and to shutdown conditions which are of concern here. The ratio of peak local heat generation rate in the hot plate to the average in the hot plate is 1.80 [A8]. It was not feasible to simulate this spatial variation in the tests. The electrically heated aluminum plates were of uniform cross-section so that the heat generation was uniform across the width and length of the plate. However the importance of span wise variations in the heating rate could be assessed by comparing the results of tests in which one side of the channel was heated to the case where both sides were heated. Thus for 2 tests conducted at the same total channel power, the heat flux for the test with one side heated is twice the flux of the 2 sides heated. The effect of axial variation in heating rate was evaluated using the RELAP5 Code and is discussed in Appendix C.

With regard to the tests in which both sides of the channel were heated, the thickness of the plate was 0.025 in., which is one-half of the fuel plate thickness. The half thickness is used to reflect the fact that in the reactor each plate is cooled on two sides by adjacent channels whereas only one channel is used in the test.

In the tests in which the channel was heated on one side only, the thickness of the heated plate was 0.050 in. The purpose here was to match the transient characteristics of the plates in the two sided heating tests. Thus for the same total channel power, the heat generation per unit volume of plate would be the same in both cases.

4. Rate of Flow Coastdown

A flywheel was mounted on each of the primary pump motors in the HFBR because of concern about downflow stability at the design flow rate of the shutdown pump. The flywheel also delayed the onset of flow reversal in the event the shutdown pump failed. This delay was beneficial in that it resulted in flow reversal occurring at a reduced afterheat power. Another consequence of the flywheel installation, that was not recognized at the time, is that the slower coastdown would tend to impede the flow reversal process. It was therefore considered important that this effect be examined in the test program. Flow coastdown measurements made on the reactor were used as a basis for establishing test conditions. These measurements were made long after the reactor was shutdown so

that there was little afterheat present. The initial condition for the measurement was a flow rate of about 1300 gpm provided by a pony motor driven primary pump. Coastdown to zero flow occurred 40 seconds after the pump was shutdown [A9]. This coastdown time was simulated in the test by means of a screw pump with a programmable speed controller to vary the speed of the pump motor.

As noted above the flow decay measurement on the reactor was made without decay heat present. If significant decay heat were present the flow rate would fall more rapidly when flow reversal occurred, because the reactor pumps are centrifugal rather than positive displacement pumps. The test program included tests at coastdown times of 30 and 60 seconds to determine the importance of this variable.

5. Flow Reversal Valve Impedance

Although the flow reversal valves are closed when the main pumps are operating at full flow, they will open at the reactor conditions corresponding to the initial conditions of the tests. It is assumed here that the shutdown pumps have also been turned off since the valves would not open if the shutdown pumps were running.

With the valves open, a fraction of the flow delivered by the primary pump(s) will bypass the core through the open valves. In addition to the valves there are other bypass paths. These include paths for control blade cooling and those formed by the spacing between the transition plate and the internal structures that penetrate it. The flow pressure drop characteristics of the flow reversal valve are based on measurements made on a prototype valve. The other bypass flows have been calculated. At a total flow rate of 1300 gpm about 18% passes through the open valves, 15% passes through the other bypass paths and the balance, 67%, passes through the core. Thus the ratio of core flow to total bypass flow is 2:1.

In the test, 3 gpm corresponded to a total flow rate in the reactor of 1300 gpm. An orifice was used to simulate the flow reversal valves and other bypass paths. An orifice size was selected to achieve the 2:1 ratio of flow rate in the heated channel to orifice flow rate.

When the pumps stop and flow reversal and natural circulation ensue, these bypass paths provide the return leg of the natural circulation loop. The flow impedance of these paths will affect the dynamics of flow reversal. To determine the importance of this parameter tests were conducted with a range of orifice sizes which corresponded to flow rate ratios from 5:1 to 1:3.4.

It should be noted that a single channel test at the maximum channel heating rate in the core does not reflect the beneficial effect of the many parallel channels that exist in the reactor and operate at lower heating rates. Flow reversal will not occur at the same time in all the channels. The return path for flow from the channel which reverses first will include the other channels still in downflow as well as the flow reversal valves and bypass paths. This effect is equivalent to a reduction in the flow impedance of the bypass path. From this viewpoint, the single channel tests with a bypass ratio of 2:1 represents a conservative bound on the reactor conditions. This issue will be discussed in greater detail in Appendix C.

6. Effect of Liquid Level

The reactor vessel liquid level at which flow reversal occurs will depend on the accident scenario. If the accident does not involve a loss of coolant, the level will remain at its nominal operating value of about 14 feet above the top of the inlet section of the fuel element. In the LOCA scenarios analyzed, the liquid level has dropped no more than 4 feet by the time flow reversal has occurred. After flow reversal, the water level continues to drop, depending on the location of the leak and could fall to a point about 2 feet above the top of inlet section of the fuel element in a leak in a beam tube. This level corresponds to the top of the thermal shield cavity.

In order to bound the effect of liquid level, tests were done with the level at 14 feet and at 3.7 feet above the top of the inlet section to the test section.

7. Effect of Pressure

Depressurization of the primary system occurs automatically in the HFBR in all loss of forced flow cooling accidents. The depressurization is accomplished by opening a valve in the helium cover gas and venting the gas to atmosphere. In some accidents flow reversal will occur when depressurization is complete, i.e., the cover gas is at atmospheric pressure. In others there may be a residual pressure above atmospheric at the time of flow reversal. The current reactor power level is based on the conservative assumption that the decay heat removal mechanism is by counter-current flow with coolant entering the core from the top only [A10]. In flooding limited models an increase in pressure will result in an increase in heat removal capacity at least in the pressure range of interest here. Other correlations of CHF (critical heat flux or dryout) in boiling in narrow rectangular channels indicate that increases in pressure cause an increase in CHF [A11, A12]. Accordingly conducting the tests at atmospheric

pressure is considered conservative.

8. Effect of Helium Evolution

In the reactor, the amount of helium gas dispersed in the reactor coolant at the time of flow reversal depends on the rate of depressurization, the coolant flow rate and the kinetics of helium dissolution. Since those factors are scenario dependent and in some cases difficult to quantify a bounding approach is taken to determine the quantity of dispersed helium present. It is assumed that during the depressurization and coastdown period (1) all the helium that can come out of solution, based on equilibrium considerations, will come out and (2) that this precipitated helium does not escape to the cover gas but remains dispersed as bubbles in the liquid. The volume fraction due to helium voids in the core region under these assumptions is about 15% [A2].

As described in Section B4 the method used to simulate helium voids in the test was to introduce helium saturated water into the loop from a separate tank which was pressurized with helium at 200 psig. The test was begun (coastdown initiated) after sufficient helium containing water was introduced to displace the helium free water originally present in the test loop. When the concept of introducing the water from a separate tank was originally proposed it was not clear how well it would work since it was possible that the gas bubbles would coalesce and separate from the liquid before coastdown began. However, the concept was much simpler than the alternative of replacing the existing loop with one designed for operation at 200 psig and was considered to be worth the modest additional cost in time and money. Fortunately the experimental approach was found capable of producing void fractions of about 10% which permitted projections to be made of the effect of a void fraction of 15% that was calculated for the reactor.

It was not possible to precisely control the helium void fraction which varied from test to test. The maximum void fraction achieved was 13%. In one of the tests the helium dissipated before flow reversal and essentially no helium voids were measured. In the two tests where significant helium voids were measured the ratio of the % change in "no trip" power to % change in void fraction was calculated. The two values were 0.29 and 0.66. The maximum helium void fraction anticipated in the reactor is 15%. Using the higher value of the ratio (0.66) to extrapolate to 15% voids, the reduction in dryout power is calculated to be 9.9%. This is used as the basis for the projected 10% reduction in power caused by 15% voids.

D. DISCUSSION OF TEST DATA FOR SELECTED TESTS

The data from two flow reversal tests have been selected to illustrate the typical results of the two possible end states of a test. Depending on the power level and the other test conditions, a flow reversal transient can lead to either natural circulation cooling of the heated section or a thermal excursion in the heated section. The two tests selected for discussion correspond to a case of safe flow reversal and a case of power trip, both under the baseline test conditions.

Test 1 - Safe Flow Reversal, Single-Sided Heating

For the test conducted under the baseline conditions, the maximum power level for safe flow reversal is 9 kW. The linear flow coastdown is evident in Fig. A7.1 which shows the measured loop (pump) flow rate. The flow rate indicates that coastdown begins 3 seconds after the initiation of data recording at time zero.

The plate temperatures at the top, middle and bottom of the heated section are shown in Figures A7.2, A7.3, and A7.4 respectively. The initial rise in wall temperature is a result of flow reduction due to pump coastdown. Initially the top wall temperature is lower than the bottom wall temperature because the forced flow is in the downward direction. At about 35 sec. the bottom wall temperature starts to decrease while the top temperature continues to rise. This is an indication of flow reversal with water from the reflector region feeding the heated section from below and hot water rising up to the top of the heated section. The top wall temperature increases to ≈225°F and remains relatively steady for the rest of the test.

The occurrence of flow reversal is also quite obvious in the temperature response of the coolant flowing in the test section. Coolant temperatures at different locations of the test loop are shown in Figure A7.5. Flow reversal is clearly demonstrated by the increase and then stabilization of the water temperature in the channel top (test section inlet).

The increase in wall temperature that accompanies the change from forced convection to free convection heat removal causes an increase in the electrical resistance of the heated plate. Since the electrical current was kept constant at ≈4 kA during the test, the increase in resistance was reflected in an upward drift in voltage across the heated section. The increase in power caused by the upward drift in voltage is shown in Figure A7.6. By the time of flow reversal, the channel power has increased from an initial value of 9 kW to 9.45 kW. The test was terminated by a manual power trip at about 155 seconds.

For this test series a bi-directional magnetic flow meters was

used to measure the water volumetric flow rate in the reflector region of the test loop. The measured reflector flow is shown in Figure A7.7. The initial positive flow direction of the reflector flow is away from the heated section (downflow). The first change in flow direction occurs at 35 sec. and from that point onward, the reflector flow fluctuates between a positive and negative direction. Based on visual observations, the flow oscillations after flow reversal have a period of about one to two seconds. The flow meter may not have accurately followed the frequent acceleration and deceleration of the coolant flow that is associated with phase changes due to boiling and condensation. The consequence is that the bi-directional magnetic flow meter may not provide accurate measurements during rapid flow transients.

Another parameter of interest is the channel pressure drop which provides indications of flow direction and voiding in the heated section. Five differential pressure transducers were used to measure the pressure drop due to friction and acceleration along the heated section. Figure A7.8 shows the overall channel pressure drop (sum of the pressure drop in each quarter of the heated section).

Mathematically the measured channel pressure drop represents,

$$\Delta P_{Channel} = P_{Top} - P_{Bottom} + H_L$$

where

P_{Top} = Static pressure at the top of the heated section.

P_{Bottom} = Static pressure at the bottom of the heated section.

H_L = Hydrostatic pressure of stagnant water equivalent to the height of the heated section.

When water is stagnant in the heated section, $\Delta P_{Channel} = 0$. Channel pressure drop is positive ($\Delta P_{Channel} > 0$) for single-phase liquid downflow and negative ($\Delta P_{Channel} < 0$) for single-phase liquid upflow. Any voiding in the channel will have a positive contribution to the channel pressure drop. In Figure A7.8 the channel pressure drop is seen to decrease during the flow coastdown and then rise rapidly at the time of flow reversal. The increase in measured pressure drop is due to voiding in the channel. A completely voided channel with zero flow would have reached a pressure drop reading of ≈0.9 psi.

The data from the baseline test at 9 kW demonstrated that natural circulation was established in the coolant channel after flow reversal and there was no overheating of the heated plates during and after the reversal.

Test 2 - Power Trip, Single-Side Heating

A wall temperature trip was the result of conducting the baseline test at an initial power level of 9.5 kW. The trip occurred a few seconds after the first change in flow direction was recorded while there was still forced downflow from the pump.

The pump flow data shown in Figure A8.1 indicates that the 40 sec. flow coastdown starts 5 seconds after the initiation of data recording at time zero.

In Figure A8.2 the temperature response of the heated plate at the top of the test section shows a rapid increase at about 38 sec. About 2 seconds later the wall temperature hits the trip setpoint. Depending on the power level, all plate temperature trips were set at a temperature of 30 - 40 degrees above the test section exit saturation temperature. Typical trip setpoint was between 260°F and 280°F. The plate temperatures at the middle and bottom of the heated section, shown in Figure A8.3 and A8.4, do not exhibit rapid temperature rise before the power trip. The drop in the bottom wall temperature at 35 sec. suggests that flow reversal has started prior to the power trip.

In this flow transient, the reversal has started but was not yet established by the time of the power trip. This observation can also be deduced from the coolant temperature data shown in Figure A8.5. The temperature of the coolant just above the top of the heated section is increasing after 35 seconds but it reaches only 185°F by the time of the trip, still 50 degrees F below the saturation temperature.

The voltage and power data shown in Figure A8.6 do not exhibit any rapid change prior to the power trip.

The behavior of the reflector flow, shown in Figure A8.7, at the time of flow reversal is typical of all flow reversal tests. At the time of flow reversal, there is a momentary increase of flow followed by a change in the flow direction of the reflector flow.

The channel pressure drop shown in Figure A8.8 reaches a peak value of 0.55 psi when the power trip occurred. The peak pressure drop for the corresponding safe flow reversal case is 0.5 psi (see Figure A7.8). Figure A8.8 shows that the overall channel pressure drop is above 0.5 psi for about 2 seconds right before the power trip. Assuming negligible pressure drop due to coolant flow, a 0.5 psi pressure drop is equivalent to about 60% (0.5/0.9) void fraction in the heated section. The data tend to support a correlation between the power trip and the channel void fraction being above a threshold value for a short period of time.

References:

[A1] Yang, B.W., et.al, 1993, "BNL Single Channel Thermal Hydraulic Test Program for the HFBR," Columbia University Heat Transfer Research Facility, CU-HTRF-93-05 (Final Report, Vol. I and II).

[A2] Tichler, P.R., 1989, "Effect of Helium Dissolution on Core Heat Transfer Following Emergency Shutdown," BNL Memorandum to Files.

[A3] Yang, B.W., et.al., 1994, "BNL Single Channel Thermal Hydraulic Test Program for the HFBR - Helium Evolution and Bypass Flow Restriction Effects," CU-HTRF-94-02 (Final Report - Vol. I and II).

[A4] Yang, B.W., et.al., 1995, "BNL Single Channel Thermal Hydraulic Test Program for the HFBR - Flow Reversal with Reduced Bypass Flow Restriction," CU-HTRF-95-03 (Final Report - Vol. I and II).

[A5] Ishii, M. and Kataoka, I., 1984, "Scaling Laws for Thermal Hydraulic System Under Single-Phase and Two-Phase Natural Circulation," Nuclear Engineering Design, Vol. 81, pp 411-425.

[A6] Tichler, P., 1996, Response to Comments by ANL on the "Flow Reversal Power Limit for the HFBR, Rev. 0," (ANL-1, Comment #2).

[A7] Cheng, L.Y., 1992, "Scaling Criteria for the Single-Channel Test," BNL Memorandum to Files.

[A8] Tichler, P., 1995, "Power Density Ratio in Hot Stripe of Hot Plate Under Shutdown Conditions," BNL Memorandum to Files.

[A9] Mevs, Ralph, 1991, "Primary Pump and Pony Motor Coastdown Flow Measurement," BNL Memorandum.

[A10] Tichler, P.R., Cheng, L.Y., and Fauske, H., 1991, "Core Cooling Under Accident Conditions at the High Flux Beam Reactor (HFBR)," Transactions ANS, Vol. 64, pp. 385-386.

[A11] Monde, M., Kusuda, H., and Uehara, H., 1982, "Critical Heat Flux during Natural Convective Boiling in Vertical Rectangular Channels Submerged in Saturated Liquid," J. Heat Transfer, 104, pp. 300-303.

[A12] Mishima, K. and Nishihara, H., 1982, "The Effect of Flow Direction and Magnitude on CHF for Low Pressure Water in Thin Rectangular Channels," Nuc. Eng. & Design, 86, pp. 165-181.

LIST OF TABLES

LIST OF FIGURES

TABLE A1 HEATED SECTION DIMENSIONS	
Single Sided Heater	
width of channel	2.160 inches
channel gap	0.10 - 0.113 inches
channel length	24.00 inches
heater width	2.25 inches
heater length	22.750 inches
heater thickness	0.050 inches
Double Sided Heater	
width of channel	2.160 inches
channel gap	0.098 - 0.116 inches
channel length	24.00 inches
heater width	2.25 inches
heater length	22.750 inches
thickness of heaters	0.025 inches

TABLE A2-1

AS-BUILT DIMENSIONS OF FLOW LOOP COMPONENTS FOR THE FIRST TEST SERIES

Upper Plenum - Rectangular Section	Width = 3 in Gap = 0.485 in Height = 3 ft
- Pipe Section	ID = 1.38 in Height = 14 ft
Inlet Section	Width = 2.46 in Gap = 0.135 in Height = 13 in
Test Section Adapter Plates (Total 2 plates: at top and bottom of test section)	Width = 2.46 in Gap = 0.126 in (top), 0.485 in (bottom) Height = 1.5 in each
Lower Plenum & Reflector Region - Vertical Section Below Test Section	ID = 2.635 in, Length = 12 in (1.5" OD insert - single-sided heater) (0.5" OD insert x 4 - double-sided heater)
- Horizontal Section	ID = 2.635 in, Length = 35 in (includes flow meter section: ID = 0.674 in, L = 12 in)
- Vertical Section	ID = 2.635 in, Length = 56 in
Flow Bypass	ID = 2.635 in, Length = 35 in (includes flowmeter section: ID = 0.674 in, L = 12 in)
Orifice Plate - Test Section Flow to Bypass Flow = 2:1	Pipe ID = 2.635 Orifice Dia. = 0.199 in
- Test Section Flow to Bypass Flow = 5:1	Pipe ID = 2.635 Orifice Dia. = 0.129 in

TABLE A2-2

AS-BUILT DIMENSIONS OF FLOW LOOP COMPONENTS FOR THE HELIUM TEST

Upper Plenum - Rectangular Section	Width = 3 in Gap = 0.485 in Height = 3 ft
- Pipe Section	ID = 1.38 in Height = 14 ft
Inlet Section	Width = 2.46 in Gap = 0.135 in Height = 13 in
Test Section Adapter Plates (Total 2 plates: at top and bottom of test section)	Top: Width = 2.46 in Gap = 0.126 in Height = 1.5 in Bottom: Width = 1.75 in Gap = 0.125 in Height = 2 in
Lower Plenum & Reflector Region - Vertical Section Below Test Section (R-1) a. Rectangular Section	Width = 1.75 in, Gap = 0.125 in, Height = 3.125
b. Pipe Section	ID = 2.635 in, Length = 1.625 in (plus a 5.5 in section extending below the junction with the inclined section.) Net flow area in pipe section = 3.66 sq. in
- Inclined Section (10°) - (R-2)	ID = 2.635 in, Length = 46 in (includes flow meter section: ID = 0.674 in, L = 12 in)
- Lower Vertical Section (R-3)	ID = 2.635 in, Length = 19.5 in
- Horizontal Section (R-4)	ID = 2.635 in, Length = 10 in
- Upper Vertical Section (R-5)	ID = 2.635 in, Length = 22 in
Flow Bypass	ID = 2.635 in, Length = 35 in (includes flowmeter section: ID = 0.674 in, L = 12 in)
Orifice Plate	0.280 in, 0.199 in, 0.129 in

TABLE A2-3

AS-BUILT DIMENSIONS OF FLOW LOOP COMPONENTS FOR THE EXTENDED BYPASS RATIO TESTS

Upper Plenum - Rectangular Section	Width = 3 in Gap = 0.485 in Height = 3 ft
- Pipe Section	ID = 1.38 in Height = 14 ft
Inlet Section	Width = 2.46 in Gap = 0.135 in Height = 13 in
Test Section Adapter Plates (Total 2 plates: at top and bottom of test section)	Width = 2.46 in Gap = 0.126 in (top), 0.485 in (bottom) Height = 1.5 in
Lower Plenum & Reflector Region - Vertical Section Below Test Section	ID = 2.635 in, Length = 7 in (plus 5 in section extending below the junction with the inclined section.) (1.5" OD insert - single-sided heater)
- Inclined Section	ID = 2.635 in, Length = 46 in (includes a 2" valve)
- Lower Vertical Section	ID = 2.635 in, Length = 13.5 in (includes a 2.25 in section of 1.097" ID pipe)
- Measurement Spool Piece in the Mid-Vertical Section	ID = 0.674 in, Length = 13.5 in
- Upper Vertical Section	ID = 2.635 in, Length = 13.5 in (includes a 2.25 in section of 1.097 in ID pipe)
Primary Flow Bypass	ID = 2.635 in, Length = 45 in (includes a 2.5" valve)
Secondary Flow Bypass	ID = 1.097 in, Length = 212 in Height = 158 in (includes flowmeter section: ID = 0.75 in, L = 12 in and a 1" valve)

TABLE A3

INSTRUMENTATION FOR THE TEST LOOPS

NAME	INSTRUMENT	DESCRIPTION
FLI1	Turbine flowmeter	Loop (pump) volumetric flow rate.
FBP	Bi-directional turbine flowmeter	Bypass volumetric flow rate.
FRE	Bi-directional turbine flowmeter	Reflector (channel) volumetric flow rate.
FBP2	Turbine flowmeter	Flow in secondary bypass (see Figure A5).
DO1	Differential pressure transducer	Pressure drop across orifice plate in the bypass line.
DRE	Differential pressure transducer	Pressure drop across turbine flowmeter in the reflector section.
RTP1	RTD	Coolant temperature in the upper plenum.
RTI1/ JTI1	RTD/thermocouple	Coolant temperature in the inlet section (channel top)
RTO1/ JTO1	RTD/Thermocouple	Coolant temperature in region below the heated section .
JT02	Thermocouple	Coolant temperature in region immediately below heated section (see Figure A5).
RTR1/ JTR1	RTD	Coolant temperature in the reflector section.
JRP1	Thermocouple	Coolant temperature in the bypass section.
JRB1	Thermocouple	Coolant temperature upstream of the heat exchanger (H.E.).
EW01-EW09	Thermocouple	Wall temperature of single-sided heater.
EW101-EW109	Thermocouple	Wall temperature of first plate in the two-sided heater.

TABLE A3

INSTRUMENTATION FOR THE TEST LOOPS

NAME	INSTRUMENT	DESCRIPTION
EW201-EW209	Thermocouple	Wall temperature of second plate in the two-sided heater.
DT1-DT4	Differential pressure transducer	Pressure drop (friction and acceleration) in each quarter of the heated section.
DT5	Differential pressure transducer	Overall pressure drop (friction and acceleration) in the heated section.
DP	Differential pressure transducer	Pressure drop in upper plenum (for estimating void fraction, see Figure A4).
PTP1	Absolute pressure transmitter	Pressure in the upper plenum.
PTIB	Absolute pressure transmitter	Pressure in the inlet section.
PTOB	Absolute pressure transmitter	Pressure in region below the heated section.
P1-P5	Absolute pressure transducer	Pressure in heated section (see Figure A5).
Vts	Voltage	Voltage across heated section.
Its	Current	Current in heated section.

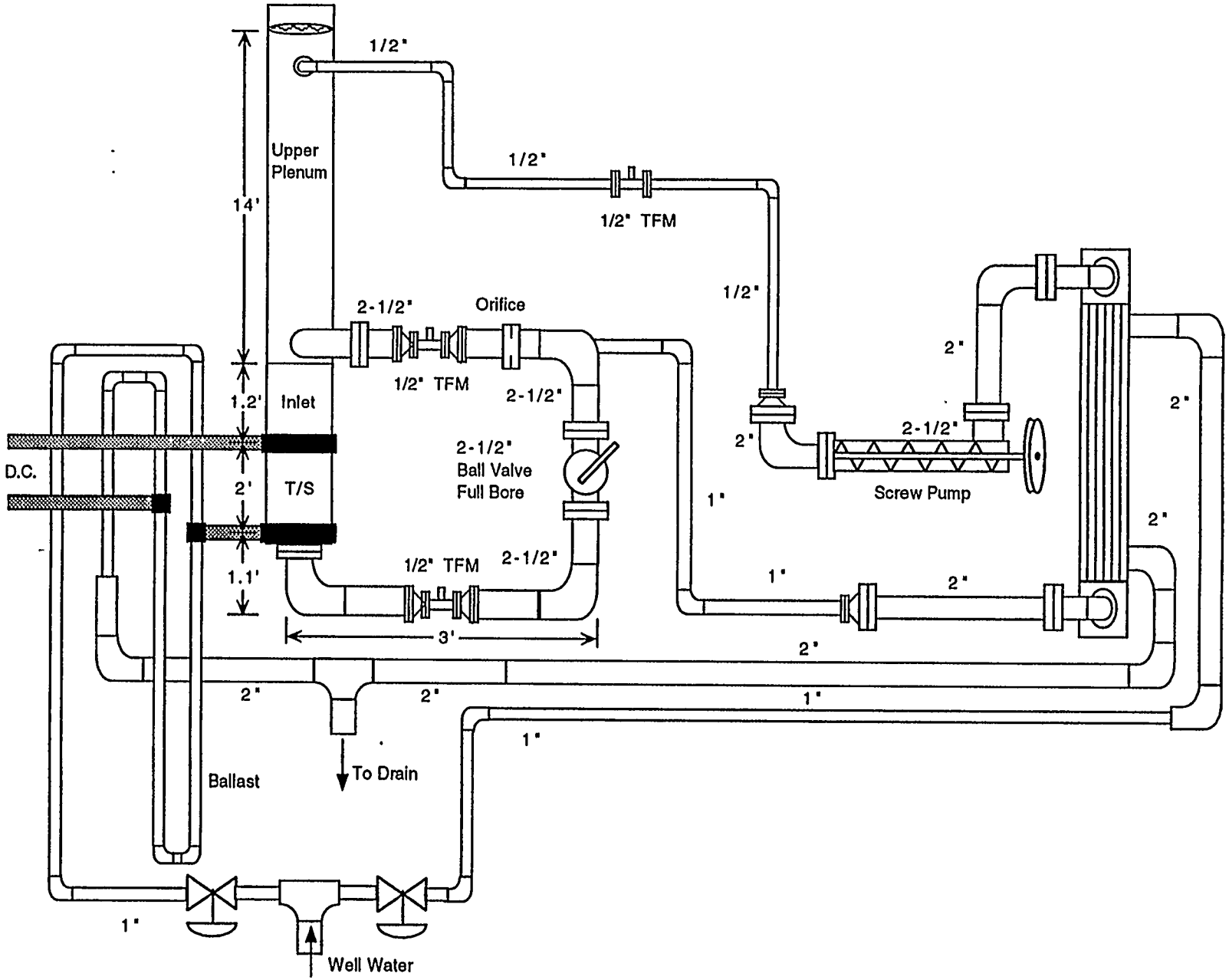

Figure A1

Schematic of the Flow Reversal Test Loop

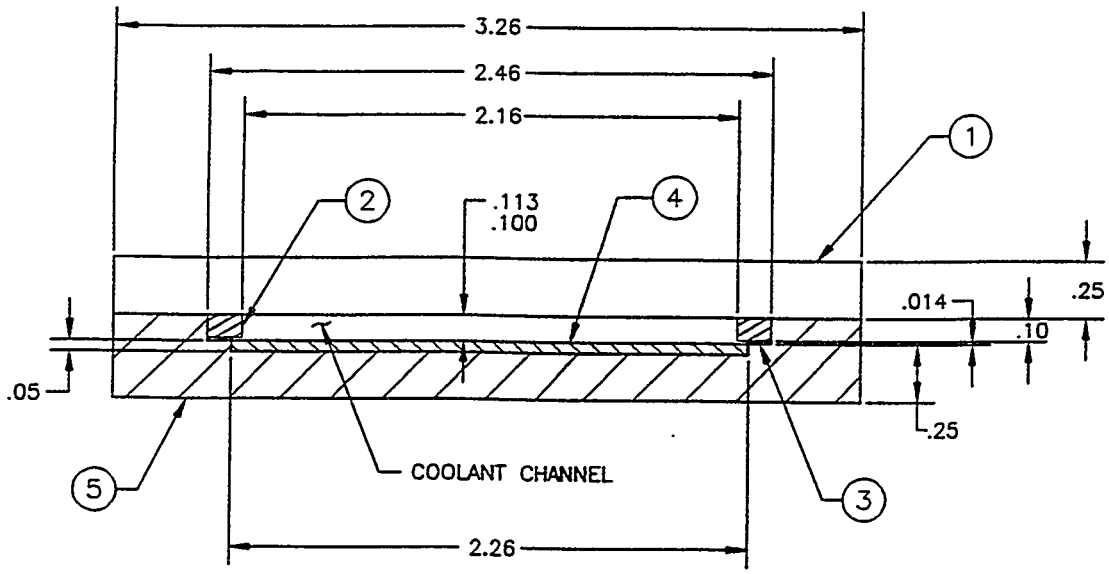

ITEM NO.	QTY.	DESCRIPTION
1	–	LEXAN
2	–	SIDE RAIL (ASBESTOS PHENOLIC)
3	–	KAPTON TAPE (4 LAYERS)
4	–	ALUMINUM HEATER STRIP (WIDTH = 2.25)
5	–	INSULATOR (PEEK)

NOTE:

1. ALL DIMENSIONS ARE NOMINAL VALUES AND IN INCHES.

Figure A2

Cross-Section of the Single-Heater Test Section

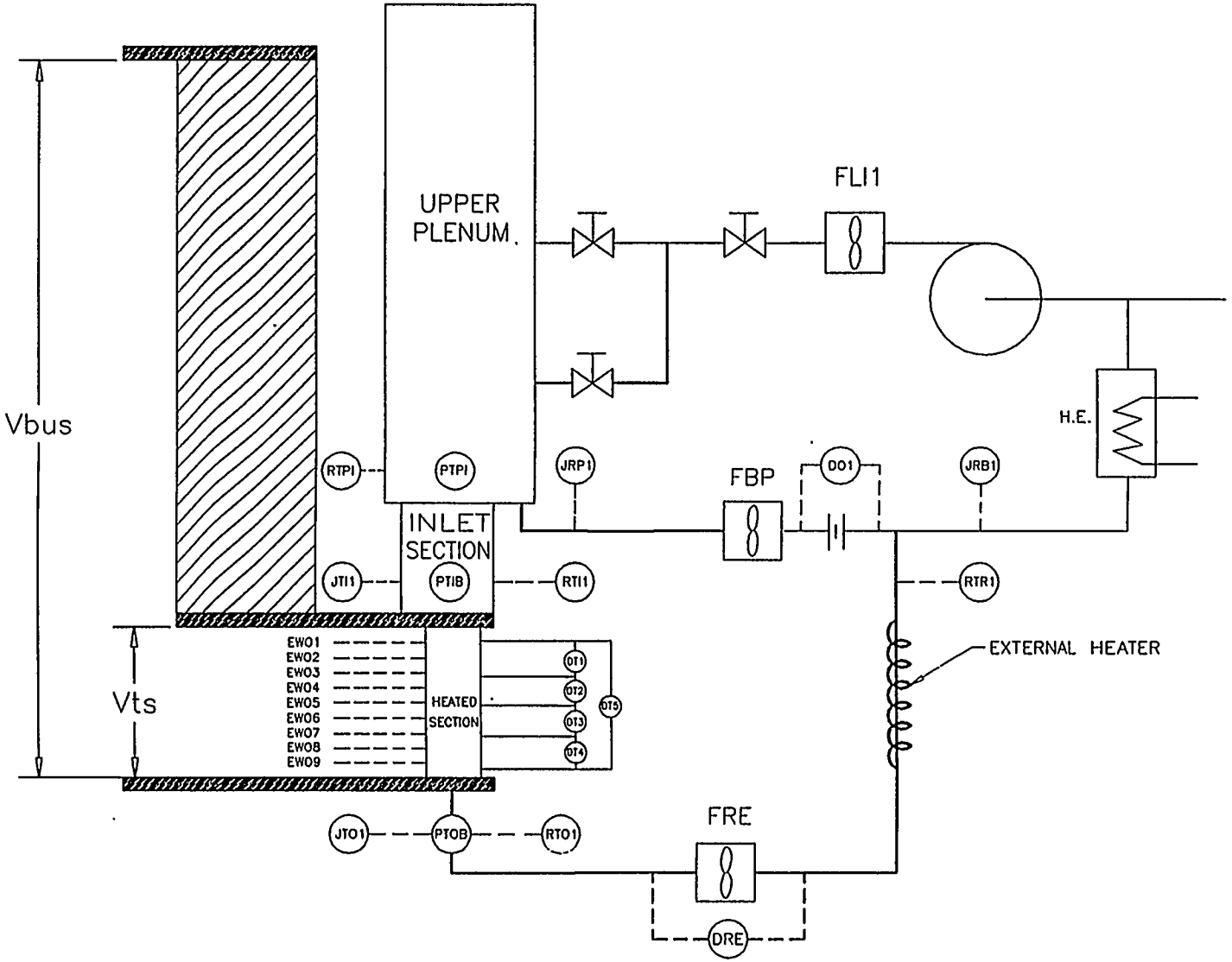

Figure A3

Schematic of Test Loop for First Test Section

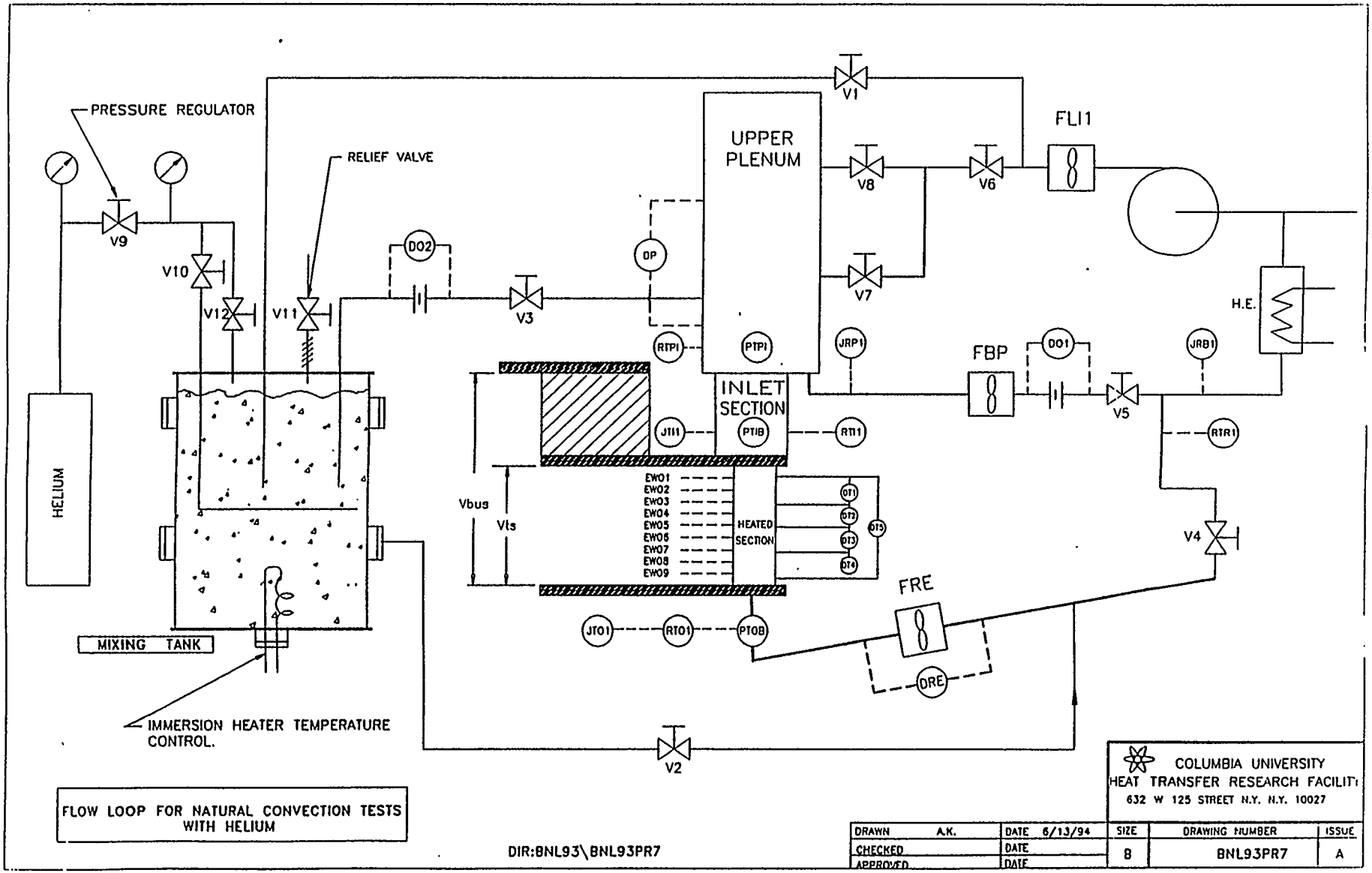

Figure A4

Schematic of Test Loop for Helium Tests

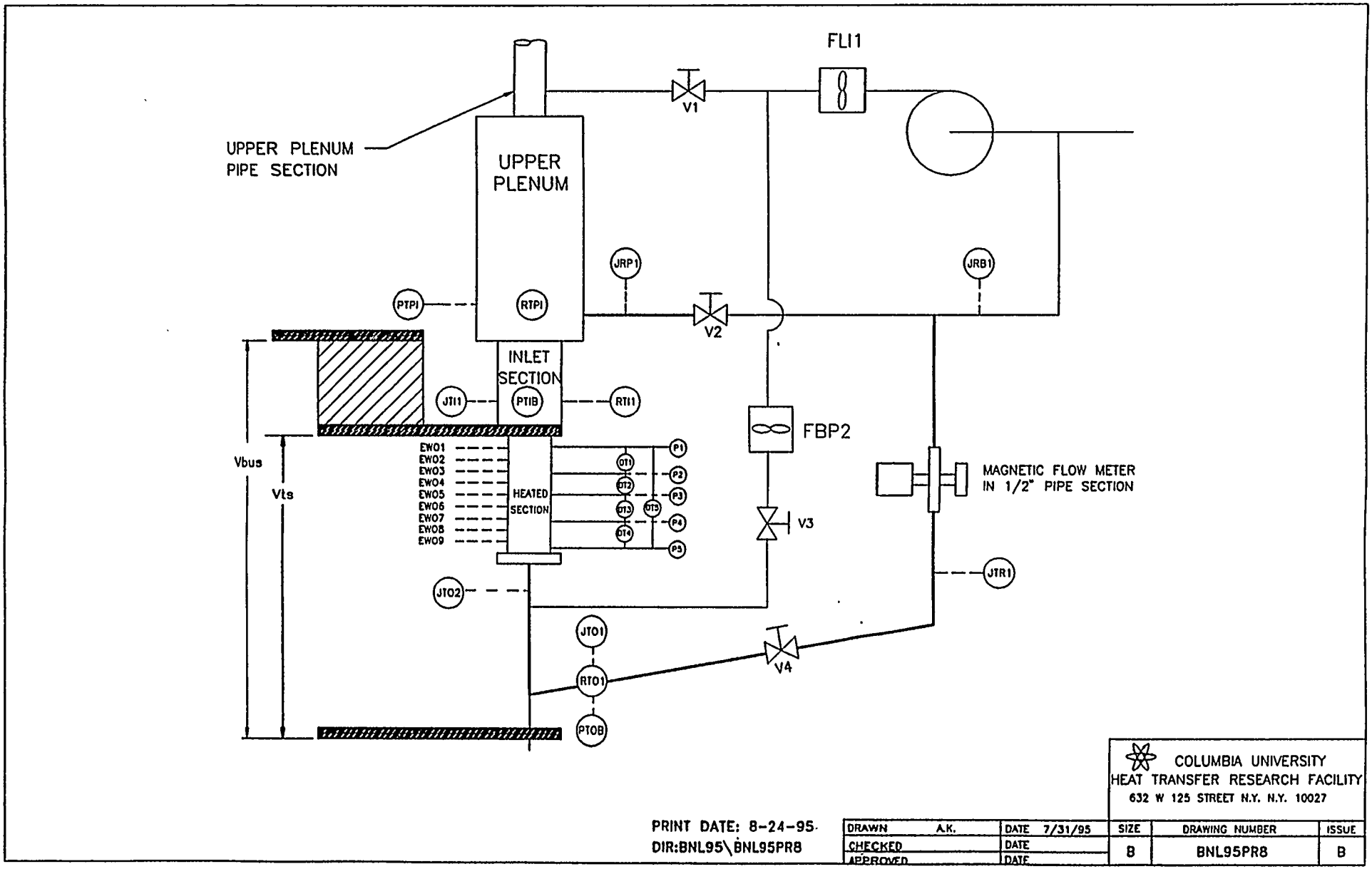

Figure A5 Schematic of Test Loop for Extended Bypass Ratio Tests

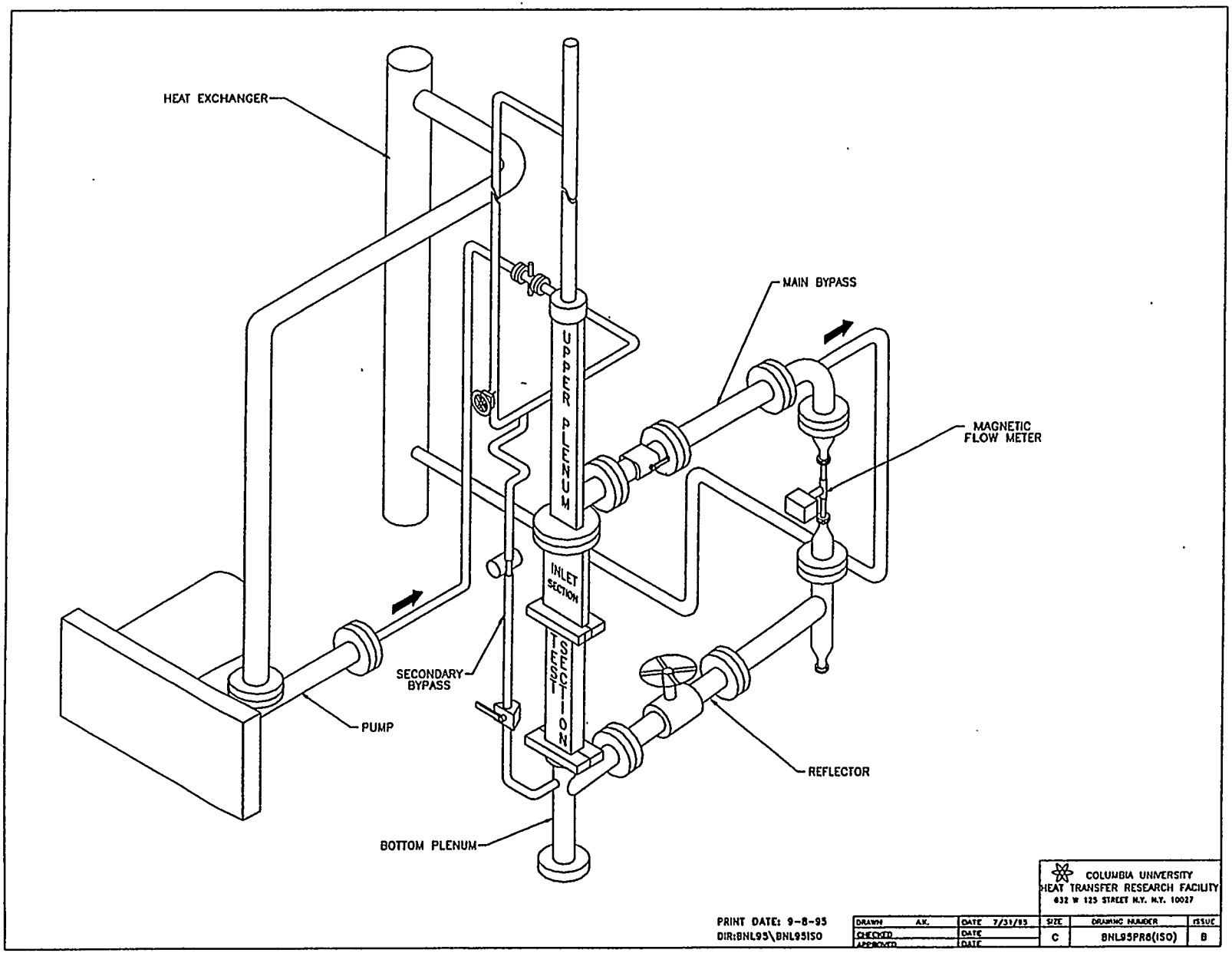

Figure A6 Isometric Drawing of the Test Loop

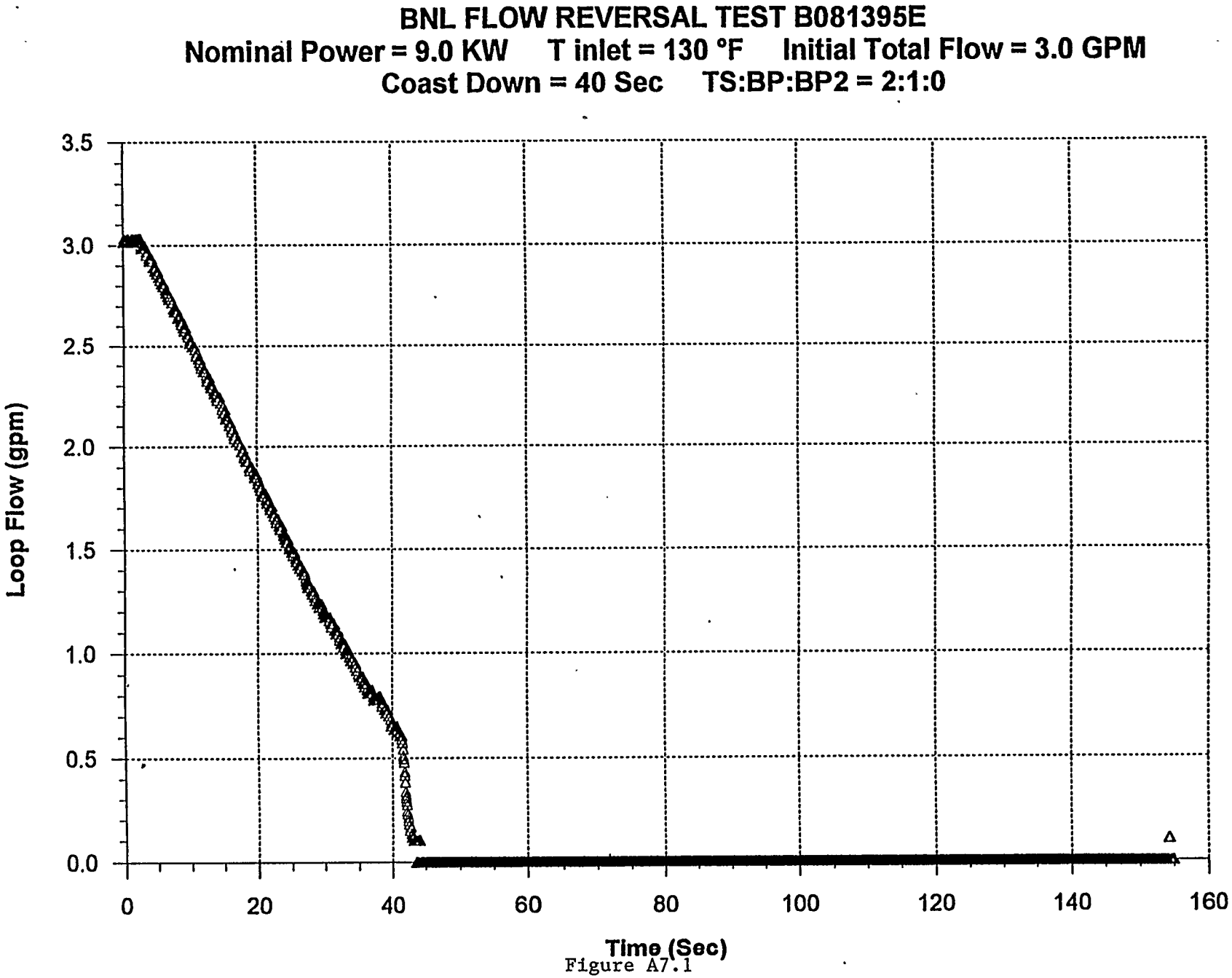
BNL FLOW REVERSAL TEST B081395E
Nominal Power = 9.0 KW T inlet = 130 °F Initial Total Flow = 3.0 GPM
Coast Down = 40 Sec TS:BP:BP2 = 2:1:0
Loop Flow (gpm)
3.5
3.0
2.5
2.0
1.5
1.0
0.5
0.0
0
20
40
60
80
100
120
140
160
Time (Sec)

Figure A7.1

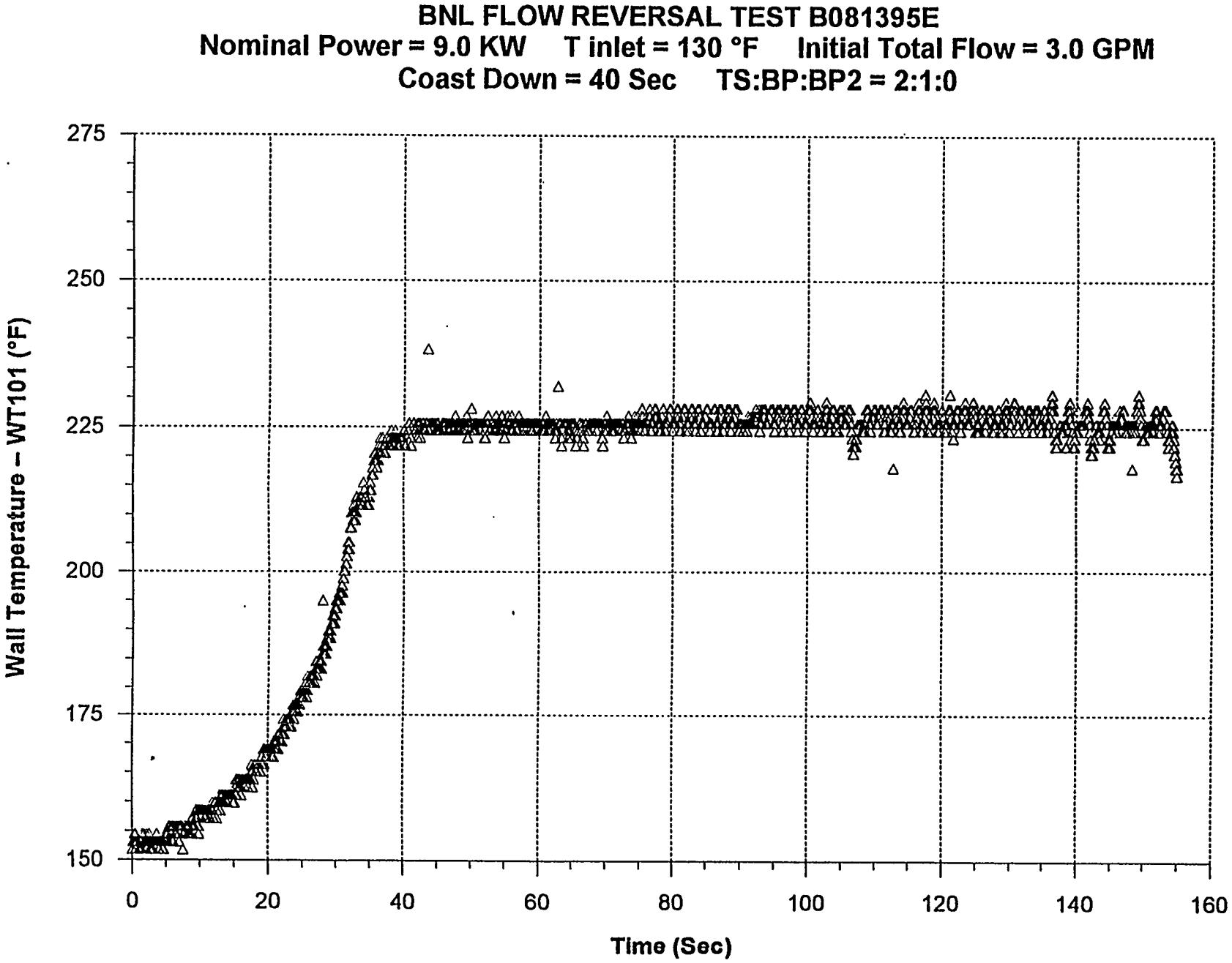
BNL FLOW REVERSAL TEST B081395E
Nominal Power = 9.0 KW T inlet = 130 °F Initial Total Flow = 3.0 GPM
Coast Down = 40 Sec TS:BP:BP2 = 2:1:0
Wall Temperature - WT101 (°F)
275
250
225
200
175
150
0
20
40
60
80
100
120
140
160
Time (Sec)

Figure A7.2

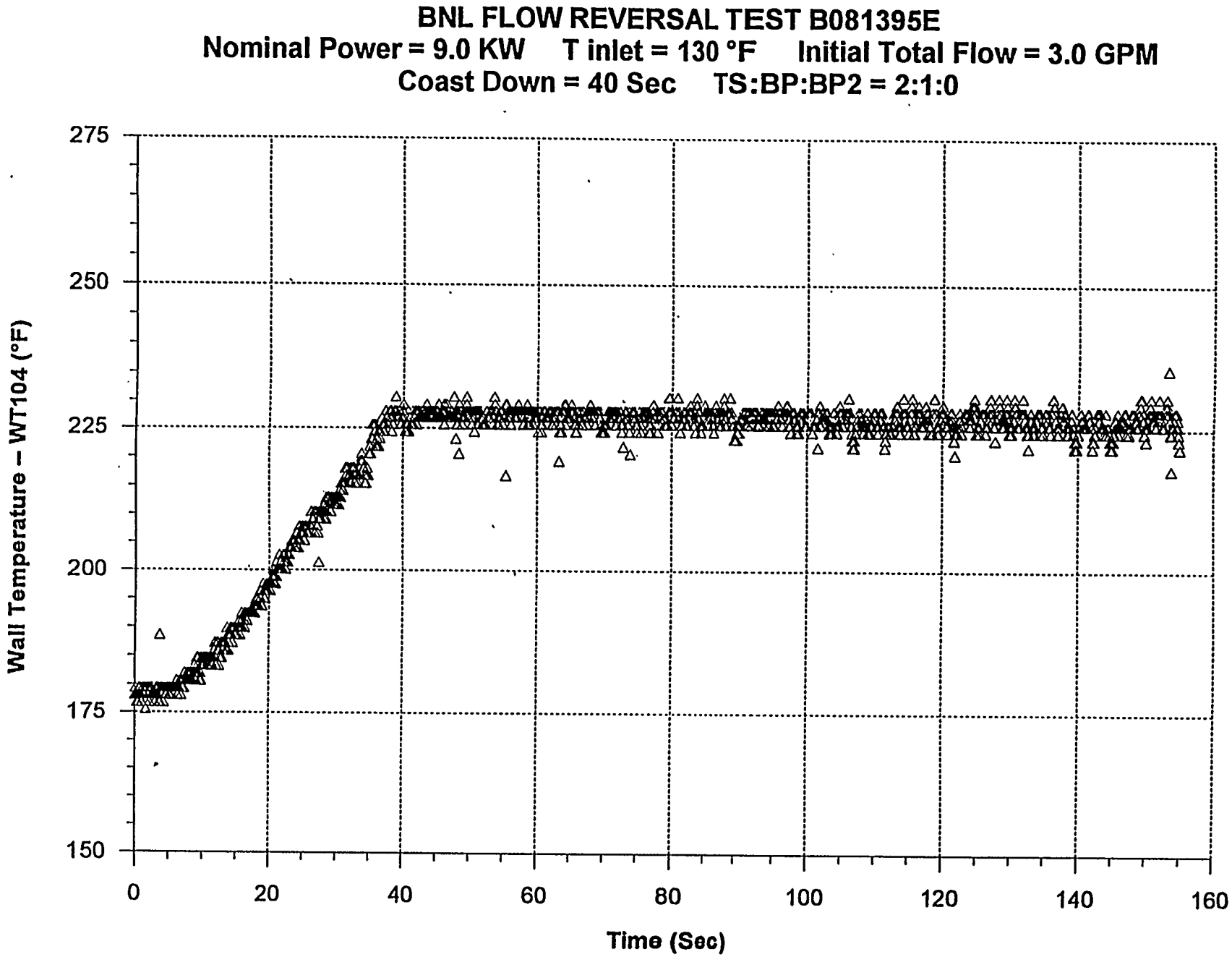
BNL FLOW REVERSAL TEST B081395E
Nominal Power = 9.0 KW T inlet = 130 °F Initial Total Flow = 3.0 GPM
Coast Down = 40 Sec TS:BP:BP2 = 2:1:0
Wall Temperature – WT104 (°F)
275
250
225
200
175
150
0
20
40
60
80
100
120
140
160
Time (Sec)

Figure A7.3

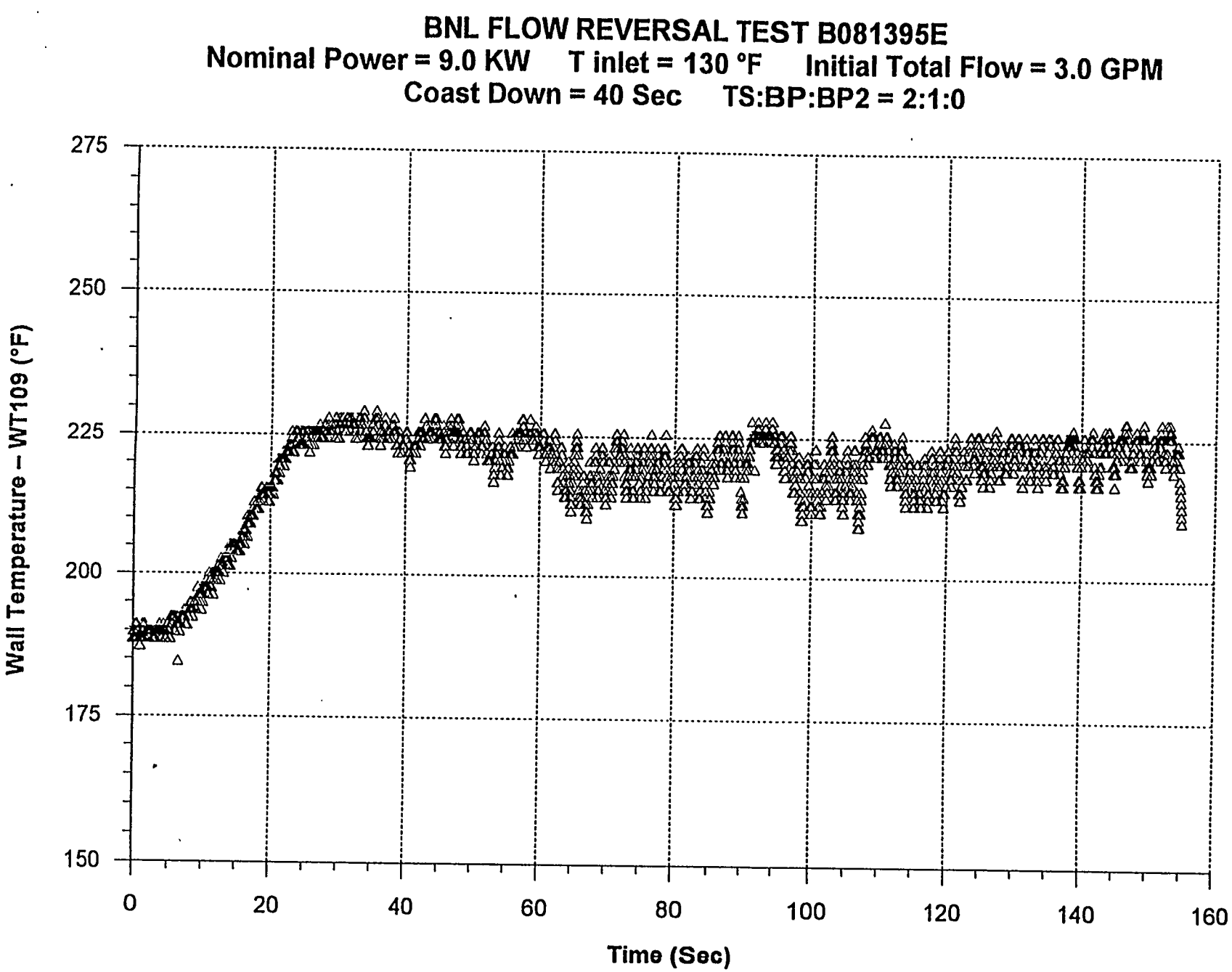
BNL FLOW REVERSAL TEST B081395E
Nominal Power = 9.0 KW T inlet = 130 °F Initial Total Flow = 3.0 GPM
Coast Down = 40 Sec TS:BP:BP2 = 2:1:0
Wall Temperature – WT109 (°F)
275
250
225
200
175
150
0
20
40
60
80
100
120
140
160
Time (Sec)

Figure A7.4

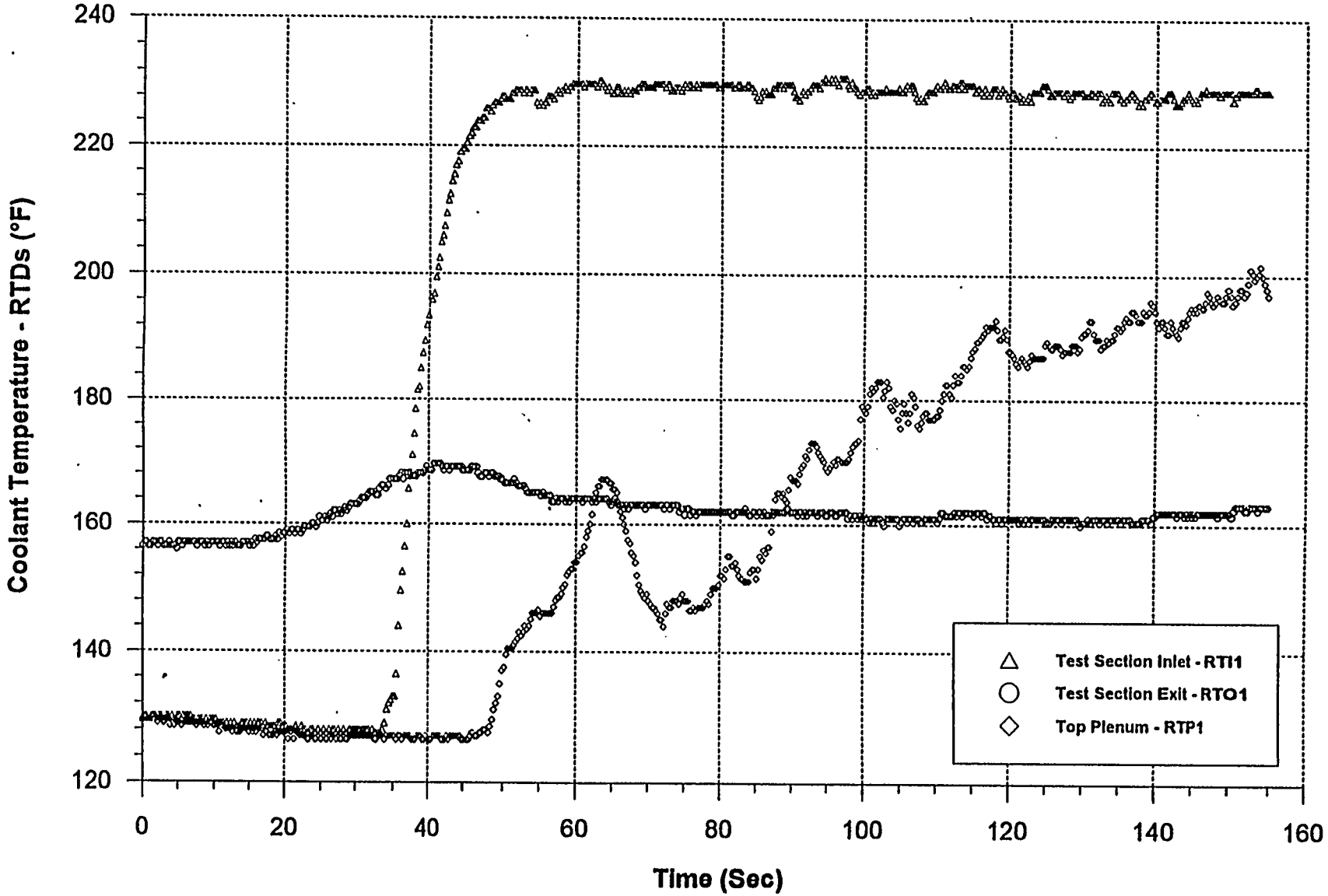
BNL FLOW REVERSAL TEST B081395E
Nominal Power = 9.0 KW T inlet = 130 °F Initial Total Flow = 3.0 GPM
Coast Down = 40 Sec TS:BP:BP2 = 2:1:0
Coolant Temperature - RTDs (°F)
240
220
200
180
160
140
120
0
20
40
60
80
100
120
140
160
Time (Sec)
Test Section Inlet - RTI1
Test Section Exit - RTO1
Top Plenum - RTP1

Figure A7.5

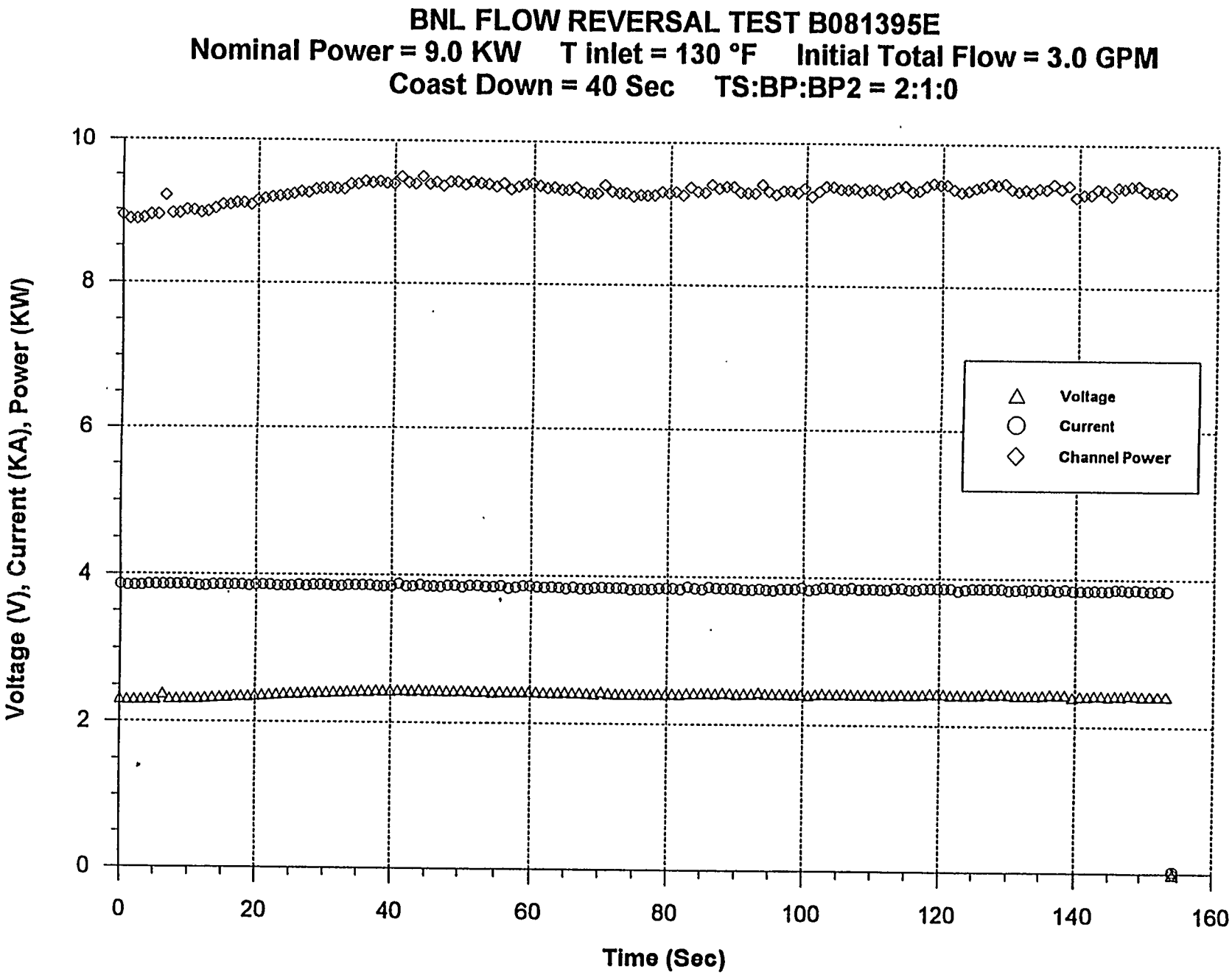
BNL FLOW REVERSAL TEST B081395E
Nominal Power = 9.0 KW T inlet = 130 °F Initial Total Flow = 3.0 GPM
Coast Down = 40 Sec TS:BP:BP2 = 2:1:0
Voltage (V), Current (KA), Power (KW)
Time (Sec)
Voltage
Current
Channel Power
0
2
4
6
8
10
0
20
40
60
80
100
120
140
160

Figure A7.6

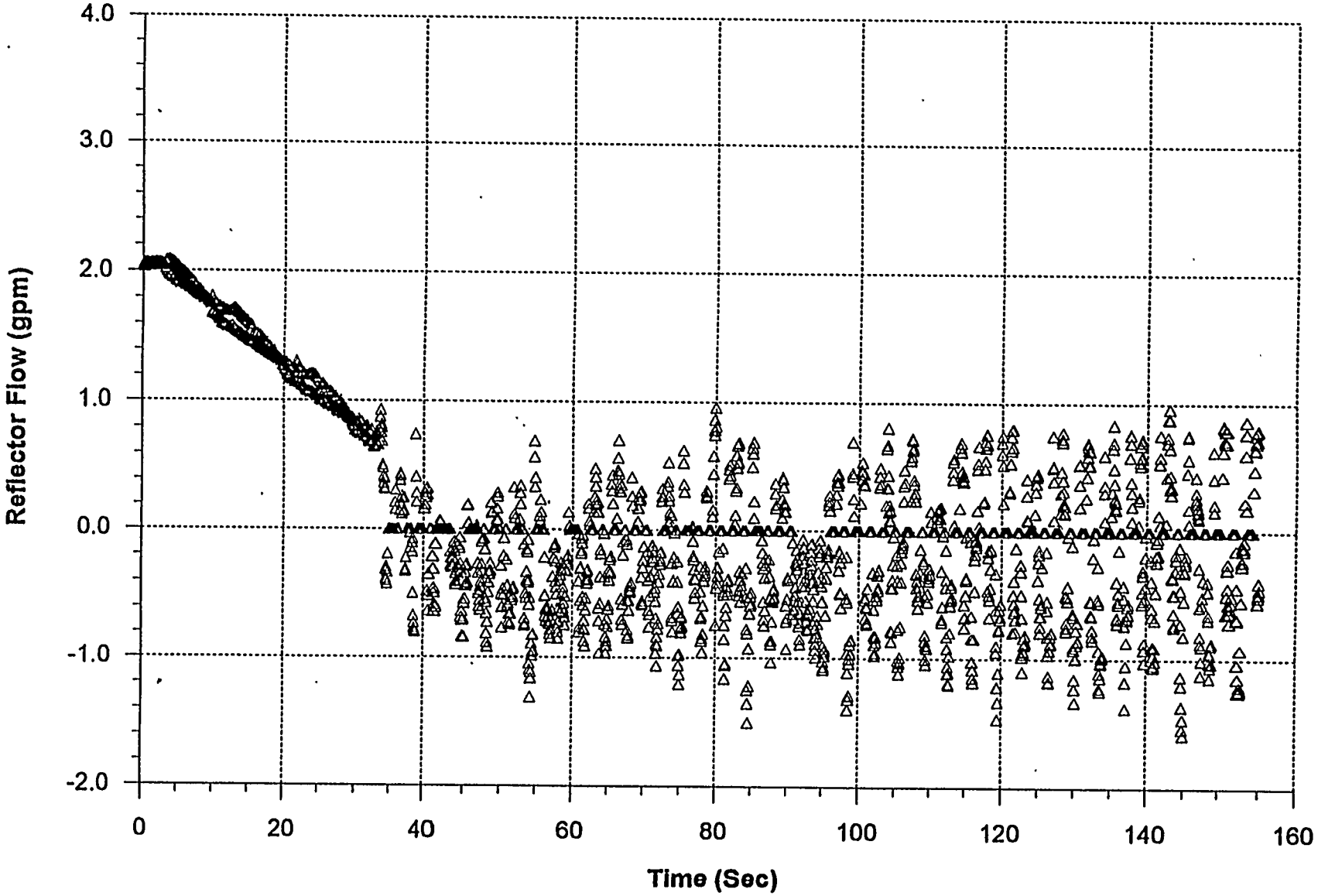
BNL FLOW REVERSAL TEST B081395E
Nominal Power = 9.0 KW T inlet = 130 °F Initial Total Flow = 3.0 GPM
Coast Down = 40 Sec TS:BP:BP2 = 2:1:0
Reflector Flow (gpm)
4.0
3.0
2.0
1.0
0.0
-1.0
-2.0
0
20
40
60
80
100
120
140
160
Time (Sec)

Figure A7.7

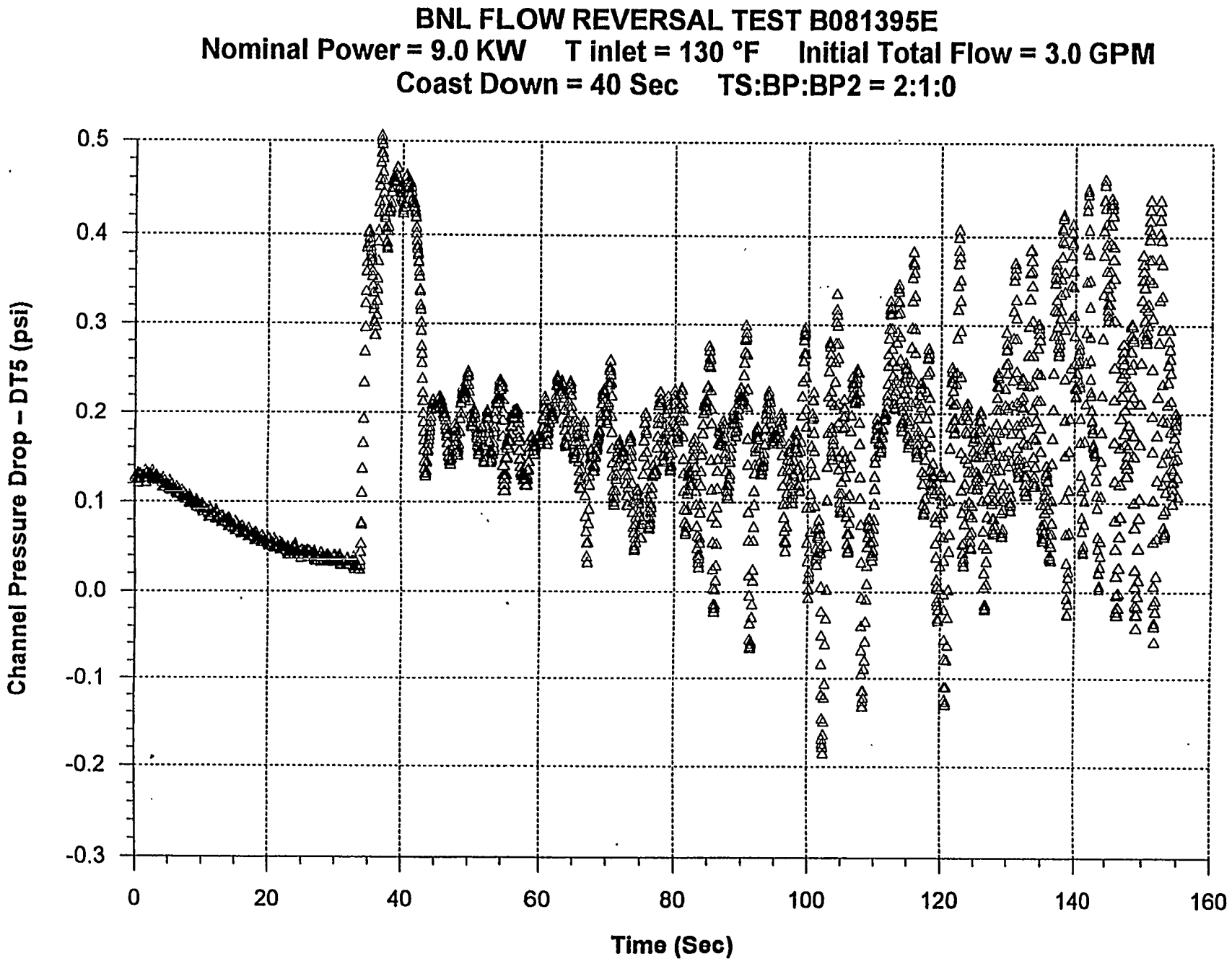
BNL FLOW REVERSAL TEST B081395E
Nominal Power = 9.0 KW T inlet = 130 °F Initial Total Flow = 3.0 GPM
Coast Down = 40 Sec TS:BP:BP2 = 2:1:0
Channel Pressure Drop – DT5 (psi)
0.5
0.4
0.3
0.2
0.1
0.0
-0.1
-0.2
-0.3
0
20
40
60
80
100
120
140
160
Time (Sec)

Figure A7.8

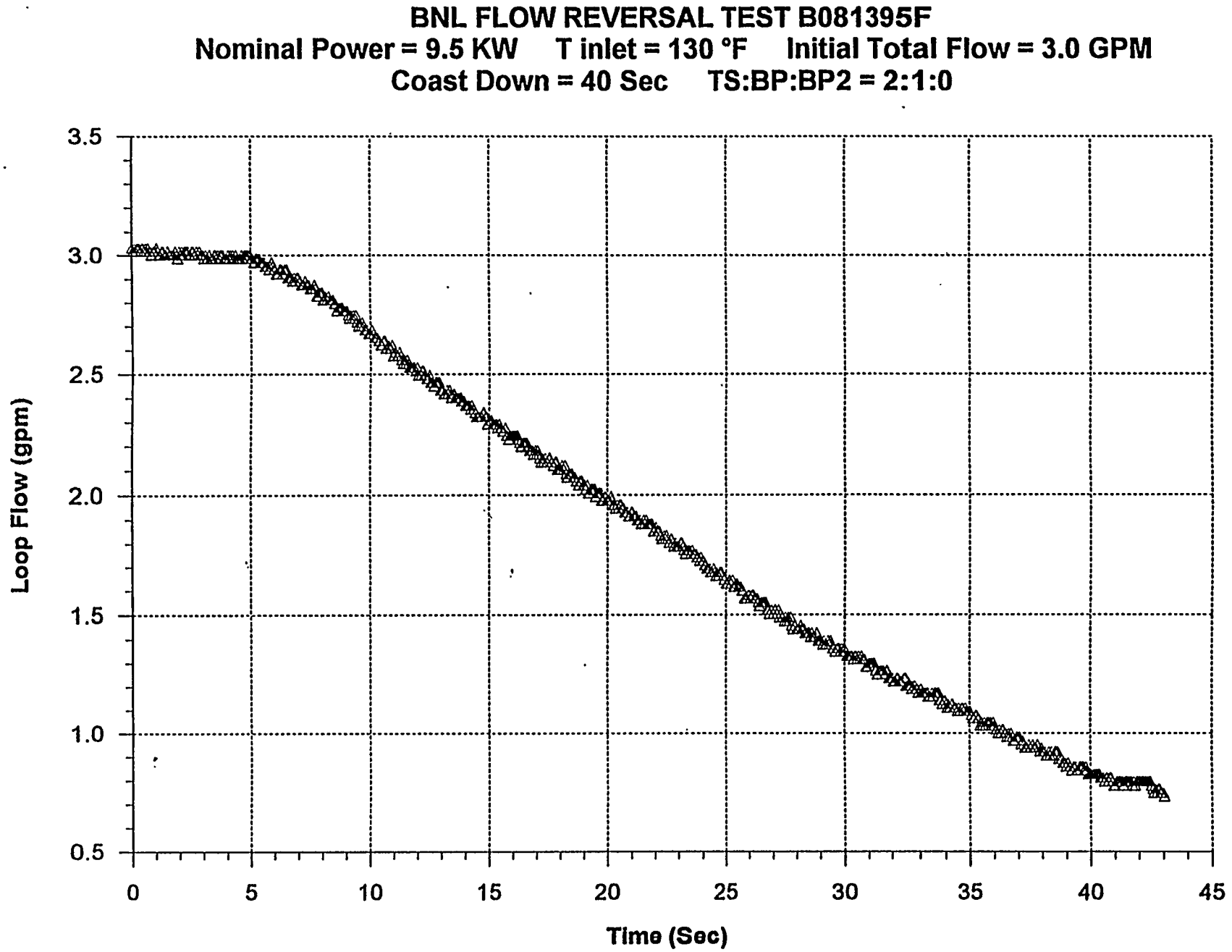
BNL FLOW REVERSAL TEST B081395F
Nominal Power = 9.5 KW T inlet = 130 °F Initial Total Flow = 3.0 GPM
Coast Down = 40 Sec TS:BP:BP2 = 2:1:0
Loop Flow (gpm)
3.5
3.0
2.5
2.0
1.5
1.0
0.5
0
5
10
15
20
25
30
35
40
45
Time (Sec)

Figure A8.1

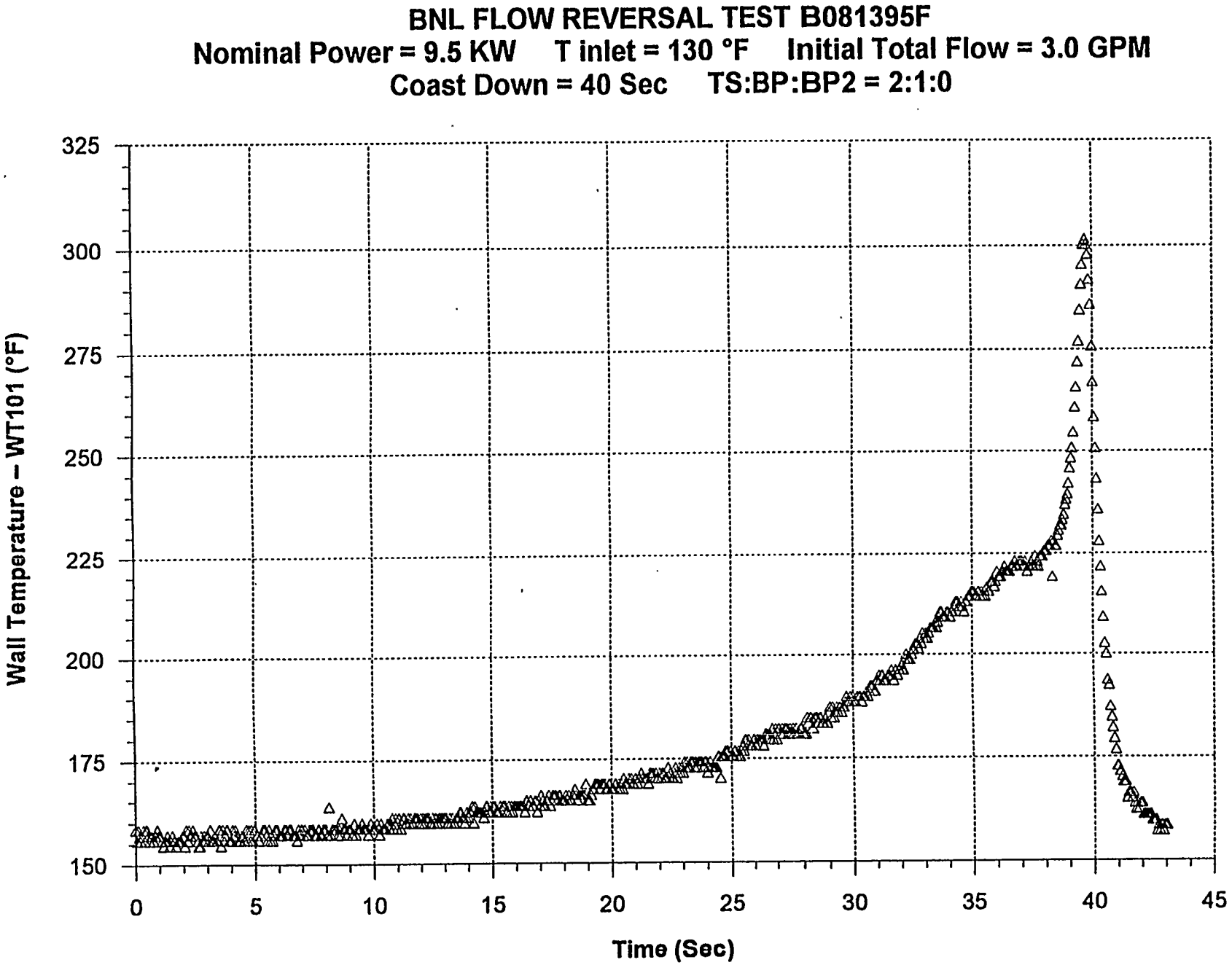
BNL FLOW REVERSAL TEST B081395F
Nominal Power = 9.5 KW T inlet = 130 °F Initial Total Flow = 3.0 GPM
Coast Down = 40 Sec TS:BP:BP2 = 2:1:0
Wall Temperature – WT101 (°F)
325
300
275
250
225
200
175
150
0
5
10
15
20
25
30
35
40
45
Time (Sec)

Figure A8.2

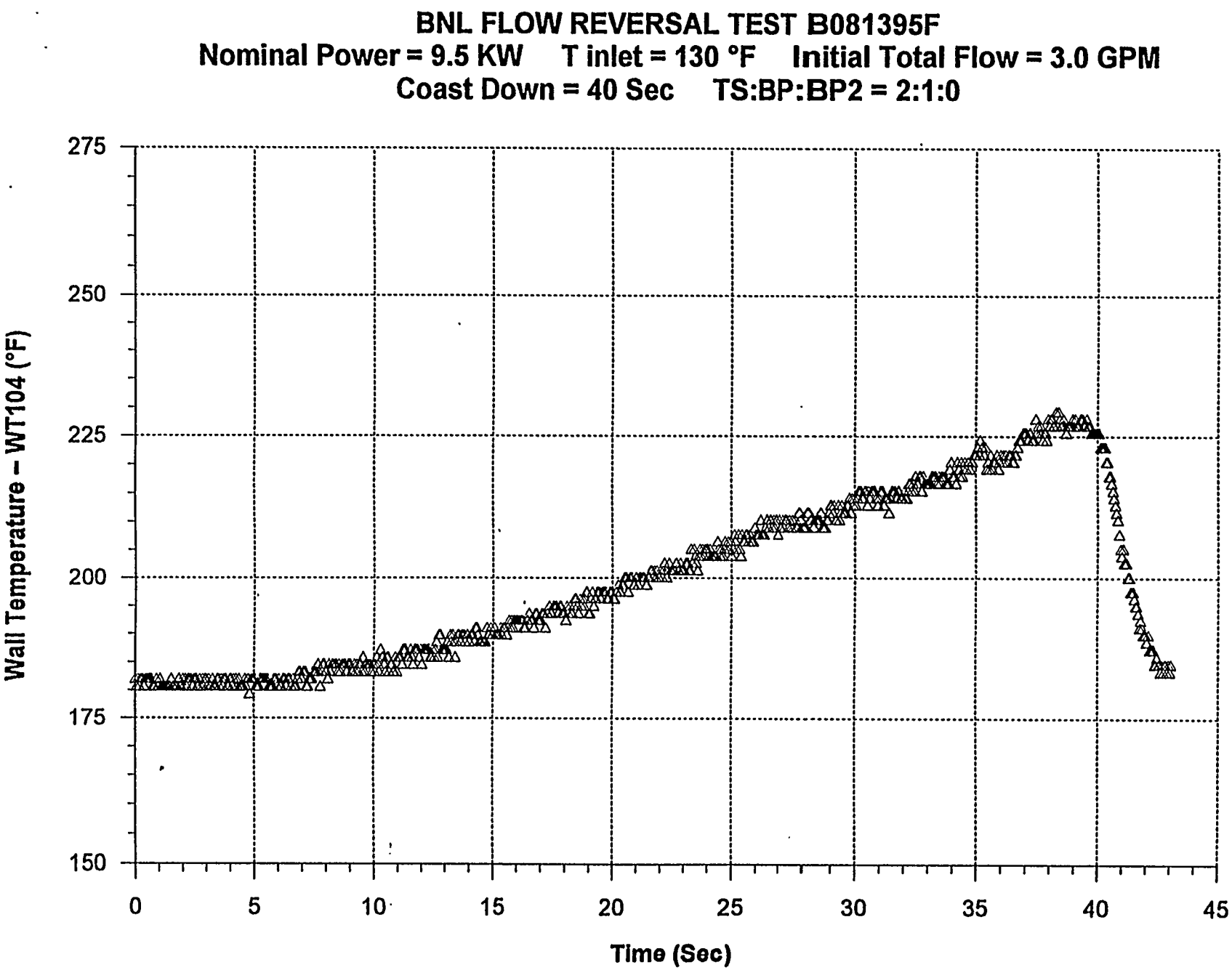
BNL FLOW REVERSAL TEST B081395F
Nominal Power = 9.5 KW T inlet = 130 °F Initial Total Flow = 3.0 GPM
Coast Down = 40 Sec TS:BP:BP2 = 2:1:0
Wall Temperature – WT104 (°F)
275
250
225
200
175
150
0
5
10
15
20
25
30
35
40
45
Time (Sec)

Figure A8.3

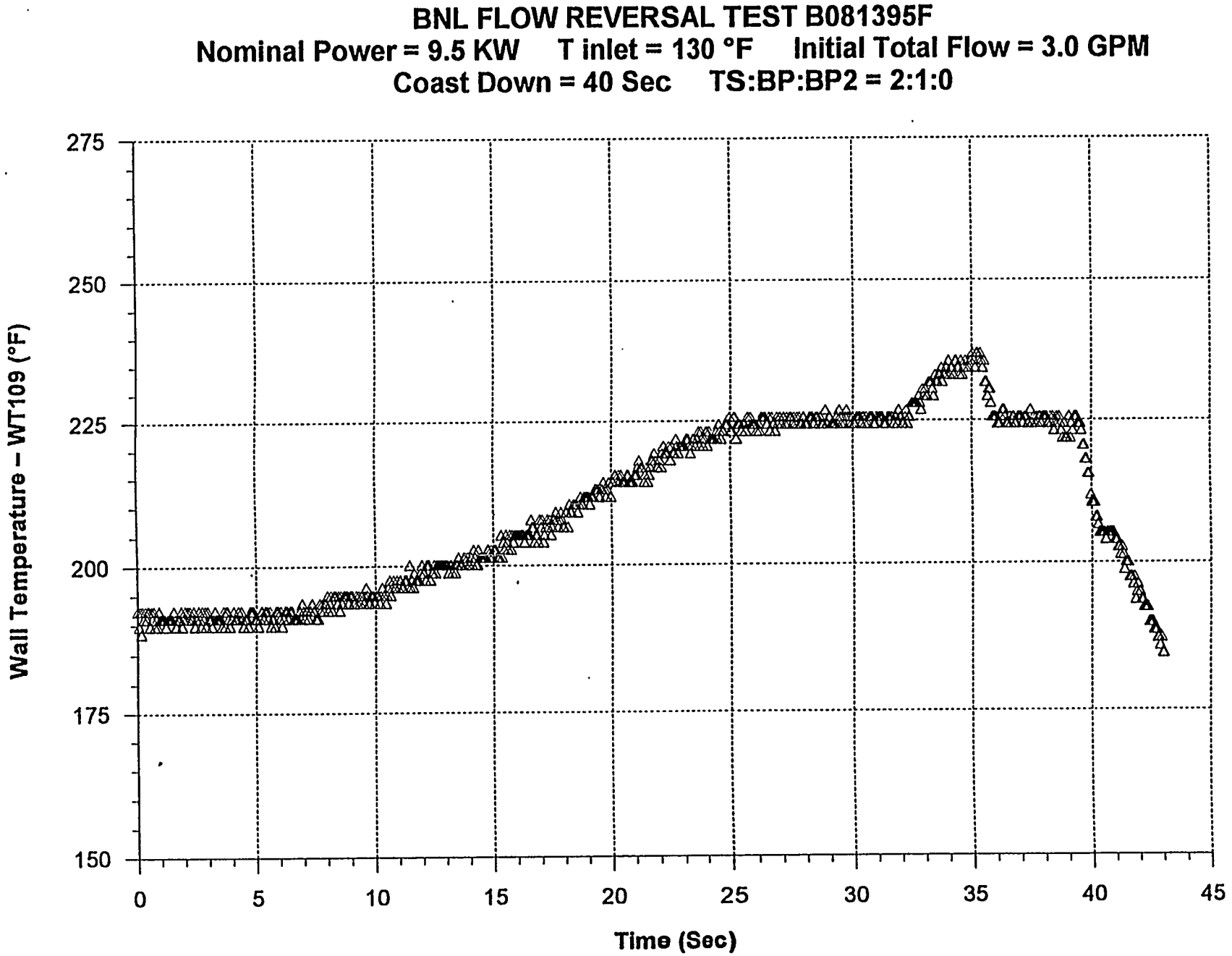
BNL FLOW REVERSAL TEST B081395F
Nominal Power = 9.5 KW T inlet = 130 °F Initial Total Flow = 3.0 GPM
Coast Down = 40 Sec TS:BP:BP2 = 2:1:0
Wall Temperature – WT109 (°F)
275
250
225
200
175
150
0
5
10
15
20
25
30
35
40
45
Time (Sec)

Figure A8.4

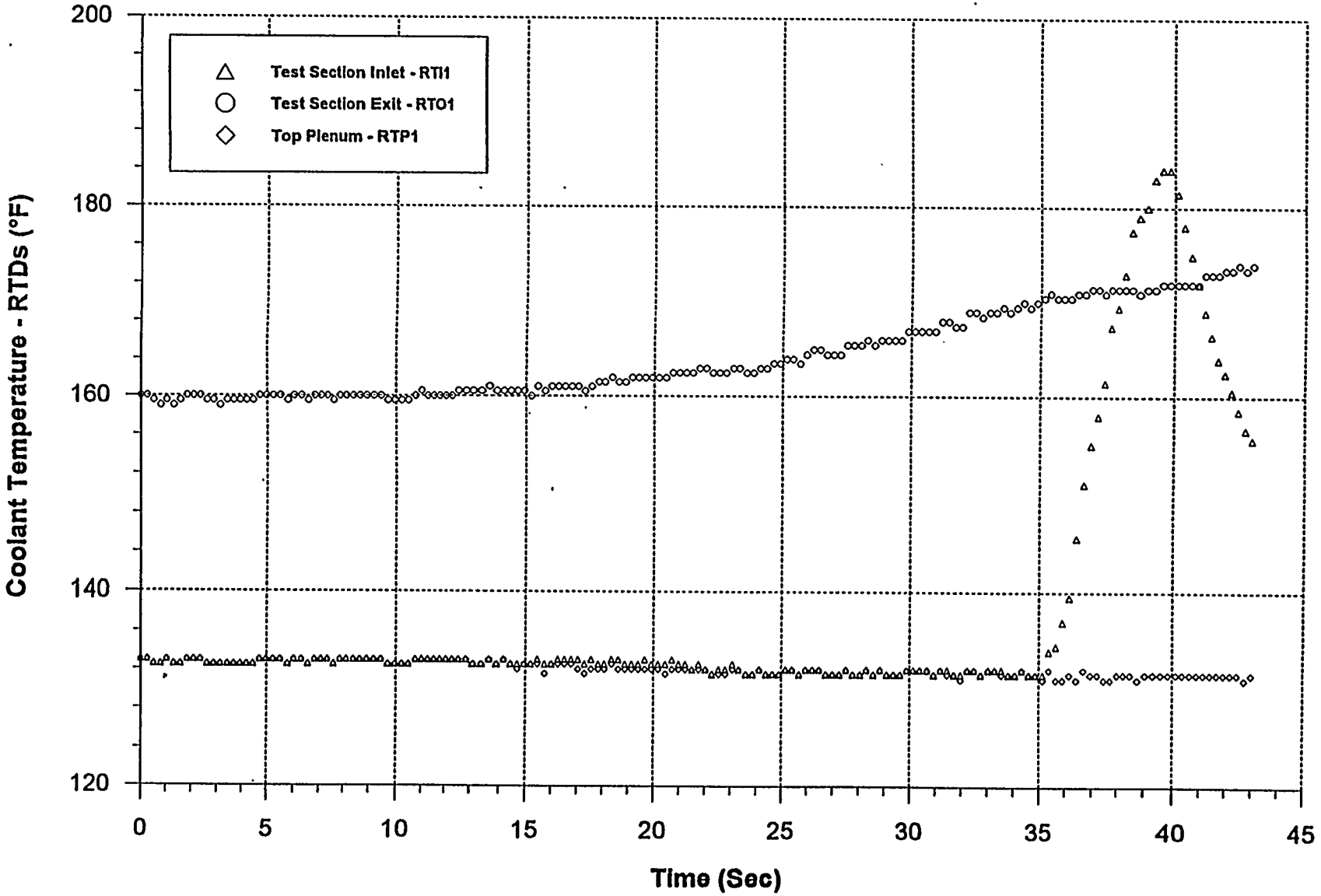
BNL FLOW REVERSAL TEST B081395F
Nominal Power = 9.5 KW T inlet = 130 °F Initial Total Flow = 3.0 GPM
Coast Down = 40 Sec TS:BP:BP2 = 2:1:0
Test Section Inlet - RTI1
Test Section Exit - RTO1
Top Plenum - RTP1
Coolant Temperature - RTDs (°F)
200
180
160
140
120
0
5
10
15
20
25
30
35
40
45
Time (Sec)

Figure A8.5

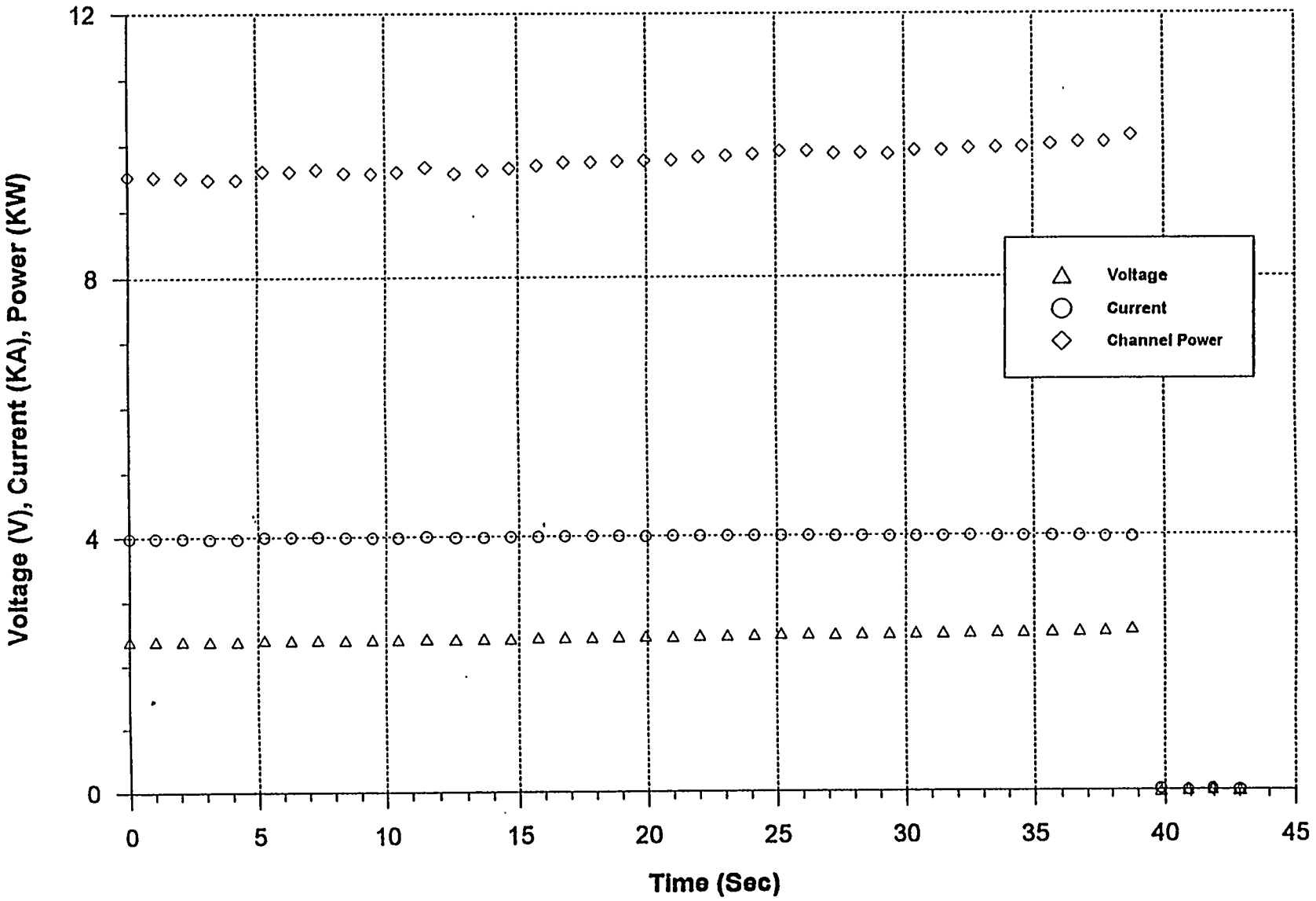
BNL FLOW REVERSAL TEST B081395F
Nominal Power = 9.5 KW T inlet = 130 °F Initial Total Flow = 3.0 GPM
Coast Down = 40 Sec TS:BP:BP2 = 2:1:0
Voltage (V), Current (KA), Power (KW)
12
8
4
0
0
5
10
15
20
25
30
35
40
45
Time (Sec)
Voltage
Current
Channel Power

Figure A8.6

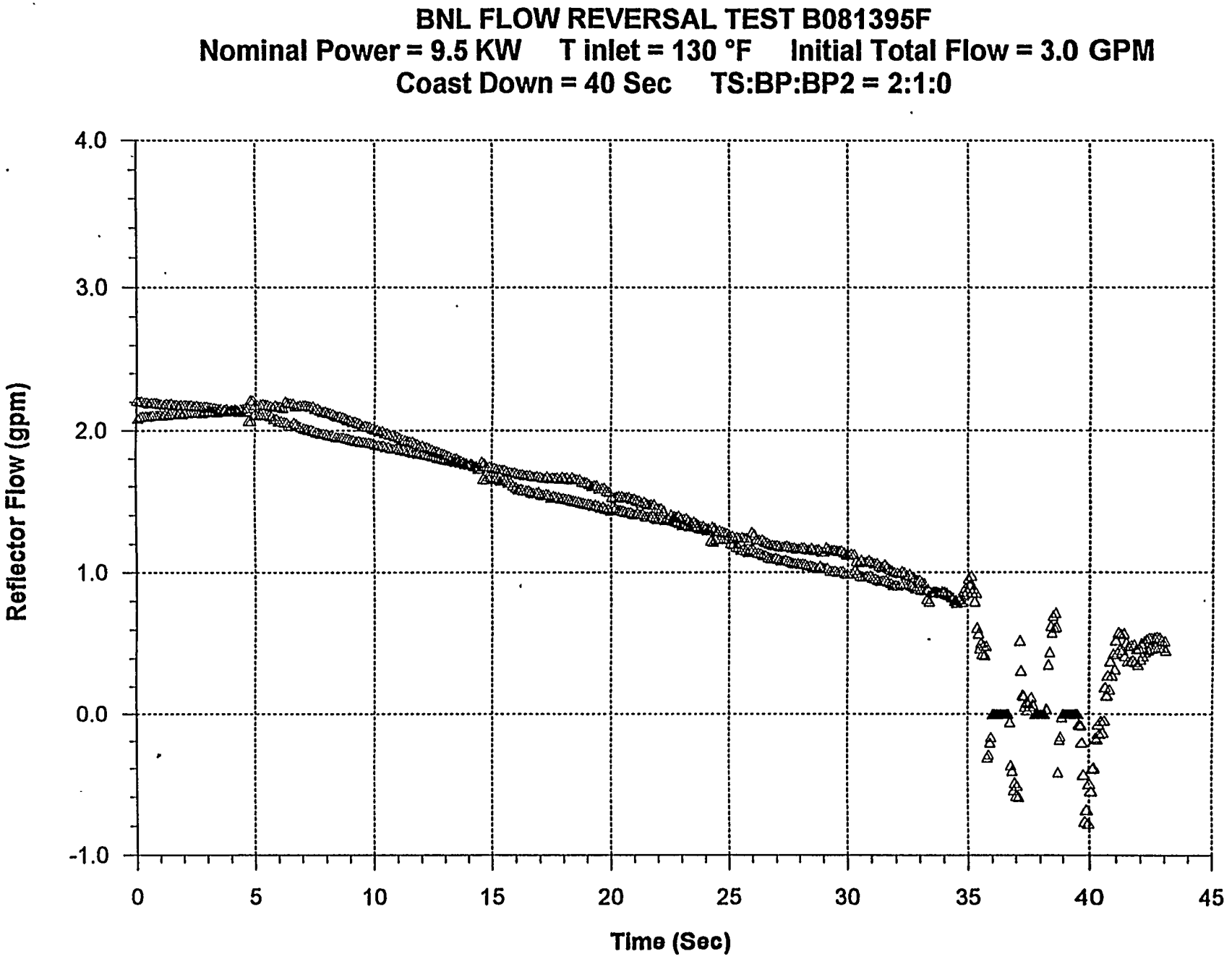
BNL FLOW REVERSAL TEST B081395F
Nominal Power = 9.5 KW T inlet = 130 °F Initial Total Flow = 3.0 GPM
Coast Down = 40 Sec TS:BP:BP2 = 2:1:0
Reflector Flow (gpm)
4.0
3.0
2.0
1.0
0.0
-1.0
0
5
10
15
20
25
30
35
40
45
Time (Sec)

Figure A8.7

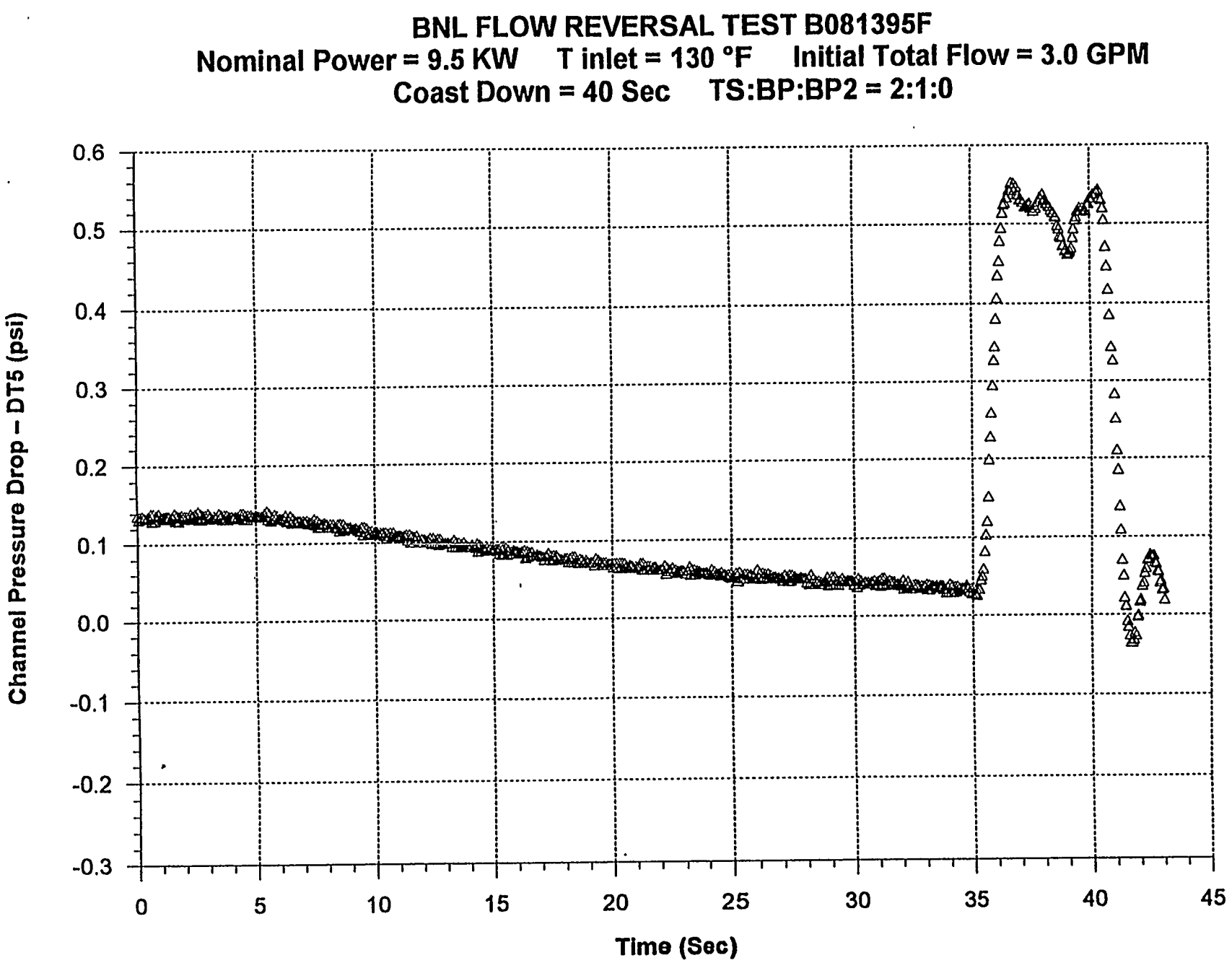
BNL FLOW REVERSAL TEST B081395F
Nominal Power = 9.5 KW T inlet = 130 °F Initial Total Flow = 3.0 GPM
Coast Down = 40 Sec TS:BP:BP2 = 2:1:0
Channel Pressure Drop – DT5 (psi)
0.6
0.5
0.4
0.3
0.2
0.1
0.0
-0.1
-0.2
-0.3
0
5
10
15
20
25
30
35
40
45
Time (Sec)

Figure A8.8

APPENDIX B

RELAP5 MODEL AND COMPARISON WITH TEST RESULTS

A. MODEL DESCRIPTION

A RELAP5 model has been developed [B1] to simulate the flow reversal tests conducted at Columbia University. The results of the numerical simulations are used to develop an analytical success criterion for safe flow reversal. The success criterion is represented by a time-averaged channel void fraction. The value of the critical void fraction is established by comparing the RELAP5 calculation with the outcome of the corresponding flow reversal test.

RELAP5 [B2] is a system thermal-hydraulic code developed at the Idaho National Engineering Laboratory (INEL) for the analysis of power reactors. Recent updates to RELAP5 has made the code more applicable to DOE research reactors [B3]. The version of RELAP5 used in the simulation of the flow reversal tests is mod 3.1.1.1 released to BNL by INEL in July 1994. During the development of the RELAP5 model for the flow reversal tests, it was observed that high steam condensation rates were calculated at the steam-water interface resulting in unrealistic simulation of the tests. The interfacial heat transfer coefficient on the liquid side was modified [B4] to reflect the conditions observed during the actual tests. In effect, the coefficients were reduced for the bubbly subcooled liquid and the slug subcooled liquid flow regimes.

The scope of the test program had been expanded twice since the first successful test conducted in February 1993. The test loop had been modified accordingly to accommodate the new test conditions. A RELAP5 representation of the test loop is shown in Figure B1. The original RELAP5 model [B1] has since been modified to reflect the three test loop configurations used in the flow reversal tests. Details of the model changes are discussed in Ref. [B5].

The RELAP5 calculations were set up to reflect the test conditions. Generally they were done in pairs, one representing safe flow reversal and the other at a slightly higher power level representing the tripped case. The principal variants of the tests were:

1. Power to the Heated Section
   The aluminum plate(s) that form the channel wall(s) was directly heated by DC power. There was an upward power drift as the plate temperatures increased during flow coastdown and flow reversal. The reference power for the safe cases was the measured power at the time of flow reversal. For the tripped cases, the reference power was the power just before the trip. Steady-state heat loss from the heated section was estimated

at 4% and 5% for the cases of single heater and double heater respectively. The actual power used in the calculation was 96% and 95% of the reference power for the safe and tripped cases respectively. The aluminum plates were assumed uniformly heated and the power were kept constant for each calculation. Each aluminum plate and the adjacent coolant channel were divided into 16 axial nodes.

2. Pump Coastdown
In the flow reversal tests, the pump was programmed to provide a linear flow coastdown. The nominal coastdown time from 3 gpm to zero flow was set at 40 seconds. Other coastdown times tested were 30 seconds and 60 seconds. Tripping the circulating pump resulted in an equivalent coastdown time of 1.5 seconds. Time dependent junctions were used in the RELAP5 calculations to represent the flows to and from the circulating pump. At any given time during the simulated coastdown, the suction flow was equal to the injection flow.

3. Initial Coolant Temperature
The initial coolant temperature of 130°F was maintained in the flow reversal test by passing the coolant through a heat exchanger located upstream of the pump. Two other coolant temperatures were used in the test, 110°F and 150°F. In RELAP5, the coolant temperature was specified in the time dependent volume that supplied flow to the time dependent junction representing the pump injection flow.

4. Initial Water Level
The normal water level in the HFBR is 14' above the transition plate. The water level was set nominally at 14' above the inlet tube section of the test loop. A lower water level of 3.67' was also tested. The test loop did not have a pressurized cover gas region as in the HFBR. The upper plenum region of the test loop actually opened to the atmosphere. In RELAP5, the initial water level was set by specifying a saturated steam condition in the hydrodynamic volumes above the free surface. A time dependent volume with saturated steam at atmospheric pressure was used to represent the ambient pressure condition above the upper plenum region of the test loop. The use of steam instead of air in the gaseous space above the water level was to avoid any unexpected complications resulting from including a non-condensable gas in a RELAP5 calculation. The heat and mass transfer across the steam/water free surface had negligible effect on the calculations because of the column of subcooled water between the heated section and the free surface.

5. Bypass Ratio
The bypass section of the test loop represented the flow paths in the HFBR that are parallel to the fuel elements. In the

forced downflow situation, these parallel flow paths divert a fraction of the total flow away from the fuel elements. The difference between the total downflow and the core flow (flow through the fuel elements) is the bypass flow. The bypass flow accounts for flow through the open flow reversal valves and flows in or around reactor vessel internal structures that penetrate the transition plate. The bypass ratio is defined to be the ratio of the core flow to the bypass flow. The bypass ratio corresponding to the initial pump flow of 3 gpm in the test was determined to be 2:1 [B6]. This bypass ratio of 2:1 was realized in the test by installing a 0.199" diameter orifice in the bypass section of the test loop. A smaller orifice of 0.129" diameter was used in the test to simulate the condition of partial loss of bypass flow path, such as the failure of one of the flow reversal values to open. The smaller orifice resulted in a bypass ratio of 5:1. In order to check the effects of a less restrictive return flow path on flow reversal, a 0.28" diameter orifice was used. This third orifice resulted in a bypass ratio of 1.5:1. The orifice plate was modeled in RELAP5 as a flow junction, using the actual orifice flow area and a user supplied loss coefficient. The loss coefficient was adjusted to achieve the proper bypass ratio for each orifice. In one series of tests a valve was used to adjust the bypass flow. For that test configuration a bypass ratio of 1:3.4 was achieved.

6. Mode of Heating

Two heated sections were used. In the single-sided heater, the coolant channel was bounded on one side by a heated plate and the other by a slab of LEXAN. In the two-sided heater, the coolant channel was bounded on each side by a heated plate. The channel gap was slightly different for the two heated sections. There was no direct measurement of the as-installed dimension of the channel gap. The design specification allowed the gap to vary between 0.10" and 0.113" for the single-sided heater, and between 0.098" and 0.116" for the two-sided heater. The RELAP5 calculations assumed the high end of the range for the channel gap. Generally a wider gap would impose a lesser resistance to flow and that is likely to translate to a lower peak wall temperature and lower void fraction in the channel during flow reversal. It is then expected that a dryout criterion developed from calculations using a wider gap would be more conservative than the case of using a smaller gap. In RELAP5 the heated plates were represented by rectangular heat structures with uniform heat sources.

7. Dissolved Helium

In one series of flow reversal tests, water saturated with dissolved helium was circulated in the test loop prior to the initiation of a flow coastdown. The effect of helium on flow reversal was assessed experimentally but no RELAP5 calculation

was done to simulate the impact of dissolved gas.

8. Secondary Bypass
In the last series of tests a second bypass line was installed to allow for the injection of unheated water into the region below the heated section. The RELAP5 model was revised accordingly to reflect this change in the test loop.

B. COMPARISON OF RELAP5 SIMULATIONS WITH TEST RESULTS

A list of flow reversal tests that have been simulated by RELAP5 is shown in Table B1. Each RELAP5 calculation was first initialized to a steady state and the flow coastdown or pump trip was then started at a time equal to 5 seconds. The focus of the RELAP5 analysis was to characterize the thermal-hydraulic response of the heated section during a flow reversal transient. Based on the test results, the timing of flow reversal was always near the end of the flow coastdown. If there was a dryout during flow reversal it generally occurred within a few seconds after the initiation of flow reversal. For all the coastdown cases, it was then adequate to carry the calculation out to 15 seconds after the forced flow has stopped.

RELAP5 run #1 represents a case of safe flow reversal under baseline test conditions. This is a simulation of test #B081395E from the last test series. The channel power was 9 kW. The 40 sec. coastdown was started at 5 sec. Figure B2.1 shows the mass flow rate at the top and bottom of the heated section. The positive flow direction is downward. The coastdown phase of the transient lasted until ≈31 sec. when the coolant began to change its flow direction. The generation of steam resulted in the expulsion of coolant out of the heated section. In this stage, the mass flow was out of the heated section at both top and bottom. The much lower mass flow rate at the bottom of the heated section was indicative of mostly steam flow out of the bottom. Flow oscillation persisted for some time after the flow had reversed from downward to upward direction. At times the mass flow at the top and bottom of the heated section were in opposite directions. The coolant flow became more in phase for times greater than ≈55 sec. and that was 10 seconds after the forced flow had completely stopped.

Figure B2.2 is a plot of the average void fraction in the heated section. This channel void fraction represents the arithmetic mean of the void fraction in the 16 coolant nodes. The channel void fraction reached a peak value of over 90% in the vapor generation stage of the flow reversal transient. In the oscillatory flow stage, each oscillation cycle resulted in more liquid reaching the heated section. This was reflected in the reduction of succeeding peaks of the channel void fraction during the oscillatory flow stage. The periodic variation of the channel void fraction in the natural circulation stage of the transient was

out of phase with the channel flow. A smaller flow results in more steam generation which led to a higher channel void fraction. The higher channel void fraction created a more favorable pressure potential for natural circulation flow. The subsequent increase in flow reduced the channel void fraction and also the pressure potential for natural circulation. In Figure B2.1 the natural circulation flow calculated by RELAP5 was seen to cycle through periods of increasing and decreasing flow while the corresponding channel void fraction was seen in Figure B2.2 to pass through periods of decreasing and increasing values.

A period of oscillation of approximately 2 seconds has been observed from both the experimental data and the RELAP5 calculation. Each oscillation cycle can be broken down into three stages. A simplified model of the process can be used to estimate the time for each stage and demonstrate that the total cycle time is in approximate agreement with 2 seconds that was visually observed and with the RELAP5 result. The calculation is based on a base case channel power of 9 kW.

Heat Up Stage:

The initial temperature of the channel water is the temperature of the reflector water. This is 161°F. The time required to heat up the water in the channel (0.20 lb) to saturation (233°F) at 9 kW is 1.69 seconds.

Steam Voiding Stage:

The time required to generate sufficient steam to completely void the channel. The channel volume is 3.4×10^{-3} ft^3 at 9 kW the time required to generate this volume of steam at a pressure corresponding to a saturation temperature of 233°F is 0.02 sec. The mass of steam vaporized is 1.84×10^{-4} lbs.

Reflood Stage:

An estimate [B7] of the time for this stage was based on a U-tube model in which one leg of the U-tube represents the channel which is initially voided and the other leg represents the reflector region which remains filled during this transient. The net hydrostatic head between the two legs which varies with time is the only driving force for coolant flow. The calculated time for this stage is 0.46 seconds.

The combined time for these 3 stages is 2.2 seconds which is in reasonable agreement with RELAP5 and experimental observation.

It follows from the above discussion that the period will be shorter for higher channel power. The period will also be

shortened by a higher temperature in the reflector region. In the course of natural circulation, the temperature of the reflector region will decrease initially due to the arrival of the cooler water from the upper plenum (nominally at 130°F). As the upper plenum heats up, the reflector region will eventually experience an increase in temperature.

The coolant temperatures as calculated by RELAP5 are shown in Figure B2.3. Flow reversal can be identified by the sudden increase in the water temperature in the inlet tube section. The initial increase in temperature in the lower plenum region during the coastdown stage of the transient was due to decreasing forced channel flow. Once the flow had reversed, coolant from the reflector region started to flow into the lower plenum region lowering its temperature. An incremental rise in temperature was also seen in the upper plenum region after flow reversal.

An example of the calculated plate temperature is shown in Figure B2.4. The calculated peak wall temperature of about 290°F (419°K) did not agree with the test data. The data showed the plate temperature to increase to the saturation temperature of ≈230°F during flow reversal. The data also did not exhibit any temperature fluctuations of more than 10 deg F while the RELAP5 calculation predicted fluctuations in the order of 20 deg F. In comparison with the test data, the calculated wall temperatures were generally higher than the measured values and fluctuations in the calculated wall temperature were of greater magnitude than the observed values.

The companion case to RELAP5 run #1 is run #2. RELAP5 run #2 represents a case of dryout during flow reversal under baseline conditions. These two RELAP5 runs correspond to the pair of flow reversal tests which bracketed the dryout power for the baseline conditions. The channel power for run #2 was 9.8 kW and it corresponded to the power level at the time of trip (minus 4% for steady-state heat loss). The results of this calculation are similar to those of run #1. The channel void fraction is shown in Figure B3. Here a couple of distinctions between the safe case and the tripped case are noted. Qualitatively, the RELAP5 calculation indicated that during the oscillatory flow stage the channel void fraction was higher and the oscillation period was shorter for the dryout case than for the safe flow reversal case.

In summary, the RELAP5 simulations of the flow reversal tests are found to reproduce the general aspects of the observed behavior of the tests. These include the timing of the onset of flow reversal, the period of flow and void oscillations, and the extensive voiding that was observed visually prior to dryout. However, the calculated plate temperatures tend to be higher than the measured values. The heat transfer correlations in RELAP5 are based primarily on data developed for rod bundle and tube

geometries and high pressure conditions applicable to power reactors. The accuracy of applying the existing heat transfer correlations to narrow channel geometry and low pressure condition has not been established. The following section summarizes the results of using channel void fraction as a dryout criterion.

C. COMPARISON OF TIME AVERAGE VOID FRACTIONS IN RELAP5 SIMULATIONS

After the RELAP5 simulations were performed it was pointed out by a reviewer that the power used in the simulation did not account for transient heat losses as discussed in Section IIC. The transient losses are losses that occur during the coastdown and flow reversal phase when temperatures are rapidly changing. The power was corrected to account for this effect. However, instead of repeating the RELAP5 simulations of all the tests, and using the new simulations to generate the time averaged void fractions, the corrected void fractions were determined by extrapolation of the original void fraction values. Extrapolation was possible because the RELAP5 calculations were performed in pairs, one representing the safe flow reversal power and the other at a slightly higher power level representing the tripped case. The change in void fraction with power was determined from these results and then was used to estimate the void fractions corresponding to the slightly lower corrected powers.

In Table B.1 for each test condition simulated, two channel powers and two corresponding maximum time-averaged void fractions are listed. The first power listed is the power used in the RELAP5 simulation and only accounts for the steady state heat loss. The first void fraction listed was determined directly from the RELAP5 result. The second power listed accounted for transient heat losses also. The second void fraction listed, as noted above, is obtained by extrapolation and corresponds to the second power.

The seventeen test conditions listed in Table B1 cover a wide range of inlet temperatures, bypass ratios and coastdown times and include both one-sided and two-sided heating tests. Figure B4.1 and B4.2 show the instantaneous and time-averaged channel void fractions for RELAP5 run numbers 1 and 2. These plots are typical of all the flow reversal simulations. A comparison of the maximum time averaged channel void fractions for the seventeen test conditions is shown in Figure B.5. The data shown in this plot correspond to the extrapolated void fraction values discussed above.

D. VALIDATION OF RELAP5

In support of applying the RELAP5 code to the analysis of flow reversal transients, comparisons have been made between RELAP5 and a drift-flux based numerical model. In addition, comparisons have been made between RELAP5 predictions and the initial steady-state

data from the flow reversal test.

A comparison was made between RELAP5 and a drift-flux model for the prediction of steady-state channel void fraction [B8]. The calculations were done for a range of coolant flow rates and channel powers which corresponded to critical heat fluxes (CHF) given by three correlations developed specifically for the narrow channel geometry. Figures B6.1 through B6.3 show the calculated channel average void fraction corresponding to each of the three CHF correlations. The results show good agreement between RELAP5 and the drift-flux model.

The ability of RELAP5 to predict natural circulation flow after flow reversal was demonstrated by a comparison with a transient drift-flux model which assumed axially uniform flow rate in a heated channel [B9]. Details of the drift-flux model are given in Reference [B10]. The comparison was for a flow reversal transient initiated by a rapid decrease in the forced downflow (equivalent to a coastdown time of 2 sec.). The channel power was constant at 10 kW. The predicted mass flow rates by the two models are shown in Figure B.7. Excellent agreement in the flow rate was observed during the coastdown phase of the transient t = 5 to 8 sec. and in the subsequent natural circulation phase after the flow reversal (t > 11 sec.). During the transition from downflow to upflow, RELAP5 and the drift-flux model (the simplified model) predicted somewhat different flow transients. The difference is mainly due to the simplifying assumption of uniform channel flow used by the drift-flux model.

The predictions of void fraction in a flow reversal transient by RELAP5 and a drift-flux model were compared to establish the trend of the maximum time-averaged channel void fraction as a function of power and the bypass flow ratio (ratio of channel flow to bypass flow). The two models were used to simulate three sets of initial conditions [B11]. The first two sets corresponded to actual test cases and they were:

Case 1

Bypass ratio = 2:1
Channel power = 9.0 kW
Initial flow in heated section = 2 gpm
Initial flow in bypass section = 1 gpm
Initial inlet temperature = 130°F
Coastdown time = 40 sec.
Reference test case = B081395E

Case 2

Bypass ratio = 1:3.4
Channel power = 13.8 kW
Initial flow in heated section = 2 gpm
Initial flow in bypass section = 6.8 gpm
Initial inlet temperature = 130°F
Coastdown time = 40 sec.
Reference test case = B081395K

A third case was for conditions similar to Case 2 but with a lower channel power of 9 kW.

Two equivalent hydraulic models were set up to simulate the three cases, one model using RELAP5 and the other using the drift-

flux formulation. As a simplifying assumption, both hydraulic models treated the upper plenum region of the test loop as a reservoir of constant pressure and temperature. The initial flow split between the heated section and the bypass section was achieved by adjusting the flow area of the bypass orifice. In the numerical simulation of the test, the initial conditions were established and maintained for five seconds and then the linear flow coastdown was started.

Two parameters from the numerical simulations are chosen for the comparison of RELAP5 and the drift-flux model. They are the time of flow reversal since the beginning of flow coastdown and the maximum 2 sec. time averaged channel void fraction. The results of the comparison are summarized in the following tables.

TIME OF FLOW REVERSAL SINCE THE BEGINNING OF FLOW COASTDOWN

	CASE 1 9 kW, 2:1	CASE 2 13.8 kW, 1:3.4	CASE 3 9 kW, 1:3.4
RELAP5	28.4 sec.	18.8 sec.	28.1 sec.
Drift-Flux	30.1 sec.	23.4 sec.	29.2 sec.
Test Data	≈30 sec.	≈16 sec.	N/A

MAXIMUM 2 SECOND TIME AVERAGED CHANNEL VOID FRACTION

	CASE 1 9 kW, 2:1	CASE 2 13.8 kW, 1:3.4	CASE 3 9 kW, 1:3.4
RELAP5	0.672	0.776	0.303
Drift-Flux	0.552	0.481	0.254

Both codes predict reasonably well the timing of flow reversal for the 9 kW (2:1) case. For the higher power case of 13.8 kW (1:3.4), the prediction by RELAP5 is much better than the drift-flux model which assumed thermal equilibrium for the coolant.

The channel void fraction calculated by RELAP5 and the drift-flux model for Case 1 are shown in Figures B7.1 and B7.2 respectively. For all three cases the void fraction predictions by RELAP5 are higher than the drift-flux model. The lower prediction by the drift-flux model is expected because one of the modeling assumptions is uniform axial flow in the heated channel. However, in RELAP5, at the initiation of flow reversal, coolant is expelled from the top and bottom of the heated section by the steam void created in the flow channel resulting in higher channel void

fraction. For a given channel power, both codes predict a lower channel void fraction for a lower bypass flow ratio (i.e., lesser bypass flow restriction). At a given bypass flow ratio, both codes indicate an increasing channel void fraction with power.

One of the means to validate a computer code is by direct comparison with test data. Two parameters from the flow reversal test data are available for comparison with the initial conditions predicted by RELAP5. They are the channel pressure drop and the water temperature downstream of the heated section. The RELAP5 comparison is with the data from test B081395E which was a 9 kW flow reversal test with a bypass ratio of 2:1 (test section to bypass section) and an inlet temperature of 130°F). The initial channel flow was 2 gpm. The inlet water temperature is shown in Figure B8.1. The measurements were from a thermocouple (JTI1) and a RTD (RTI1). The measured initial temperature was about one to two degrees below the nominal value of 130°F which was used in the RELAP5 calculation. The calculated outlet temperature is shown in Figure B8.2 together with the measured values from a thermocouple (JTO1) and a RTD (RTO1). The initial measured outlet temperature is about 5 degrees F below the predicted value. About two degrees of the difference can be explained by the lower than expected inlet temperature. The rest of the difference is mainly due to the higher than actual power assumed by RELAP5. The assumed constant power in the RELAP5 calculation corresponded to the maximum power experienced by the heated section at the time of flow reversal. For the test B081395E the power assumed in RELAP5 is about 6% above the actual initial power. Thus for a nominal water temperature rise of 32 degrees F (outlet minus inlet), the 6% over-power corresponds to 2 degrees F in water temperature. After accounting for the corrections in inlet temperature and initial power the RELAP5 prediction of the channel outlet temperature agrees well with the test data. It shall be noted that in Figure B8.1, the response of the RTD (RTI1) after flow reversal (at ≈35 sec.) is slower than the response of the thermocouple (JTI1). This is because the RTD has relatively larger thermal capacity than the thermocouple.

The channel pressure drop calculated by RELAP5 and corrected for the hydrostatic pressure is shown in Figure B8.3 with the measured data. The comparison between RELAP5 and the test data shows very good agreement in the initial steady-state (time < 5 sec.) channel pressure drop. In Figure B8.3, the measured channel pressure drop (DT5) is more steady than the calculated pressure drop after flow reversal at a time of ≈35 sec. Possible causes for this discrepancy in the transient pressure drop are damping in the lines between the pressure taps and pressure sensors and differences in the time lags in these lines.

In conclusion, similar flow behavior was calculated by RELAP5 and the drift-flux model in the simulation of flow reversal. Both

models were able to predict steady natural circulation after flow reversal. The two models compared favorably in the prediction of steady-state channel void fraction. Good agreement was observed between the RELAP5 predictions and available steady-state data from the flow reversal test.

References:

[B1] Cheng, Lap Y., 1995, "A RELAP5 Model of the Flow Reversal Tests," BNL Memorandum to Files.

[B2] Carlson, K.E., et.al., 1990, "RELAP5 Mod 3 Code Manual Volume I: Code Structure, System Models, and Solution Methods," NUREG/CR-5535 (Draft).

[B3] RELAP5 3.1.1 Input Manual, transmitted to BNL from Nancy Larson of INEL via letter number nsl-148-93.

[B4] Cheng, Lap Y., 1995, "Modifications to Interfacial Heat Transfer Coefficient in RELAP5," BNL Memorandum to Files.

[B5] Cheng, Lap Y., 1995, "RELAP5 Inputs for Analyzing Flow Reversal Tests," BNL Memorandum to Files.

[B6] Cheng, Lap Y., 1991, "Fraction of Bypass Flow and Pressure Loss in the Single-Channel Test," BNL Memorandum to Files.

[B7] Cheng, Lap Y. 1996, "Estimation of Time of Refill a Voided Channel," BNL Memorandum to Files.

[B8] Cheng, Lap Y., 1996, "Comparison of Steady-State Void Fraction Calculated by RELAP5 and a Drift-Flux Model," Revised September 24, 1996, BNL Memorandum to Files.

[B9] Cheng, Lap Y., 1995, "Comparison of RELAP5 and a Drift-Flux Model in the Calculation of Multi-Channel Flow Reversal," BNL Memorandum to Files.

[B10] Cheng, Lap Y., 1993, "A Single-Velocity Drift-Flux Model of Flow Reversal Transients," BNL Memorandum to Files.

[B11] Cheng, Lap Y., 1996, "Comparison of Void Fraction Predictions by RELAP5 and a Drift-Flux Model for the Flow Reversal Experiments," Revised September 24, 1996, BNL Memorandum to Files.

LIST OF TABLE

LIST OF FIGURES

TABLE B1

LIST OF RELAP5 SIMULATIONS OF FLOW REVERSAL TESTS

RELAP5 RUN NO.	REFERENCE* TEST NO.	TEST' OUTCOME	CHANNEL+ POWER (kW)	ORIFICE'' DIAMETER (in.)	BYPASS'' RATIO	NUMBER SIDES HEATED	INLET TEMP. (°F)	COASTDOWN TIME (sec.)	MAXIMUM++ VOID FRACTION
101	B021393F[1]	FR	7.0/6.7	0.199	2:1	1	130	40	0.696/.663
102	B021393H[1]	Trip	7.6/7.3	0.199	2:1	1	130	40	0.761/.728
103	B021393I[1]	FR	7.6/7.3	0.199	2:1	1	130	30	0.716/.688
104	B021393K[1]	Trip	8.4/8.1	0.199	2:1	1	130	30	0.789/.761
107	B021393Q[1]	FR	8.3/8.0	0.199	2:1	1	110	40	0.704/.678
108	B021393R[1]	Trip	9.1/8.8	0.199	2:1	1	110	40	0.771/.745
109	B030493D[1]	FR	6.9/6.6	0.199	2:1	1	130	40	0.762/.739
110	B030493E[1]	Trip	7.8/7.5	0.199	2:1	1	130	40	0.829/.807
112	B080394D[1]	Trip	6.8/6.5	0.129	5:1	1	130	40	0.884/.866
113	B080394E[1]	FR	6.4/6.1	0.129	5:1	1	130	40	0.860/.841
114	B080394G[1]	FR	7.9/7.6	0.28	1.5:1	1	130	40	0.739/.711
115	B080394H[1]	Trip	8.2/7.9	0.28	1.5:1	1	130	40	0.766/.739
302	B101694B[2]	FR	7.5/7.2	0.199	1.42:1	1	130	40	0.819/.793
303	B101694C[2]	Trip	8.5/8.2	0.199	1.42:1	1	130	40	0.904/.878
304	B101694F[2]	Trip	7.4/7.1	0.199	1.42:1	1	130	60	0.851/.819
305	B101694G[2]	FR	6.7/6.4	0.199	1.42:1	1	130	60	0.777/.744
306	B101694K[2]	Trip	6.9/6.6	0.129	2.78:1	1	130	40	0.895/.893
307	B101694L[2]	FR	6.7/6.4	0.129	2.78:1	1	130	40	0.894/.892

TABLE B1 (CONTINUED)

LIST OF RELAP5 SIMULATIONS OF FLOW REVERSAL TESTS

RELAP5 RUN NO.	REFERENCE' TEST NO.	TEST# OUTCOME	CHANNEL+ POWER (kW)	ORIFICE** DIAMETER (in.)	BYPASS## RATIO	NUMBER SIDES HEATED	INLET TEMP. (°F)	COASTDOWN TIME (sec.)	MAXIMUM++ VOID FRACTION
201	B061293E(1)	FR	8.3/8.0	0.199	2:1	2	130	40	0.784/.766
202	B061293G(1)	Trip	8.9/8.6	0.199	2:1	2	130	40	0.819/.801
204	B061293I(1)	Trip	7.3/7.0	0.199	2:1	2	150	40	0.824/.797
205	B061293J(1)	FR	6.4/6.1	0.199	2:1	2	150	40	0.743/.715
206	B061293K(1)	Trip	7.5/7.2	0.199	2:1	2	130	60	0.775/.737
207	B061293L(1)	FR	6.9/6.6	0.199	2:1	2	130	60	0.701/.664
1	B081395E(3)	FR	9.0/8.7	-	2:1:0	1	130	40	0.713/.690
2	B081395F(3)	Trip	9.8/9.5	-	2:1:0	1	130	40	0.774/.751
10	B081395K(3)	FR	13.8/13.6	-	1:3.4:0	1	130	40	0.860/.850
21	B081395N(3)	FR	13.8/13.6	-	1:3.4:0.6	1	130	40	0.668/.656
6	B081395U(3)	FR	11.5/11.2	-	2:1:1.2	1	125	40	0.55/.53
5	B081395V(3)	Trip	13.2/13.0	-	2:1:1.2	1	130	40	0.667/.653
11	B081795C(3)	FR	19.0/19.0	-	1:3.4:0.6	1	130	1.5	0.718/.718

Notes:

* The number in parenthesis after the test number is the test loop configuration: (1) refers to Figure 3; (2) refers to Figure 4; (3) refers to Figure 5.

\# FR means a successful flow reversal without a power trip for 30 seconds after initiation of flow reversal.

\+ Channel power corresponds to either the flow reversal power or the trip power given in Tables 2. The first number is the channel power after a reduction of 4% and 5% to account for steady-state heat loss from the single-sided and two-sided heaters respectively. The second number is the effective channel power after accounting for the higher of steady-state and transient heat losses.

** A numerical value indicates orifice diameter in bypass path in test configurations (1) and (2). A (-) indicates use of throttling valve in bypass path.

\## Refers to ratio of flow rates under initial conditions. First number applies to section flow, second number applies to primary bypass flow and third number, if present, applies to secondary bypass flow in test configuration 3.

++ Maximum time-averaged void fraction during the 10 second interval following reversal in RELAP5 calculation. The time averaging period is two seconds. The first number is based on a channel power accounting only for steady-state heat loss. The second number is based on the effective channel power which accounts for the higher of steady-state and transient heat losses.

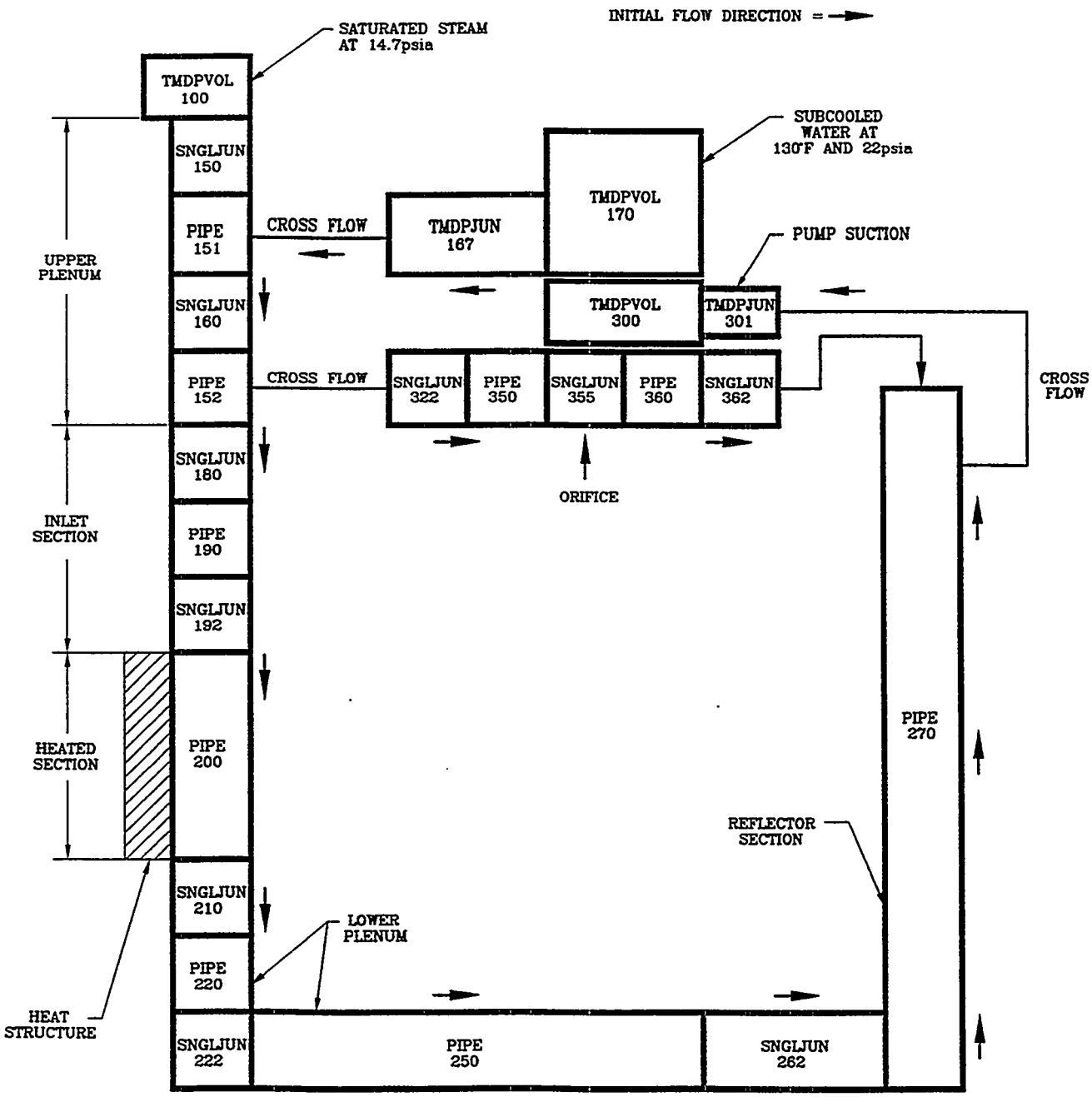

Figure B1 RELAP5 Representation of the Flow Reversal Test

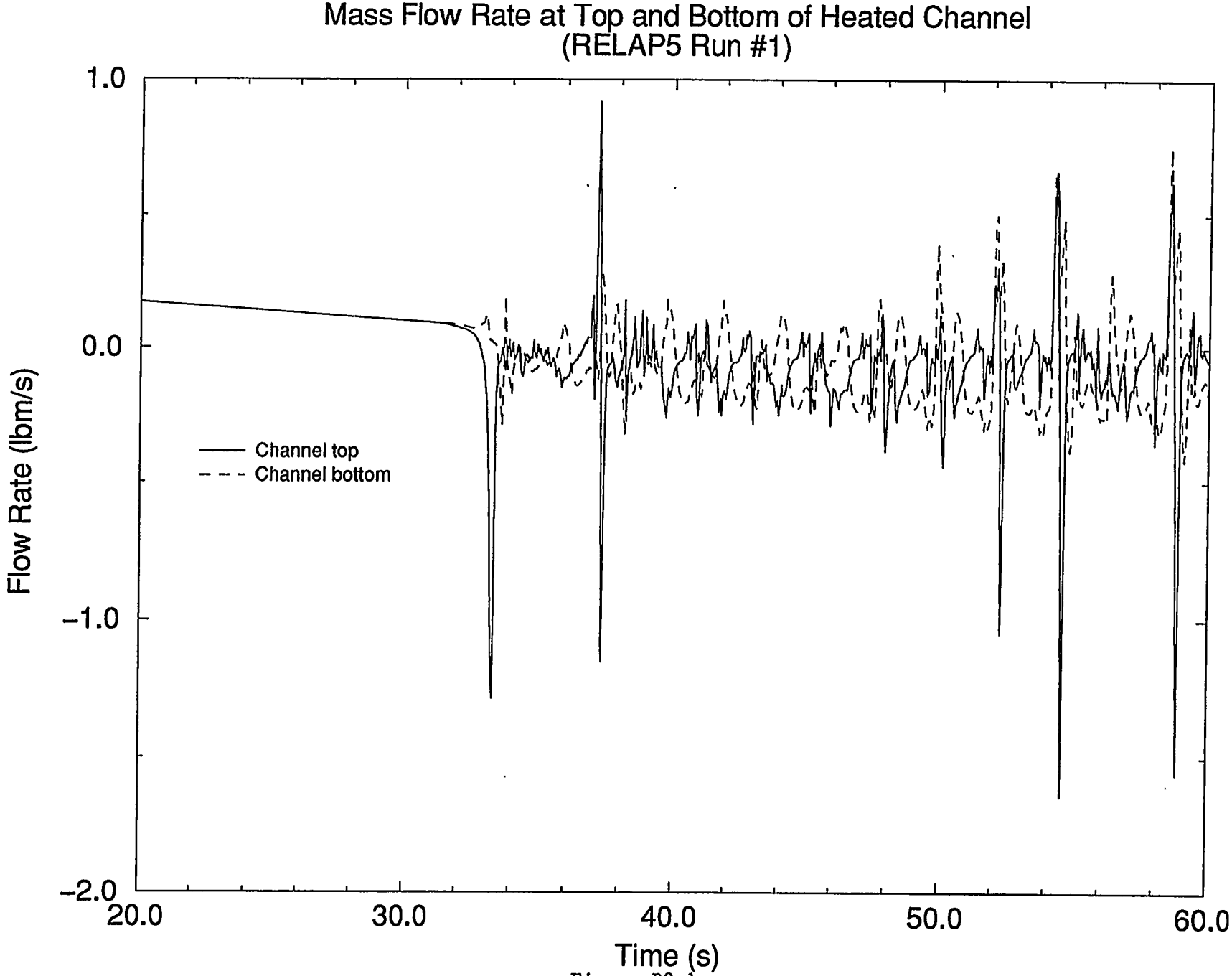
Mass Flow Rate at Top and Bottom of Heated Channel
(RELAP5 Run #1)
1.0
0.0
-1.0
-2.0
Flow Rate (lbm/s)
Channel top
Channel bottom
20.0
30.0
40.0
50.0
60.0
Time (s)

Figure B2.1

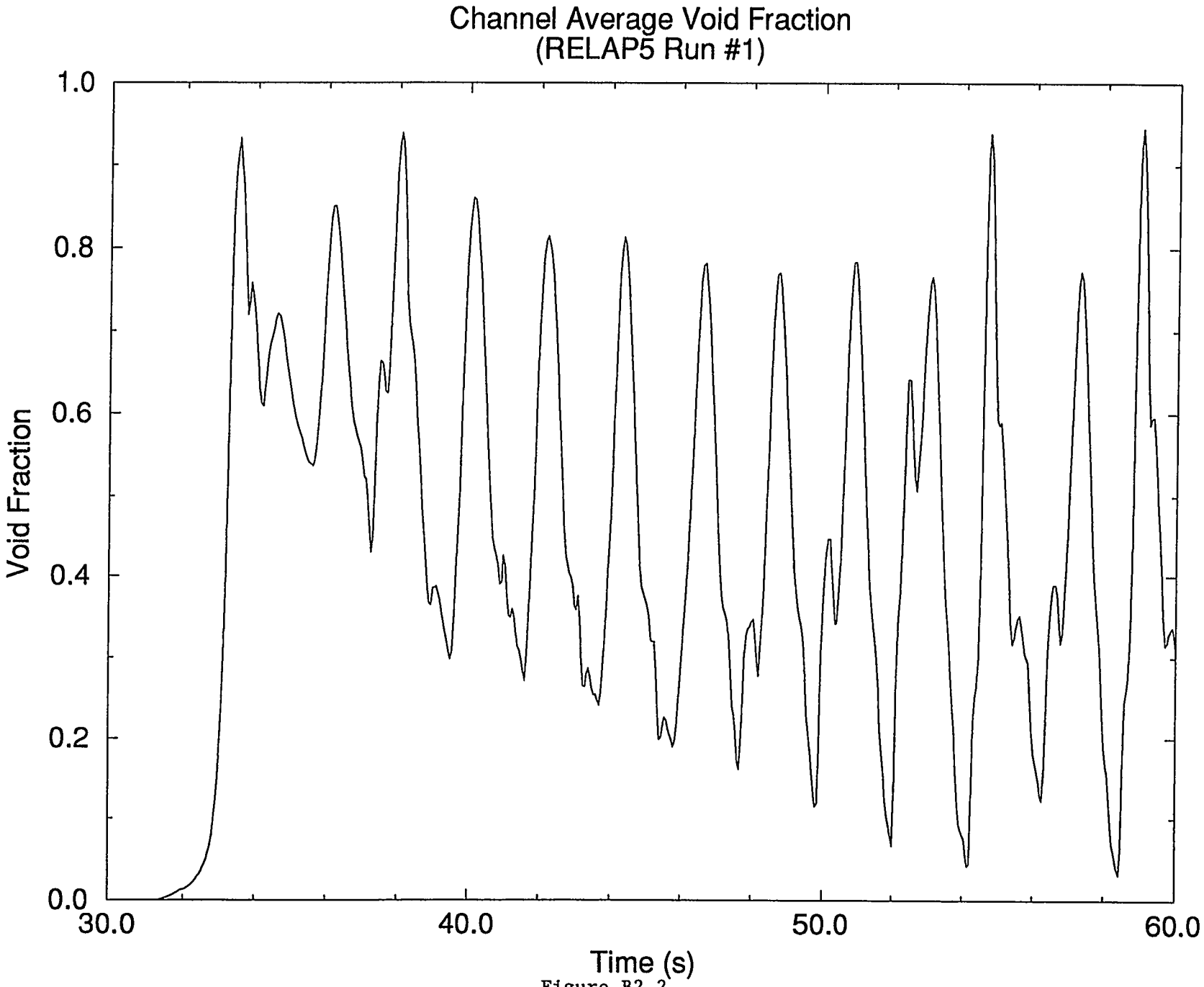
Channel Average Void Fraction
(RELAP5 Run #1)
Void Fraction
1.0
0.8
0.6
0.4
0.2
0.0
30.0
40.0
50.0
60.0
Time (s)

Figure B2.2

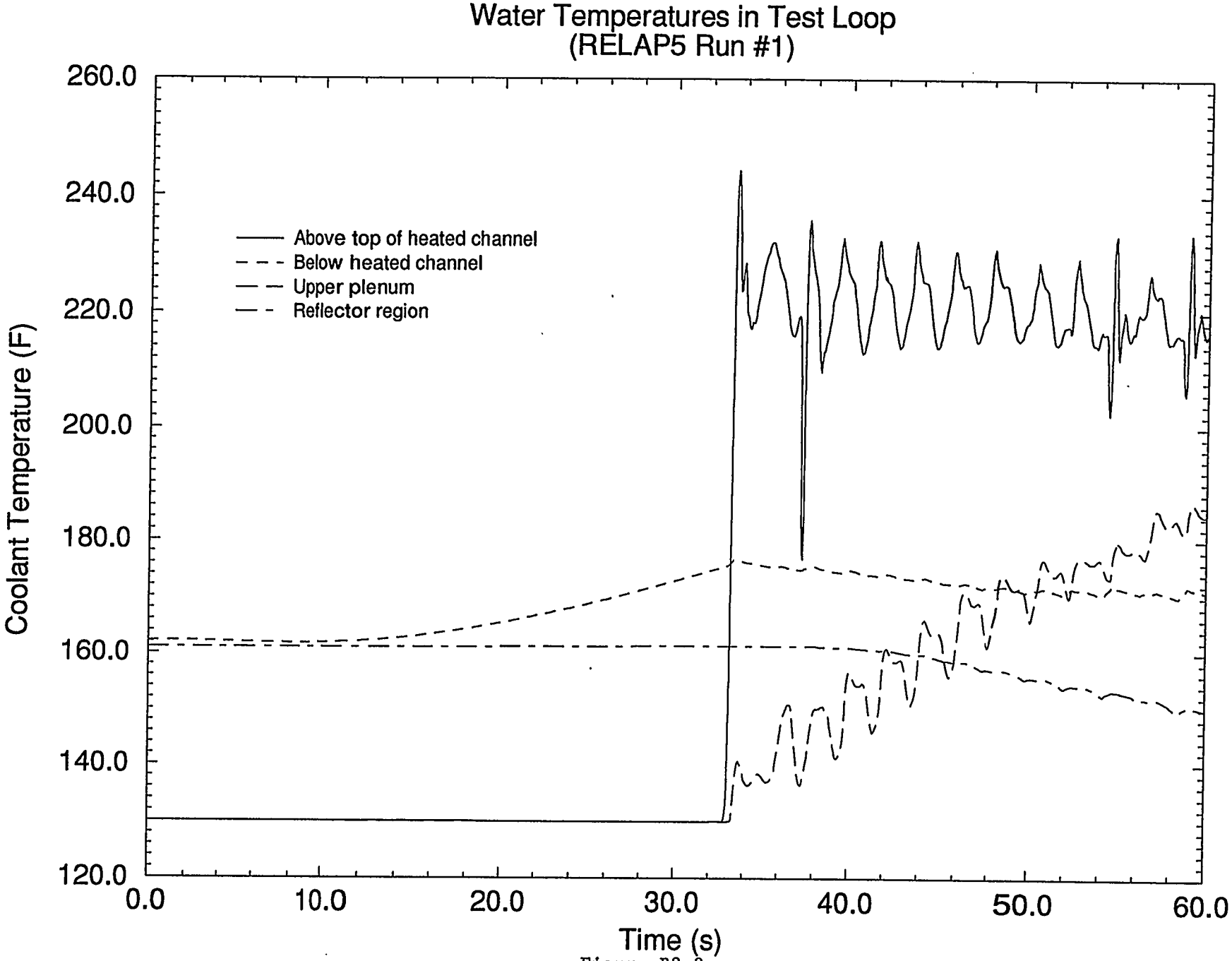
Water Temperatures in Test Loop
(RELAP5 Run #1)
Above top of heated channel
Below heated channel
Upper plenum
Reflector region
Coolant Temperature (F)
260.0
240.0
220.0
200.0
180.0
160.0
140.0
120.0
0.0
10.0
20.0
30.0
40.0
50.0
60.0
Time (s)

Figure B2.3

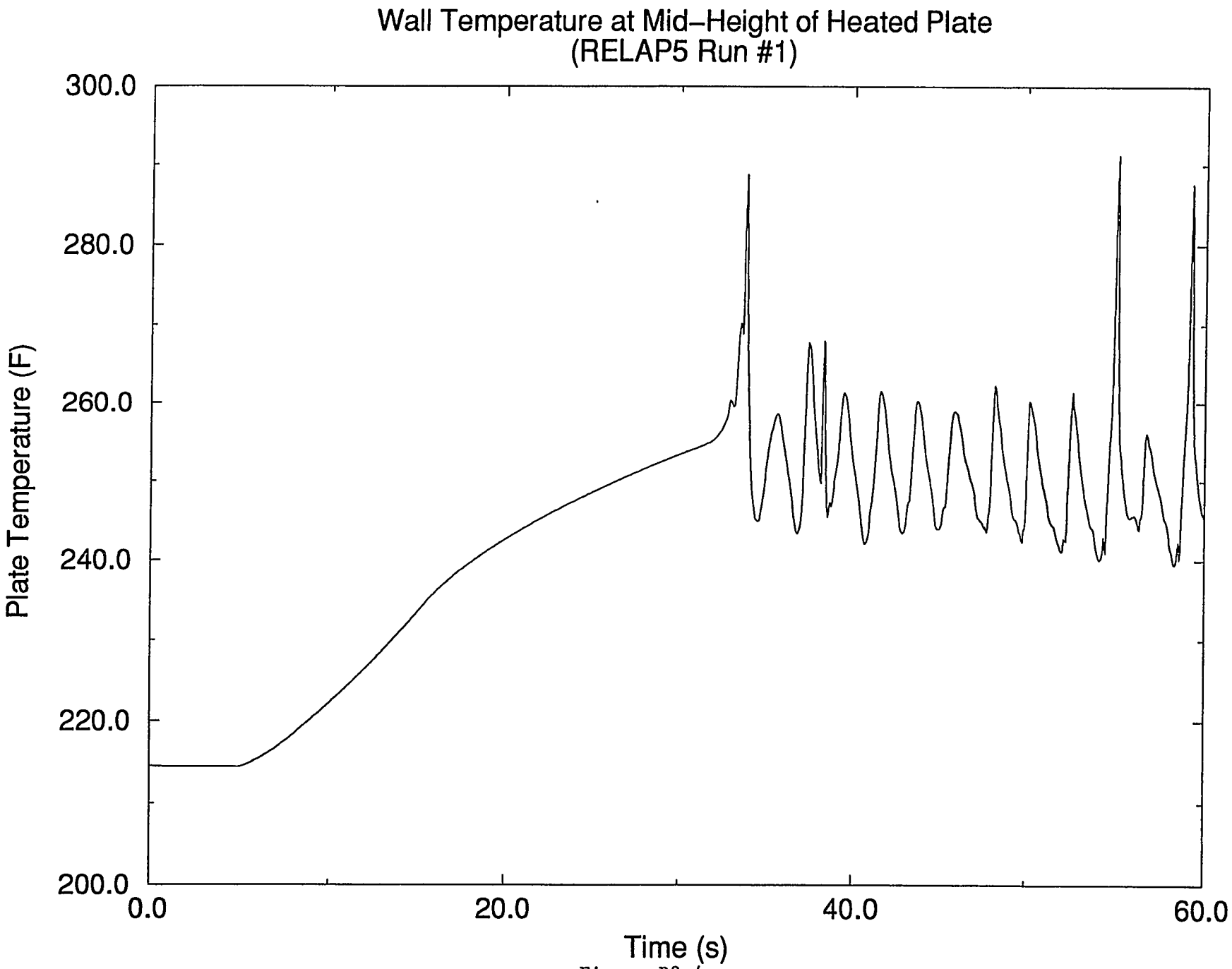
Wall Temperature at Mid-Height of Heated Plate
(RELAP5 Run #1)
300.0
280.0
260.0
240.0
220.0
200.0
Plate Temperature (F)
0.0
20.0
40.0
60.0
Time (s)

Figure B2.4

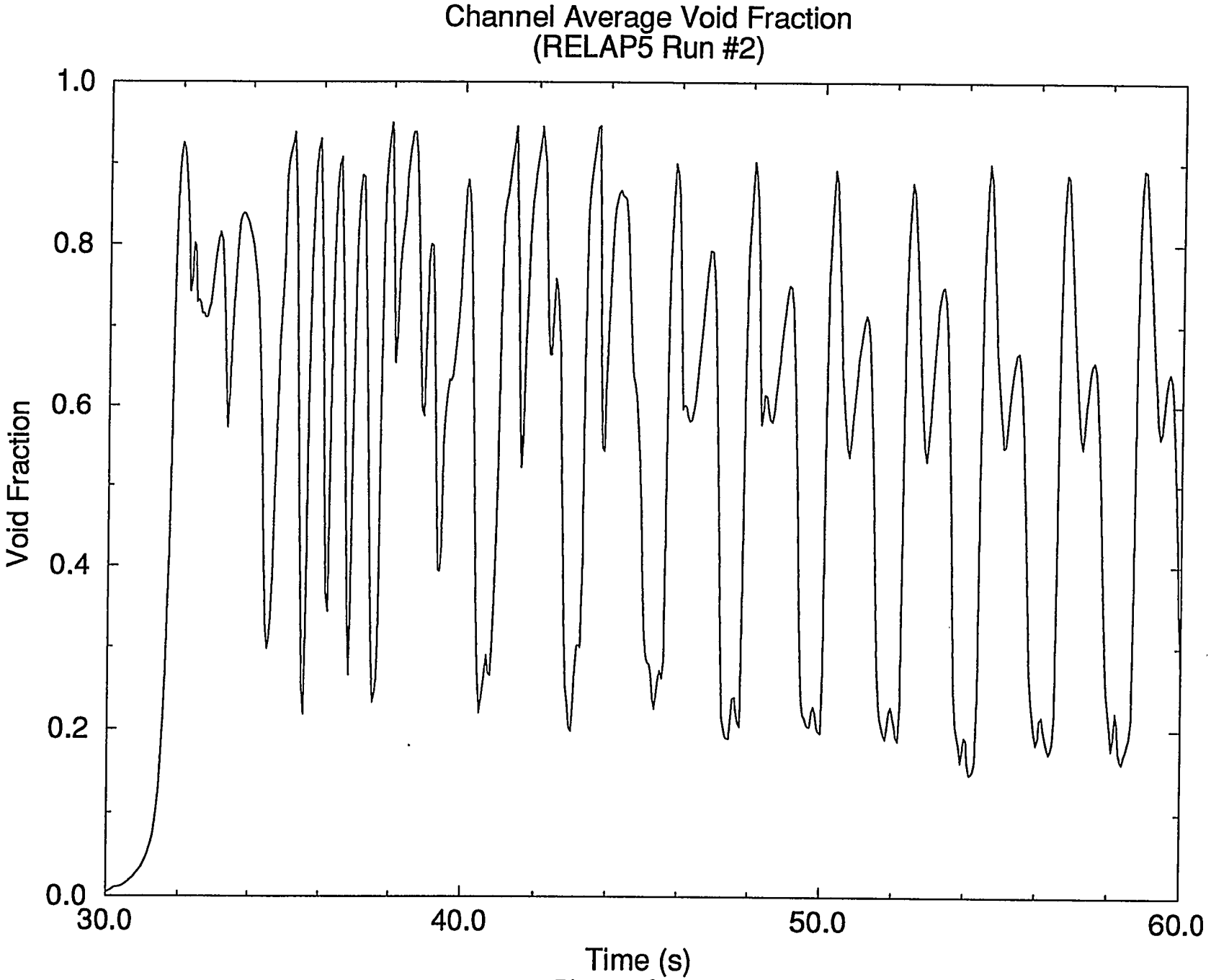
Channel Average Void Fraction
(RELAP5 Run #2)
Void Fraction
1.0
0.8
0.6
0.4
0.2
0.0
30.0
40.0
50.0
60.0
Time (s)

Figure B3

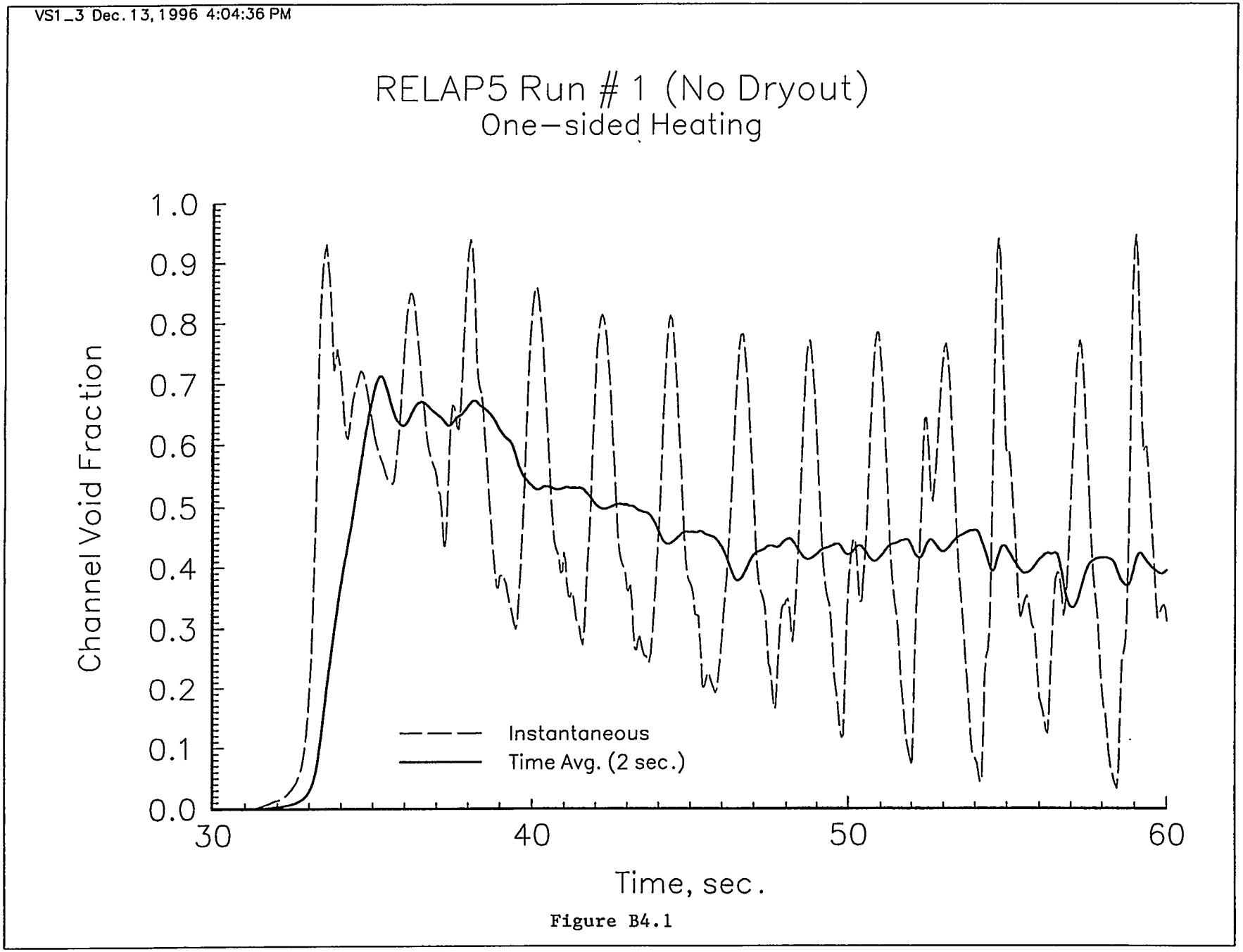
VS1_3 Dec. 13, 1996 4:04:36 PM
RELAP5 Run # 1 (No Dryout)
One-sided Heating
Channel Void Fraction
1.0
0.9
0.8
0.7
0.6
0.5
0.4
0.3
0.2
0.1
0.0
30
40
50
60
Time, sec.
Instantaneous
Time Avg. (2 sec.)

Figure B4.1

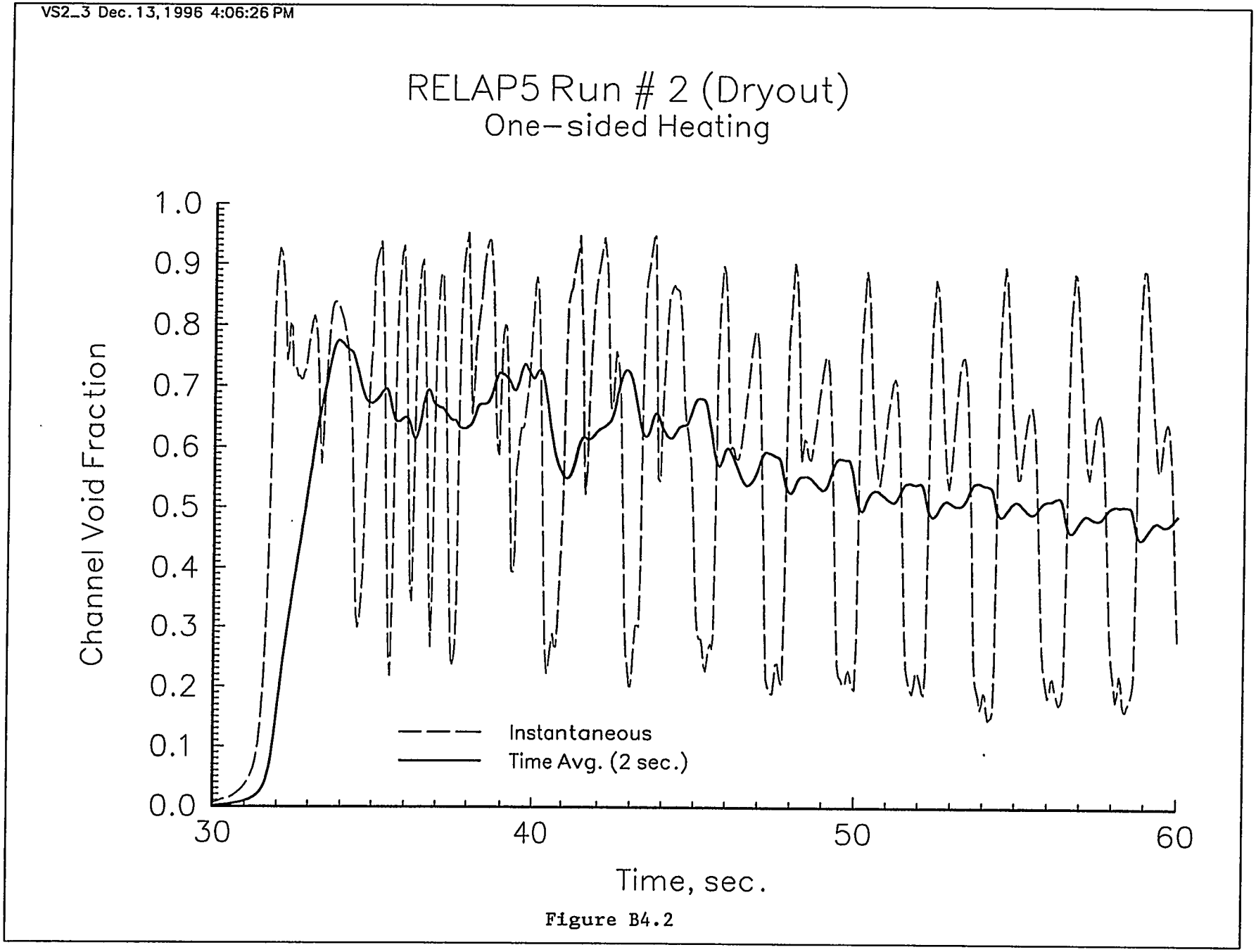
VS2_3 Dec. 13, 1996 4:06:26 PM
RELAP5 Run # 2 (Dryout)
One-sided Heating
Channel Void Fraction
1.0
0.9
0.8
0.7
0.6
0.5
0.4
0.3
0.2
0.1
0.0
30
40
50
60
Time, sec.
Instantaneous
Time Avg. (2 sec.)

Figure B4.2

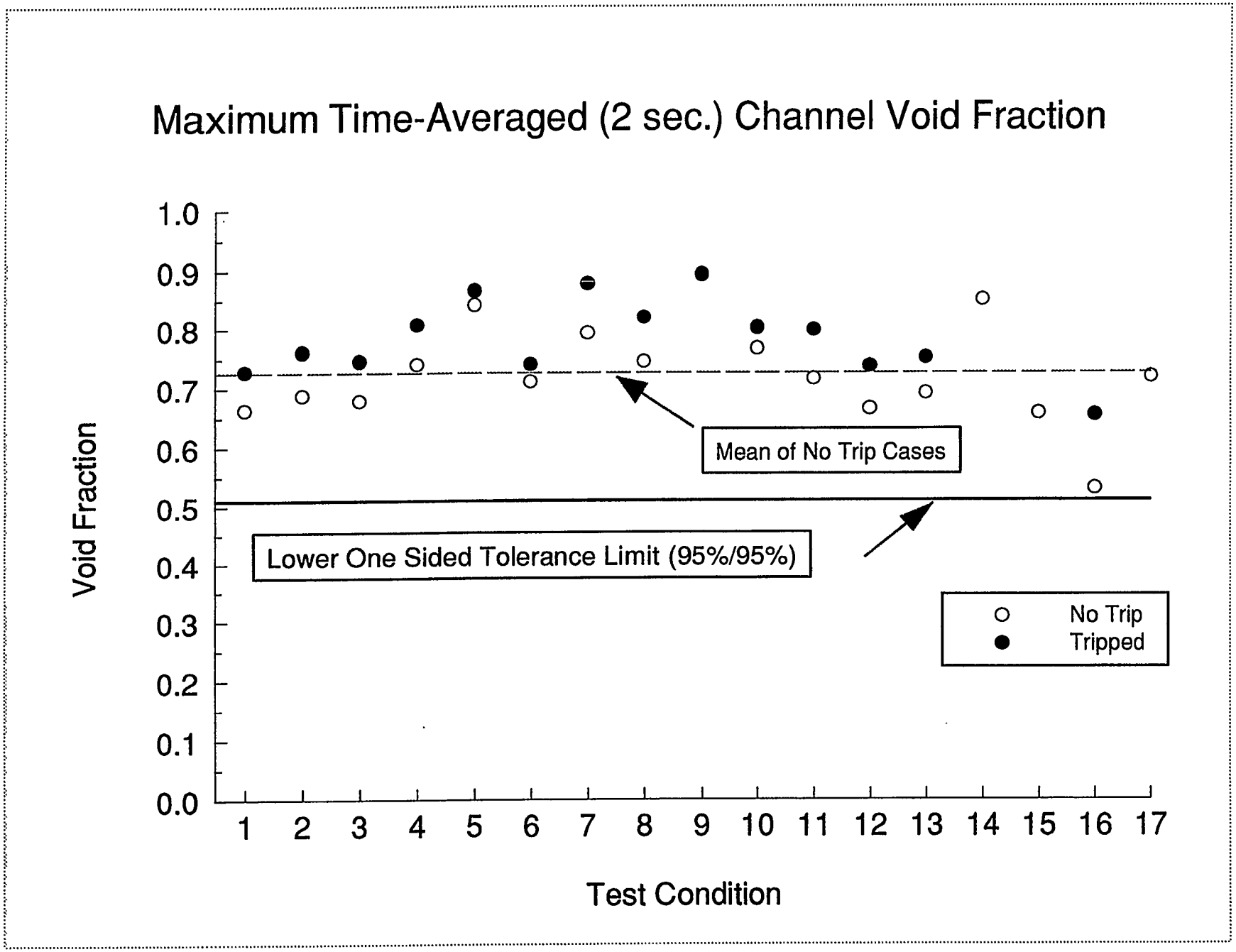
Maximum Time-Averaged (2 sec.) Channel Void Fraction
Void Fraction
1.0
0.9
0.8
0.7
0.6
0.5
0.4
0.3
0.2
0.1
0.0
1
2
3
4
5
6
7
8
9
10
11
12
13
14
15
16
17
Test Condition
Mean of No Trip Cases
Lower One Sided Tolerance Limit (95%/95%)
No Trip
Tripped

Figure B5

chvoid1 Dec. 13, 1996 4:17:12 PM

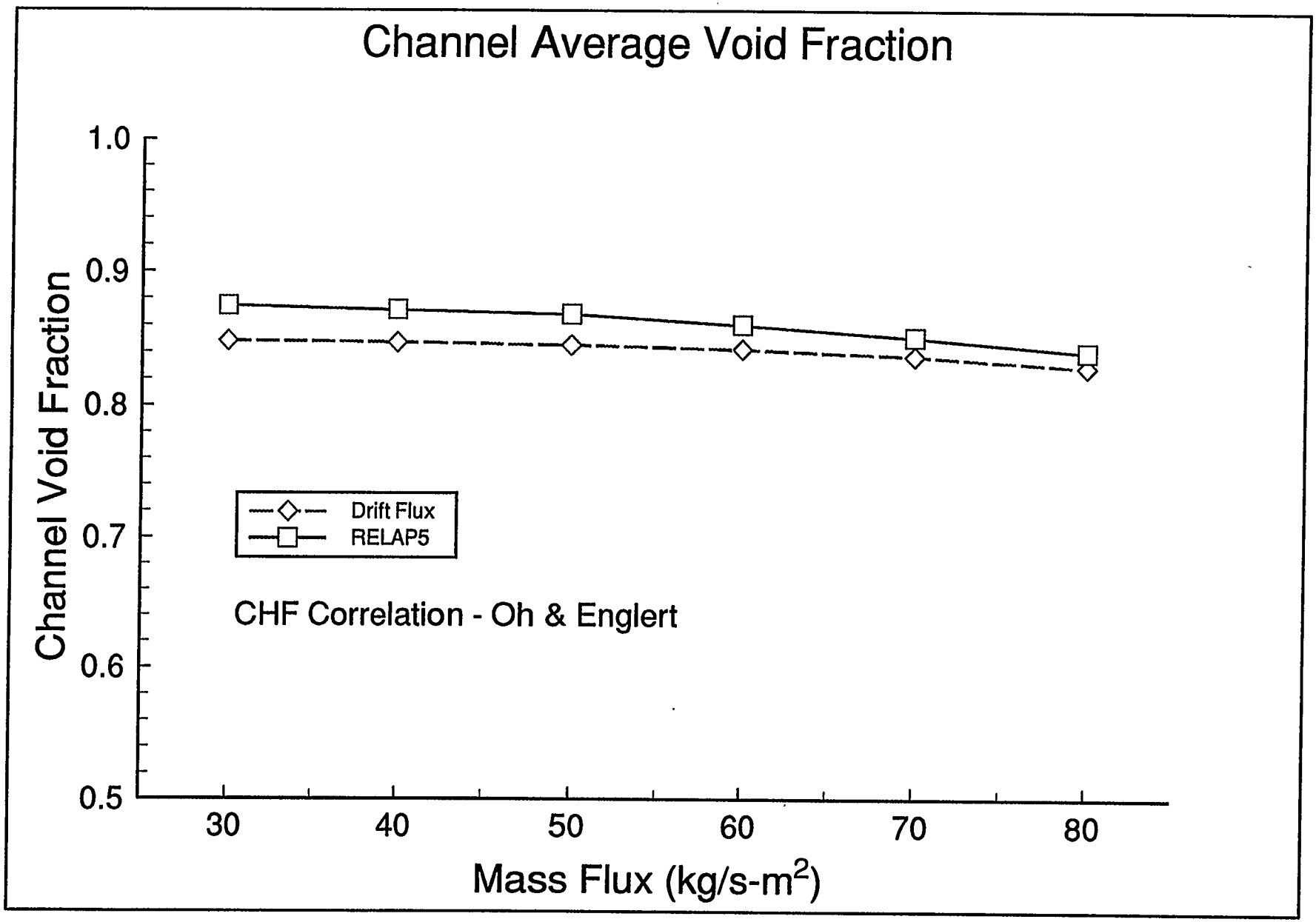

Figure B6.1

chvoid2 Dec. 13, 1996 4:30:03 PM

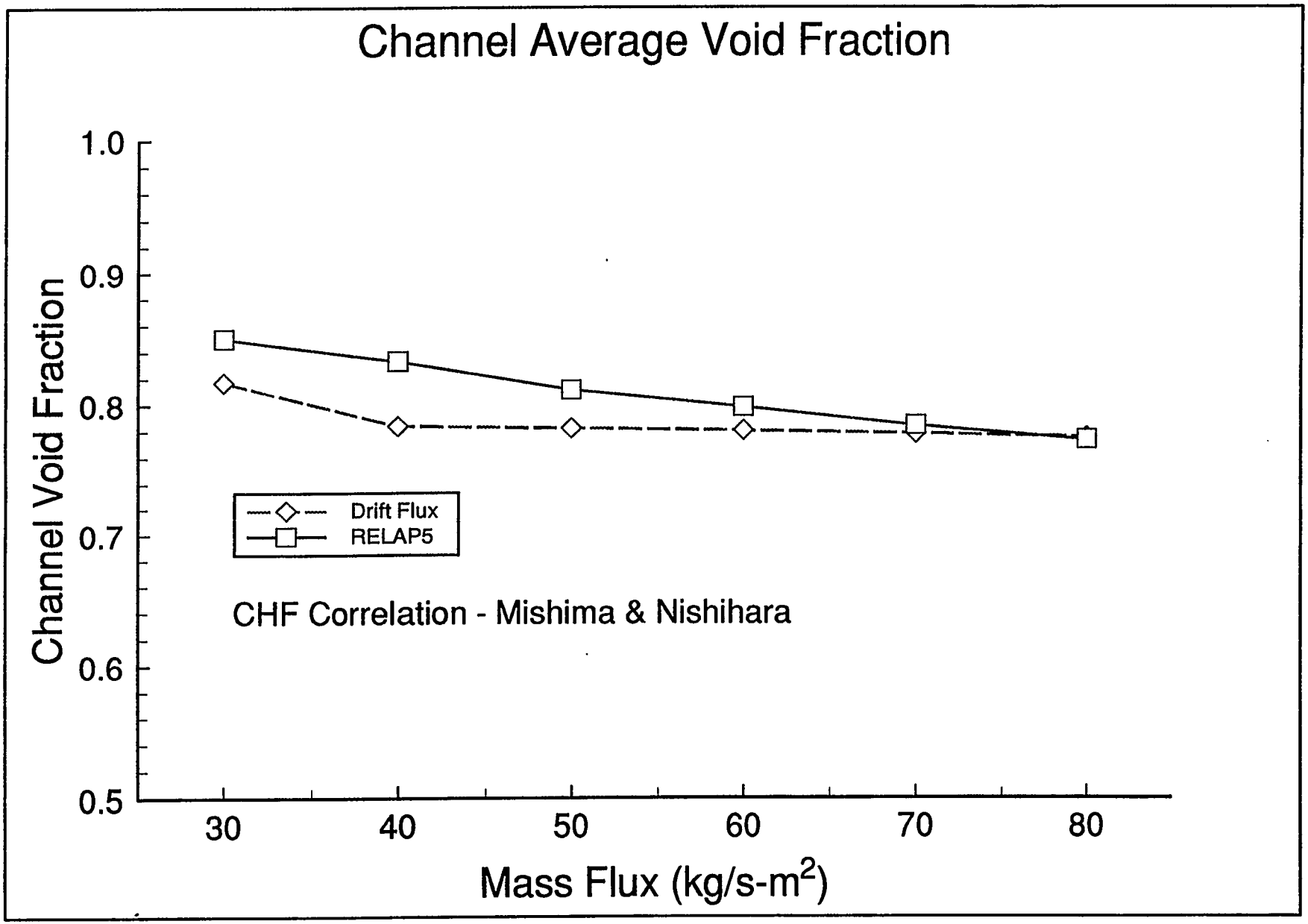

Figure B6.2

chvoid3 Dec. 13, 1996 4:29:34 PM

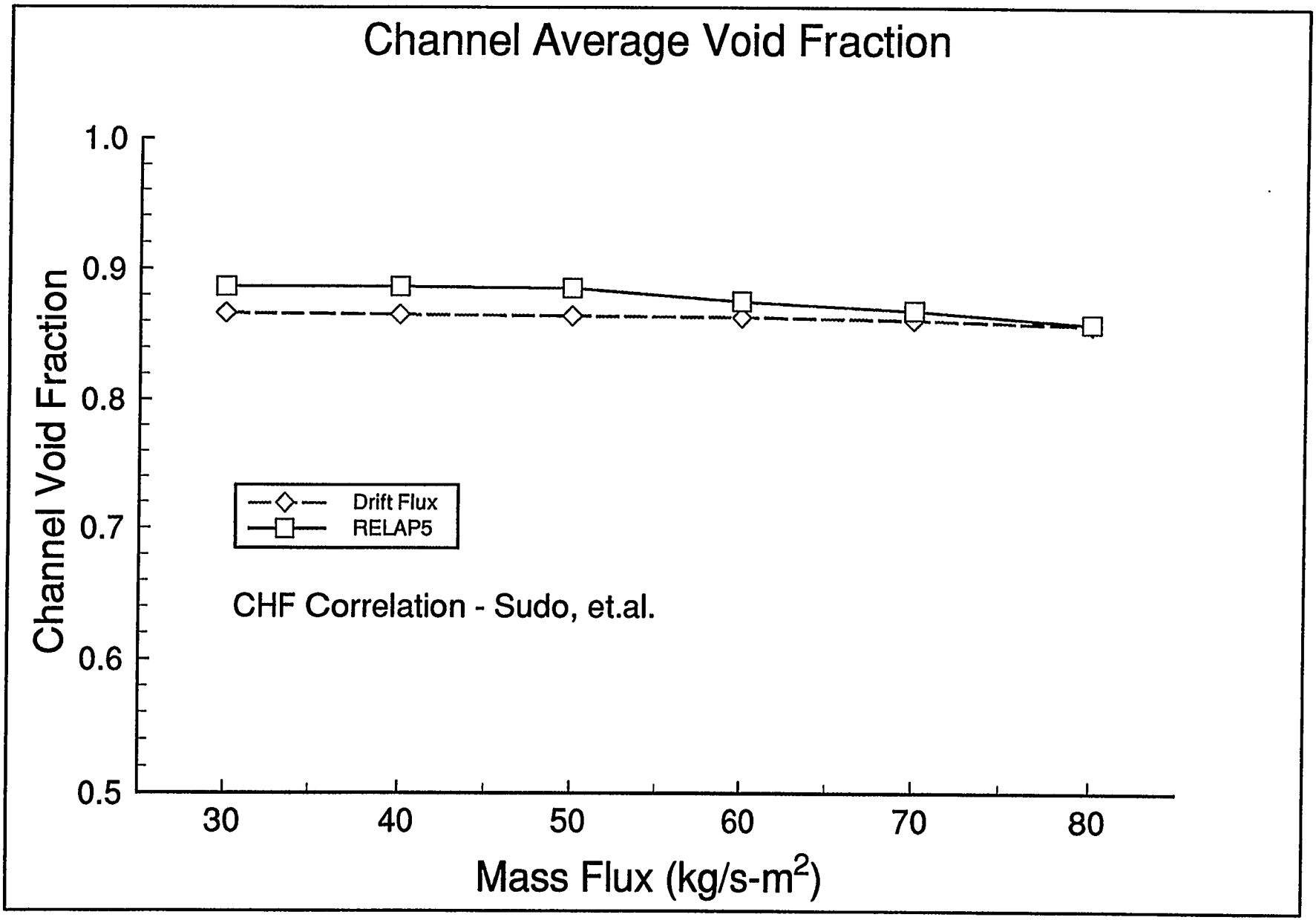

Figure B6.3

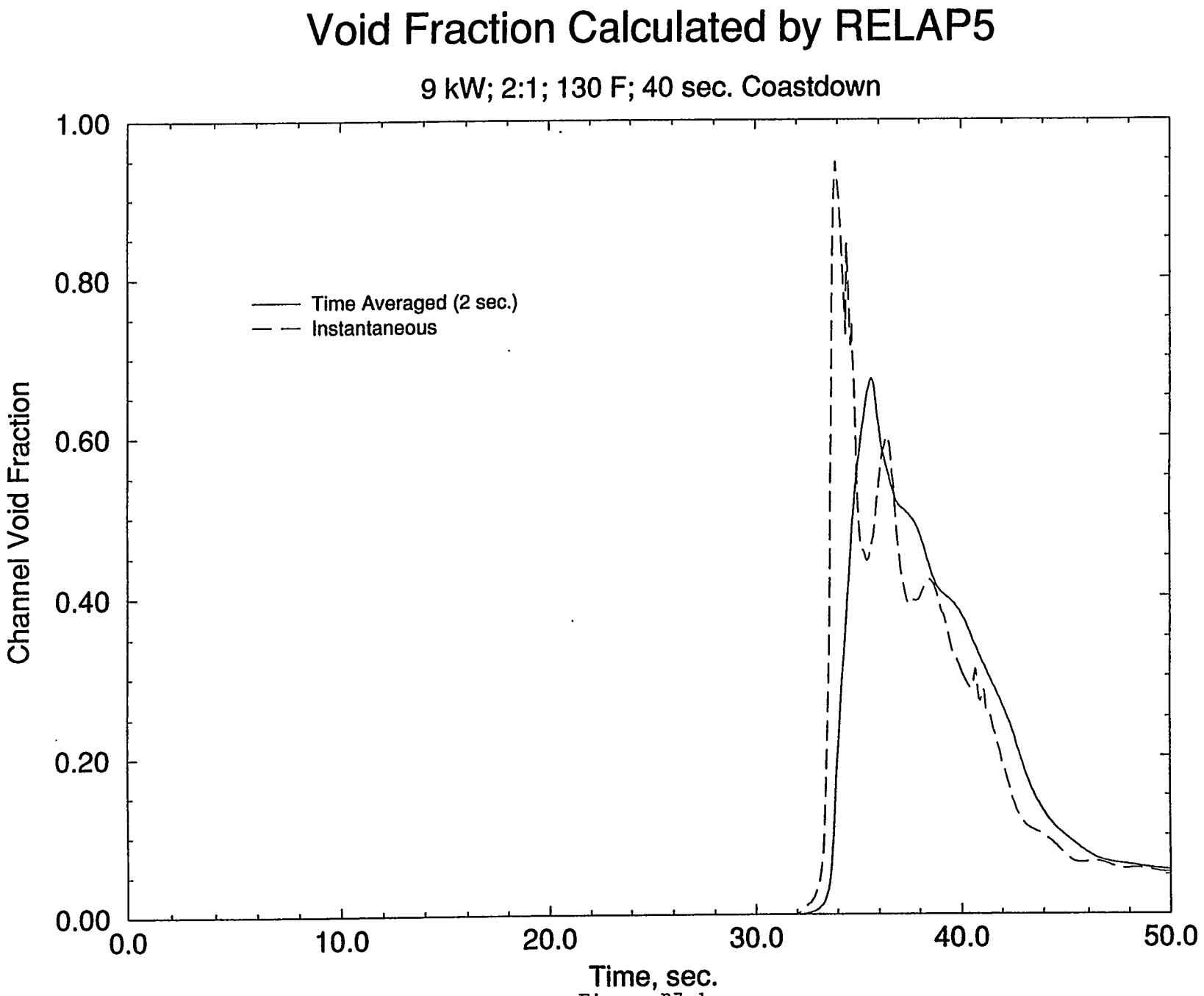
Void Fraction Calculated by RELAP5
9 kW; 2:1; 130 F; 40 sec. Coastdown
Time Averaged (2 sec.)
Instantaneous
Channel Void Fraction
1.00
0.80
0.60
0.40
0.20
0.00
0.0
10.0
20.0
30.0
40.0
50.0
Time, sec.

Figure B7.1

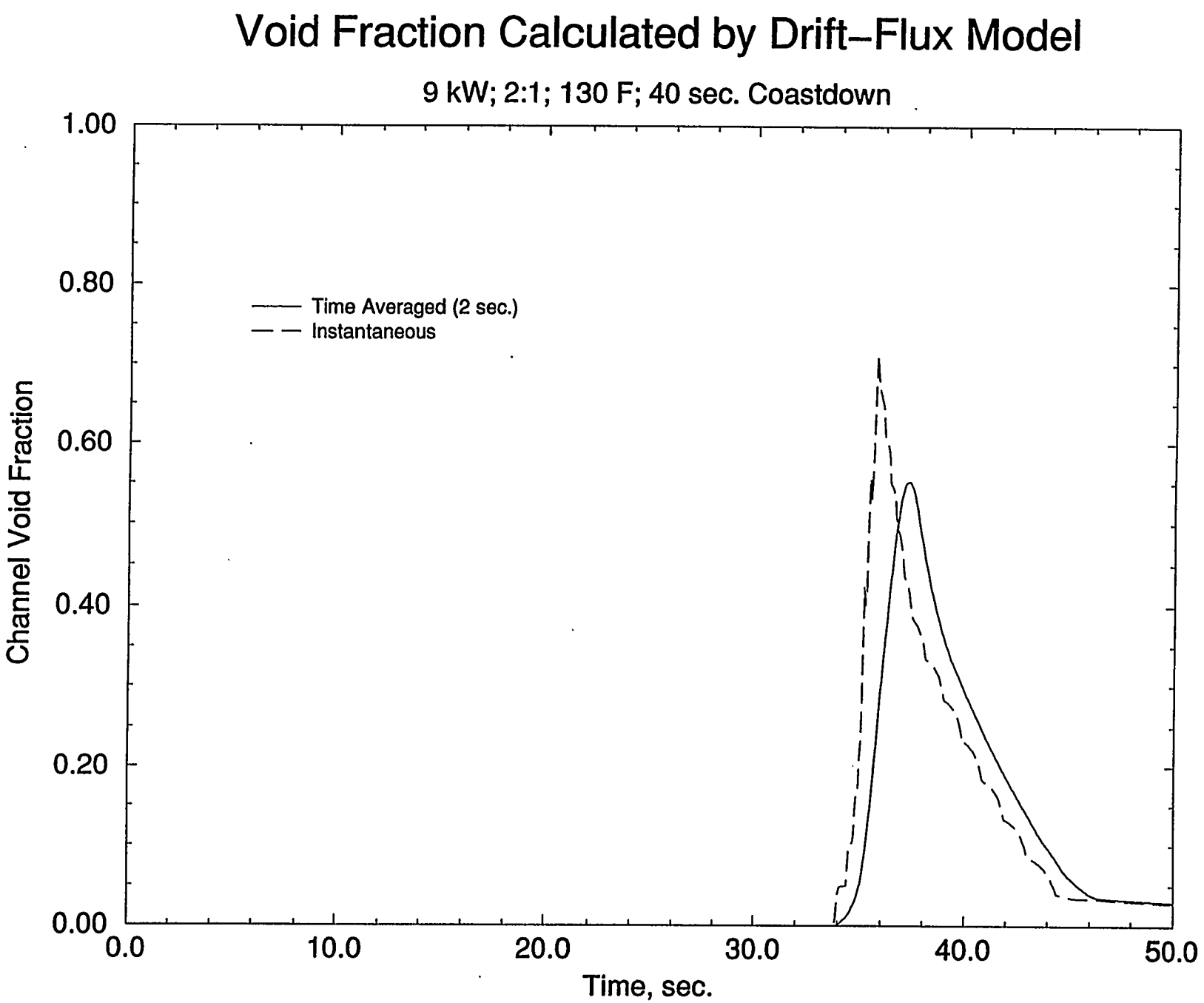
Void Fraction Calculated by Drift–Flux Model
9 kW; 2:1; 130 F; 40 sec. Coastdown
Time Averaged (2 sec.)
Instantaneous
Channel Void Fraction
1.00
0.80
0.60
0.40
0.20
0.00
0.0
10.0
20.0
30.0
40.0
50.0
Time, sec.
Figure B7.2

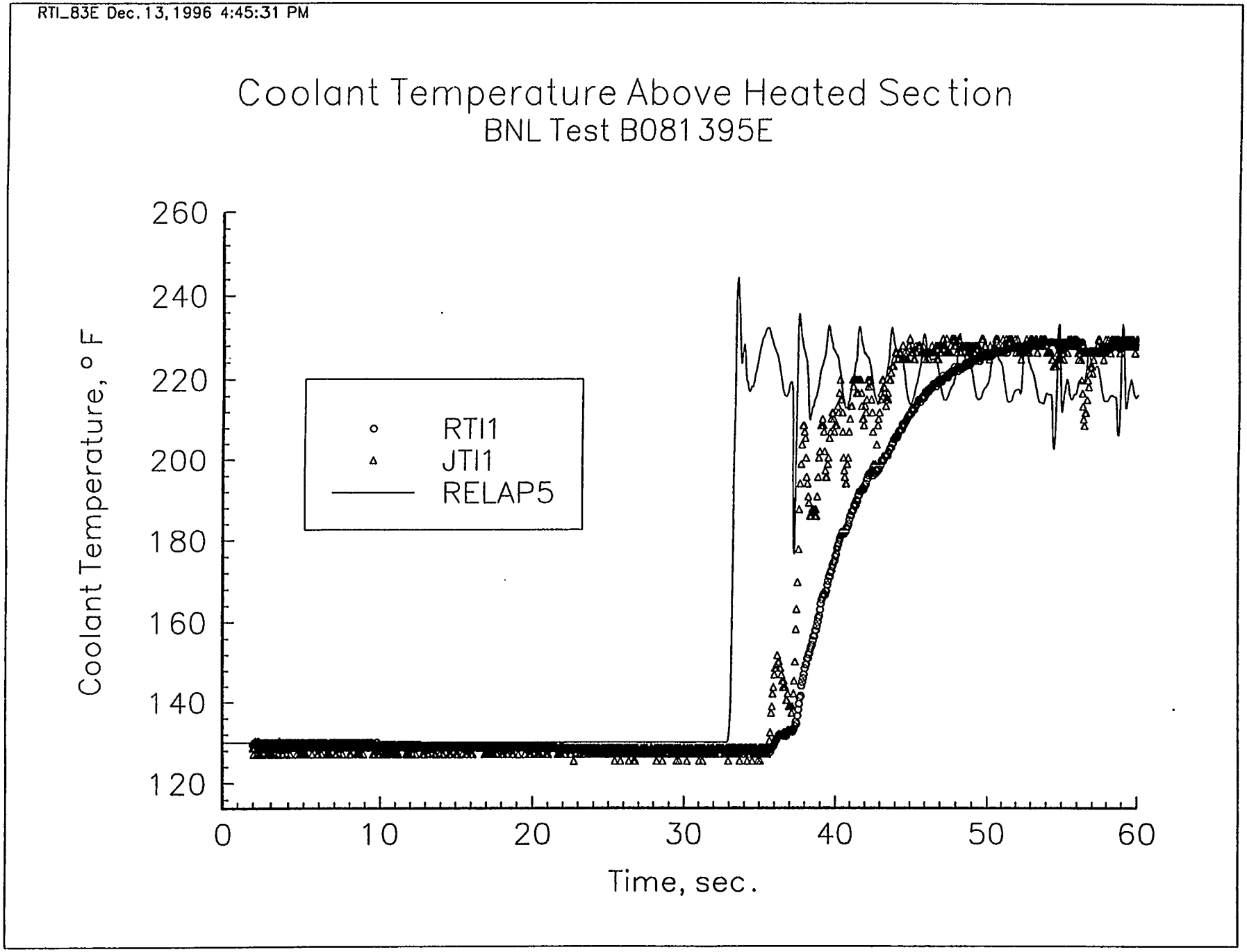
RTI_83E Dec. 13, 1996 4:45:31 PM
Coolant Temperature Above Heated Section
BNL Test B081395E
Coolant Temperature, ° F
260
240
220
200
180
160
140
120
RTI1
JTI1
RELAP5
0
10
20
30
40
50
60
Time, sec.

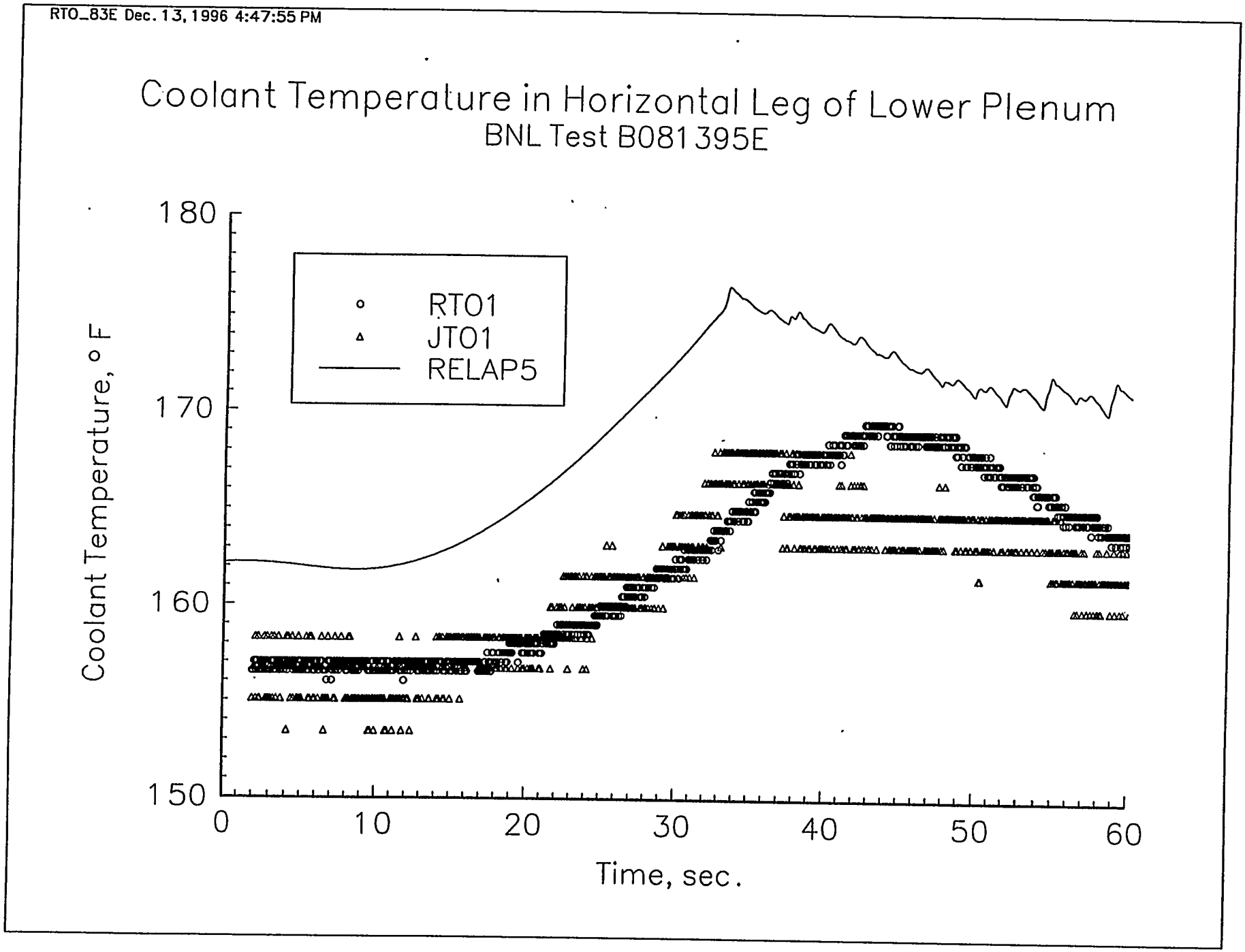
RTO_83E Dec. 13, 1996 4:47:55 PM
Coolant Temperature in Horizontal Leg of Lower Plenum
BNL Test B081395E
RTO1
JTO1
RELAP5
Coolant Temperature, °F
180
170
160
150
0
10
20
30
40
50
60
Time, sec.

Figure B8.2

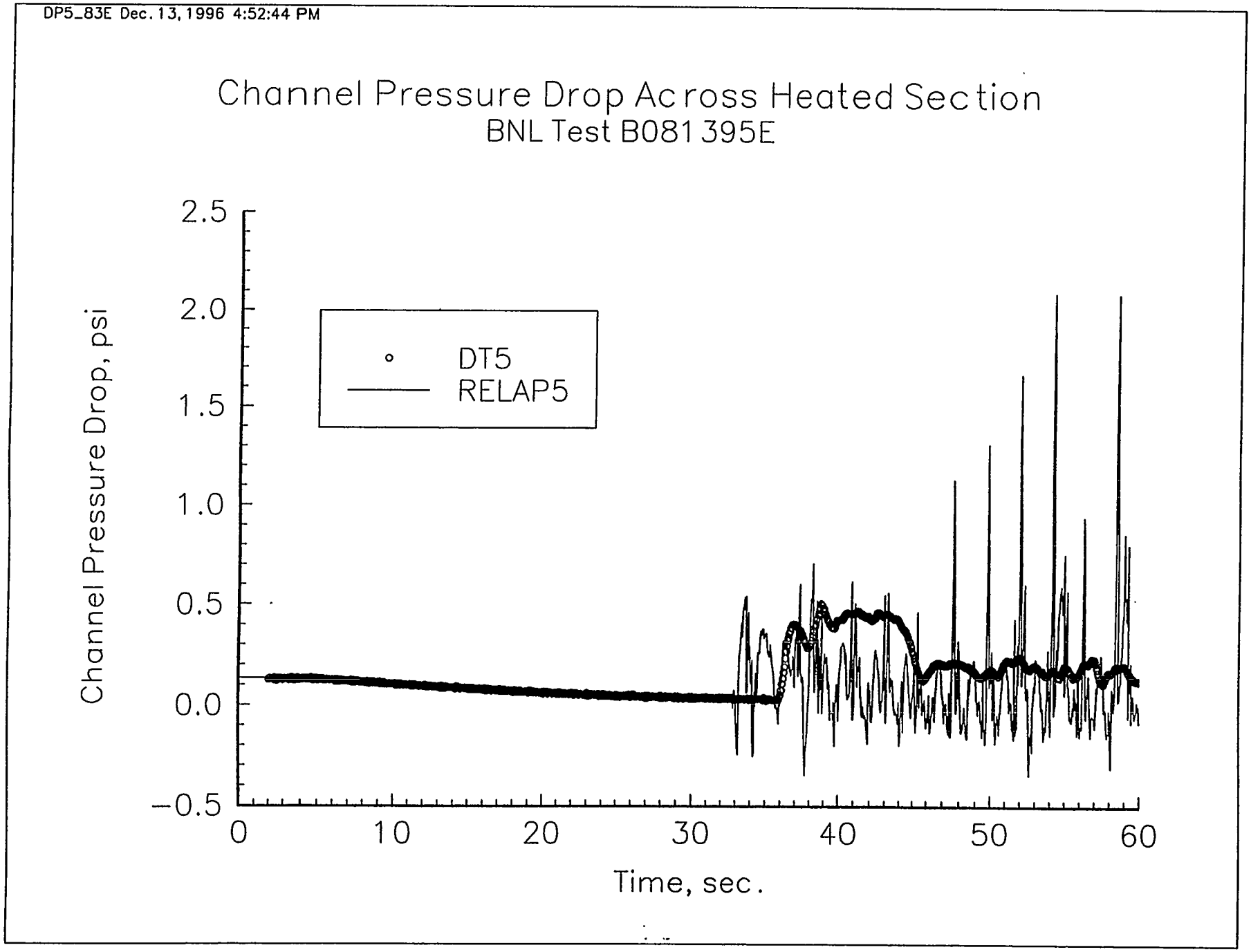
DP5_83E Dec. 13, 1996 4:52:44 PM
Channel Pressure Drop Across Heated Section
BNL Test B081 395E
Channel Pressure Drop, psi
2.5
2.0
1.5
1.0
0.5
0.0
-0.5
DT5
RELAP5
0
10
20
30
40
50
60
Time, sec.

APPENDIX C

SIMULATION OF REACTOR ACCIDENTS WITH RELAP5

A. MODEL DESCRIPTION

The RELAP5 model of the reactor is described in detail in Reference [C1]. A RELAP5 node diagram of the reactor vessel and the primary loop is shown in Figure C1. Important features of the model are summarized below:

1. Core Region

   a. The 532 (28 x 19) coolant channels in the HFBR core were divided into two channel types, hot and average. The RELAP5 model of the HFBR had 3 hot channel groups and 7 average channel groups. In the hottest fuel assembly, coolant channels #2, 3 and 4 were the highest powered channels [C2]. The 3 hot channel groups in the RELAP5 model corresponded to coolant channel #2, 3 and 4 respectively. Each hot channel group was equivalent to 14 coolant channels and the total number of hot channels was 42. The remaining 490 coolant channels were divided into 7 groups of geometrically identical average channels.

   b. Fission and decay heat power were modeled as a volumetric source that was uniformly distributed in the cermet embedded in the fuel plates. Heat was then conducted through the aluminum cladding to the coolant. The heat transfer area in each lumped channel was proportional to the number of individual coolant channels represented by the lumped channel. There was a variation in the power density of the fuel plate corresponding to each lumped channel. For the base case, the axial and spanwise power distribution was assumed uniform. The effect of axial variation in power density was also examined. The time dependence of power density following reactor shutdown was modeled.

   c. For the base case calculation at a nominal 60 MW, a safety factor which accounts for normal variations and instrument uncertainties had been included. The resulting RELAP5 base case power was 64.05 MW (see Table C1). For decay power, an additional safety factor of 1.23 was included. This factor reflected an uncertainty of 11.6% in the calculation of the decay power [C3] and another 10% to account for the helium evolution effect. The 10% factor was based on the flow reversal experiments which showed that helium evolution will reduce the safe flow reversal power by no more than 10%. The application of this factor reflected the fact that helium evolution

was not explicitly modeled in the RELAP5 calculation.

d. A fraction of the fission product gamma decay power (37.5%) was deposited directly in the reflector region of the reactor.

2. Other Primary System Components

a. The 4 flow reversal valves were lumped into one equivalent valve.

b. All the core bypass paths (control rod cooling, transition plate clearances, etc.) were lumped into one bypass path.

c. The two parallel loops in the primary system, which includes the two pumps and heat exchangers were lumped into one equivalent loop.

d. Shutdown pumps and pony motors were conservatively assumed not operating.

e. Plant data were used to benchmark the primary pump model and the depressurization of the reactor via the depressurization valve HCe-102.

3. Trip Settings and Instrument Response Times

These were obtained from the 60 MW accident analysis [C2].

a. Reactor trip will occur at a vessel water level of 209 inches with a 2.6 second delay or at a cover gas pressure of 180 psig with a 0.5 second delay.

b. Primary pump trip will occur at a water level of 197 inches with a 2.6 second delay or at a cover gas pressure of 120 psig with a 0.5 second delay.

c. Both the depressurization valve HCe-102 and the syphon break valve will open with a 1.5 second delay if both the water level has reached 197 inches and a pump trip has occurred.

4. Initial Conditions

The initial conditions for the RELAP5 calculation were based on combining the 60 MW design basis value [C2] with the worst case anticipated variation and instrument uncertainty. A list of the initial conditions for the base case of the RELAP5 calculations is shown in Table C1. The conditions were chosen to represent the scenario in which flow reversal will occur with minimum delay following reactor trip. This maximizes the power at the time of

flow reversal. A higher initial power, a lower primary flow rate, a lower cover gas pressure and a higher core inlet temperature all lead to an earlier flow reversal.

B. ACCIDENT SCENARIOS ANALYZED

The accidents that will lead to flow reversal were those involving a loss of forced flow cooling. Of these there were two categories of interest. One category is a loss of forced flow cooling without a loss of coolant. For this to occur in the HFBR it would be necessary to assume that the shutdown pumps and pony motors were not operating. While the shutdown pumps were not powered by a qualified power supply, the pony motors were and were currently required to be operational as a Technical Safety Requirement. However, for operational reasons it may be desirable in the future to relax this requirement. One of the accidents analyzed was therefore, a loss of forced flow cooling without loss of coolant. The accident of this type that leads to the most severe flow reversal condition (highest decay power and lowest pressure) was one involving a breach in the cover gas system. The design basis breach in the 60 MW FSAR was a circular orifice with an area of 1.39 in^2 and this was used in the current analysis. A break of this size, in the cover gas system results in a rapid depressurization of the reactor with a tripping of the reactor and the primary pumps within 2 seconds after breach initiation. This accident scenario was the most severe because the pump trip occurs with little delay after the reactor trip. This maximizes the decay heat at the time of flow reversal. The rapid depressurization also lowers the saturation temperature and results in flow reversal occurring at a lower pressure (atmospheric) which was another unfavorable factor. This contrasts with a depressurization due to accidental opening of depressurization valve HCe-102 which results in a relatively slow depressurization.

The other event which would lead to flow reversal was a LOCA which results in the liquid level in the reactor vessel dropping below 197 inches. Two bounding accidents of this type were examined in which the break size was the same as previously assumed. In one the break location was in a beam tube and the other was at the primary pump discharge. The latter location maximizes the leak rate because the pressure at the leak location was the highest. However, in both these LOCAs, the rate of depressurization was relatively slow compared to the breach in the cover gas system, because the volumetric leak rate for a liquid was much lower than for a gas for the same hole size and pressure drop. The consequence of this was that there was a significant delay between reactor trip and pump trip. This delay results in the flow reversal occurring at a decay power that was lower than the decay power at which flow reversal occurs in the accident involving a breach in the cover gas system. In addition, at the time of flow reversal in the LOCA scenarios, the cover gas system has not fully

depressurized. This factor also results in a more favorable condition for flow reversal. Accordingly the accident involving a breach in the cover gas system was considered the bounding accident with respect to flow reversal and the discussion which follows will focus on this accident.

C. RESULTS OF ACCIDENT ANALYSIS

1. Overview

Several variations of the cover gas depressurization accident were performed using RELAP5 to determine the effect of changes in some of the input parameters. The following cases were analyzed:

a. Base Case (Case 1)

Reactor power: 64.05 MW (includes safety factor)
Fuel plate heating: assumed uniform
Flow reversal valve operating: 4
Pump coastdown: based on plant data

b. Case 2

Reactor power: 2 x base case = 128.1 MW
All other parameters were the same as base case.

c. Case 3

Reactor power: 128.1 MW
3 flow reversal valves operating, one not operating.
All other parameters were the same as the base case.

d. Case 4

Reactor power: 128.1 MW
Increased the pump friction torque coefficient by a factor of 1.5. This reduced the pump coastdown time from 57.4 to 46.2 sec. All other parameters were the same as the base case.

e. Case 5

Reactor power: 128.1 MW
Decreased the pump friction torque coefficient by a factor of 1.5. This increased the coastdown time by about 20%. All other parameters were the same as the base case.

f. Case 6

The axial power density distribution was assumed to have chopped cosine shape. All other parameters were the same

as the base case.

g. Case 7

The axial power density distribution was assumed to have an inverted chopped cosine shape. In other words the maximum power density occurred at the top and bottom of the fuel plate. All other parameters were the same as the base case.

h. Case 8 [C4]

The gap of coolant channels in hot channel group #1 was reduced from 0.117" to 0.112". All other parameters were the same as the base case.

i. Case 9 [C5]

The core was modeled by three hot channels, representing coolant channel #2, 3, and 4 respectively, and one average channel group consisting of 529 channels. All other parameters were the same as the base case.

j. Case 10 [C5]

The core was modeled by one hot fuel element and one average channel group. The hot fuel element had a common inlet tube section shared by three hot channels and an average channel representing the other sixteen channels. One fuel plate separated hot channels #1 and 2 and another fuel plate was between hot channels #2 and 3. All other parameters were the same as the base case.

k. Case 11 [C5]

The case was similar to Case 9 except in the representation of the fuel plates adjacent to the hot channels. In Case 11 there was a common fuel plate between two hot channels, one between coolant channels #2 and 3 and another between coolant channels #3 and 4.

l. Case 12 [C5]

This case was similar to Case 10 except the gap of the three hot channels in the hot fuel element was reduced by 0.005".

m. Case 13 [C6]

The flow coefficient (C_v) of the flow reversal valve in the backward flow direction was multiplied by a factor of

1.2. All other parameters were the same as the base case.

n. Case 14 [C6]

The flow coefficient (C_v) of the flow reversal valve in the backward flow direction was multiplied by a factor of 0.88. All other parameters were the same as the base case.

o. Case 15 [C7]

The case was similar to the base case except the gap of the average channels was reduced from 0.0984" to 0.0969".

The general characteristics of the base case results will be discussed first and will be followed by a comparison of the calculated maximum 2 second time averaged channel void fraction for the various cases.

A more detailed description of the calculations and results are given in References [C1] and [C4] through [C7].

2. Base Case

The initial power for the base case was 64.05 MW and that corresponded to a nominal reactor power of 60 MW. The flow reversal transient was initiated by a breach of the reactor vessel in the cover gas region. The location of the breach was selected to result in the shortest time interval between the reactor trip and the primary pump trip. Both the reactor trip and the primary pump trip were activated by the low pressure trip setpoints for the cover gas. Figure C2.1 shows the rapid depressurization of the cover gas following the break initiation at time zero. The reactor was depressurized to the ambient pressure at 14.3 sec. The condition of zero cover gas pressure was similar to the single channel flow reversal test which had the upper plenum region opened to the atmosphere.

The primary pump coastdown began in less than one second after the reactor trip. Figure C2.2 shows the angular velocity of the primary pump as a function of time. Coastdown from initial operating speed to zero speed took about 55 seconds. The corresponding primary flow in units of gpm was shown in Figure C2.3.

The junction mass flow rates at the top and bottom of the heated section of the three hot channel groups are shown in Figures C2.4 and C2.5 respectively. In these figures the positive flow direction was downward. The first flow reversal in the three hot channel groups occurred at about the same time (≈47 sec. after

reactor trip). Among the three hot channel groups, the first to go through flow reversal was group number 3 which had the lowest power of the hot channels but the narrowest channel gap (0.095 inches).

The junction flow rates for the 7 average channels are shown in Figures C2.6 through C2.9. For the average channel groups, it was the highest powered group (group number 7) that first went through flow reversal.

Flows through the flow reversal valve and the core bypass flow path are shown in Figures C2.10 and C2.11 respectively. The flow reversal valve started to open at about 9 sec. (see Figure C2.12) and it stayed open for the rest of the transient. The check valve in the primary loop was partially open till the end of the flow coastdown. In Figure C2.13, the check valve was seen to remain almost fully closed after the primary pump had stopped at 57 sec.

The oscillatory behavior of the coolant channel mass flow rates shown in Figures C2.4 through C2.9 is somewhat similar to the results of the RELAP5 calculations done for the single channel test (see Appendix A). One of the major differences between the reactor and the test is the presence of multiple natural circulation flow paths in the reactor. The effect of multiple heated channels on natural circulation is that at any given time the flow direction does not have to be the same in all flow channels. This aspect of multi-channel effect is shown clearly by the individual channel mass flow rate which oscillates between upflow and downflow. The average behavior of the natural circulation flow through the HFBR core can be characterized by the time averaged flow rate in the flow paths which constitute the natural circulation loop. In the following calculation the flow through the core region is represented by the mass flow rates at the lower end of the heated channels (see Figures C2.5, C2.8 and C2.9). The flow rates are time averaged between 50 and 100 seconds.

Flow Path	**Time Averaged Mass Flow Rate (kg/s)**
Hot channel #1	-0.69
Hot channel #2	-0.63
Hot channel #3	-0.51
Average channel #1	2.3
Average channel #2	2.2
Average channel #3	-0.51
Average channel #4	-0.69
Average channel #5	-1.9
Average channel #6	-2.4
Average channel #7	-2.7
Core bypass	2.5
Flow reversal valve	2.9

Σ upflow channels = 10. kg/sec.
Σ downflow channels = 4.5 kg/sec.

The time averaged mass flow rates show that the upflows were balanced roughly by the downflows (i.e., downflow channels + core bypass + flow reversal valve) as to be expected for a situation of closed loop natural circulation. Another observation to be made from the above tabulation is that the magnitude of upflows is proportional to flow area and channel power.

The state of the coolant in the flow channel is reflected by the average channel void fraction which is shown in Figures C2.14 through C2.16 for the ten channel groups. The periodic behavior of the channel void fraction can be characterized by three stages, a boiling stage, a heat up stage and a reflood stage. When the coolant reached the boiling condition, the generation of steam voids in a channel resulted in a rapid increase in the channel void fraction (the boiling stage). Flow began to enter the channel because of the density difference between the coolant channel and the reflector region. The coolant quickly condensed or displaced the steam in the channel and cooled down the heated wall (the reflood stage). When the channel was occupied by single-phase liquid, the mass flow was reduced and the coolant in the channel began to heat up to boiling again (the heat up stage). The flow in the heated channel was seen to alternate between two-phase and single-phase conditions depending on the thermal state of the coolant.

The 2-second time average channel void fractions for the hot and average channels are shown in Figures C3.1 through C3.10. The maximum time-averaged (2 sec.) channel void fraction calculated for the base case is less than 0.31. The corresponding decay power used in the base case for the highest powered coolant channel in the HFBR was 7.8 kW at the time of flow reversal (see Figure C4). This channel power is in the range of the power levels tested in the flow reversal experiments. It should also be noted that the safe flow reversal power was higher for shorter coastdown times and was in excess of 19 kW for a very rapid coastdown (pump trip).

These considerations and the relatively low void fractions calculated for the HFBR core indicate that flow reversal in the multiple, parallel channel HFBR core occurs under conditions which were closer to a pump trip rather than a long coastdown.

In the case of the HFBR with variable heating rates in the channels, flow reversal does not occur simultaneously in all channels. With some of the channels in upflow while others in downflow, the coolant from the downflow channels becomes an extra source for feeding the upflow channels. This extra source supplements the core bypass flow and the flow through the flow reversal valves. In effect the existence of downflow channels is equivalent to an increase in the bypass orifice used in the single-channel flow reversal test. The apparent increase in the bypass flow area in the HFBR is the principal cause of a lower channel void fraction for the reactor than the single-channel test.

Based on the mass flow rates calculated by RELAP5 for the 10 channel groups of the HFBR core, an estimate of the ratio of channel flow to bypass flow is made with respect to the first flow reversal. From Figures C2.5 and C2.9, hot channel group #3 is seen first to go through flow reversal at about 48 sec. Within a couple of seconds, hot channel groups nos. 1, and 3, and average channel groups nos. 6, and 7 also go through flow reversal. Thus the number of coolant channels involved in the first flow reversal is,

3 x 14 (3 hot groups with 14 coolant channels per group) +
2 x 70 (2 average groups with 70 coolant channels per group) = 182

The remaining coolant channels are still in downflow and their number is 350 (532-182). In addition, the core bypass flow and the flow through the reversal valves also contribute to the total downflow. Nominally, these two flow streams amount to half of the total core flow and can be viewed as 266 (532/2) coolant channels. Therefore, the ratio of channel flow to bypass flow at the time of first flow reversal is equivalent to,

$$\frac{\text{total upflow channels}}{\text{total downflow channels}} = \frac{182}{350 + 266} = \frac{1}{3.4}$$

With each channel flow reversal there is an incremental change in the net buoyancy head generated in the core region. The increased buoyancy head tends to speed up the coastdown of the primary flow. This is similar to the case of a pump trip in the single channel flow reversal test. A rapid flow coastdown results in minimal opposition from the forced downflow to flow reversal. The rapid flow coastdown associated with flow reversal in the HFBR is seen in Figure C2.3 which shows the rapid drop in primary flow at the time of first flow reversal as calculated by RELAP5.

An indication of the propensity toward safe flow reversal is the maximum time-averaged channel void fraction at the time of reversal. A lower maximum channel void fraction means the required buoyancy head to induce a flow reversal is lower. The above discussion of the multi-channel effect is consistent with the calculated channel void fraction being lower in a multi-channel configuration (HFBR) and higher in a single channel (flow reversal test) all other conditions being equal.

3. Sensitivity Study

a. Non-uniform axial power distribution (Cases 6 and 7)

The power density variations that exist within each plate were not accounted for in the base case calculation. The axial power density shape is a function of time in the operating cycle and varies from plate to plate at a given cycle time. To address this issue an axial flux shape

which was close to the shape in a peripheral fuel element in a freshly fueled core was selected for Case 6. All the plates in the core had the same normalized shape. In this shape the peak power density occurs at the midplane and the power density is lowest at the top and bottom. For Case 7 the shape was inverted so that the maximum power density occurred at the top and bottom and the midplane has the lowest value. The normalized power densities are shown below for 8 of the 16 axial nodes used in the calculation:

Node	Case 6	Case 7
1	0.4659	1.3666
2	0.5794	1.2866
3	0.8110	1.2608
4	1.0378	1.1920
5	1.1920	1.0378
6	1.2608	0.8110
7	1.2866	0.5794
8	1.3666	0.4659

The axial nodes are numbered in ascending order from top to bottom. Nodes 9 to 16 are mirror images of Nodes 1 through 8.

There were differences in the channel void fraction between the cases of uniform and non-uniform axial power distribution. However, in all the channel groups regardless of the axial power shape, the maximum time-averaged channel void fraction is in the range of 0.25 and 0.31. The maximum time averaged channel void fraction is thus not sensitive to the axial power shape in the core. Hence it is justifiable to use a uniform axial power distribution in RELAP5 calculations to determine the maximum time-averaged channel void fraction.

b. Effect of Doubling Reactor Power (Case 2)

The base case calculation indicates that flow reversal will be successful in the HFBR because the maximum time-averaged channel void fraction for the coolant channels is below the critical void fraction of 0.51. In order to establish the margin to dryout during flow reversal, the channel power needs to be increased to a level such that the maximum time-averaged channel void fraction approaches the critical void fraction. Another RELAP5 calculation was done with the reactor power and the decay power increased by a factor of two over the base case value. A comparison with the result of the base case shows that, for the case of a higher channel power, the

time to flow reversal from pump trip is shortened and the maximum time-averaged channel void fraction is increased to 0.5 (see Figure C5) . For this higher power case, the initial reactor power is 128.1 MW and the multiplier applied to the decay power is 1.2276 (1.116 x 1.1). Including the multiplier, the decay power used in the calculation is equivalent to a reactor power of 157.26 MW. Even at this elevated power, the maximum time-averaged channel void fraction is still less than the critical void fraction. It is also noted that RELAP5 did not predict a continued increase in the wall temperature. This implies that at decay heat levels corresponding to 157.26 MW, the wall temperature calculated by RELAP5 is low enough to permit rewetting.

c. Effect of One Closed Flow Reversal Valve (Case 3)

A variation of the accident scenario is the failure of one of the four flow reversal valves to open. With one valve remaining closed, there is a reduction in the area available to the coolant flow that bypasses the core. The previous RELAP5 calculation (Case 2) was redone with one flow reversal valve closed. As compared to Case 2, the time of flow reversal is delayed slightly in Case 3. This is because of a slight increase in the channel flow when the effective bypass flow area is reduced. The maximum time-averaged channel void fraction during flow reversal is slightly lower for Case 3 than Case 2, (0.47 verses 0.50). Thus the failure of one of the flow reversal valves to open has negligible effect on the maximum time-averaged void fraction.

d. Effect of a Shorter Coastdown (Case 4)

The simulation of a shorter primary pump coastdown was done by increasing the pump friction torque coefficient used in RELAP5 by a factor of 1.5. The same reactor power as in Case 2 (128.1 MW) was used for this case of a shorter coastdown. The pump speed became zero at 46.3 sec. as compared to 57.4 sec. in Case 2. It is noted that a shorter coastdown results in an earlier flow reversal and thus a higher corresponding channel power at flow reversal. However, the negative effect on flow reversal from the forced downflow is mitigated by a faster flow coastdown. According to the RELAP5 results the comparison of the time-averaged channel void fraction between Case 2 and Case 4 is mixed. While some of the channels are showing a higher channel void fraction for a shorter coastdown, there were other channels showing a lower channel void fraction. The net effect of an approximately 20% reduction in the coastdown time on the maximum time-averaged channel void fraction is shown to

be negligible. The maximum void fraction remains unchanged at 0.5.

e. Effect of a Longer Coastdown (Case 5)

A longer coastdown was simulated by reducing the pump friction torque coefficient by a factor of 1.5. For the same reactor power as in Case 2 (128.1 MW), the time of zero pump speed was delayed to ≈67.4 sec. (the calculation ended at 60 sec. and the time of zero pump speed was obtained by extrapolation from the pump speed at 60 sec.). The net effect of an approximately 20% increase in the coastdown time on the maximum time-averaged channel void fraction is negligible. The maximum void again remains unchanged at 0.5.

f. Effect of Modeling Individual Channels in a Fuel Element (Cases 9, 10, 11)

The base case model of the HFBR core had the 532 coolant channels divide according to their power into 10 channel groups. In the HFBR core, coolant channels and their associated fuel plates are organized in the form of fuel elements. The base case RELAP5 model of the HFBR core differs from the configuration of a fuel element in three aspects.

I. Each group in the base case model had multiple channels of identical size and power. Different channels in a fuel element have different size and power.

II. Each channel group had its own unheated inlet tube section. In a fuel element all 19 coolant channels with varying power share a common inlet tube.

III. Each heat structure in the base case model provided power to one channel only. A fuel plate in a fuel element transfers heat to two adjacent channels.

A study [C5] of the effects of the three areas in which the base case RELAP5 model of the HFBR core deviated from the configuration of a fuel element found that the base case model produced results that were conservative as compared to the alternative models. These alternative models [C5] had features that made the coolant channels resemble the arrangement in a fuel element. The model for Case 10 [C5] had a hot fuel element which consisted of three hot channels and an average channel group representing the remaining 16 channels in an element.

g. Effect of Channel Dimension Variations Due to Manufacturing Tolerances (Cases 8, 12, 15)

A review of the specifications for the HFBR fuel element shows,

a. For each coolant channel the maximum deviation of the average channel gap is 0.005" from the nominal value [C8].

b. Assuming the most unfavorable tolerance limit in a fuel element it is possible that an average channel group in the base case model could have a gap size which is 0.0015" less than the nominal value of 0.0984" [C7, C9].

Three sets of RELAP5 calculations were done to assess the effect of a channel gap reduction on the maximum time averaged channel void fraction. The calculations and their results are:

I. Case 8 - The gap of hot channel group #1 was reduced from 0.117" (nominal value) to 0.112" [C4]. The overall maximum time averaged channel void fraction for this new case is almost identical with that of the base case.

II. Case 15 - The gap of the seven average channel groups in the base case was reduced from 0.0984" (nominal value) to 0.0969" [C7]. The results showed an increase in the maximum time averaged channel void fraction from 0.307 for the base case to 0.314 for the reduced gap case.

III. Case 12 - The gaps of the three hot channels in the hot fuel element of Case 10 were reduced by 0.005". The maximum time averaged void fraction was slightly different for the two cases, 0.211 for the reduced gap case and 0.203 for the nominal gap case.

Based on the above sensitivity study it is concluded that the uncertainty in the channel gap due to manufacturing tolerances will not have a significant effect on the results predicted by RELAP5 for the reactor.

h. Effect of Uncertainty in the Pressure Loss Coefficient for the Flow Reversal Valves (Cases 13, 14)

The RELAP5 model of the flow reversal valves assumed that the valves had the same pressure loss characteristics for the forward and reverse flow direction. A calculation [C10] estimated that the uncertainty of the pressure loss in the reverse flow direction is within 30% of the pressure loss in the forward flow direction. Two RELAP5 sensitivity calculations were done in which the loss coefficient for reverse flow was decreased and increased by 30% [C6]. The 30% decrease and increase in the pressure loss coefficient corresponds to a multiplication of the valve flow coefficient (C_v) by a factor of 1.2 (Case 13) and 0.88 (Case 14) respectively. The results showed that the uncertainty in the loss coefficient for the flow reversal valve had negligible effect on the maximum time averaged void fraction.

References:

[C1] Cheng, Lap Y., 1995, "Flow Reversal Limited Operating Power for the HFBR," BNL Reactor Division Calculation No. SEG-57-0.

[C2] Tichler, P., 1982, "Addendum to the HFBR FSAR for 60 MW Operation," BNL Report.

[C3] Tichler, P., 1989, "Decay Heating in HFBR Hot Channels," BNL Memorandum to Files.

[C4] Cheng, Lap Y., 1996, "Effects of Reduced Channel Gap on the RELAP5 Analysis of the Reactor," BNL Memorandum to Files.

[C5] Cheng, Lap Y., 1996, "A RELAP5 Analysis of the Reactor with One Hot Fuel Element and an Average Core Group," BNL Memorandum to Files.

[C6] Cheng, Lap Y., 1996, "Sensitivity of RELAP5 Analysis to the Uncertainty in the Pressure Loss Coefficient for the Flow Reversal Valve," BNL Memorandum to Files.

[C7] Cheng, Lap Y., 1996, "A RELAP5 Analysis of the Reactor with Reduced Average Channel Flow Area," BNL Memorandum to Files.

[C8] BNL Drawing No. HFBR-M-706-5, Rev. A, "HFBR Fuel Element Type KM Assembly."

[C9] Tichler, P., 1996, "Effect of Fabrication Tolerance on Flow Area of 'Average' Channel in HFBR," BNL Memorandum to Files.

[C10] Tichler, P., 1996, "Flow Characteristics of the Flow Reversal Valve for Flow in the Forward and Reverse Direction," BNL Memorandum to Files.

LIST OF TABLE

LIST OF FIGURES

TABLE C1

INITIAL CONDITIONS FOR THE BASE CASE OF THE RELAP5 CALCULATIONS OF THE HFBR

Variable	Design Basis Value	Anticipated Variation	Uncertainty	RELAP5 Base Case
Reactor Power (MW)	61	59-61	±5%	64.05
Primary Flow Rate (gpm)	17,900	17900-18500	±3%	17,400
Cover Gas Pressure (psig)	200	200-210	±5	195
Liquid Level (inches)	230	230-240	±1	241
Core Inlet Temperature (°C)	56.5 (133.8°F)	50-56.5	±1	57.5 (135.5°F)

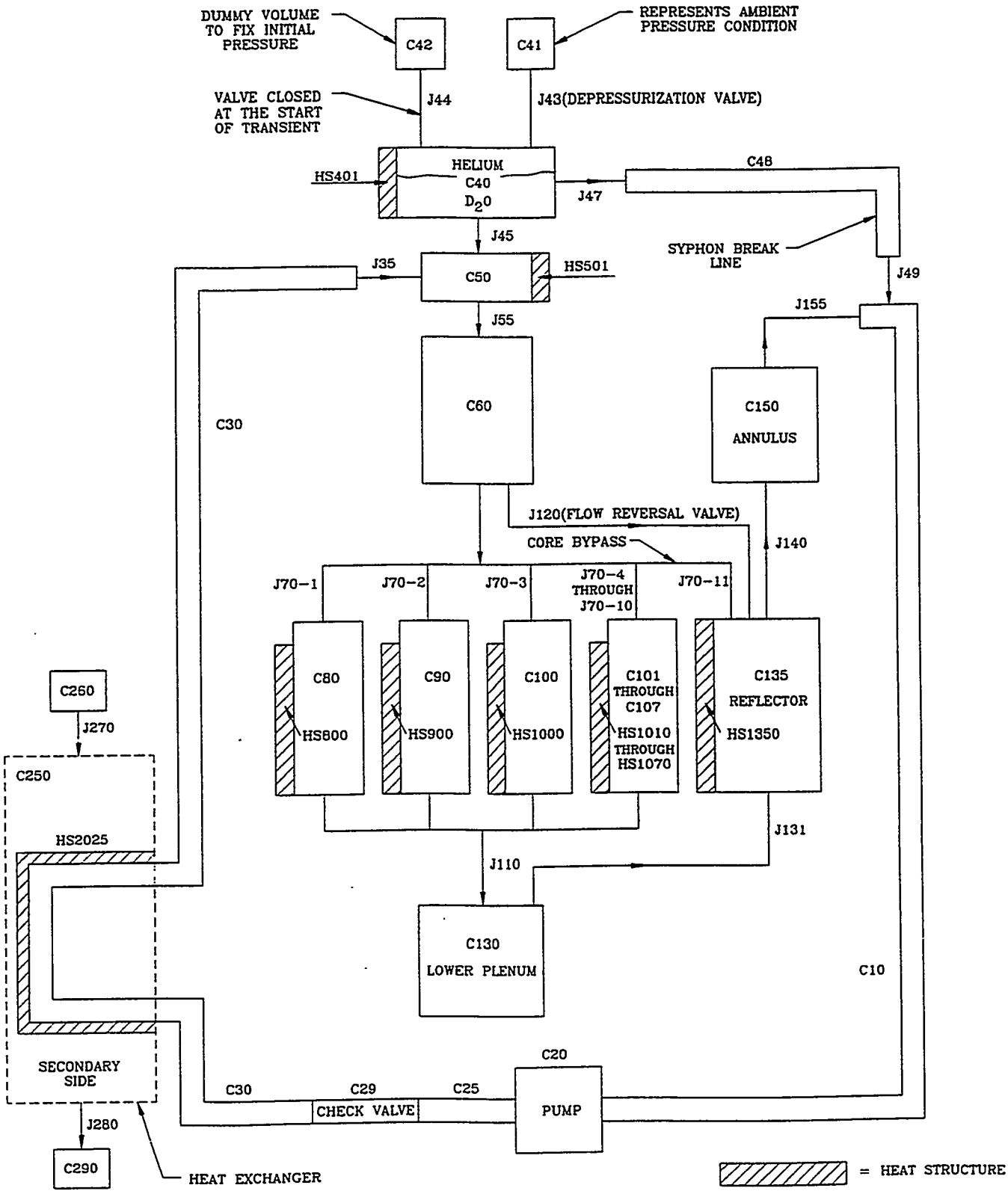

Figure C1 RELAP5 Node Diagram of the HFBR Vessel and Primary Loop

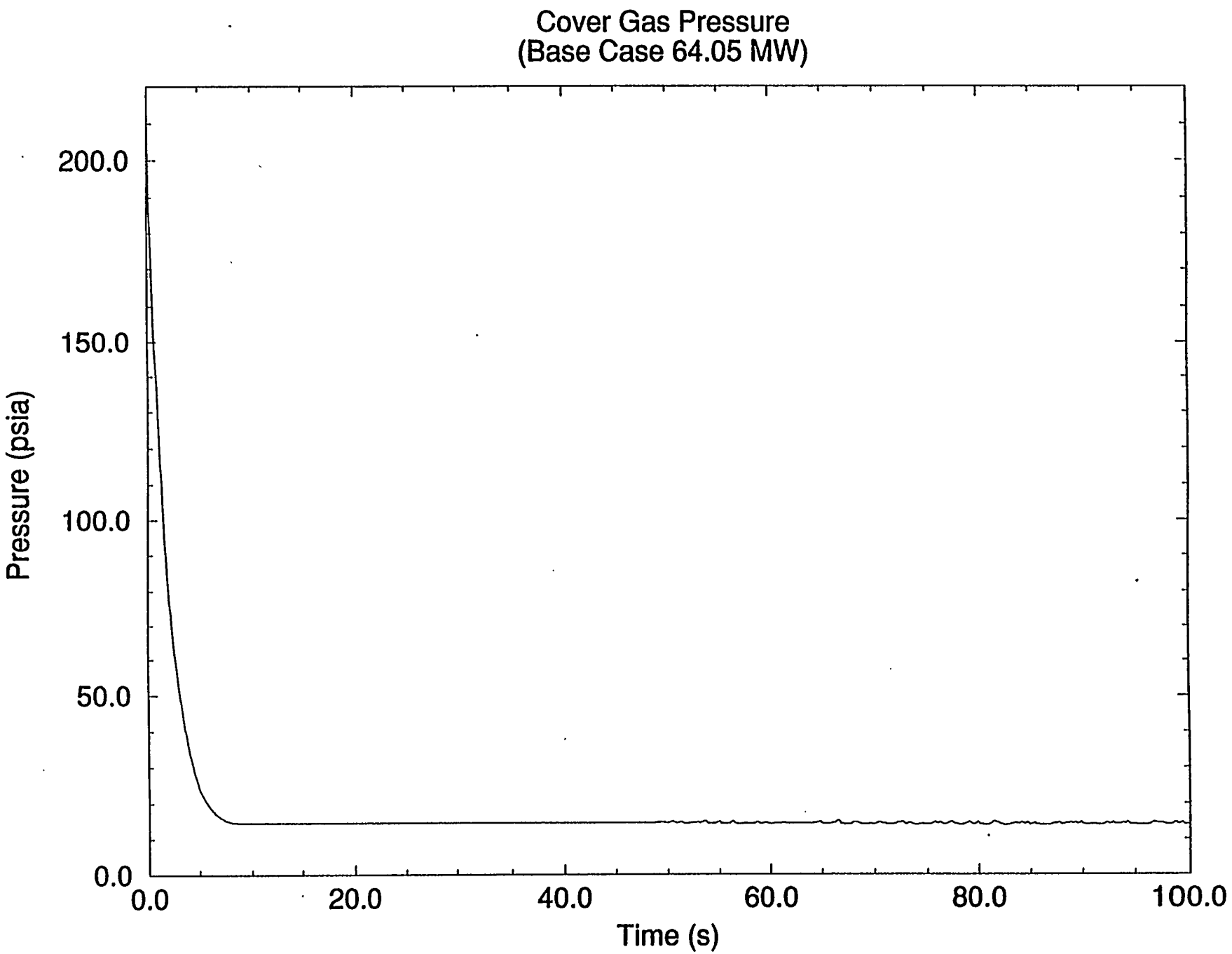
Cover Gas Pressure
(Base Case 64.05 MW)
Pressure (psia)
200.0
150.0
100.0
50.0
0.0
0.0
20.0
40.0
60.0
80.0
100.0
Time (s)

Figure C2.1

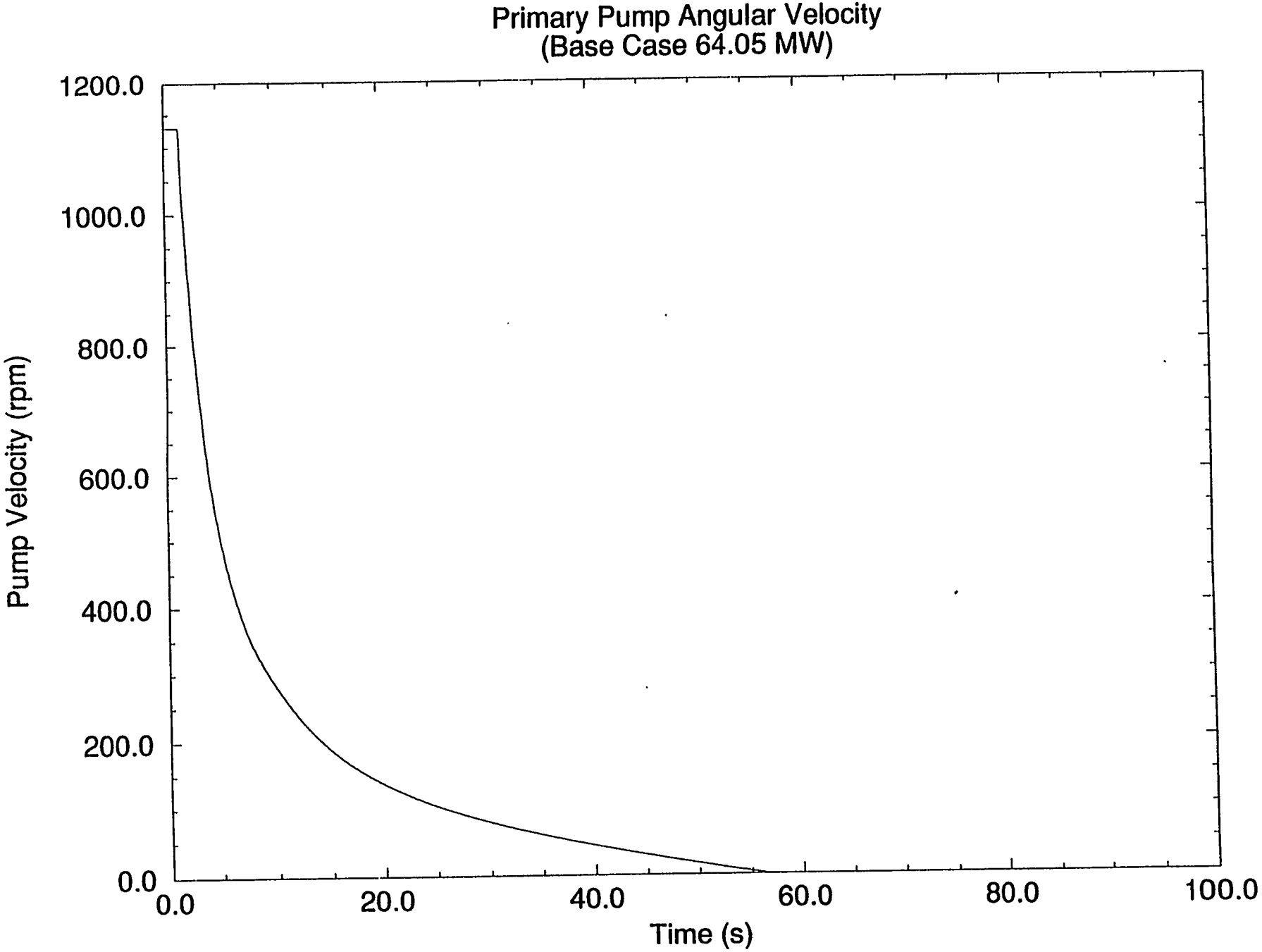
Primary Pump Angular Velocity
(Base Case 64.05 MW)
1200.0
1000.0
800.0
600.0
400.0
200.0
0.0
Pump Velocity (rpm)
0.0
20.0
40.0
60.0
80.0
100.0
Time (s)

Figure C2.2

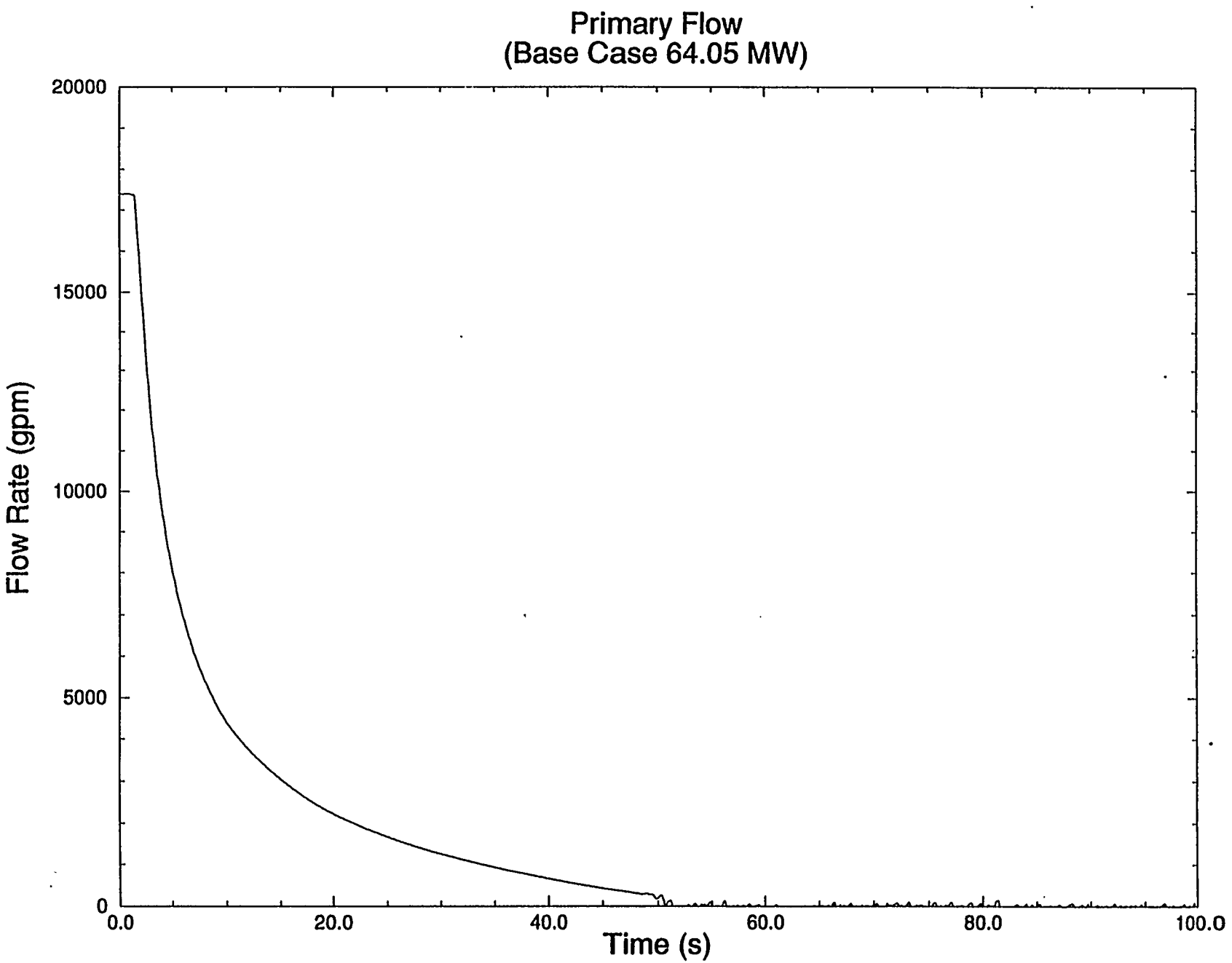
Primary Flow
(Base Case 64.05 MW)
Flow Rate (gpm)
20000
15000
10000
5000
0
0.0
20.0
40.0
60.0
80.0
100.0
Time (s)

Figure C2.3

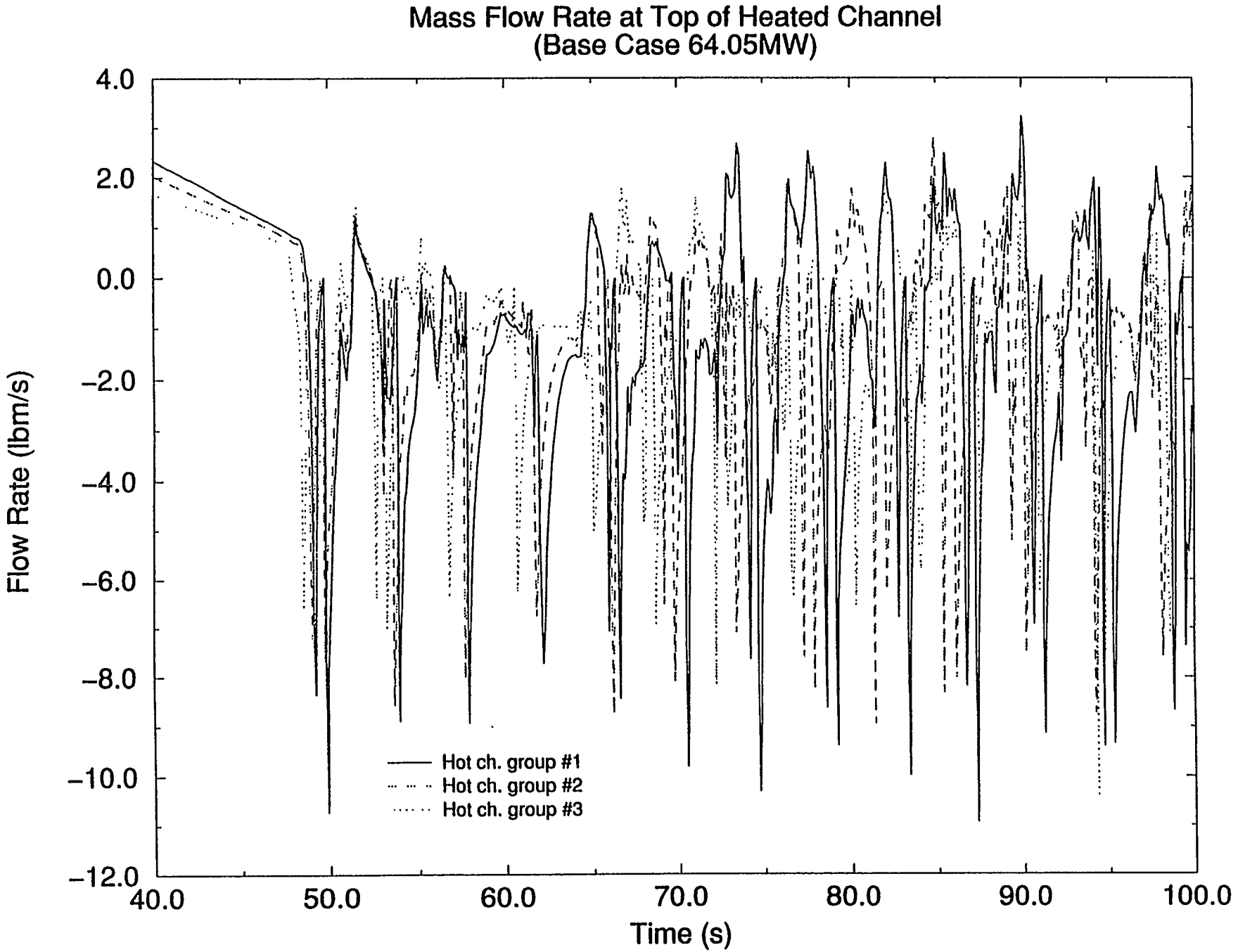
Mass Flow Rate at Top of Heated Channel
(Base Case 64.05MW)
4.0
2.0
0.0
-2.0
-4.0
-6.0
-8.0
-10.0
-12.0
Flow Rate (lbm/s)
40.0
50.0
60.0
70.0
80.0
90.0
100.0
Time (s)
Hot ch. group #1
Hot ch. group #2
Hot ch. group #3

Figure C2.4

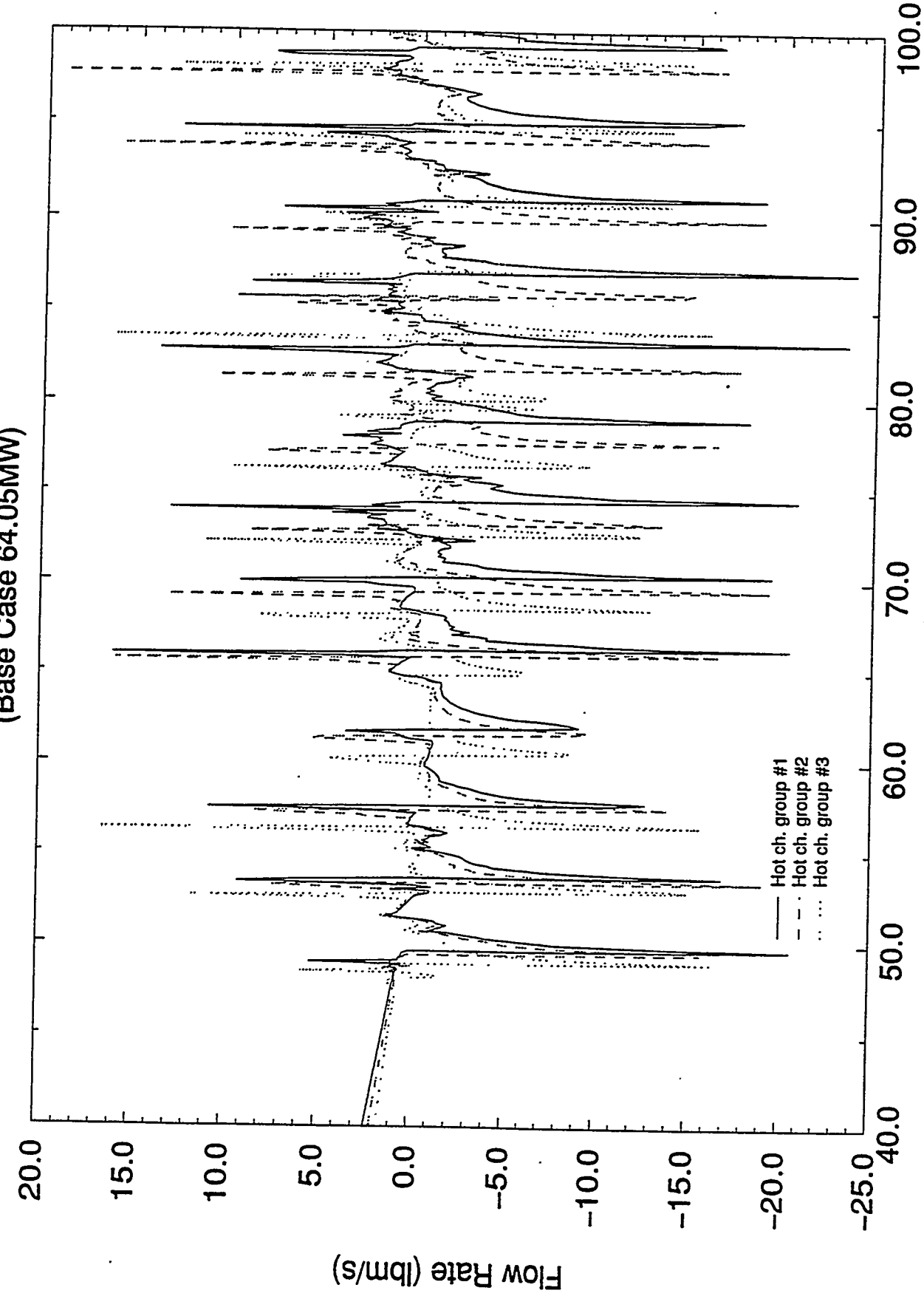
Mass Flow Rate at Bottom of Heated Channel
(Base Case 64.05MW)
Flow Rate (lbm/s)
20.0
15.0
10.0
5.0
0.0
-5.0
-10.0
-15.0
-20.0
-25.0
40.0
50.0
60.0
70.0
80.0
90.0
100.0
Time (s)
Hot ch. group #1
Hot ch. group #2
Hot ch. group #3

Figure C2.5

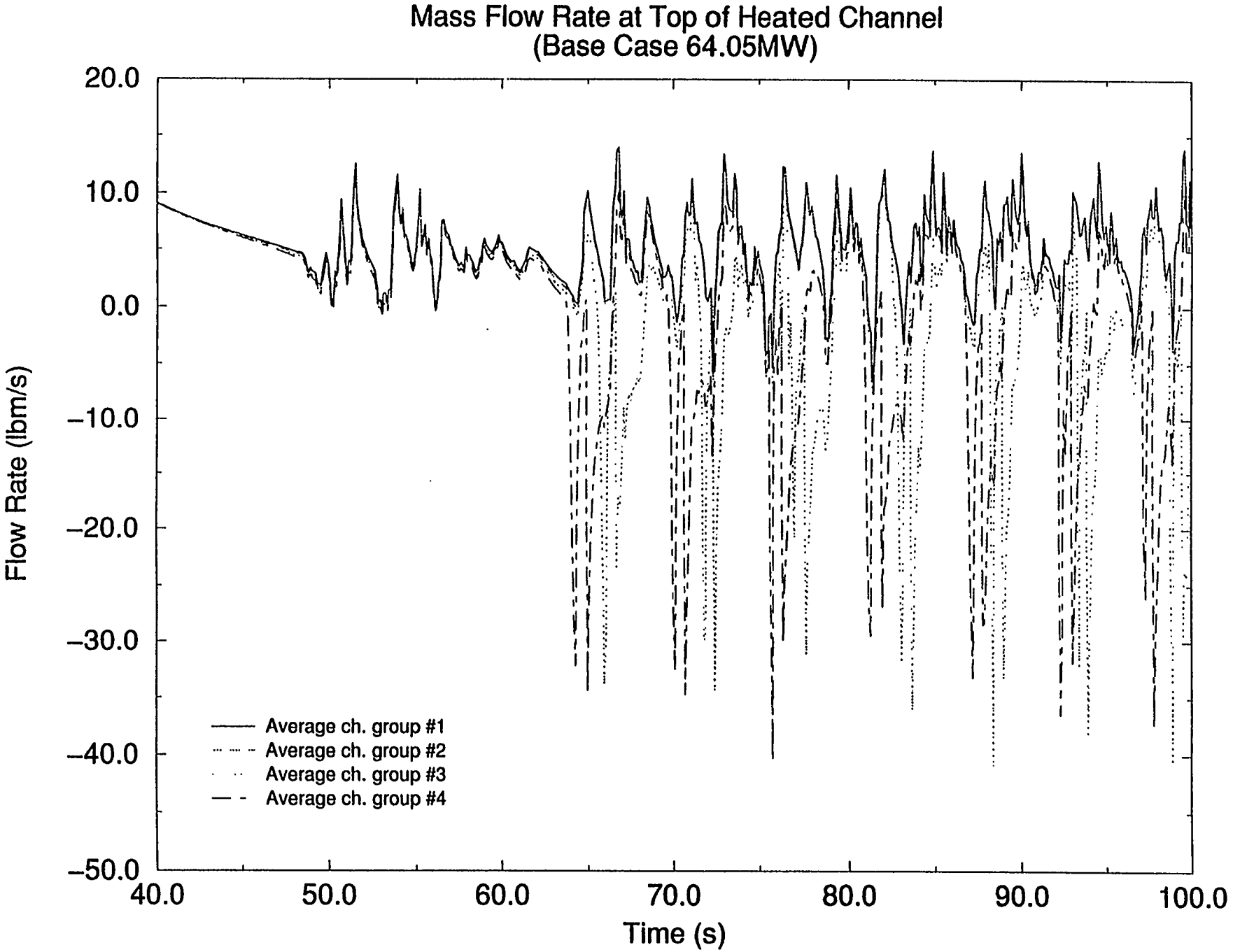
Mass Flow Rate at Top of Heated Channel
(Base Case 64.05MW)
20.0
10.0
0.0
-10.0
-20.0
-30.0
-40.0
-50.0
Flow Rate (lbm/s)
40.0
50.0
60.0
70.0
80.0
90.0
100.0
Time (s)
Average ch. group #1
Average ch. group #2
Average ch. group #3
Average ch. group #4

Figure C2.6

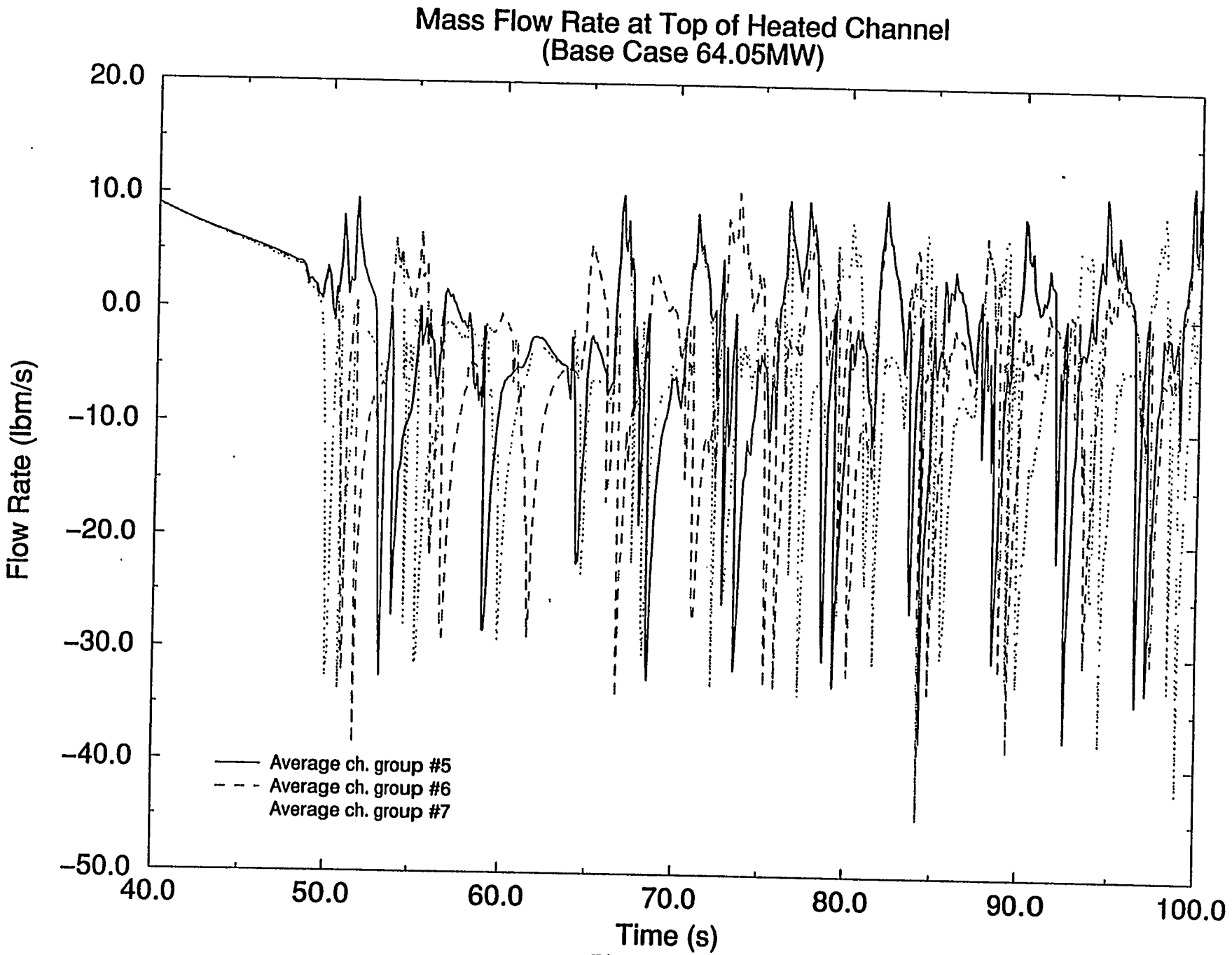
Mass Flow Rate at Top of Heated Channel
(Base Case 64.05MW)
20.0
10.0
0.0
-10.0
-20.0
-30.0
-40.0
-50.0
Flow Rate (lbm/s)
40.0
50.0
60.0
70.0
80.0
90.0
100.0
Time (s)
Average ch. group #5
Average ch. group #6
Average ch. group #7

Figure C2.7

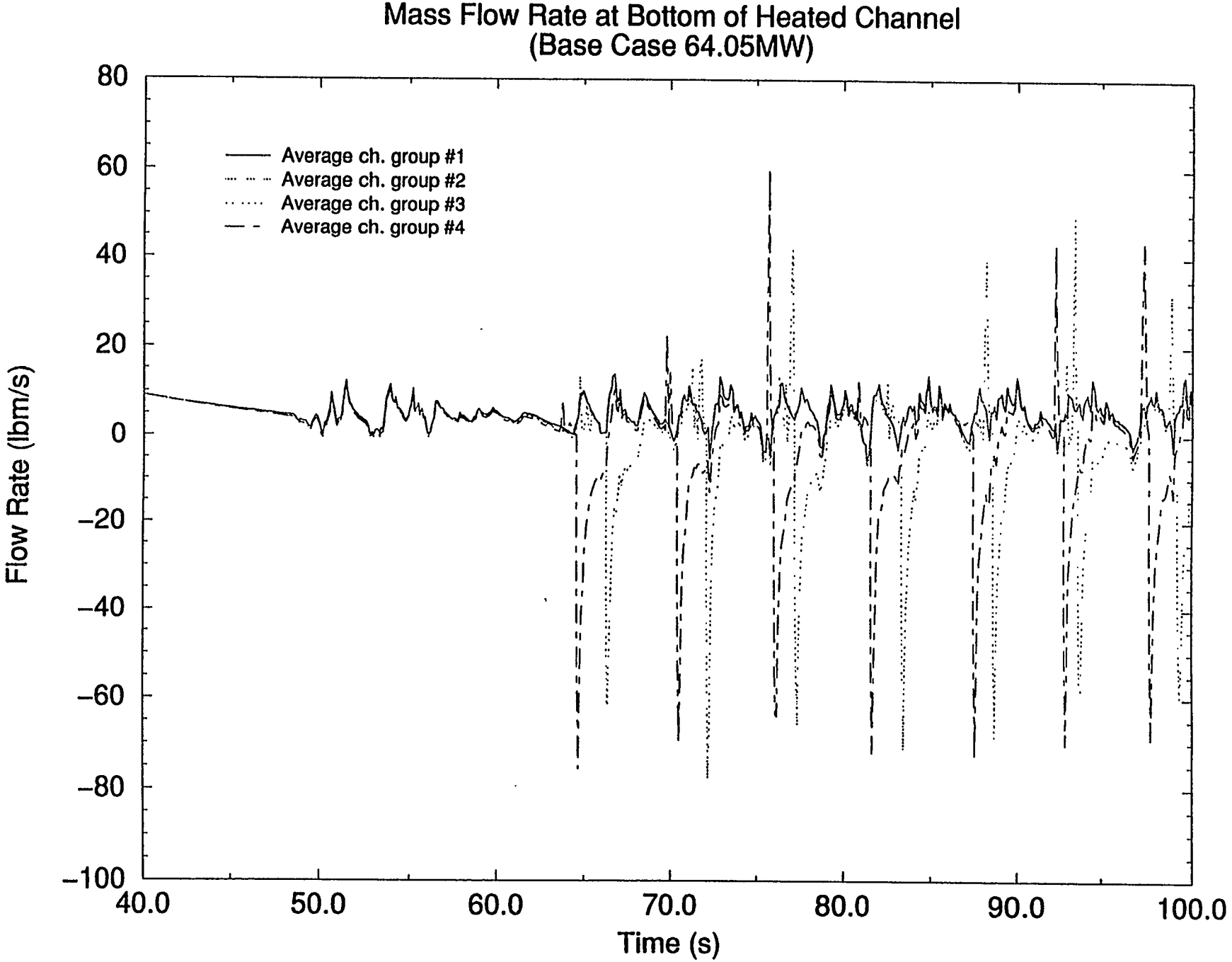
Mass Flow Rate at Bottom of Heated Channel
(Base Case 64.05MW)
Average ch. group #1
Average ch. group #2
Average ch. group #3
Average ch. group #4
Flow Rate (lbm/s)
80
60
40
20
0
-20
-40
-60
-80
-100
40.0
50.0
60.0
70.0
80.0
90.0
100.0
Time (s)

Figure C2.8

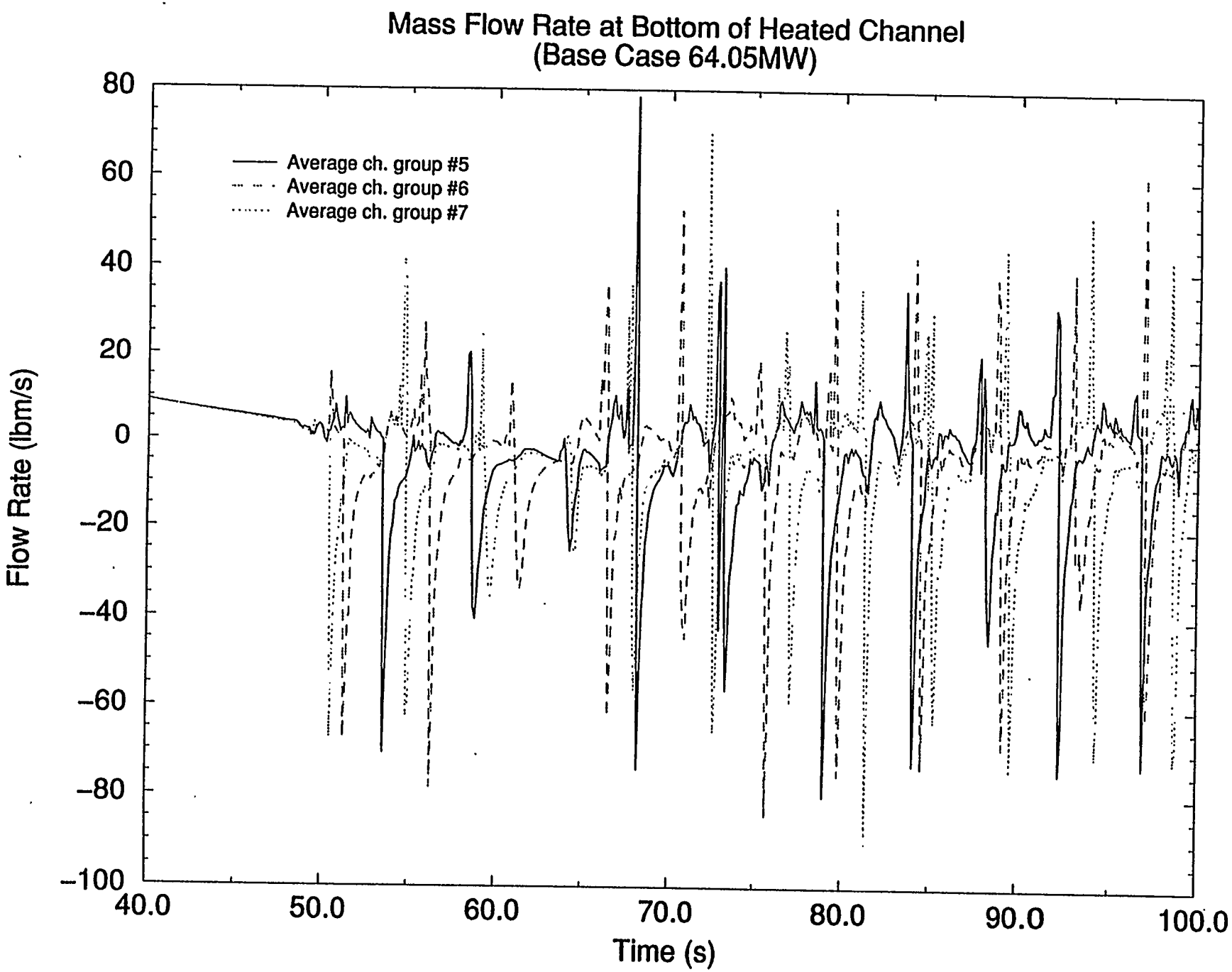
Mass Flow Rate at Bottom of Heated Channel
(Base Case 64.05MW)
Average ch. group #5
Average ch. group #6
Average ch. group #7
Flow Rate (lbm/s)
80
60
40
20
0
-20
-40
-60
-80
-100
40.0
50.0
60.0
70.0
80.0
90.0
100.0
Time (s)

Figure C2.9

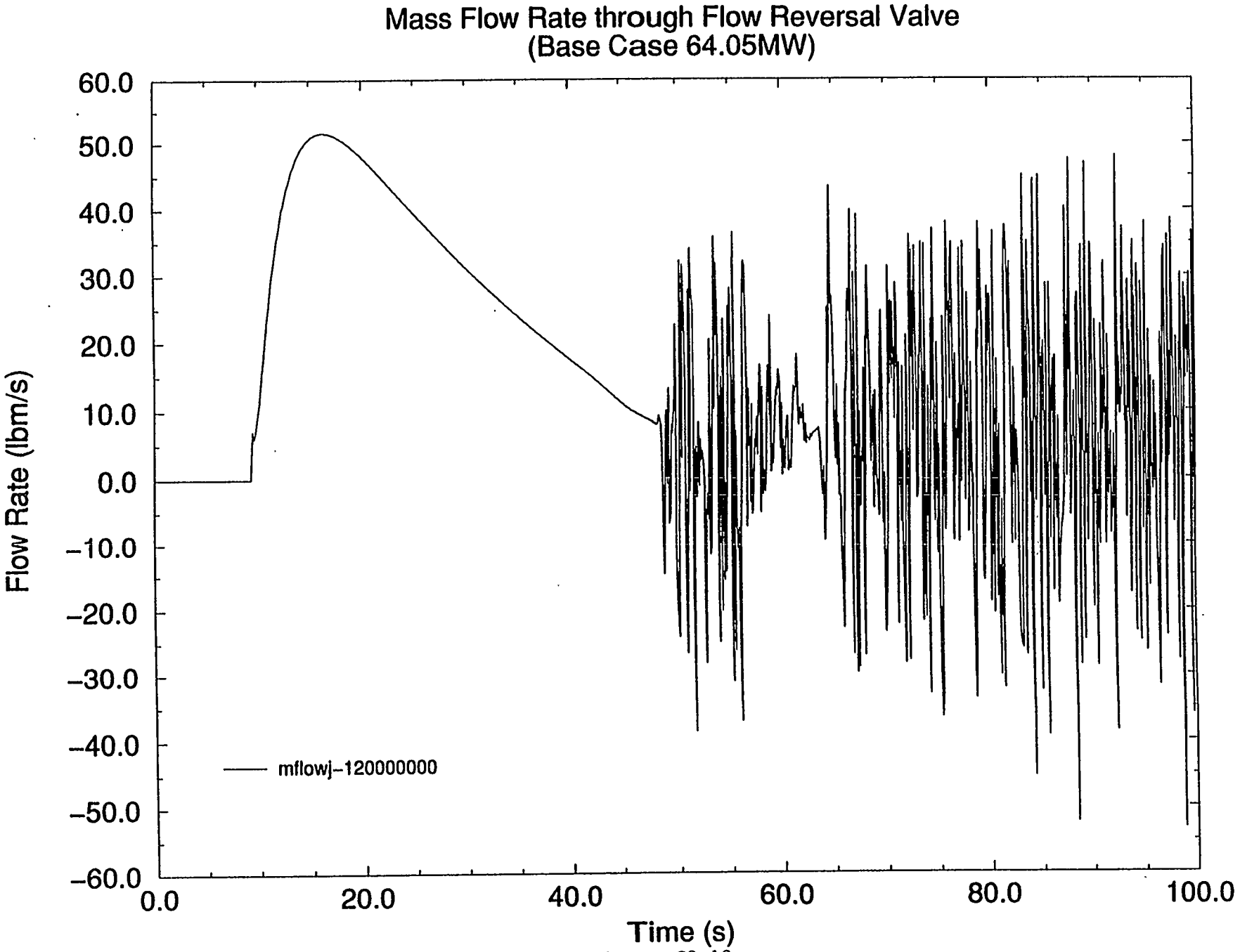
Mass Flow Rate through Flow Reversal Valve
(Base Case 64.05MW)
Flow Rate (lbm/s)
60.0
50.0
40.0
30.0
20.0
10.0
0.0
-10.0
-20.0
-30.0
-40.0
-50.0
-60.0
0.0
20.0
40.0
60.0
80.0
100.0
Time (s)
mflowj-120000000

Figure C2.10

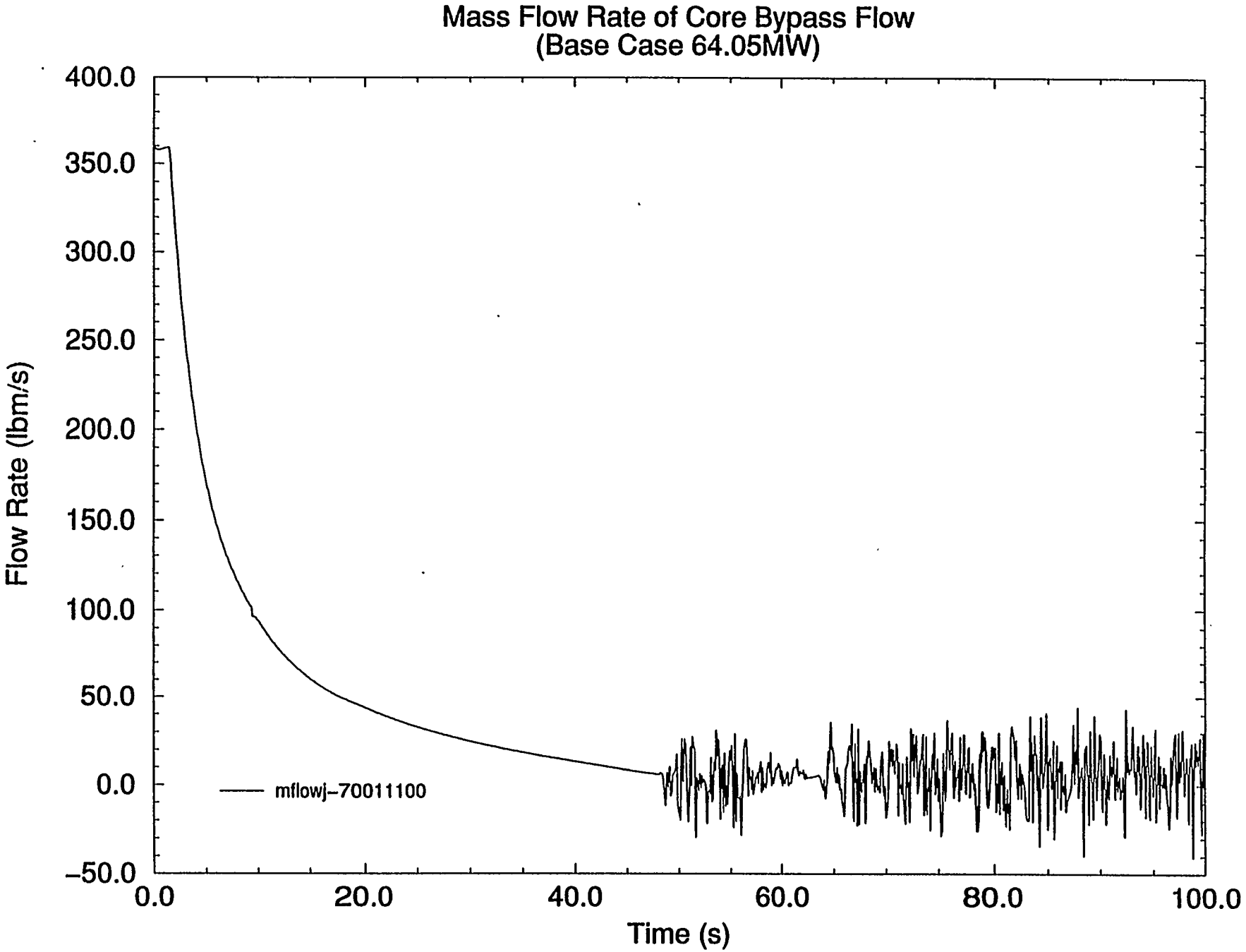
Mass Flow Rate of Core Bypass Flow
(Base Case 64.05MW)
400.0
350.0
300.0
250.0
200.0
150.0
100.0
50.0
0.0
-50.0
Flow Rate (lbm/s)
0.0
20.0
40.0
60.0
80.0
100.0
Time (s)
mflowj-70011100

Figure C2.11

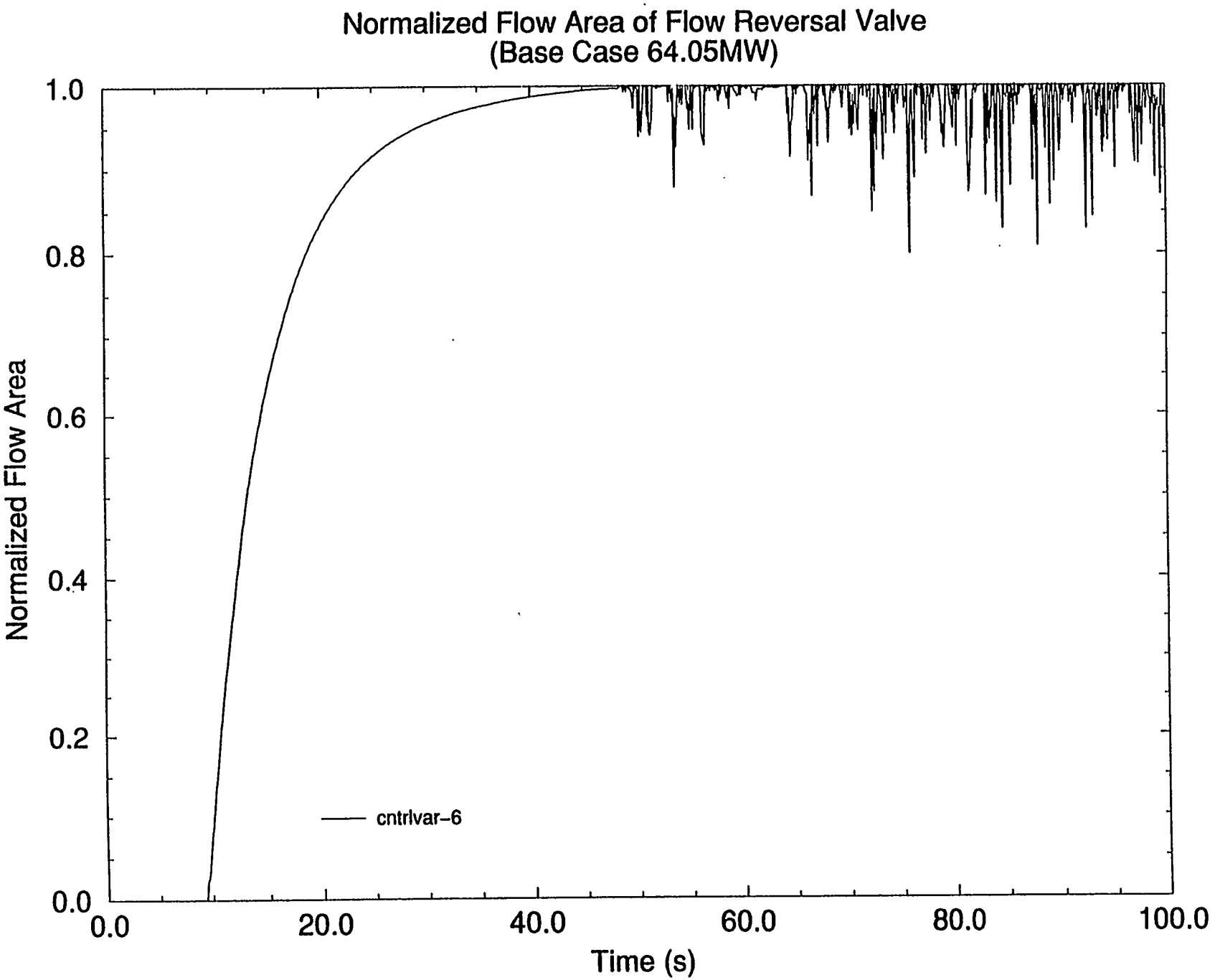
Normalized Flow Area of Flow Reversal Valve
(Base Case 64.05MW)
Normalized Flow Area
1.0
0.8
0.6
0.4
0.2
0.0
0.0
20.0
40.0
60.0
80.0
100.0
Time (s)
cntrlvar-6

Figure C2.12

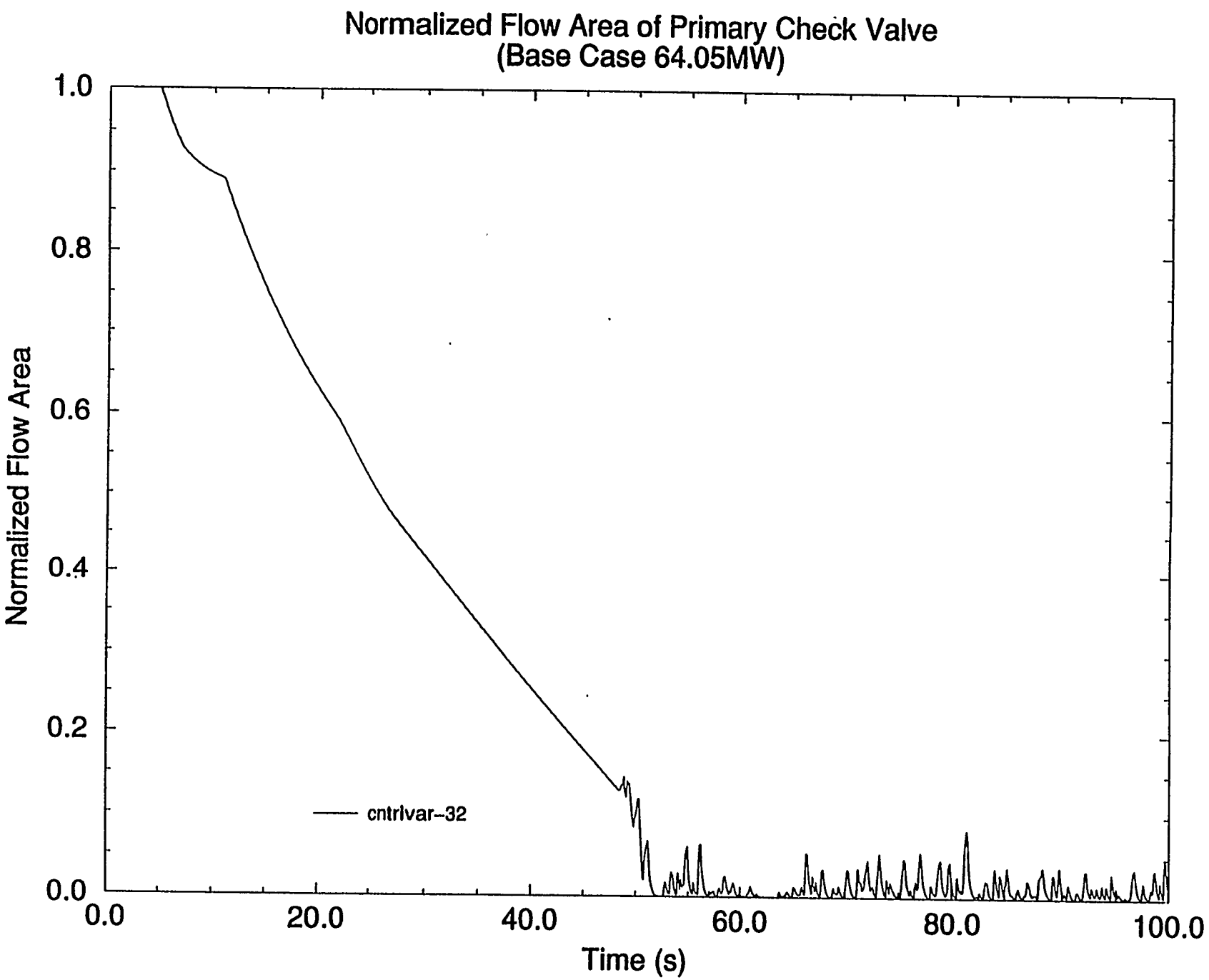
Normalized Flow Area of Primary Check Valve
(Base Case 64.05MW)
Normalized Flow Area
1.0
0.8
0.6
0.4
0.2
0.0
cntrlvar--32
0.0
20.0
40.0
60.0
80.0
100.0
Time (s)

Figure C2.13

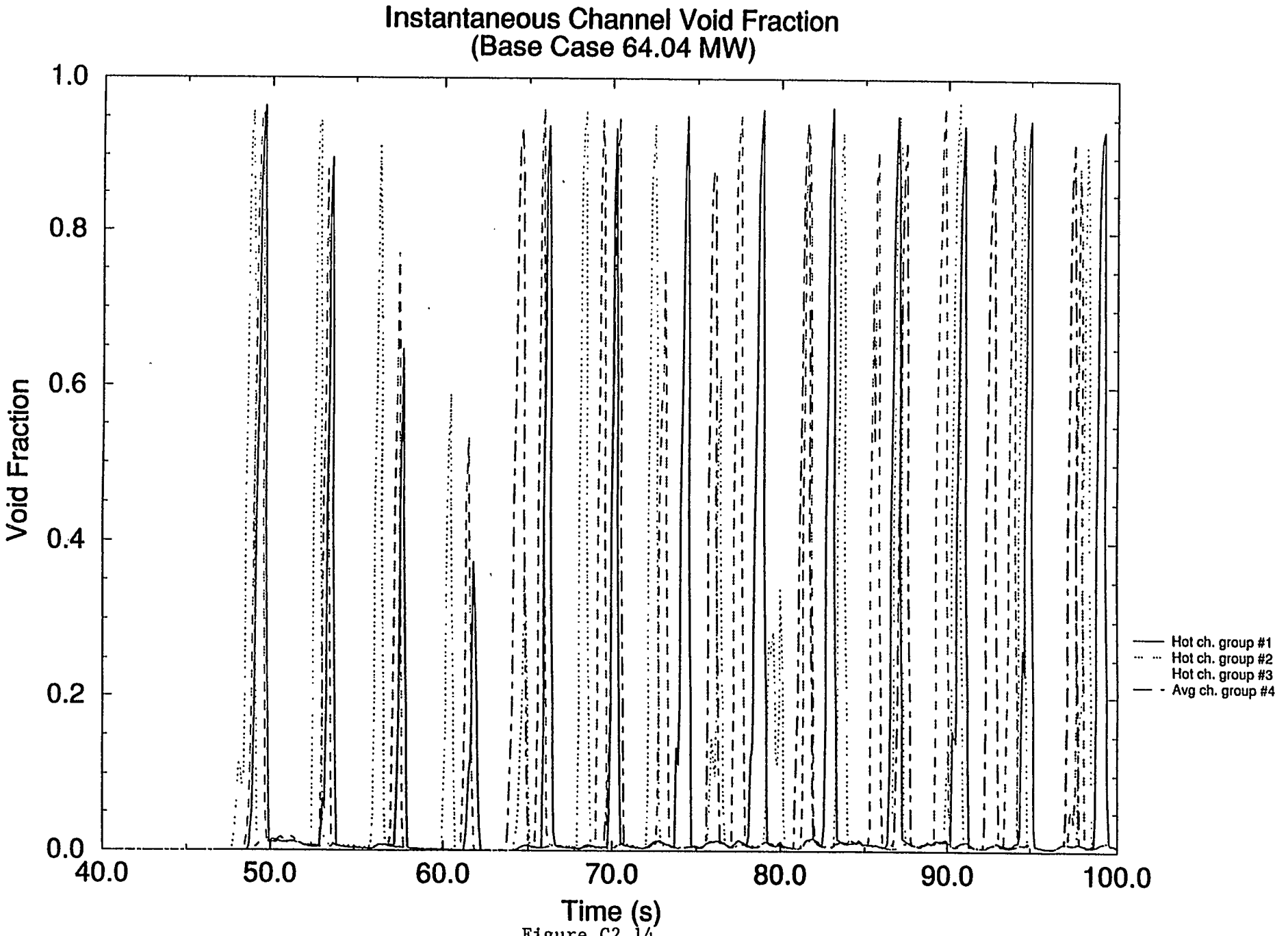
Instantaneous Channel Void Fraction
(Base Case 64.04 MW)
Void Fraction
1.0
0.8
0.6
0.4
0.2
0.0
40.0
50.0
60.0
70.0
80.0
90.0
100.0
Time (s)
Hot ch. group #1
Hot ch. group #2
Hot ch. group #3
Avg ch. group #4

Figure C2.14

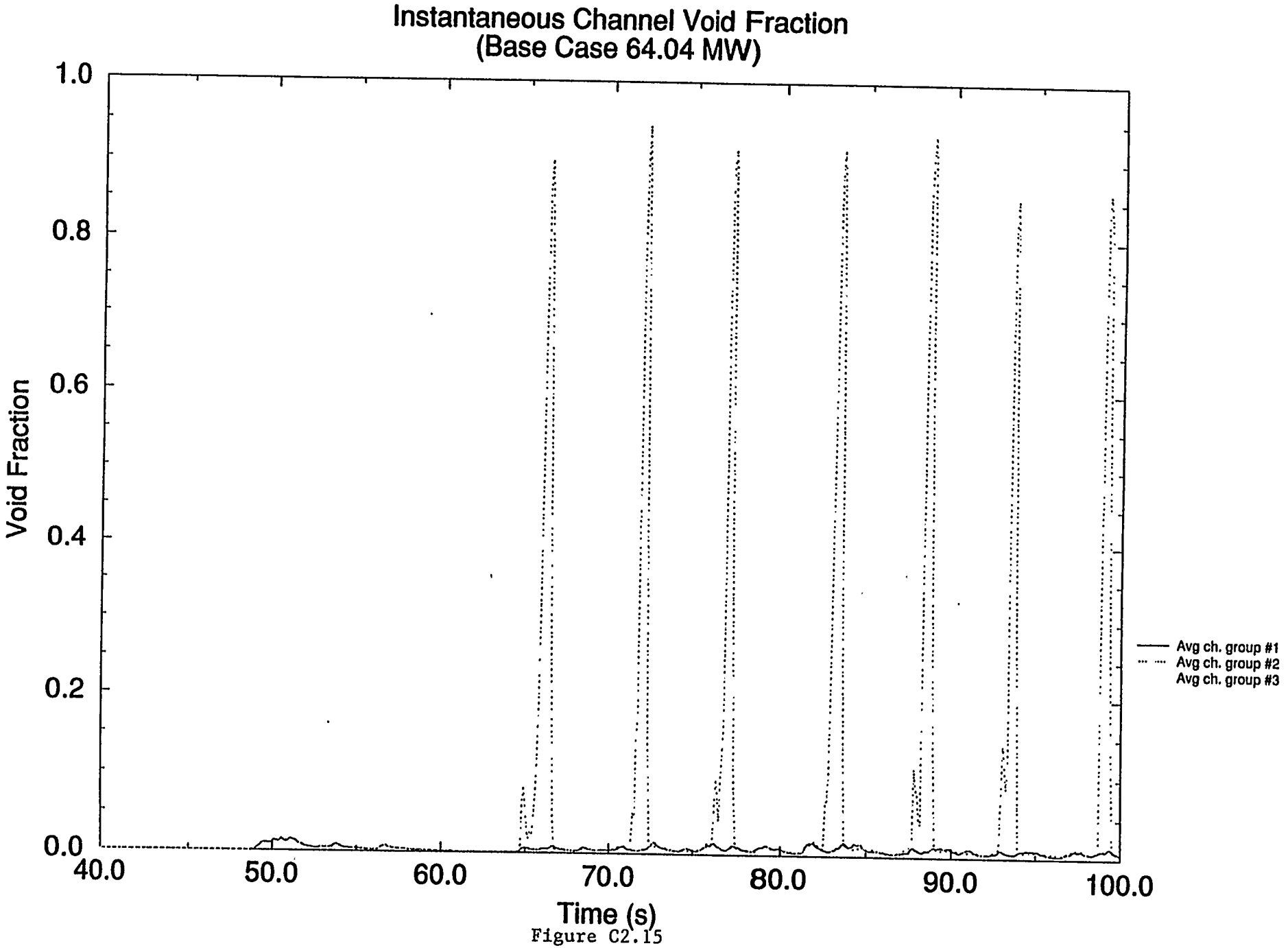
Instantaneous Channel Void Fraction
(Base Case 64.04 MW)
Void Fraction
1.0
0.8
0.6
0.4
0.2
0.0
40.0
50.0
60.0
70.0
80.0
90.0
100.0
Time (s)
Avg ch. group #1
Avg ch. group #2
Avg ch. group #3

Figure C2.15

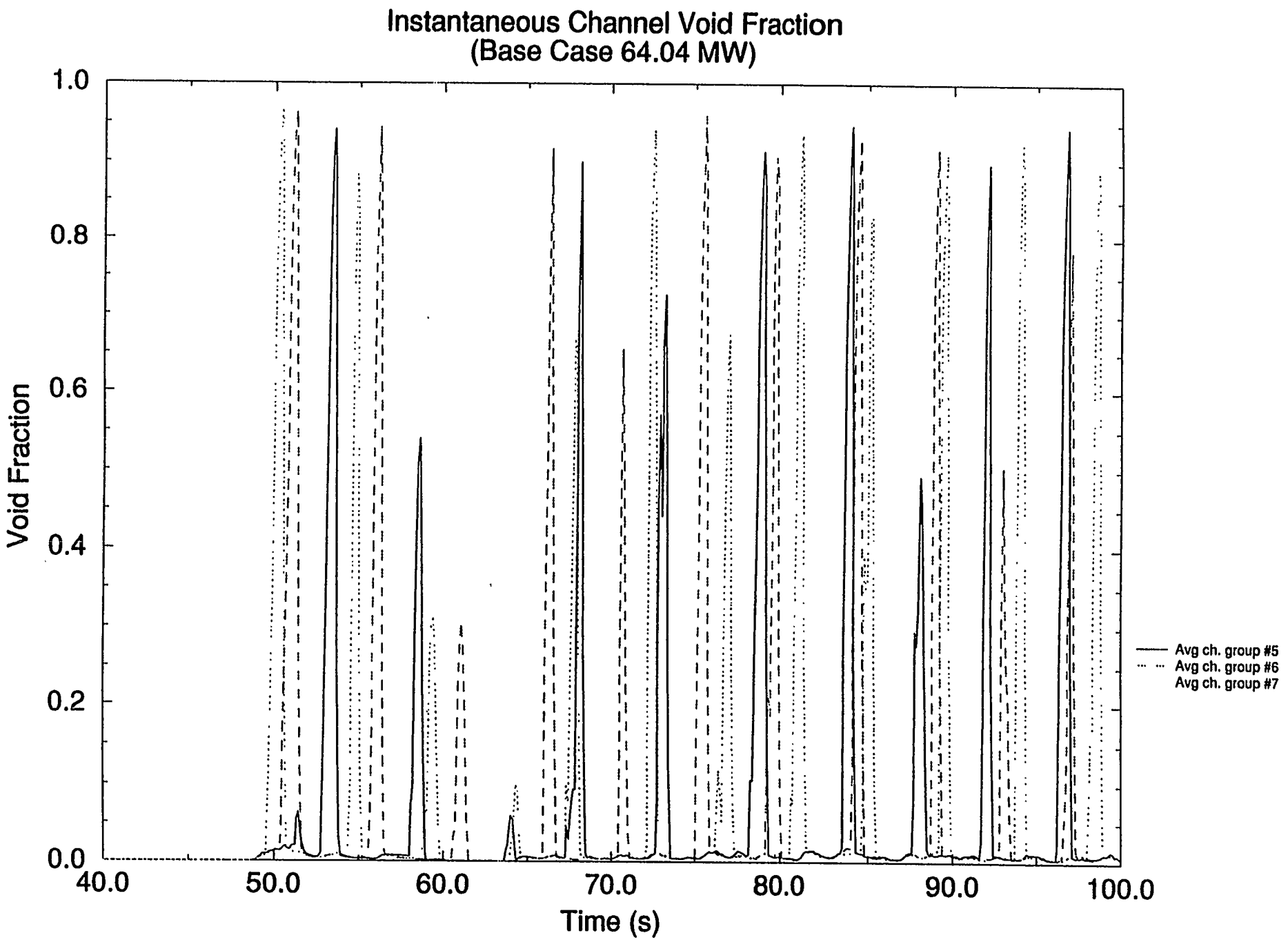
Instantaneous Channel Void Fraction
(Base Case 64.04 MW)
Void Fraction
1.0
0.8
0.6
0.4
0.2
0.0
40.0
50.0
60.0
70.0
80.0
90.0
100.0
Time (s)
Avg ch. group #5
Avg ch. group #6
Avg ch. group #7

Figure C2.16

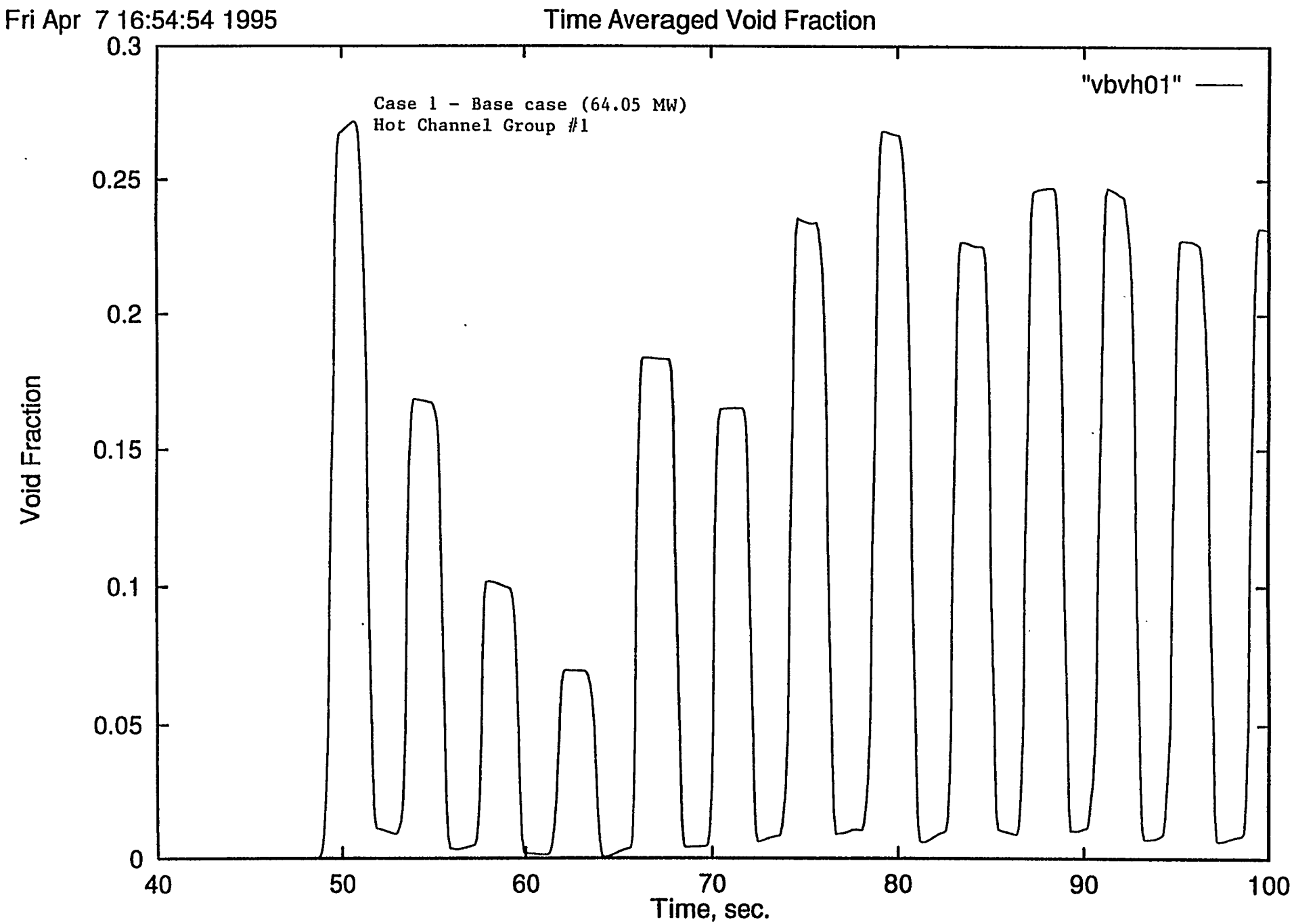
Fri Apr 7 16:54:54 1995
Time Averaged Void Fraction
Case 1 - Base case (64.05 MW)
Hot Channel Group #1
"vbvh01"
Void Fraction
0.3
0.25
0.2
0.15
0.1
0.05
0
40
50
60
70
80
90
100
Time, sec.

Figure C3.1

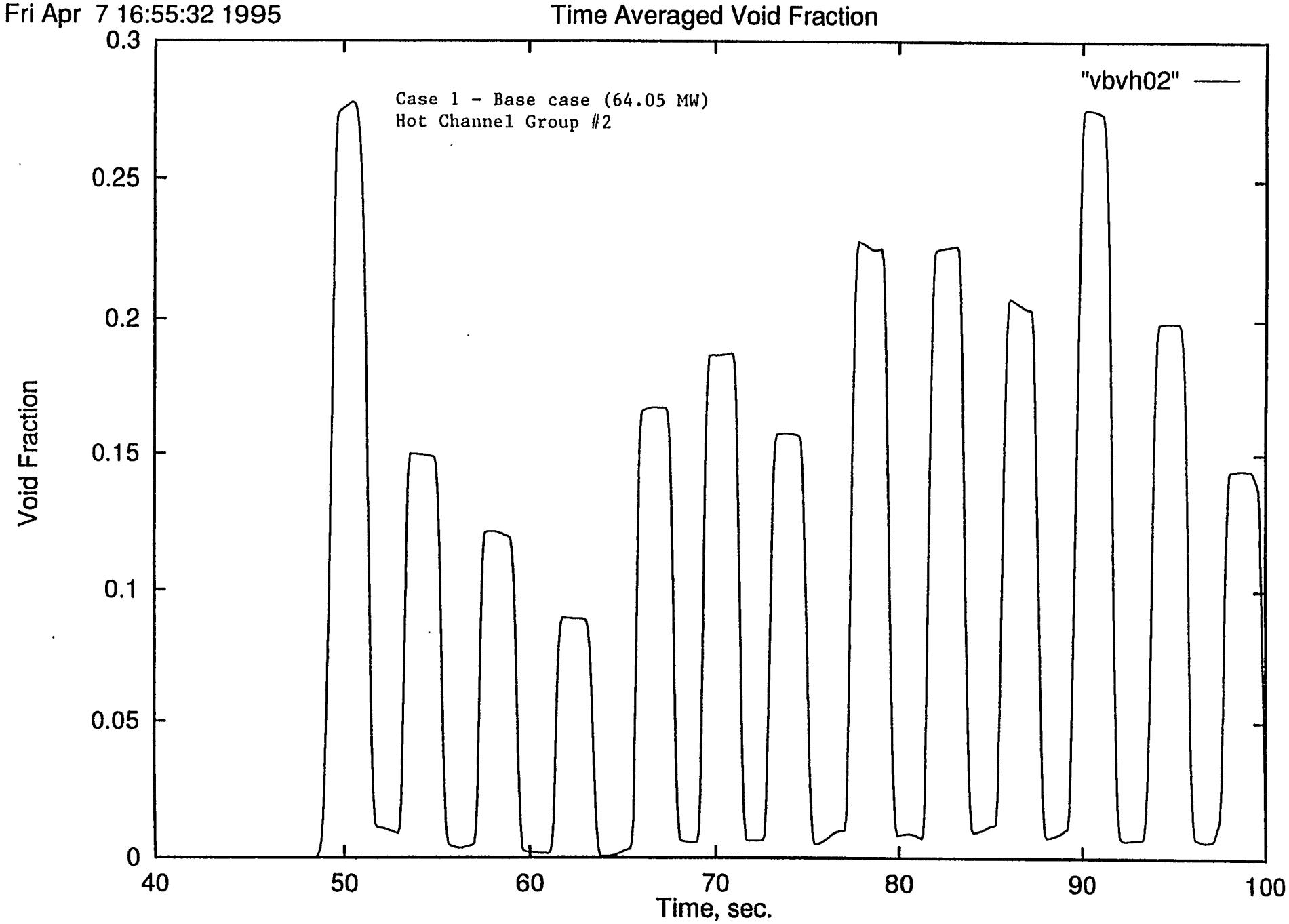
Fri Apr 7 16:55:32 1995
Time Averaged Void Fraction
Case 1 - Base case (64.05 MW)
Hot Channel Group #2
"vbvh02"
Void Fraction
0.3
0.25
0.2
0.15
0.1
0.05
0
40
50
60
70
80
90
100
Time, sec.

Figure C3.2

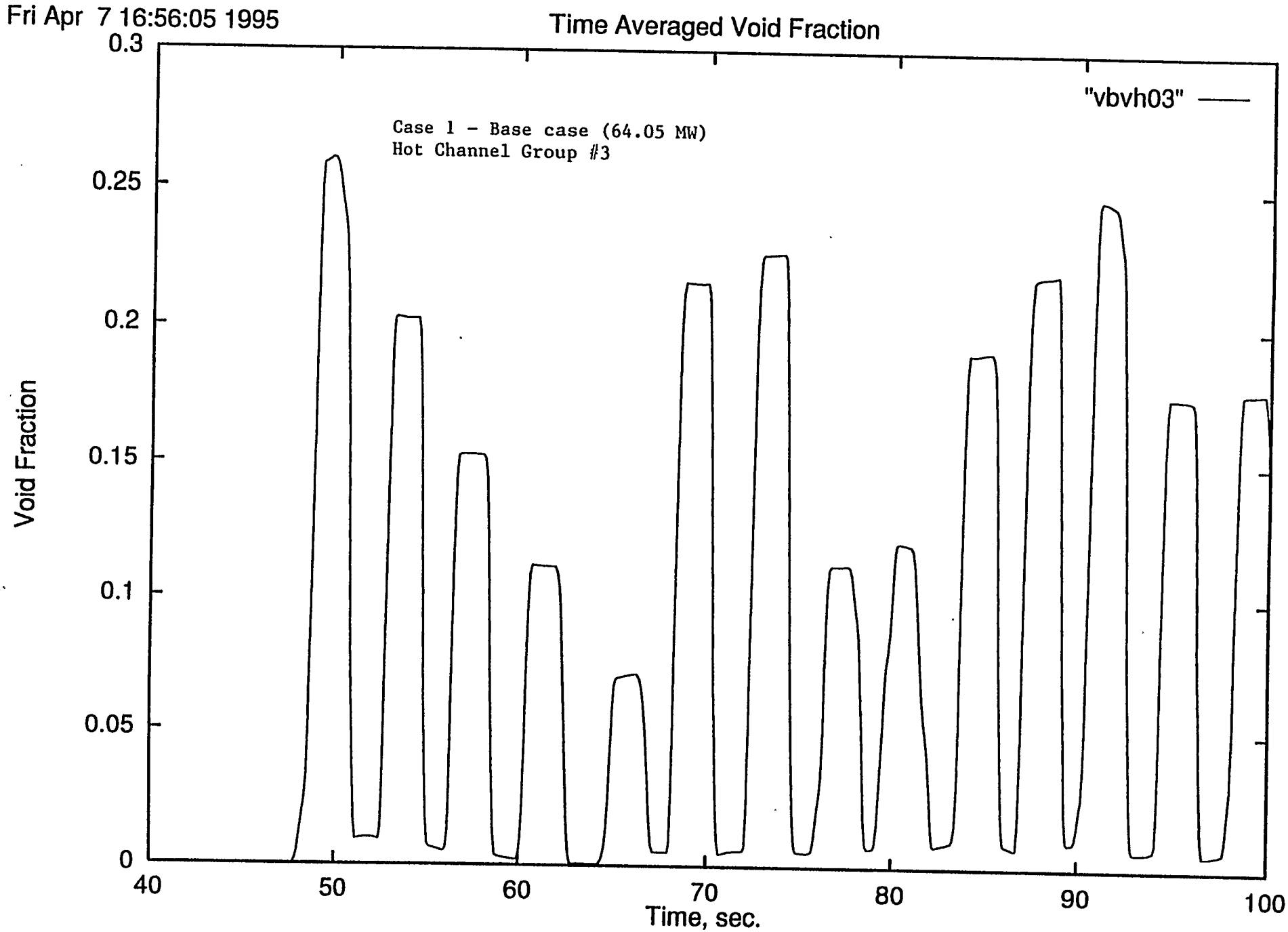
Fri Apr 7 16:56:05 1995
Time Averaged Void Fraction
"vbvh03"
Case 1 - Base case (64.05 MW)
Hot Channel Group #3
Void Fraction
0.3
0.25
0.2
0.15
0.1
0.05
0
40
50
60
70
80
90
100
Time, sec.

Figure C3.3

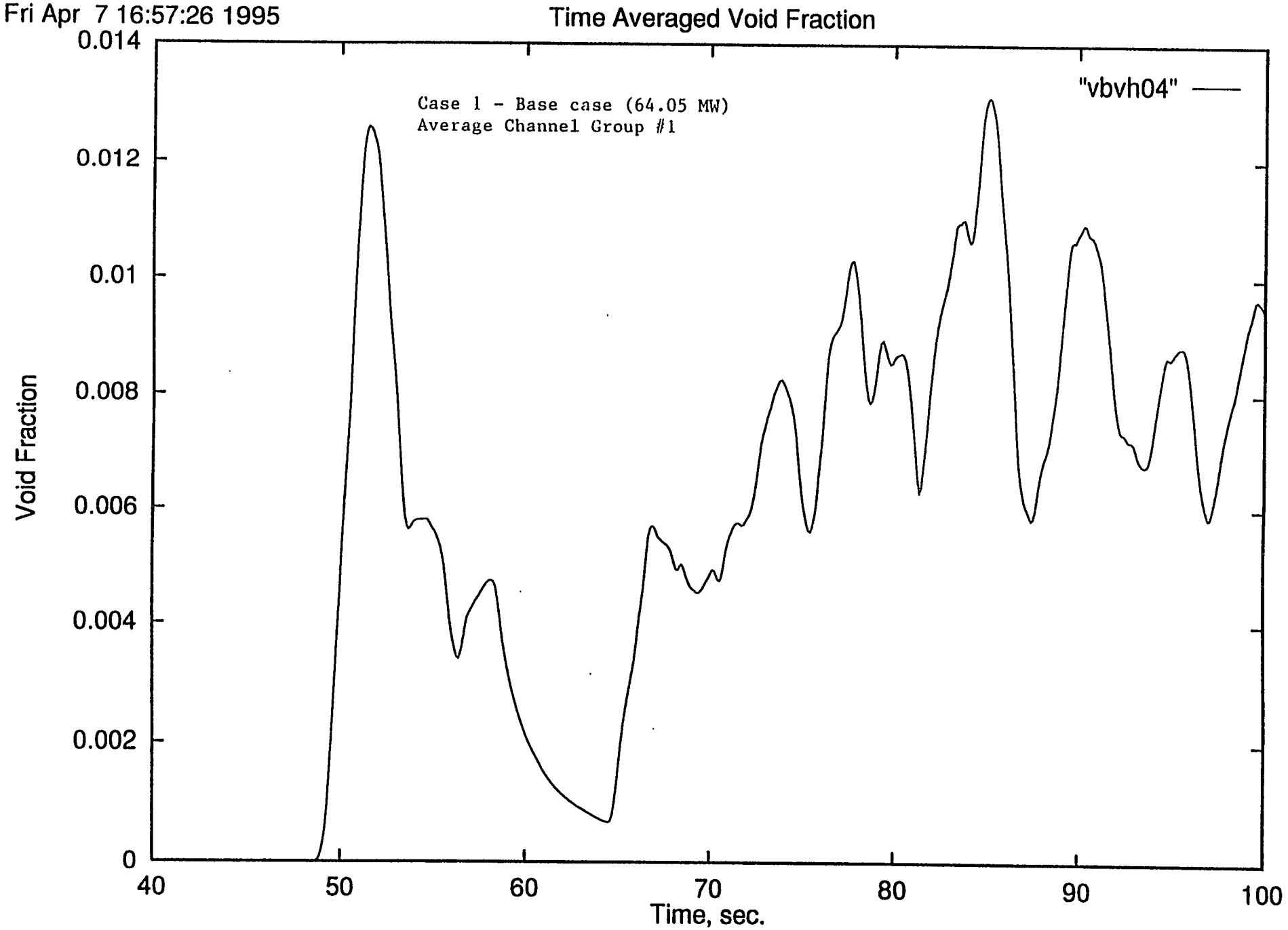
Fri Apr 7 16:57:26 1995
Time Averaged Void Fraction
Case 1 - Base case (64.05 MW)
Average Channel Group #1
"vbvh04"
Void Fraction
0.014
0.012
0.01
0.008
0.006
0.004
0.002
0
40
50
60
70
80
90
100
Time, sec.

Figure C3.4

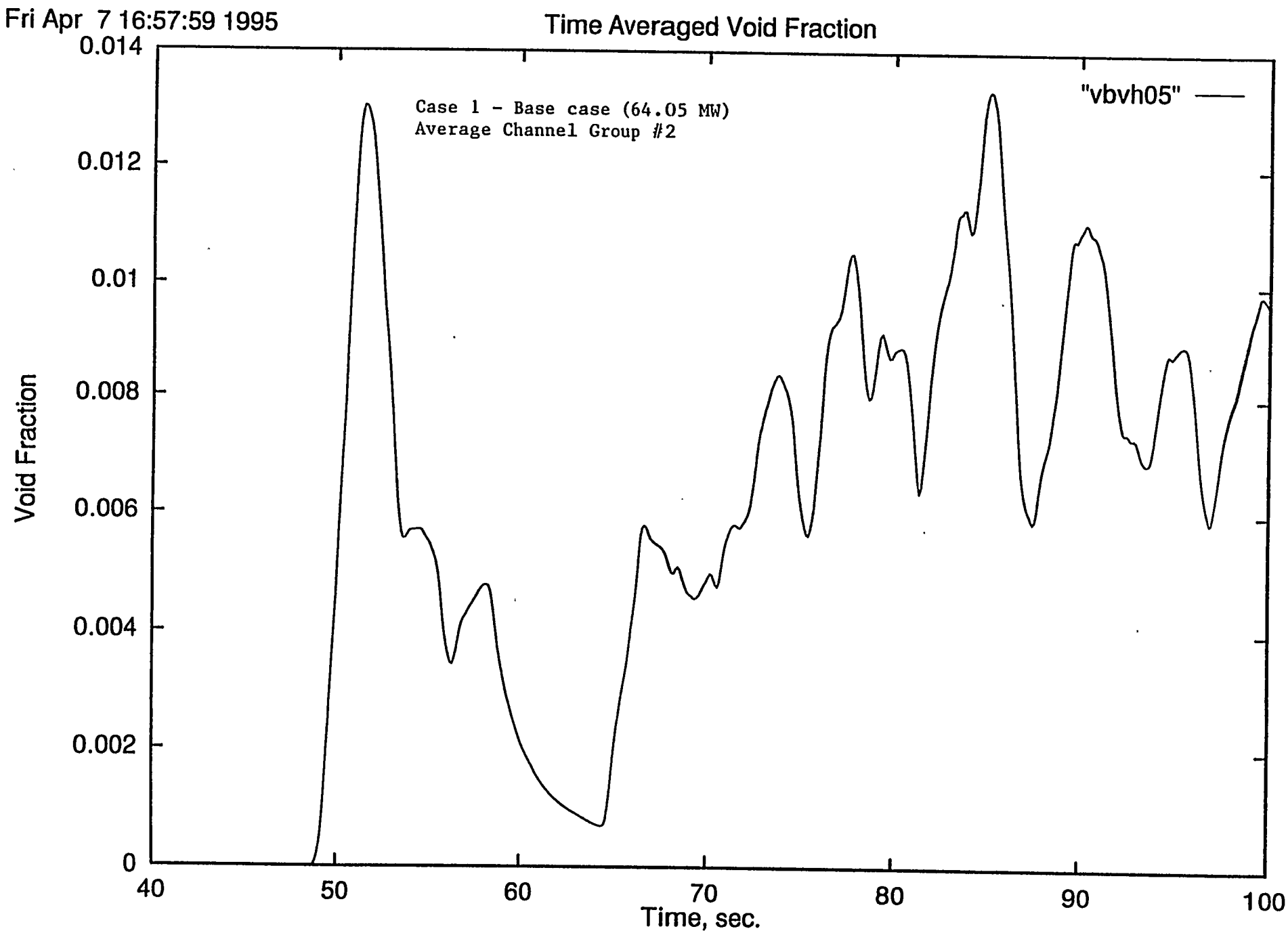
Fri Apr 7 16:57:59 1995
Time Averaged Void Fraction
Case 1 - Base case (64.05 MW)
Average Channel Group #2
"vbvh05"
Void Fraction
0.014
0.012
0.01
0.008
0.006
0.004
0.002
0
40
50
60
70
80
90
100
Time, sec.

Figure C3.5

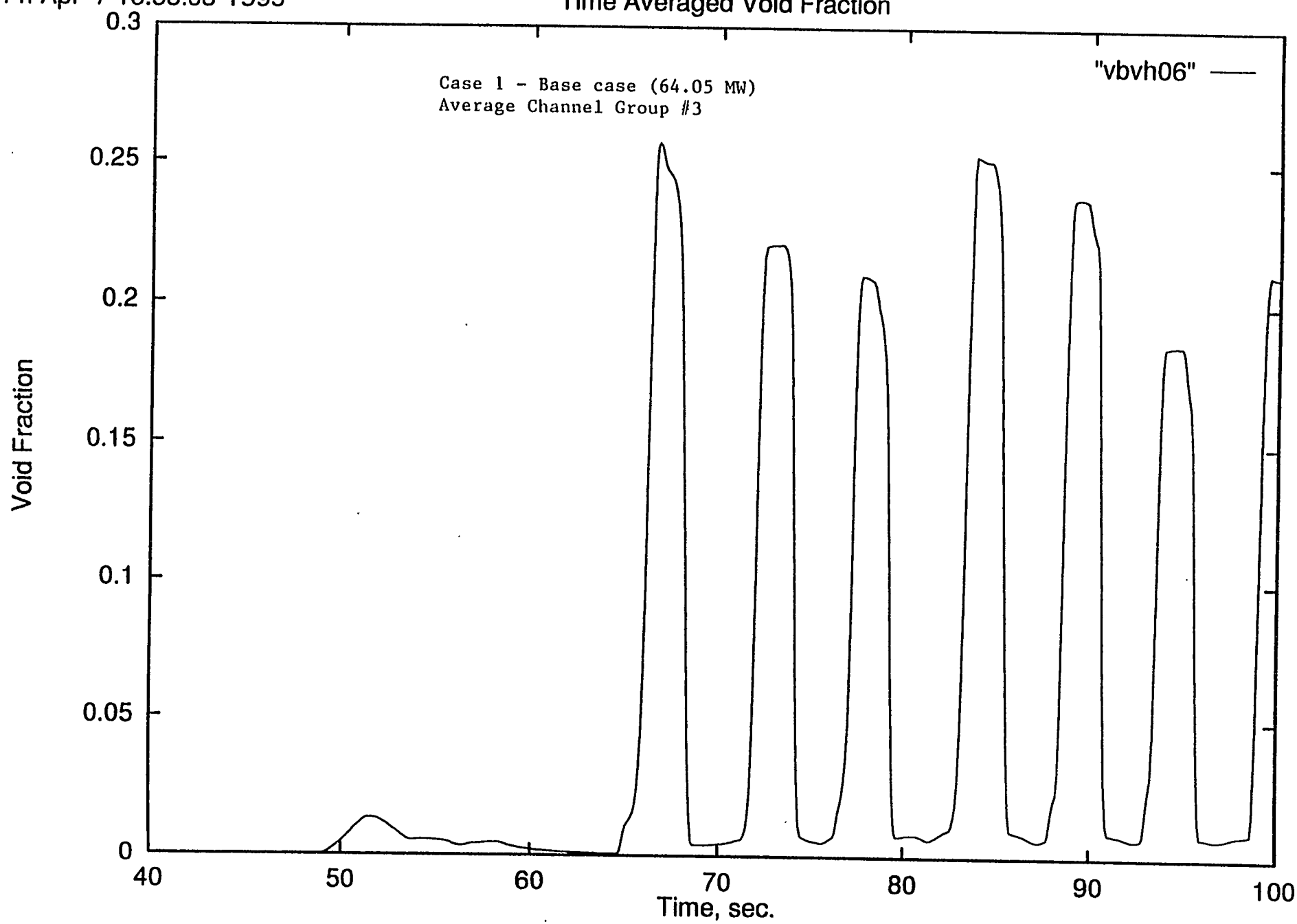
Fri Apr 7 16:58:38 1995
Time Averaged Void Fraction
Case 1 - Base case (64.05 MW)
Average Channel Group #3
"vbvh06"
Void Fraction
0.3
0.25
0.2
0.15
0.1
0.05
0
40
50
60
70
80
90
100
Time, sec.

Figure C3.6

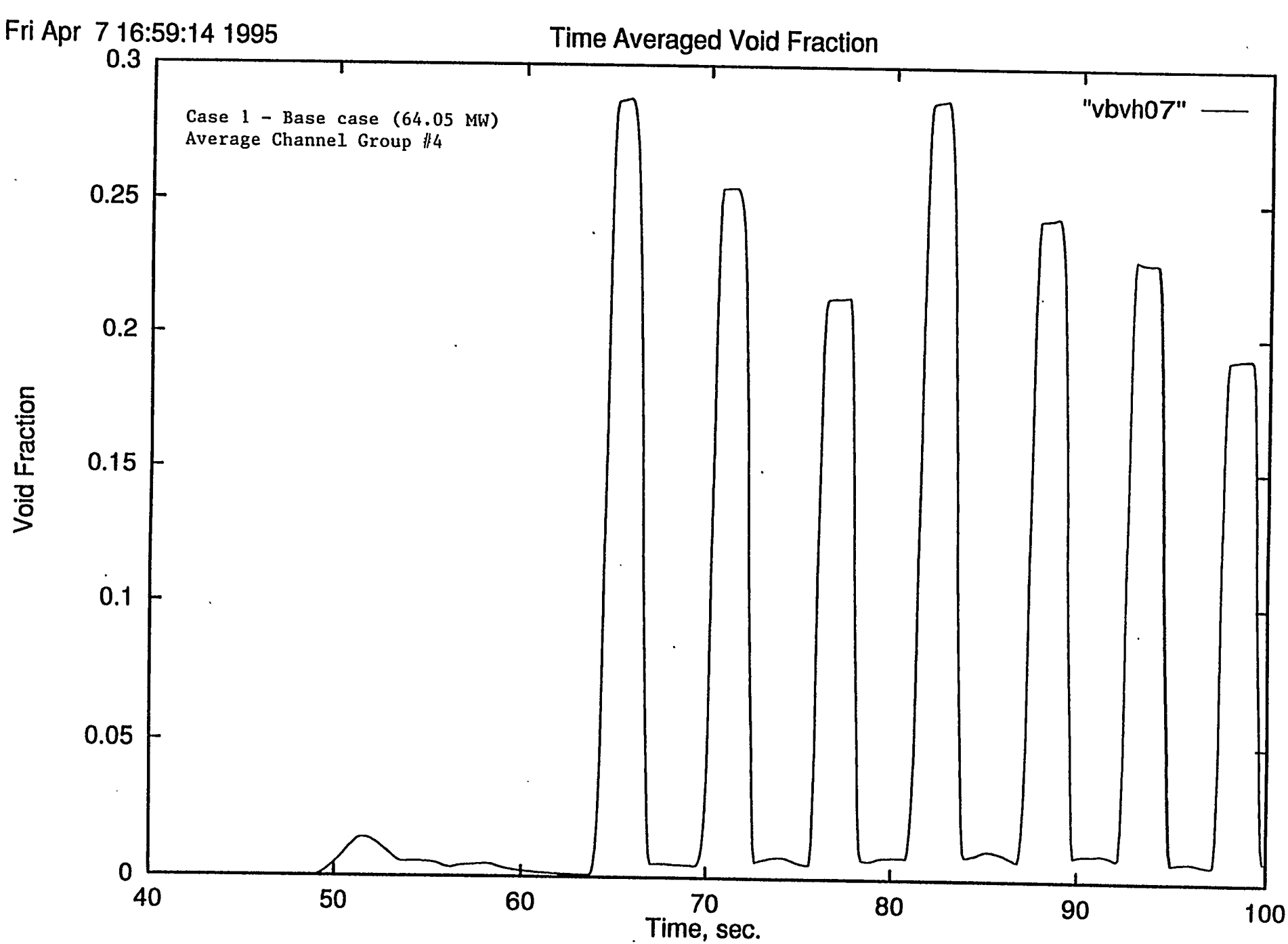
Fri Apr 7 16:59:14 1995
Time Averaged Void Fraction
Case 1 - Base case (64.05 MW)
Average Channel Group #4
"vbvh07"
Void Fraction
0.3
0.25
0.2
0.15
0.1
0.05
0
40
50
60
70
80
90
100
Time, sec.

Figure C3.7

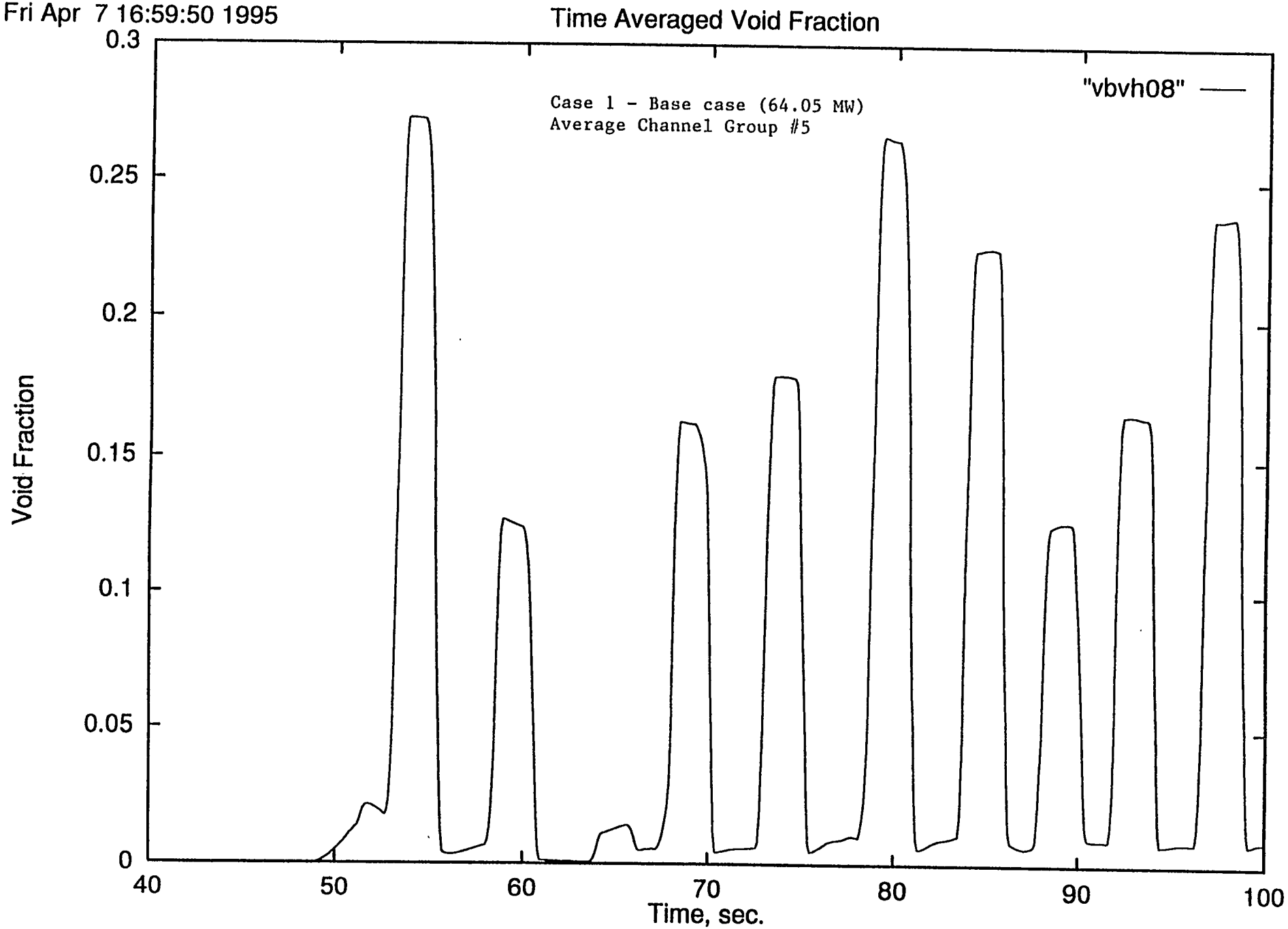
Fri Apr 7 16:59:50 1995
Time Averaged Void Fraction
"vbvh08"
Case 1 - Base case (64.05 MW)
Average Channel Group #5
Void Fraction
0.3
0.25
0.2
0.15
0.1
0.05
0
40
50
60
70
80
90
100
Time, sec.

Figure C3.8

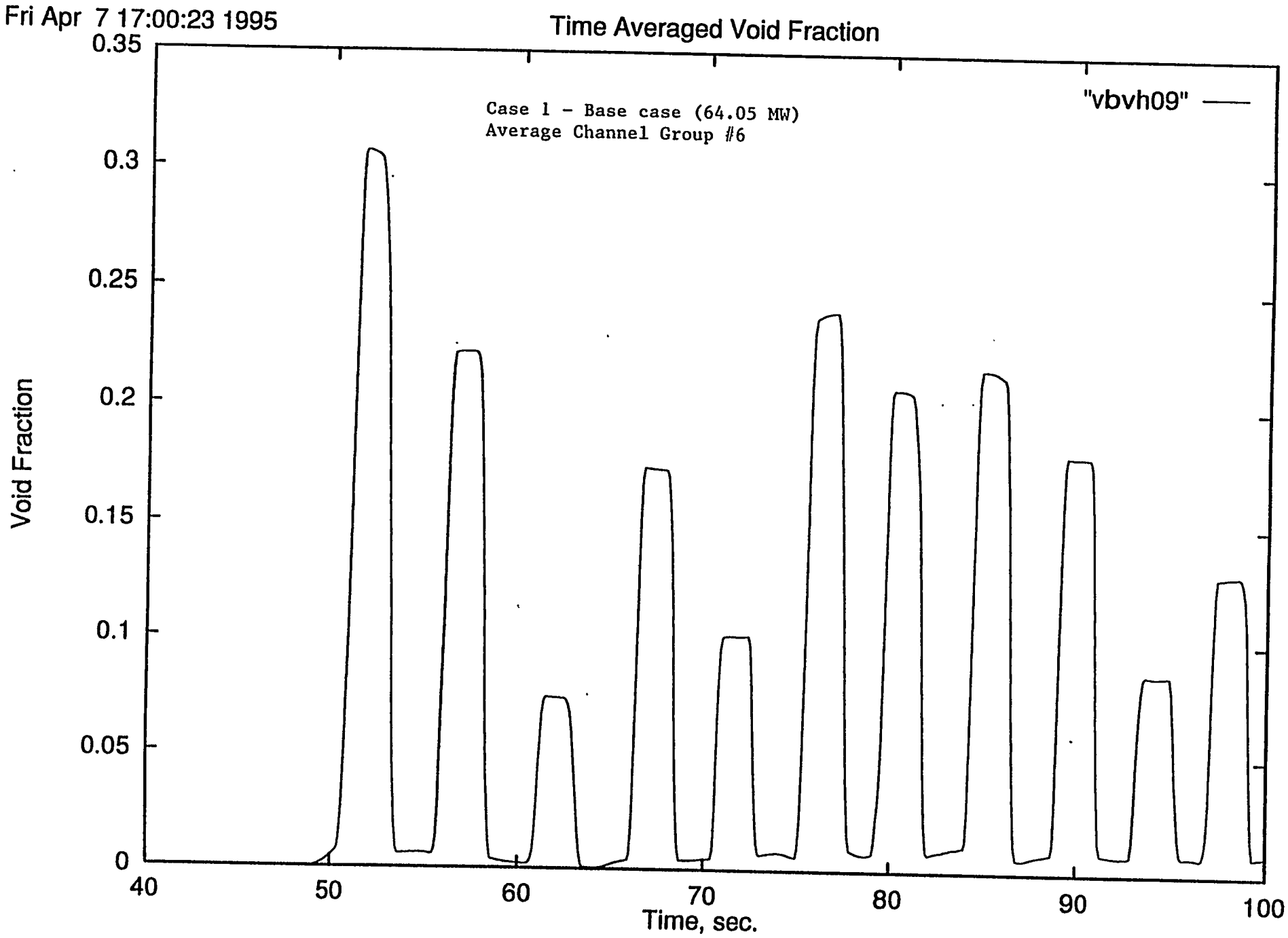
Fri Apr 7 17:00:23 1995
Time Averaged Void Fraction
Case 1 - Base case (64.05 MW)
Average Channel Group #6
"vbvh09"
Void Fraction
0.35
0.3
0.25
0.2
0.15
0.1
0.05
0
40
50
60
70
80
90
100
Time, sec.

Figure C3.9

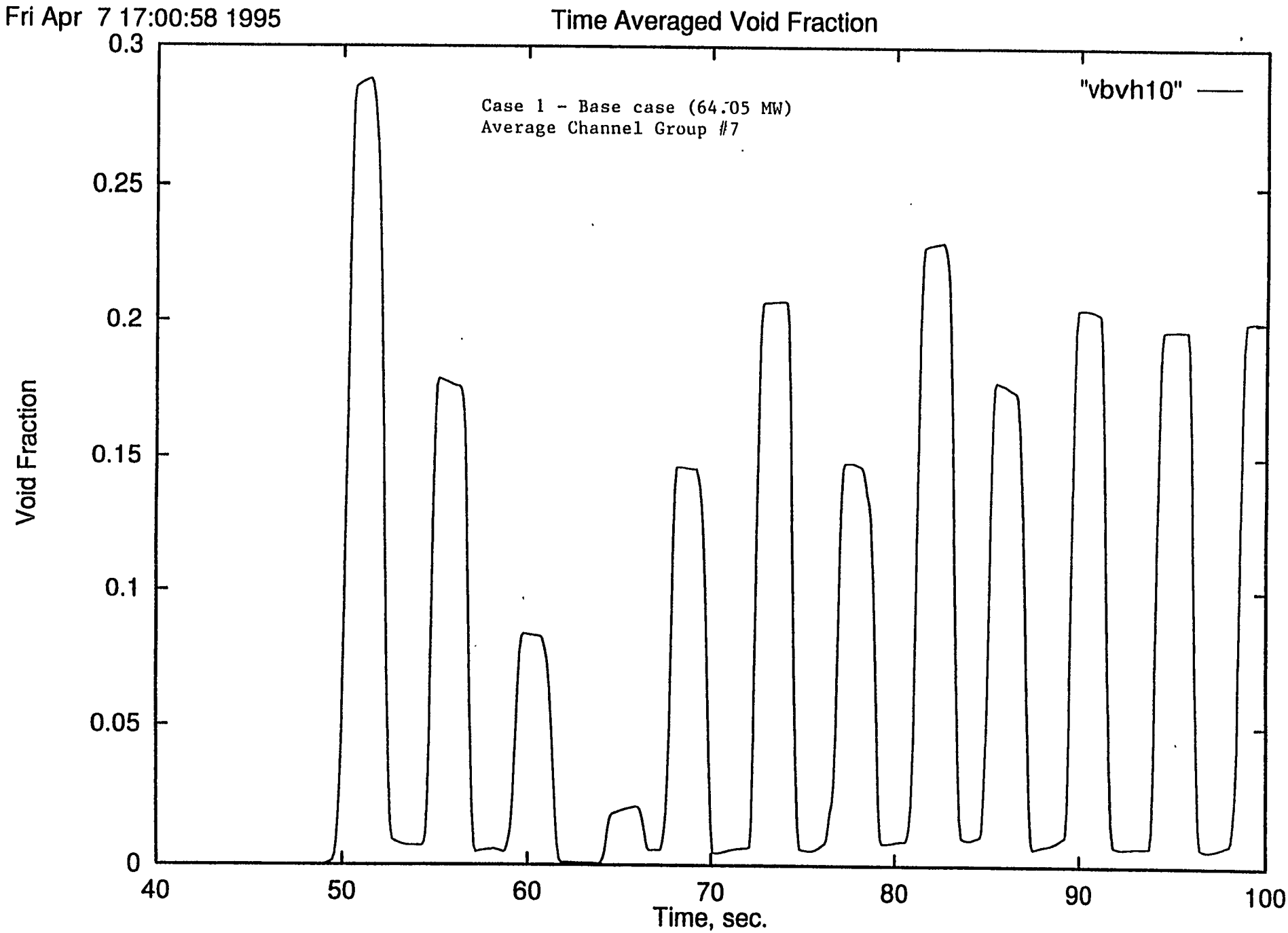
Fri Apr 7 17:00:58 1995
Time Averaged Void Fraction
"vbvh10"
Case 1 - Base case (64.05 MW)
Average Channel Group #7
Void Fraction
0.3
0.25
0.2
0.15
0.1
0.05
0
40
50
60
70
80
90
100
Time, sec.

Figure C3.10

DECAY2 Apr. 18, 1995 10:53:09 AM

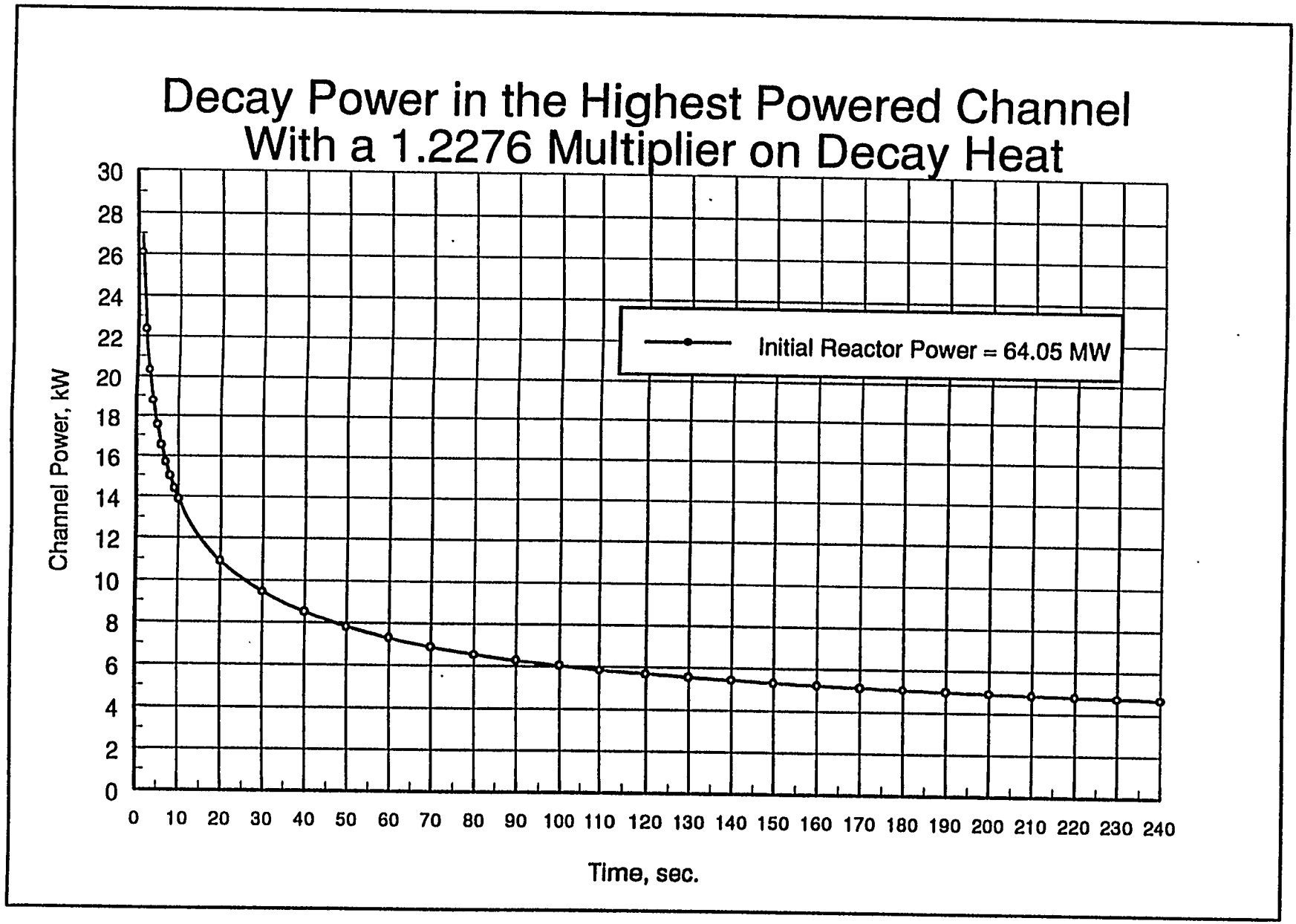

Figure C4

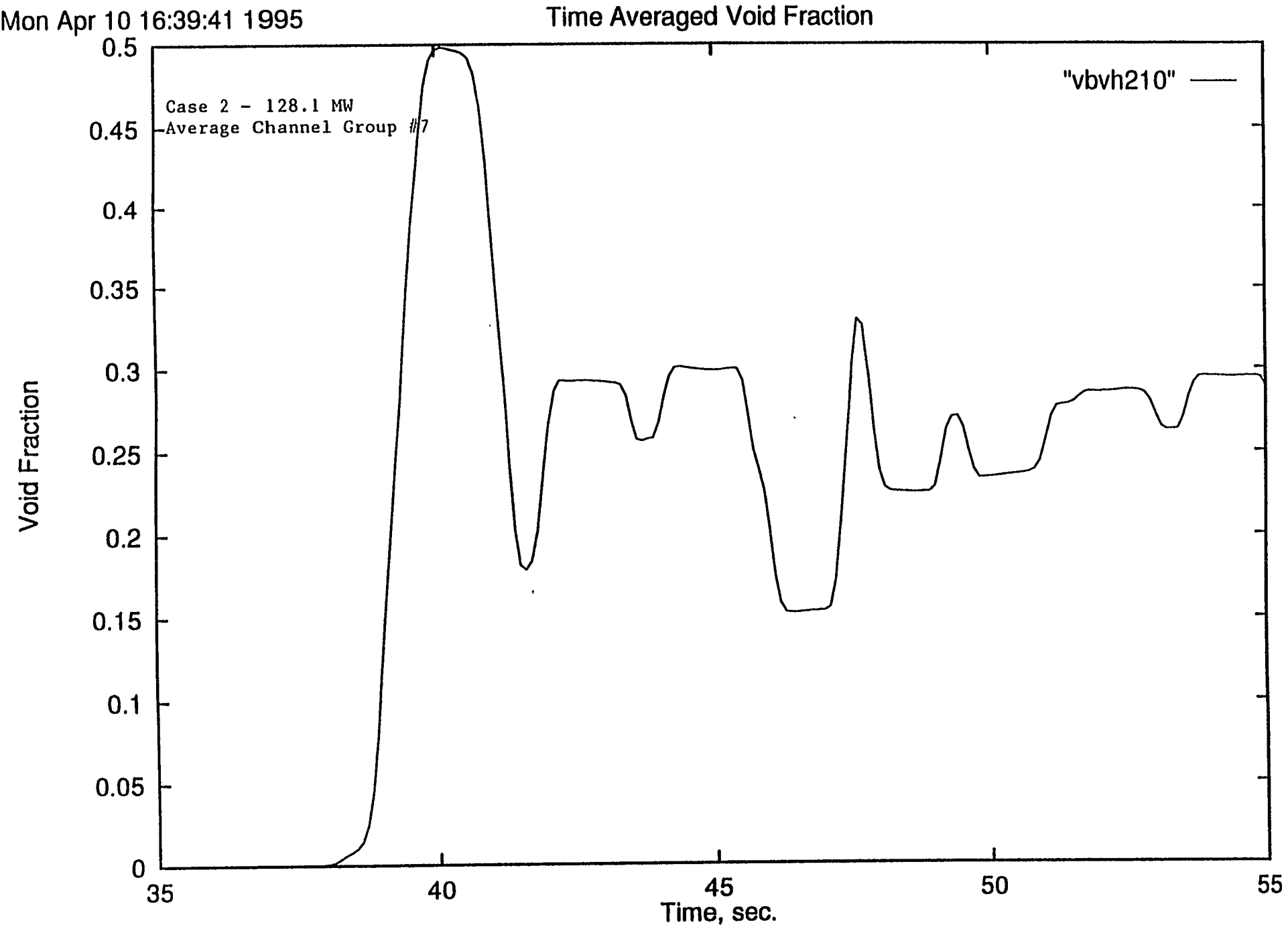
Mon Apr 10 16:39:41 1995
Time Averaged Void Fraction
"vbvh210"
Case 2 - 128.1 MW
Average Channel Group #7
Void Fraction
0.5
0.45
0.4
0.35
0.3
0.25
0.2
0.15
0.1
0.05
0
35
40
45
50
55
Time, sec.

Figure C 5